Synthesis of Precursors and Reactivity Studies of Nitrosocarbonyl Intermediates

By

Saghar Nourian

A dissertation submitted to Johns Hopkins University in conformity with the requirements for the degree of Doctor of Philosophy

Baltimore, Maryland

July, 2017

Abstract

Nitroxyl (HNO), a potential heart failure therapeutic, is a reactive species that spontaneously dimerizes to yield hyponitrous acid, which dehydrates to generate nitrous oxide (N_2O). Due to its inherent chemical reactivity, HNO cannot be used directly, and therefore, donors are required for its *in situ* generation. Here, we report *N*-substituted hydroxamic acids with pyrazolone leaving groups (**NHPY**) and *O*-substituted hydroxamic acids with pyrazolone leaving groups (**OHPY**) as novel precursors to nitrosocarbonyl intermediates, which subsequently provide HNO. Nitrosocarbonyls are transient electrophiles that react with nucleophiles, including water, to produce HNO. We found that pyrazolones are efficient nitrosocarbonyl traps under physiologically relevant conditions, undergoing an *N*-selective nitrosocarbonyl aldol reaction. This trapping reaction has been used to confirm the involvement of nitrosocarbonyls as intermediates in the observed chemistry.

Time-resolved infrared (TRIR) spectroscopy is a powerful tool for studying photochemically generated reactive intermediates in solution. Applying this technique, we examined the reactivity of a photo-generated nitrosocarbonyl intermediate with a pyrazolone and reported the rate constant for this trapping reaction.

Advisor: Professor John P. Toscano

Readers: Professor Thomas Lectka

Professor Kenneth D. Karlin

Acknowledgments

I would like to thank Professor John P. Toscano for granting me the opportunity to work in his research group. He taught me how to think, independently, as a scientist, and gave different opportunities to challenge myself. I sincerely thank him for being such a thoughtful advisor.

Also, I would like to thank Professor Thomas Lectka and Professor Kenneth D. Karlin for serving on my thesis committee. I thank my lab mates: Dr. Gizem Keceli, Dr. Daryl A. Guthrie, Dr. Tyler A. Chavez, Dr. Christopher L. Bianco, Dr. Vinayak Khodade, Hyunah Cho, Blaze Pharoah, Christopher Chang, Zachary A. Zilber, and Robert P. Lesko, for very helpful discussions and all the scientific work we had in last five years.

Most of all, my sincere thanks go to my dad. I wouldn't be who I am today without his encouragements and thoughtfulness. He is always in my heart. Also, I am very grateful to my mom for supprting me with my decisions. She is a true example of kindness and patience. I want to thank my brother and sister for always being so helpful to me, and supporting me through ups and downs of my life. I would also like to thank my parents-in-law for their constant support.

I would like to dedicate this thesis to my love, Ashkan. Thanks for everything!

Table of Contents

List of Figures

List of Schemes

List of Tables

Chapter 1.

Introduction

1.1 Nitroxyl (Azanone, HNO)

Nitric oxide (NO) is a biological signaling agent that has been shown to modulate numerous physiological processes.[1-3] This endogenously produced small molecule plays an important role in blood pressure control, the immune response and neurotransmission. [2,4]

Peroxynitrite ($ONOO^-$), nitrite (NO_2^-), and nitrogen dioxide (NO_2) can be formed through oxidation of NO in certain aerobic and biological environments.[5] Many reports have demonstrated the importance of these molecules as biological effectors.[6] The role of NO was preliminary thought to be as an oxidative agent, so research mainly studied NO species with higher oxidation states, and less consideration focused on reduced species such as the one-electron reduced form of NO, nitroxyl (HNO).

Although the endogenous generation of NO is well established, the endogenous generation of HNO has not been demonstrated. HNO has been shown to enhance both vasorelaxation and myocardial contractility, which makes it a potential therapeutic for treatment of heart failure.[7-11]

There are some proposed biosynthetic pathways that suggest the possibility of endogenous generation of HNO. Nitric oxide synthases (NOS) is an enzyme that converts argenine to cirtulline and NO in presence of the cofactor tetrahydrobiopterin (THB).[12] Generation of HNO using isolated neuronal NOS has been demonstrated in the absence of THB.[13] Also, generation of HNO has been shown by oxidation of hydroxylamine (NH_2OH) with heme-containing proteins.[14] Interconversion of NO and HNO in presence of superoxide dismutase (SOD) is another possible pathway that suggests the endogenous generation of HNO.[15] Recently, the reaction of hydrogen sulfide (H_2S) with NO potentially to form thionitrous acid (HSNO) has attracted attentions.[16,17] Upon reaction with H_2S, HSNO can produce HNO. Although these results may demonstrate the possibility of endogenous generation of HNO, more investigations are required to provide direct evidence for *in vivo* HNO formation.

A complication of studying HNO chemistry is its high reactivity. As shown in Scheme 1-1, HNO spontaneously dimerizes ($k = 8 \times 10^6\ M^{-1}s^{-1}$) to hyponitrous acid (HON=NOH), which subsequently dehydrates to produce nitrous oxide (N_2O).[18] Detection of N_2O has served as a marker for the presence of HNO.

Scheme 1-1. HNO Dimerization

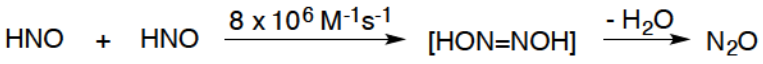

The pK_a of HNO has been evaluated to be 11.4.[18,19] Thus, under physiological conditions HNO exists mostly in its protonated form. The deprotonation of HNO, which is a ground state singlet,[20,21] to generate NO^-, with a triplet ground state,[22,23] is presumed to be quite slow due to the spin-forbidden nature of this process.

One major target for biochemical reactivity of HNO appears to be thiols (Scheme 1-2). Depending on the concentration of thiol, HNO reactivity results in the formation of sulfinamides or disulfides.[24,25] The second-order rate constant for reaction of HNO with glutathione and cysteine were determined to be 2×10^6 $M^{-1}s^{-1}$ and 5×10^5 $M^{-1}s^{-1}$, respectively. The pK_a of the reacting thiol is thought affect the trapping rate, with thiols of lower pK_a values reacting faster with HNO.[26]

Scheme 1-2. HNO Reactivity with Thiols

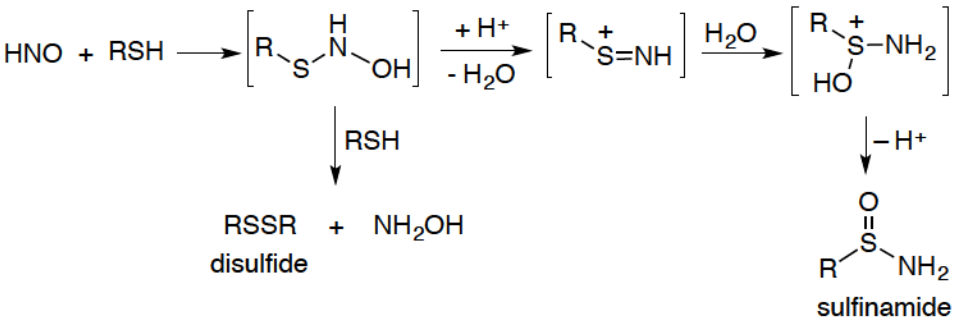

Recently, the reaction of carbon based nucleophiles with HNO has been studied under physiological conditions.[27-29] Also, transition metal centers are known to be targets for HNO in biological systems. HNO reduces ferric hemes to

generate ferrous heme-nitrosyl complexes through reductive nitrosylation reactions.[30-33] The same reductive properties of HNO with other metals such as copper (Cu)[34] and manganese (Mn)[35] have also been reported.

1.2 HNO Donors

As discussed above, HNO is a very reactive molecule and rapidly dimerizes through an irreversible process, so donors are needed for the *in situ* generation of HNO. Angeli's salt (**AS**) is a well-known HNO donor that was first reported in 1896.[36] Piloty's acid (**PA**) is another HNO donor that was reported in the same year.[37] There are also other HNO donors reported in literature (Figure 1-1), including primary amine based diazeniumdiolates, such as **IPA/NO**,[38,39] acyloxy nitroso compounds (**AcON**)[40,41], *N*-hydroxycyanamide,[42-45] *N*-substituted hydroxylamine with pyrazolone leaving groups (**HAPY**),[27] *N*-substituted hydroxylamines with barbituric acid leaving groups (**HABA**),[28] and nitrosocarbonyl (**NC**) precursors[46,47].

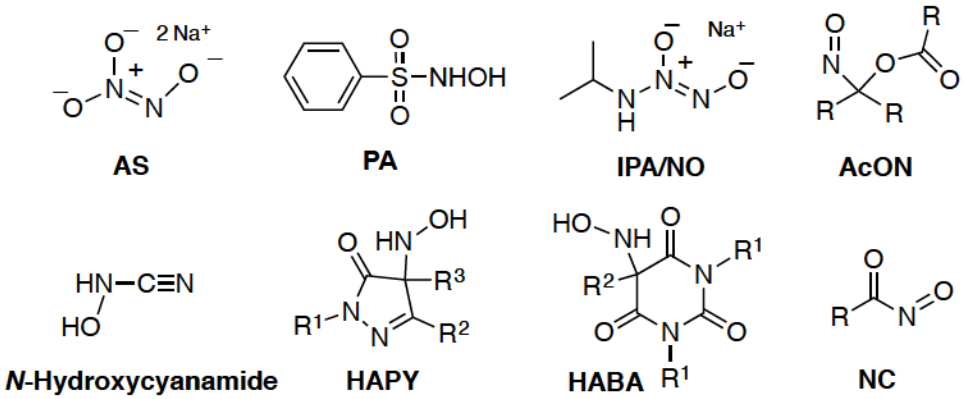

Figure 1-1. Representative examples of HNO donors.

1.2.1. Angeli's Salt

Angeli's salt (**AS**) is an oxygen-based diazeniumdiolate, and efficient HNO donor with a half-life of ~ 3 min under physiological conditions.[48,49] **AS** is the most prevalent donor that has been used to study HNO chemistry and pharmacology. Decomposition of **AS** involves protonation following by tautomerization to produce HNO and nitrite as the end products.[50] **AS** becomes an NO donor at pH< 4 and the decomposition mechanism is through tautomerization to a higher energy species[51] as shown in Scheme 1-3. Under physiological conditions, **AS** is an efficient HNO donor, but modification of its structure to access corresponding HNO donors with longer half-lives has not yet been reported. Thus, other donors are required to investigate the physiological effects of chronic delivery of HNO.

Scheme 1-3. Decomposition Pathways of Angeli's Salt

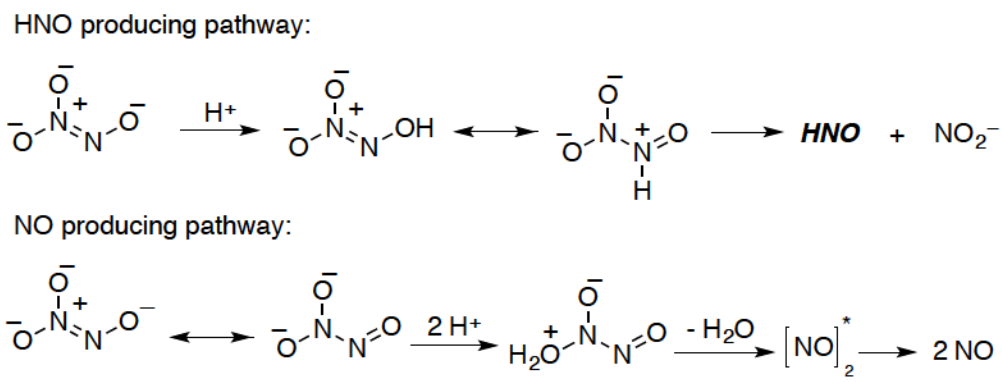

1.2.2. Amine-Based Diazeniumdiolates

Keefer and co-workers have reported a range of secondary amine-based diazeniumdiolates as efficient NO donors in biological studies.[52-55] Miranda and colleagues have investigated primary amine-based diazeniumdiolates as potential

HNO donors.[38,39] Depending on pH and amine backbone, these primary amine derivatives can serve as both HNO and NO donors. The isopropyl amine derivative **IPA/NO** is a well-known primary amine-based diazeniumdiolates that under physiological conditions releases equimolar amounts of HNO and NO as shown in Scheme 1-4.

Scheme 1-4. Decomposition Pathways of IPA/NO

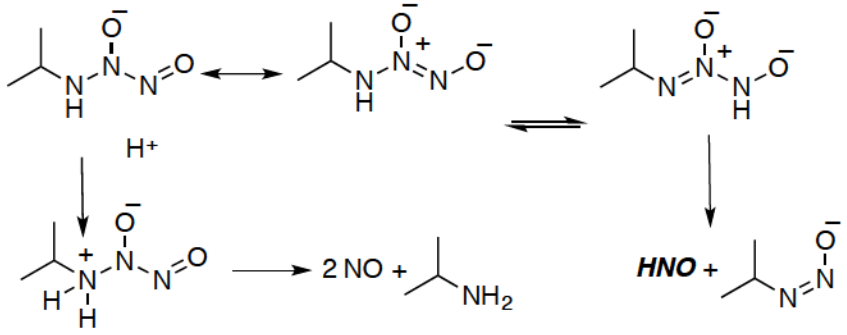

1.2.3. Piloty's Acid Derivatives

Piloty's acid (**PA**) was first synthesized by the German chemist, Oskar Piloty, in 1896.[37] **PA** is an *N*-substituted hydroxylamine derivative with a sulfinate as the leaving group, and can generate HNO under basic conditions (Scheme 1-5).[56,57] The first step for decomposition is the deprotonation of hydroxylamino group.[56,58,59] Doctorovich and co-workers studied different **PA** derivatives with various pK_a values. It was shown that the highest rate of HNO generation was at pH values where the **PA** derivatives is fully deprotonated.[60] This suggests a barrier for HNO release from anionic **PA**, which could be reflected in reversible HNO generation as sodium benzenesulfinate is known to slow the decomposition rate of **PA**. Under physiological conditions, **PA** is oxidized and becomes an NO donor. [61]

Scheme 1-5. Decomposition Pathways for Piloty's Acid

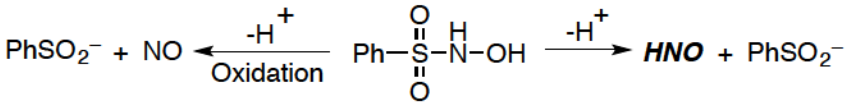

To promote HNO generation from Piloty's acid derivatives, bulky groups or electron withdrawing groups have been added to the phenyl ring.[62-64] Electron withdrawing groups can decrease the pK_a value of the donor and stabilize the sulfinate leaving group, thereby facilitating HNO generation. Interestingly, crystallographic analysis confirmed that **PA** derivatives with electron withdrawing groups have shorter N-O bond distances, which may suggest more facile HNO generation.[60]

Our lab has synthesized a variety of **PA** derivatives including 2-bromo-*N*-hydroxybenzenesulfonamide (2-bromo-Piloty's acid).[62] This compounds is an excellent HNO donor with the half-life of 2.4 min under physiologically relevant conditions.

1.2.4. Acyloxy Nitroso Compounds

Acyloxy nitroso compounds (**AcON**) can hydrolyze to release HNO (Scheme 1-6).[65-66] **AcON** compounds can be synthesized via oxidation of oximes in the presence of carboxylic acids. The rate of HNO generation depends on pH and the ester group structure. Based on decomposition studies, the chemistry of **AcON** compounds is more complicated than preliminarily expected. Upon hydrolysis of the ester group, as shown in Scheme 1-6, an alpha hydroxyl nitroso intermediate is

formed, which can further decompose to release HNO (Path A). In presence of thiols, formation of hydroxysulfenamide, disulfide, and hydroxylamine are reported, suggesting the generation of HNO. However, a non HNO-producing pathway, direct reaction of the thiolate with the acyloxy nitroso compound (Scheme 1-6, Path B), can compete with HNO generation forming disulfides as identical end products. Thus, the decomposition of **AcON** compounds can go through competing pathways.

Scheme 1-6. Decomposition Pathways of Acyloxy Nitroso Compounds

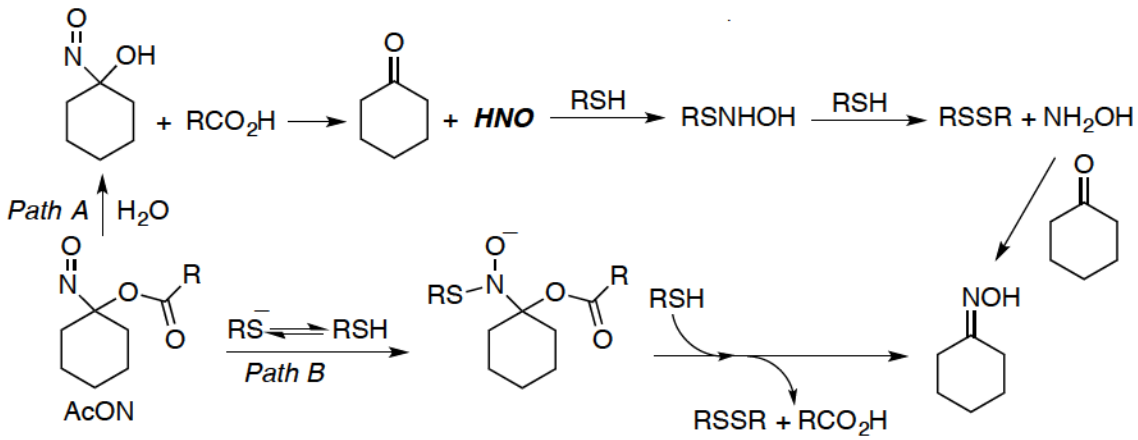

1.2.5. Cyanamide

Aldehyde dehydrogenase (AlDH) is an enzyme that catalyzes the conversion of acetaldehyde to acetate. After consumption of alcohol, inhibition of AlDH causes acetaldehydemia. HNO can inhibit AlDH via its reaction with the active site cysteine residue.[42-45] Cyanamide is an alcohol deterrent that has been used in Europe, Canada, and Japan and can release HNO upon metabolic activation (Scheme 1-7). *N*-hydroxycyanamide is the proposed intermediate that can be formed upon bioactivation of cyanamide. This *N*-substituted hydroxylamine derivative is

unstable, and decomposes to either produce HNO or upon oxidative metabolism, generates nitrosyl cyanide, which further can hydrolyze and release HNO (Scheme 1-7). Beside HNO, four other products are formed: HCN, HNO_2, CO_2, and NH_3. Following derivatization of cyanamide compounds, *N*,*O*-dibenzoyl derivatives of *N*-hydroxycyanamide **1** have been synthesized (Scheme 1-7), but this compound generates HNO only in presence of esterase or base.[67]

Scheme 1-7. Cyanamide Decomposition Pathways

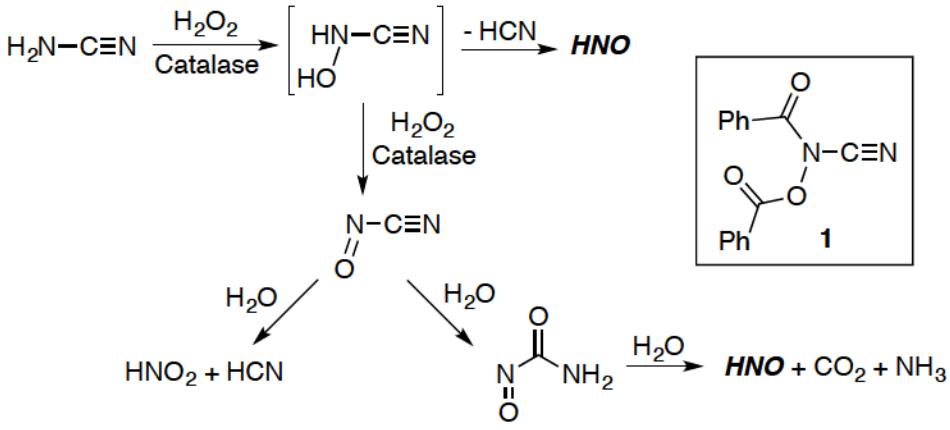

1.2.6. Hydroxylamines with Carbon Based Leaving Groups

Recently, Toscano et al. have reported three new classes of highly tunable HNO donors based on hydroxylamino Meldrum's acid **HAMA**, hydroxylamino barbituric acid **HABA**, and hydroxylamino pyrazolone **HAPY** scaffolds.[27-29] These compounds are examples of *N*-substituted hydroxylamines with carbon-based leaving groups. Employing these donors, the idea is to generate HNO along with a stable carbanion at neutral pH. The mechanism of decomposition is through deprotonation of the hydroxylamino moiety and subsequent HNO generation

(Scheme 1-8). Beside the importance of donors pK_a that significantly affect the rate of HNO release, the acidity of the leaving group has strong impact on the stability of these donors under physiological conditions.

After decomposition of **HAMA** compounds, it is expected that HNO be generated with an equimolar amount of Meldrum acid. Meldrum acids have low pK_a values because upon deprotonation, delocalization of the lone pair of electrons through the ring can effectively stabilize the carbanion. However, the carbonyls of Meldrum acids ring are prone to nucleophilic attack.[68] Based on reported evidence, formation of acetone upon hydrolysis of **HAMA** compounds competes with HNO formation, which may limit the application of this class of compounds. [29]

Scheme 1-8. HNO Release from HAMA, HABA, and HAPY compounds

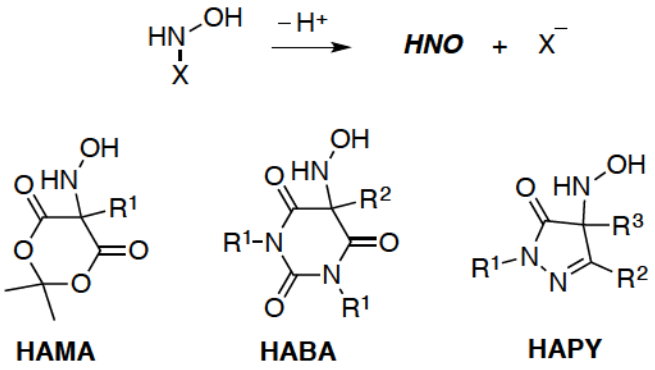

Barbituric acids are stable to hydrolysis, and have low pK_a values. The initial report presented an *N*-substituted hydroxylamine with a barbituric acid leaving group (R^1 = Me, R^2 = C(=NOMe)Me) that has a short half-life (0.7 min) and excellent HNO yield (> 95%) upon decomposition. However, there is a non-HNO producing pathway that competes with HNO release for these barbituric acid derivatives.

Based on reported experiments, it is possible for some barbituric acid derivatives to rearrange to hydantoin, and therefore, inhibit HNO formation. Following decomposition of different **HABA** compounds, the propensity to rearrangement was examined in order to develop strategies that favor HNO generation. It has been shown that 1,3-unsubstituted barbituric acid derivatives (R^1 = H) do not undergo this rearrangement, and the barrier to rearrangement can be increased by modification of R^2 substitutions. Using these strategies, an extensive series of **HABA** compounds with various half-lives (19-107 min) have been reported.[28]

The **HAPY** compounds are efficient HNO donors with no observed rearrangement of the pyrazolone ring. Additionally, the reported pyrazolone derivatives were shown to be stable to hydrolysis, and therefore, did not undergo non-HNO producing pathways. A correlation between half-lives of **HAPY** compounds and donor pK_a values was found. **HAPY** compounds with low pK_a values are short-lived HNO donors. With these findings, Toscano et al. reported different **HAPY** derivatives with excellent HNO yields and various half-lives (4-5674 min) under physiologically relevant conditions.

1.2.7. Nitrosocarbonyl Precursors

Nitrosocarbonyls are reactive electrophiles that can react with nucleophiles, including water, to generate HNO (Scheme 1-9).[46,69-71] These intermediates can be generated by a variety of chemical processes including oxidation of hydroxamic acids using oxidants such as periodate salts,[72] lead and silver oxides,[73] and Dess-Martin periodinane.[74] Other methods for nitrosocarbonyl generation include

thermal fragmentation of Diels-Alder adducts,[46,71,75] oxidation of nitrile oxide,[76,77] photocleavage of 1,2,4-oxadiazole-4-oxides,[78] and the rearrangement of nitrosocarbenes.[79-82] In general, these methods are not suitable for HNO generation under physiological conditions. *N*,*O*-bis-acylated derivatives, such as *N*,*O*-dibenzoyl-*N*-hydroxycyanamide, are other examples of nitrosocarbonyl precursors. As mentioned in Section 1.2.5., enzymatic or basic treatments for HNO release from this compound are required, which potentially limits the scope of HNO generation under physiological conditions.[67] Recently, Toscano et al. reported modified *N*,*O*-bis-acylated hydroxylamine derivatives with arenesulfonyl leaving groups that can produce HNO nonenzymatically under physiological conditions.[83] However, mechanistic studies revealed that the chemistry of decomposition is more complicated than originally expected. Acyl migration and amide hydrolysis are two non-HNO producing pathways that compete with nitrosocarbonyl formation and can inhibit HNO release.

Scheme 1-9. Formation of nitrosocarbonyl compounds

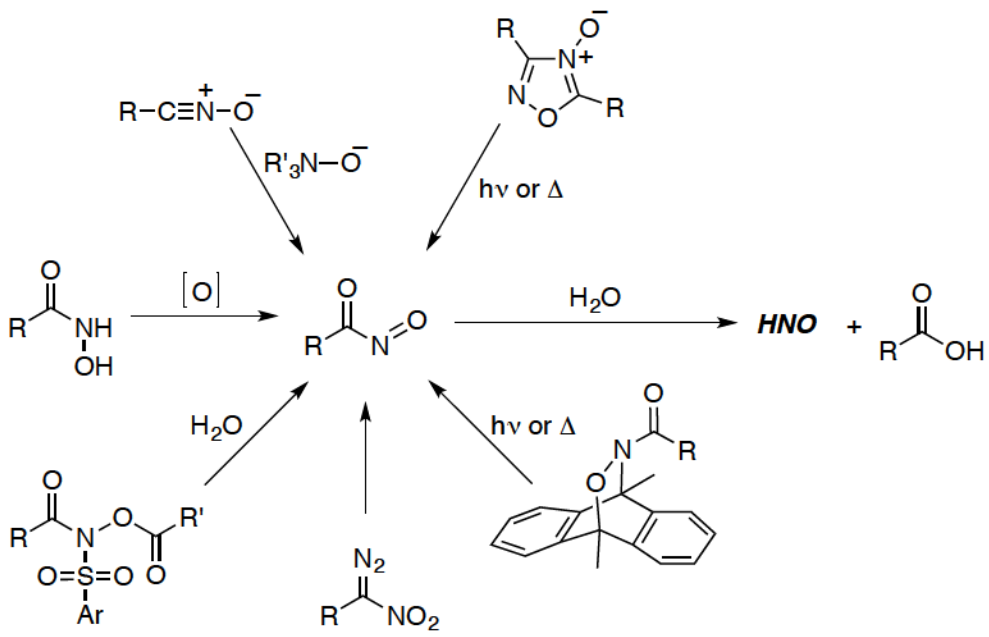

Nitrosocarbonyl compounds are reactive molecules that have not yet been isolated in stable form. Using time-resolved infrared (TRIR) spectroscopy, Toscano et al. reported the first direct detection of these reactive intermediates in organic solution.[47,84] Nitrosocarbonyls were generated by laser photolysis of nitrosocarbonyl photoprecursors, and rate constants were measured for the reaction with amines, thiols, and a diene. It was reported that the mechanism of nitrosocarbonyl reaction with primary amines involved general base catalysis, however, aminolysis by secondary amines was bimolecular. Unlike thiols, thiolates were reported to be very reactive with nitrosocarbonyls on the microsecond time scale, and the mechanism of the reaction was proposed to be through the formation of a detectable tetrahedral intermediate. Based on previous studies of the dienophilic character of nitrosocarbonyls, trapping of a nitrosocarbonyl with 1,3-

cyclohexadiene was monitored by TRIR and the rate constant was measured and reported for the formation of a final Diels-Alder adduct.

Reaction of nitrosocarbonyls with triphenylphosphines was first studied by Kirby and co workers (Scheme 1-10).[85] The reaction mechanism was proposed to be through deoxygenation following by a rearrangement to form an isocyanate and phosphine oxide. However, the reaction of nitrosoformates with triphenylphosphine turned out to be complicated. Alkoxy groups have low tendency for migration, and upon deoxygenation of the nitrosoformate, alkoxycarbonylnitrenes are proposed to be potentially formed.

Scheme 1-10. Reaction of Nitrosocarbonyls with Triphenylphosphine

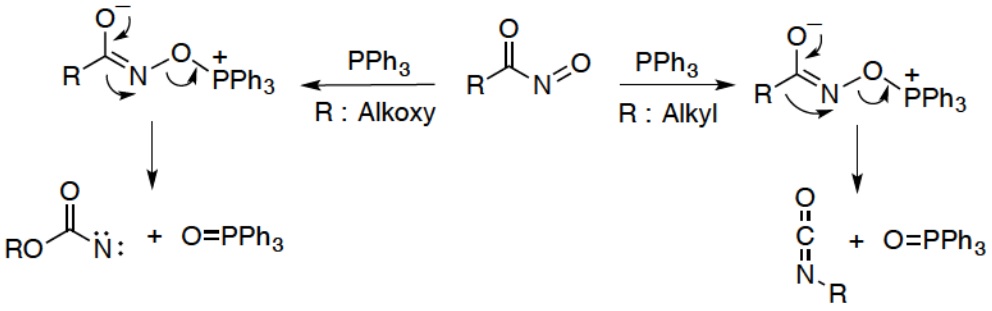

In addition to HNO generation, nitrosocarbonyls have attracted attention as potential tools in organic synthesis.[86-106] Mild aerobic oxidation of hydroxamic acids to generate nitrosocarbonyls has expanded the synthetic utility of these reactive intermediates. Nitrosocarbonyls can react with nucleophiles at the carbonyl carbon to generate HNO. As has been demonstrated recently,[93-106] it is also possible for the nucleophile to react at either nitrogen or oxygen through a nitrosocarbonyl aldol

reaction. These reactions are nitrosocarbonyl electrophilic reactions, which yield stable end products.

Scheme 1-11. Reaction of Nitrosocarbonyl Intermediates with Nucleophiles

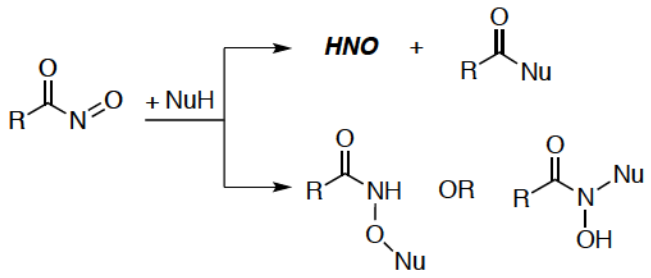

The utility of nitrosocarbonyls as synthetic tools in Diels-Alder reactions, ene reactions, and nitrosocarbonyl aldol reactions has been reported in the preparation of various functionalized molecules. Using the aerobic mild oxidation process for *in situ* generation of nitrosocarbonyls (Scheme 1-12), it is possible to synthesize *N*- or *O*-substituted hydroxamic acid derivatives selectively. Also, synthesis of both alpha-amino and alpha-hydroxy carbonyls was reported by starting with hydroxamic acid derivatives that can be further manipulated after formation of *N*- or *O*-substituted hydroxamic acid derivatives. [93,94]

Scheme 1-12. Recent Advances on α-Functionalization of Carbonyl Groups

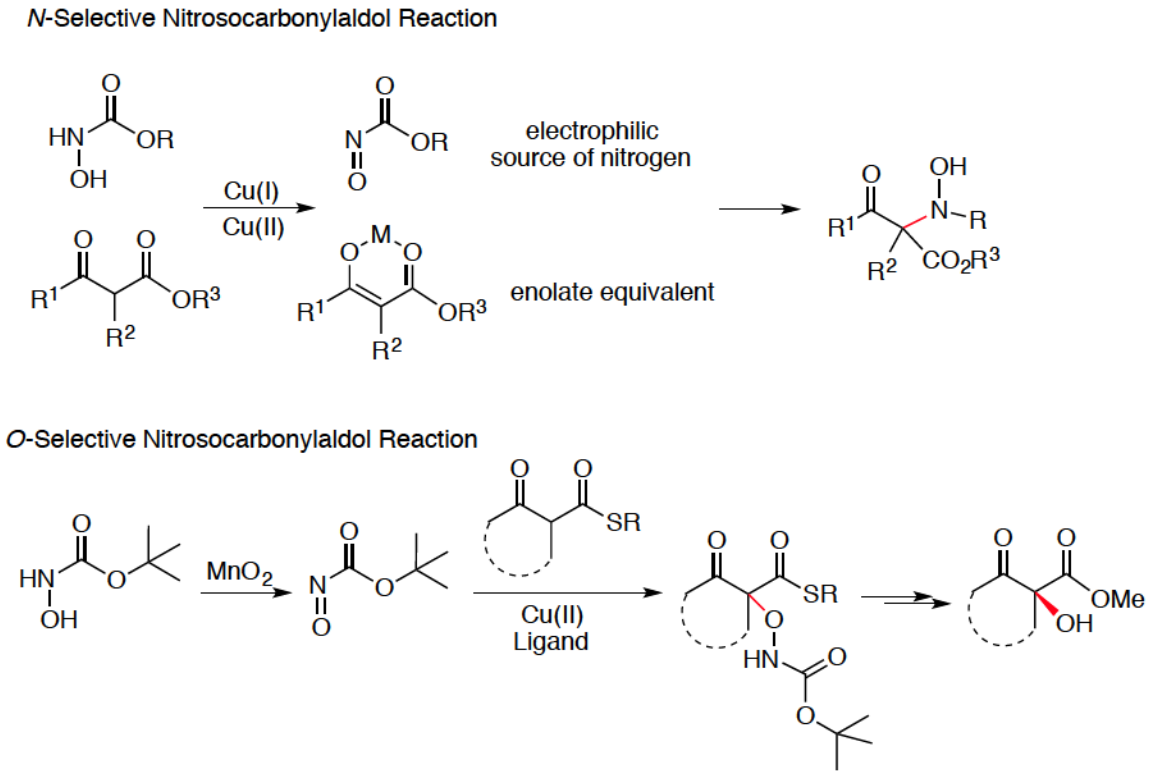

1.3. Current Studies

As mentioned in section 1.2.5., **HAPY** compounds have been reported as excellent HNO precursors with various half-lives. Pyrazolones have been shown to be efficient leaving groups and also are edaravone derivatives. Edaravone (Scheme 1-13) is a potent antioxidant, and is currently in clinical use for treatment of stroke and cardiovascular diseases.[107,108] Also, as discussed in section 1.2.6., hydrolysis of nitrosocarbonyls is an efficient pathway for HNO generation. Nitrosocarbonyl compounds are important intermediates not only for HNO release, but also as an intermediate that can be used in different synthetic procedures. Here, we have designed and synthesized two novel classes of nitrosocarbonyl precursors, *N*- and *O*-substituted hydroxamic acids with pyrazolone leaving groups (**NHPY** and **OHPY**

compounds, Scheme 1-13).[109,110] These compounds generate nitrosocarbonyls under physiological conditions, which subsequently produce HNO. In addition to gas chromatographic (GC) analysis to quantify the amount of N_2O produced, we have applied ^1H NMR spectroscopy to monitor the decomposition of our newly developed donors at physiological pH and temperature. For the first time, we have found that pyrazolones are efficient nitrosocarbonyl traps, undergoing an *N*-selective nitrosocarbonyl aldol reaction. This trapping reaction has been used to confirm the involvement of nitrosocarbonyls as intermediates in the observed chemistry. Additionally, we have shown that **NHPY** compounds generate nitrosocarbonyls under mild basic conditions in organic solvent, and may therefore also enjoy synthetic utility.

Scheme 1-13. Nitrosocarbonyl Release from NHPY and OHPY Compounds

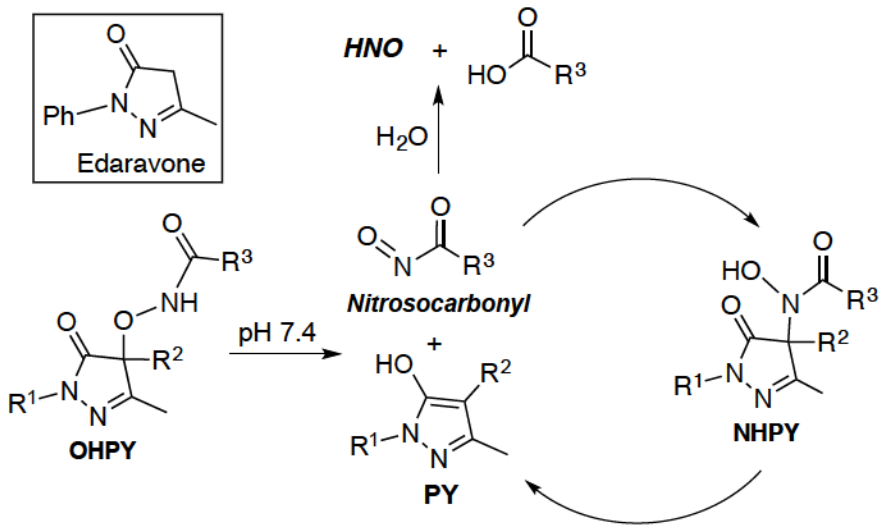

As mentioned in section 1.2.7, the reactivity of photogenerated nitrosocarbonyl intermediates was previously studied by TRIR spectroscopy, reporting on the photogeneration of these reactive compounds with characteristic IR bands around 1735 cm^{-1} from 9,10-dimethylanthracene adducts and 1,2,4-oxadiazole-4-oxide.[47] Given our observation that pyrazolones are excellent nitrosocarbonyl traps in both aqueous and organic solutions,[109,110] we tried to examine this reaction by TRIR spectroscopy and compare that to the reaction with amines. Since the nature of the nitrosocarbonyl intermediate RC(O)N=O (R = Me, OMe, and NMe_2) has a significant effect on its reactivity, we hope to clarify the relative reactivity of different nitrosocarbonyl intermediates by examining their reactions with amines and pyrazolones by TRIR spectroscopy.

1.4. References

(1) Palmer, R. M.; Ferrige, A. G.; Moncada, S. *Nature.* **1987**, *327*, 524–526.

(2) Moncada, S.; Palmer, R. M. J.; Higgs, E. A. *Pharmacol. Rev.* **1991**, *43*, 109–142.

(3) Li, L.; Hsu, A.; Moore, P. K. *Pharmacol. Ther.* **2009**, *123*, 386–400.

(4) Calabrese, V.; Cornelius, C.; Rizzarelli, E.; Owen, J. B.; Dinkova-Kostova, A. T.; Butterfield, D. A. *Antioxid. Redox Signal.* **2009**, *11*, 2717–2739.

(5) Fukuto, J. M.; Bartberger, M. D.; Dutton, A. S.; Paolocci, N.; Wink, D. A.; Houk, K. N. *Chem. Res. Toxicol*. **2005**, *18*, 790–801.

(6) Miranda, K. M.; Espey, M. G.; Jourd'heuil, D.; Grisham, M. B.; Fukuto, J. M.; Feelisch, M.; Wink, D. A. The chemical biology of nitric oxide. In Nitric Oxide Biology and Pathobiology; Ignarro, L. J., Ed.; Academic Press: San Diego, 2000; Chapter 3, pp 41–55.

(7) Paolocci, N.; Saavedra, W. F.; Miranda, K. M.; Martignani, C.; Isoda, T.; Hare, J. M.; Espey, M. G.; Fukuto, J. M.; Feelisch, M.; Wink, D. A.; Kass, D. A. *Proc. Natl. Acad. Sci. U.S.A.* **2001**, *98*, 10463–10468.

(8) Paolocci, N.; Katori, T.; Champion, H. C.; St. John, M. E.; Miranda, K. M.; Fukuto, J. M.; Wink, D. A.; Kass, D. A. *Proc. Natl. Acad. Sci. U.S.A.* **2003**, *100*, 5537–5542.

(9) Paolocci, N.; Jackson, M. I.; Lopez, B. E.; Miranda, K.; Tocchetti, C. G.; Wink, D. A.; Hobbs, A. J.; Fukuto, J. M. *Pharmacol. Ther.* **2007**, *113*, 442–458.

(10) Tocchetti, C. G.; Wang, W.; Froehlich, J. P.; Huke, S.; Aon, M. A.; Wilson, G. M.; Di Benedetto, G.; O'Rourke, B.; Gao, W. D.; Wink, D. A.; Toscano, J. P.; Zaccolo,

M.; Bers, D. M.; Valdivia, H. H.; Cheng, H.; Kass, D. A.; Paolocci, N. *Circ. Res.* **2007**, *100*, 96–104.

(11) Froehlich, J. P.; Mahaney, J. E.; Keceli, G.; Pavlos, C. M.; Goldstein, R.; Redwood, A. J.; Sumbilla, C.; Lee, D. I.; Tocchetti, C. G.; Kass, D. A.; Paolocci, N.; Toscano, J. P. *Biochemistry* **2008**, *47*, 13150–13152.

(12) Sakai, N.; Kaufman, S.; Milstein, S. *Mol. Pharmacol*. **1993**, *43*, 6–10.

(13) Adak, S.; Wang, Q.; Stuehr, D. J. *J. Biol. Chem*. **2000**, *275*, 33554–33561.

(14) Choe, C.-u.; Lewerenz, J.; Fischer, G.; Uliasz, T. F.; Espey, M. G.; Hummel, F. C.; King, S. B.; Schwedhelm, E.; Böger, R. H.; Gerloff, C.; Hewett, S. J.; Magnus, T.; Donzelli, S. *J. Neurochem*. **2009**, *110*, 1766–1773.

(15) Murphy, M. E.; Sies, H. *Proc. Natl. Acad. Sci. U.S.A*. **1991**, *88*, 10860–10864.

(16) Filipovic, M. R.; Miljkovic, J. L.; Nauser, T.; Royzen, M.; Klos, K.; Shubina, T.; Koppenol, W. H.; Lippard, S. J.; Ivanović-Burmazović, I. *J. Am. Chem. Soc*. **2012**, *134*, 12016–12027.

(17) King, B.; Miao, Z. *Nitric Oxide* **2016**, *57*, 1–14.

(18) Shafirovich, V.; Lymar, S. V. *Proc. Natl. Acad. Sci. U.S.A.* **2002**, *99*, 7340–7345.

(19) Bartberger, M. D.; Liu, W.; Ford, E.; Miranda, K. M.; Switzer, C.; Fukuto, J. M.; Farmer, P. J.; Wink, D. A.; Houk, K. N. *Proc. Natl. Acad. Sci. U.S.A.* **2002**, *99*, 10958–10963.

(20) Orgel, L. E. *J. Chem. Soc.* **1953**, 1276–1278.

(21) Walsh, A. D. *J. Chem. Soc.* **1953**, 2266–2288.

(22) Szmytkowski, C.; Maciag, K. *J. Phys. B: At. Mol. Phys.* **1991**, 4273–4279.

(23) Tennyson, J. *J. Phys. B: At. Mol. Phys.* **1986**, *19*, 4025–4033.

(24) Doyle, M. P.; Mahapatro, S. N.; Broene, R. D.; Guy, J. K. *J. Am. Chem. Soc.* **1988**, *110*, 593–599.

(25) Wong, P. S. Y.; Hyun, J.; Fukuto, J. M.; Shirota, F. N.; DeMaster, E. G.; Shoeman, D. W.; Nagasawa, H. T. *Biochemistry* **1998**, *37*, 5362–5371.

(26) Filipovic, M. "HNO-Thiol Relationship" In *The Chemistry and Biology of Azanone (HNO)*; Marti, M.A., Doctorovich, F., Farmer, P., Eds; Elsevier, **2016**, 105–126.

(27) Guthrie, D. A.; Ho, A.; Takahashi, C. G.; Collins, A.; Morris, M.; Toscano, J. P. *J. Org. Chem.* **2015**, *80*, 1338–1348.

(28) Guthrie, D. A.; Nourian, S.; Takahashi, C. G.; Toscano, J. P. *J. Org. Chem.* **2015**, *80*, 1349–1356.

(29) Guthrie, D. A.; Nourian, S.; Toscano, J. P. "Hydroxylamines with Organic-Based Leaving Groups as HNO Donors." In *The Chemistry and Biology of Azanone (HNO)*; Marti, M.A., Doctorovich, F., Farmer, P., Eds; Elsevier, **2016**, 37–51.

(30) Bazylinski, D. A.; Hollocher, T. C. *J. Am. Chem. Soc.* **1985**, *107*, 7982–6.

(31) Farmer, P. J.; Sulc, F. *J. Inorg. Biochem.* **2005**, 99, 166–184.

(32) Sulc, F.; Immoos, C. E.; Pervitsky, D.; Farmer, P. J. *J. Am. Chem. Soc.* **2004**, *126*, 1096–1101.

(33) Immoos, C. E.; Sulc, F.; Farmer, P. J.; Czarnecki, K.; Bocian, D. F.; Levina, A.; Aitken, J. B.; Armstrong, R. S.; Lay, P. A. *J. Am. Chem. Soc.* **2005**, *127*, 814–815.

(34) Murphy, M. E.; Sies, H. *Proc. Natl. Acad. Sci. U.S.A.* **1991**, *88*, 10860–10864.

(35) Marti, M. A.; Bari, S. E.; Estrin, D. A.; Doctorovich, F. *J. Am. Chem. Soc.* **2005**, *127*, 4680–4684.

(36) Angeli, A. *Gazz. Chim. Ital.* **1896**, *26*, 17–25.

(37) Piloty, O. *Ber. Dtsch. Chem. Ges.* **1896**, *29*, 1559–1567.

(38) Miranda, K. M.; Katori, T.; Torres de Holding, C. L.; Thomas, L.; Ridnour, L. A.; McLendon, W. J.; Cologna, S. M.; Dutton, A. S.; Champion, H. C.; Mancardi, D.; Tocchetti, C. G.; Saavedra, J. E.; Keefer, L. K.; Houk, K. N.; Fukuto, J. M.; Kass, D. A.; Paolocci, N.; Wink, D. A. *J. Med. Chem.* **2005**, *48*, 8220–8228.

(39) Salmon, D. J.; Torres de Holding, C. L.; Thomas, L.; Peterson, K. V.; Goodman, G. P.; Saavedra, J. E.; Srinivasan, A.; Davies, K. M.; Keefer, L. K.; Miranda, K. M. *Inorg. Chem.* **2011**, *50*, 3262–3270.

(40) Sha, X.; Isbell, T. S.; Patel, R. P.; Day, C. S.; King, S. B. *J. Am. Chem. Soc.* **2006**, *128*, 9687–9692.

(41) Shoman, M. E.; DuMond, J. F.; Isbell, T. S.; Crawford, J. H.; Brandon, A.; Honovar, J.; Vitturi, D. A.; White, C. R.; Patel, R. P.; King, S. B. *J. Med. Chem.* **2011**, *54*, 1059–1070.

(42) Shoeman, D. W.; Shirota, F. N.; DeMaster, E. G.; Nagasawa, H. T. *Alcohol* **2000**, *20*, 55–59.

(43) DeMaster, E. G.; Redfern, B.; Nagasawa, H. T. *Biochem. Pharmacol.* **1998**, *55*, 2007–2015.

(44) Nagasawa, H. T.; DeMaster, E. G.; Redfern, B.; Shirota, F. N.; Goon, D. J. W. *J. Med. Chem.* **1990**, *33*, 3120–3122.

(45) Shirota, F. N.; Goon, D. J. W.; DeMaster, E. G.; Nagasawa, H. T. *Biochem. Pharmacol.* **1996**, *52*, 141–147.

(46) Corrie, J. E. T.; Kirby, G. W.; Mackinnon, J. W. M. *J. Chem. Soc., Perkin Trans. 1* **1985**, 883–886.

(47) Cohen, A. D.; Zeng, B. B.; King, S. B.; Toscano, J. P. *J. Am. Chem. Soc.* **2003**, *125*, 1444–1445.

(48) Hughes, M.N.; Wimbledon, P.E. *J. Chem. Soc., Dalton Trans.* **1976**, 703–707.

(49) Maragos, C.M.; Morley, D.; Wink, D.A.; Dunams, T.M.; Saavedra, J.E.; Hoffman, A.; Bove, A. A.; Isaac, L.; Hrabie, J. A.; Keefer, L. K. *J. Med. Chem.* **1991**, *34*, 3242–3247.

(50) Basudhar, D.; Bharadwaj, G.; Salmon, D.J.; Miranda, K.M. "HNO Donors: Angeli's Salt and Related Diazeniumdiolates" In *The Chemistry and Biology of Azanone (HNO)*; Marti, M.A., Doctorovich, F., Farmer, P., Eds; Elsevier, **2016**, 11-36.

(51) Dutton, A. S.; Fukuto, J. M.; Houk, K. N. *J. Am. Chem. Soc.* **2004**, *126*, 3795–3800.

(52) Hansen, T. J.; Croisy, A. F.; Keefer, L. K. *IARC Sci Publ* **1982**, *41*, 21–29.

(53) Keefer, L. K.; Flippen-Anderson, J. L.; George, C.; Shanklin, A. P.; Dunams, T. M.; Christodoulou, D.; Saavedra, J. E.; Sagan, E. S.; Bohle, D. S. *Nitric Oxide* **2001**, *5*, 377–394.

(54) Davies, K. M.; Wink, D. A.; Saavedra, J. E.; Keefer, L. K. *J. Am. Chem. Soc.* **2001**, *123*, 5473–5481.

(55) Hrabie, J. A.; Klose, J. R.; Wink, D. A.; Keefer, L. K. *J. Org. Chem.* **1993**, *58*, 1472–1476.

(56) Bonner, F.T.; Ko, Y. *Inorg. Chem.* **1992**, *31*, 2514–2519.

(57) Zamora, R.; Grzesiok, A.; Weber, H.; Feelisch, M. *Biochem. J.* **1995**, *312*, 333–339.

(58) Exner, O.; Juska, T. *Collect Czech Chem Commun* **1984**, *49*, 51–57.

(59) Exner O. *Collect Czech Chem Commun* **1964**, *29*, 1337–1343.

(60) Sirsalmath, K.; Suarez, S. A.; Bikiel, D. E.; Doctorovich, F. *J. Inorg. Biochem.* **2013**, *118*, 134–139.

(61) Zamora, R.; Grzesiok, A.; Weber, H.; Feelisch, M. *Biochem J* **1995**, *312*, 333–339.

(62) Toscano, J. P.; Brookfield, F. A.; Cohen, A. D.; Courtney, S. M.; Frost, L. M.; Kalish, V. J. *N*-Hydroxylsulfonamide derivatives as new physiologically useful nitroxyl donors. US0080330356.

(63) Porcheddu, A.; De Luca, L.; Giacomelli, G. A *Synlett* **2009**, *13*, 2149–2153.

(64) Aizawa, K.; Nakagawa, H.; Matsuo, K.; Kawai, K.; Ieda, N.; Suzuki, T., Miyata, N. *Bioorganic Med Chem Lett* **2013**, *23*, 2340–2343.

(65) Sha, X.; Isbell, T. S.; Patel, R. P.; Day, C. S.; King, S. B. *J. Am. Chem. Soc.* **2006**, *128*, 9687–9692.

(66) Shoman, M. E.; DuMond, J. F.; Isbell, T. S.; Crawford, J. H.; Brandon, A.; Honovar, J.; Vitturi, D. A.; White, C. R.; Patel, R. P.; King, S. B. *J. Med. Chem.* **2011**, *54*, 1059–1070.

(67) Nagasawa, H. T.; Lee, M. J.; Kwon, C. H.; Shirota, F. N.; DeMaster, E. G. *Alcohol* **1992**, *9*, 349–353.

(68) Pihlaja, K.; Matti, S. *Acta Chem Scand* **1968**, *22*, 3053–3062.

(69) King, S. B.; Nagasawa, H. T. *Methods Enzymol.* **1999**, *301*, 211–220.

(70) Atkinson, R. N.; Storey, B. M.; King, S. B. *Tetrahedron Lett.* **1996**, *37*, 9287–9290.

(71) Kirby, G. W.; Sweeny, J. G. *J. Chem. Soc. Perkin Trans. 1* **1981**, 3250–3254.

(72) Kirby, G. W.; Sweeny, J. G. *J. Chem. Soc., Chem. Commun.* **1973**, 704–705.

(73) Dao, L. H.; Dust, J. M.; Mackay, D.; Watson, K. N. *Can. J. Chem.* **1979**, *57*, 1712–1719.

(74) Jenkins, N. E.; Ware, R. W.; Atkinson, R. N.; King, S. B. *Synth. Commun.* **2000**, *30*, 947–953.

(75) Zeng, B; Huang, J.; Wright, M. W.; King, S. B. *Bioorg. Med. Chem.* **2004**, *14*, 5565–5568.

(76) Quadrelli, P.; Invernizzi, A. G.; Caramella, P. *Tetrahedron Lett.* **1996**, *37*, 1909–1912.

(77) Quadrelli, P.; Mella, M.; Caramella, P. *Tetrahedron Lett.* **1998**, *39*, 3233–3236.

(78) Quadrelli, P.; Mella, M.; Caramella, P. *Tetrahedron Lett.* **1999**, *40*, 797–800.

(79) O'Bannon, P. E.; William, D. P. *Tetrahedron Lett.* **1988**, *29*, 5719–5722.

(80) O'Bannon, P. E.; Dailey, W. P. *J. Org. Chem.* **1989**, *54*, 3096–3101.

(81) Chemagin, A. V.; Yashin, N. V.; Grishin, Y. K.; Kuznetsova, T. S.; Zefirov, N. S. *Synthesis* **2010**, 259–266.

(82) So, S. S.; Mattson, A. E. *J. Am. Chem. Soc.* **2012**, *134*, 8798–8801.

(83) Sutton, A. D.; Williamson, M.; Weismiller, H.; Toscano, J. P. *Org. Lett.* **2012**, *14*, 472–475.

(84) Evans, A. S.; Cohen, A. D.; Gurard-Levin, Z. A.; Kebede, N.; Celius, T. C.; Miceli, A. P.; Toscano, J. P. Can. J. Chem. 2010, 89, 130–138.

(85) Kirby, G. W.; McGuigan, H.; Mackinnon, J. W. M.; McLean, D.; Sharma, R. P. *J. Chem. Soc. Perkin Trans. I.* **1985**, 1437–1442.

(86) Ritter, A. R.; Miller, M. J. *J. Org. Chem.* **1994**, *59*, 4602–4611.

(87) Streith, J.; Defoin, A. *Synthesis* **1994**, *1994*, 1107–1117.

(88) Vogt, P. F.; Miller, M. J. *Tetrahedron* **1998**, *54*, 1317–1348.

(89) Frazier, C. P.; Engelking, J. R.; Read de Alaniz, J. *J. Am. Chem. Soc.* **2011**, *133*, 10430–10433.

(90) Fakhruddin, A.; Iwasa, S.; Nishiyama, H.; Tsutsumi, K. *Tetrahedron Lett.* **2004**, *45*, 9323–9326.

(91) Yamamoto, Y.; Yamamoto, H. *European J. Org. Chem.* **2006**, *2006*, 2031–2043.

(92) Chaiyaveij, D.; Cleary, L.; Batsanov, A. S.; Marder, T. B.; Shea, K. J.; Whiting, A. *Org. Lett.* **2011**, *13*, 3442–3445.

(93) Sandoval, D.; Frazier, C. P.; Bugarin, A.; Read de Alaniz, J. *J. Am. Chem. Soc.* **2012**, *134*, 18948–18951.

(94) Baidya, M.; Griffin, K. A.; Yamamoto, H. *J. Am. Chem. Soc.* **2012**, *134*, 18566–18569.

(95) Selig, P. *Angew. Chemie Int. Ed.* **2013**, *52*, 7080–7082.

(96) Palmer, L.; Frazier, C.; Read de Alaniz, J. *Synthesis.* **2013**, *46*, 269–280.

(97) Baidya, M.; Yamamoto, H. *Synthesis.* **2013**, *45*, 1931–1938.

(98) Frazier, C. P.; Sandoval, D.; Palmer, L. I.; Read de Alaniz, J. *Chem. Sci.* **2013**, *4*, 3857–3862.

(99) Yang, W.; Huang, L.; Yu, Y.; Pflasterer, D.; Rominger, F.; Hashmi, S. K. *Chem. Eur. J.* **2014**, *20*, 3927–3931.

(100) Yu, C.; Song, A.; Zhang, F. Wang, W. *ChemCatChem.* **2014**, *6*, 1863–1865.

(101) Sandoval, D.; Samoshin, A. V; Read de Alaniz, J. *Org. Lett.* **2015**, *17*, 4514–4517.

(102) Ramakrishna, I.; Grandhi, G. S.; Sahoo, H.; Baidya, M. *Chem. Commun.* **2015**, *51*, 13976–13979.

(103) Maji, B.; Yamamoto, H. *Angew. Chem.* **2014**, *126*, 14700–14703.

(104) Maji, B.; Yamamoto, H. *Bull. Chem. Soc. Jpn.* **2015**, *88*, 753–762.

(105) Xu, C.; Zhang, L.; Luo, S. *Angew. Chem. Int. Ed.* **2014**, *53*, 4149–4153.

(106) Merino, P.; Tejero, T.; Delso, I.; Matute, R. *Synthesis* **2016**, *48*, 653–676.

(107) Higashi, Y.; Jitsuiki, D.; Chayama, K.; Yoshizumi, M. *Recent Pat. Cardiovasc. Drug Discovery* **2006**, *1*, 85–93.

(108) Watanabe, T.; Tahara, M.; Todo, S. *Cardiovasc. Ther*. **2008**, *26*, 101–114.

(109) Nourian, S.; Zilber, Z. A.; Toscano, J. P. *J. Org. Chem.* **2016**, *81*, 9138–9146.

(110) Nourian, S.; Lesko, R. P.; Guthrie, D. A.; Toscano, J. P. *Tetrahedron* **2016**, *72*, 6037–6042.

Chapter 2.

Development of *N*-Substituted Hydroxamic Acids with Pyrazolone Leaving Groups as Nitrosocarbonyl Precursors

2.1. Abstract

A novel class of nitrosocarbonyl precursors, *N*-substituted hydroxamic acids with pyrazolone leaving groups (**NHPY**), has been synthesized. Under physiological conditions, these compounds generate nitrosocarbonyl intermediates, which upon hydrolysis release nitroxyl (azanone, HNO) in excellent yields. The amount and rate of nitrosocarbonyl generation are dependent on the nature of the pyrazolone leaving groups and significantly on the structural properties of the **NHPY** donors. Pyrazolones have been found to be efficient nitrosocarbonyl traps, undergoing an *N*-selective nitrosocarbonyl aldol reaction. This trapping reaction has been used to confirm the involvement of nitrosocarbonyl intermediates in **NHPY** aqueous decomposition. In addition, **NHPY** compounds are shown to generate

nitrosocarbonyls efficiently under mild basic conditions in organic solvent, and may therefore also enjoy synthetic utility.

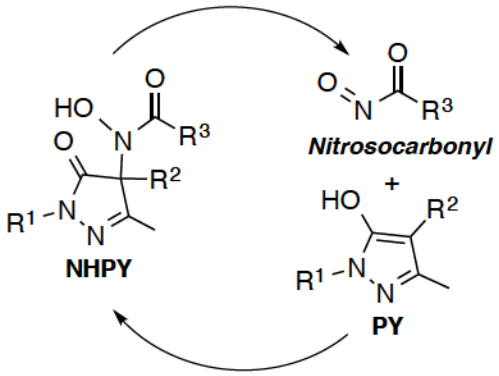

2.2. Introduction

Nitroxyl (azanone, HNO) is the one-electron reduced and protonated relative of nitric oxide (NO) that has recently been proposed as a potential alternative to current treatments for cardiac failure.[1-9] HNO possesses unique physiological properties that affect vasorelaxation and enhancement of cardiac contractility, and may also find use in the treatment of alcoholism and cancer.[8-9]

HNO is a very reactive molecule that spontaneously dimerizes to yield hyponitrous acid (HON=NOH), which subsequently dehydrates to nitrous oxide (N_2O).[10] Because of this inherent chemical reactivity, donors are needed for the generation and study of HNO. Angeli's salt (**AS**, Figure 2-1) is a well known HNO donor with a relatively short half-life of 2-3 min under physiological conditions.[11] Accessing other HNO donors with different release rates under physiological conditions is important to assess the impact that HNO may potentially have on the treatment of diseases. Piloty's acid (**PA**) derivatives,[12] acyloxy nitroso (**AcON**) compounds,[13] (hydroxylamino)pyrazolone (**HAPY**),[14,15a] and

(hydroxylamino)barbituric acid (**HABA**) derivatives[16] (Figure 2-1), are among a limited number of physiologically compatible HNO donors with tunable half-lives that have been reported.[17-19] Continued efforts are required to develop other potential HNO donors that can be used under physiological conditions.

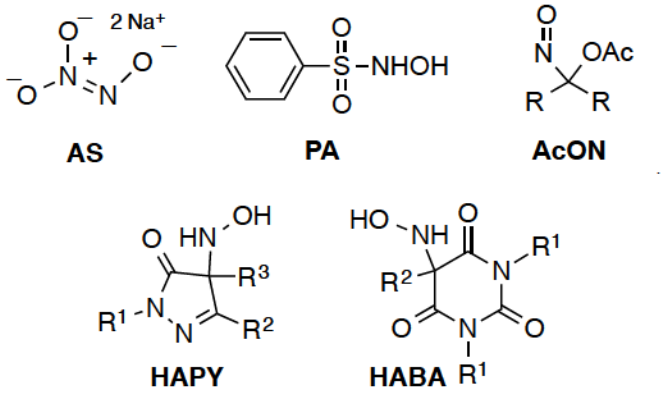

Figure 2-1. Representative examples of HNO donors.

One approach that has been used to generate HNO is based on the hydrolysis of nitrosocarbonyl intermediates.[20] Nitrosocarbonyls are transient electrophiles that can react with nucleophiles including water to release HNO. These intermediates can be generated by a variety of chemical processes including oxidation of hydroxamic acids, thermal fragmentation of Diels-Alder adducts,[21-23] photocleavage of 1,2,4-oxadiazole-4-oxides,[24] and the rearrangement of nitrocarbenes.[25-28] In general, these methods are not suitable for HNO generation under physiological conditions. Notable among compounds reported to generate HNO through nitrosocarbonyl hydrolysis are *N,O*-bis-acylated derivatives such as *N,O*-dibenzoyl-*N*-hydroxycyanamide that release HNO under enzymatic or basic conditions.[29] Based on this initial work, we reported modified *N,O*-bis-acylated

hydroxylamine derivatives with arenesulfonyl leaving groups that produce nitrosocarbonyls nonenzymatically under physiological conditions.[17] Mechanistic studies revealed that the chemistry of these donors is complicated, and that non-HNO producing pathways (acyl migration and amide hydrolysis) can be dominant. Nitrosocarbonyls have been used as important components in a variety of synthetic approaches.[30-50] Aerobic oxidation of hydroxamic acids under mild conditions that avoid overoxidation of products has been used to generate nitrosocarbonyl intermediates.[33-50] These reactive species can also be generated via metal catalysis and have been extensively utilized in ene reactions, Diels-Alder reactions, or as electrophiles in nitrosocarbonyl aldol reactions.

Herein, we report a new class of nitrosocarbonyl donors that decompose based on the general strategy shown in Scheme 2-1. *N*-Substituted hydroxamic acids with pyrazolone leaving groups (**NHPY**, shown in Scheme 2-2) are efficient nitrosocarbonyl donors that upon *O*-deprotonation and loss of HX (HX = pyrazolone) generate nitrosocarbonyl intermediates either under physiological conditions or in basic organic solvent. In aqueous solutions, subsequent hydrolysis of the nitrosocarbonyl (Path A) generates a carboxylic acid and HNO in excellent yield. In organic solution, as has been elegantly demonstrated in recent reports,[37,39,40,44-46,49] nitrosocarbonyl intermediates can react with nucleophiles at the nitrogen of the nitroso group through an *N*-selective nitrosocarbonyl aldol reaction (Path B) to produce *N*-substituted hydroxamic acid adducts. We have observed this same reactivity using pyrazolone traps that have also been used to confirm nitrosocarbonyl generation upon **NHPY** decomposition.

Scheme 2-1. Reactivity of *N*-Substituted Hydroxamic Acids with Good Leaving Groups X

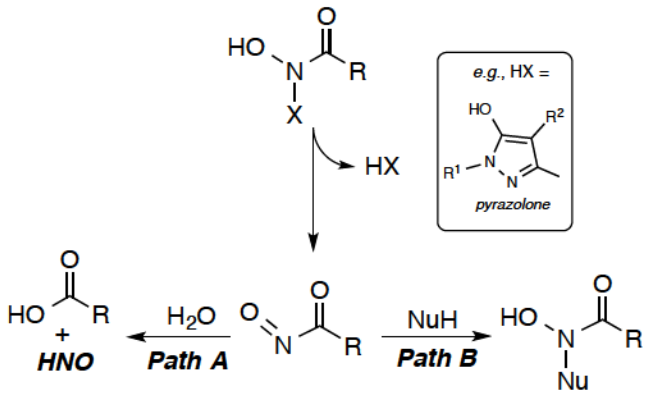

On the basis of previously reported **HAPY** donors,[14,15a] pyrazolones have been shown to be efficient leaving groups with the rate of **HAPY** decomposition dependent on the nature of the pyrazolone. This observation was utilized to design **HAPY** donors with varying half-lives. In this report, we demonstrate that the rate of nitrosocarbonyl generation from **NHPY** compounds depends both on the nature of the leaving groups and also unexpectedly on the structural properties of the substituted hydroxylamino group as discussed in detail below.

2.3. Result and Discussion

2.3.1. Synthesis

We have developed two general methodologies for the synthesis of **NHPY** derivatives: (1) the reaction of the corresponding brominated pyrazolone (Br-PY) with an *O*-*tert*-butoxycarbonyl protected hydroxamic acid, followed by subsequent acid deprotection (Scheme 2-2, method A); and (2) an *N*-selective nitrosocarbonyl aldol reaction initiated by oxidation of hydroxamic acids in the presence of

pyrazolones (Scheme 2-2, method B). A 50% v/v aqueous ethanol solution enhances the solubility of reactants and potassium carbonate is used to adjust the pH of solution in the range of 7-8 to favor nitrosocarbonyl reaction with the deprotonated pyrazolone.

Scheme 2-2. Strategies for the Synthesis of NHPY Derivatives

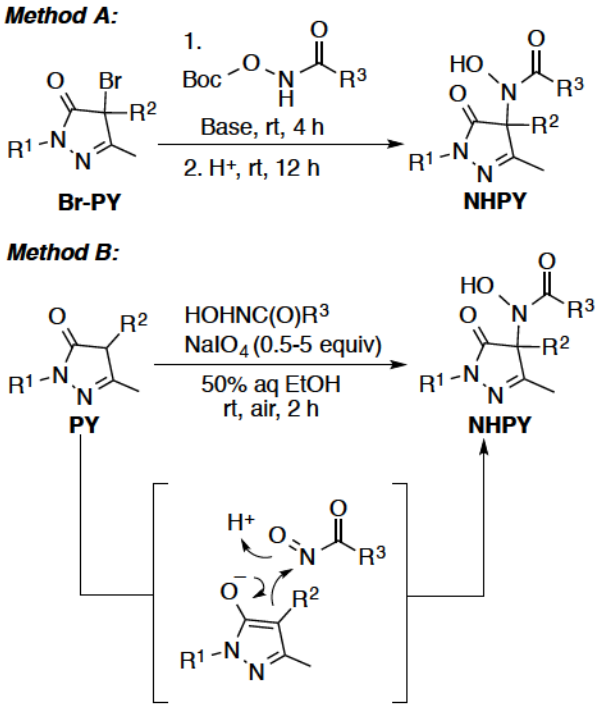

We first synthesized **NHPY** donors **1a-b** using the two described methods; yields are reported in Table 2-1. Method A provides **1a-b** in very poor yields, whereas the nitrosocarbonyl aldol reaction affords these precursors in much higher yields (73%-75%). The synthesis of donors **1c-d** via either of two methods resulted in moderate to good yields (48%-71%). Methods A and B gave donors **1e-g** in low to moderate yields (11%-48%). The nitrosocarbonyl aldol reaction (method B) is straightforward, single pot, and scalable; donor **1a** can be prepared on a gram scale

under conditions identical to a 100 mg scale without any significant loss in isolated yield. For future studies, it may be possible to expand this synthetic route to other active enolates that may undergo further synthetic manipulation.

Table 2-1. Synthetic Yields for NHPY Donors

NHPY	R^1	R^2	R^3	% Yield Method A	% Yield Method
1a	Ph	C(=NOMe)Me	Me	<10	73
1b	Me	C(=NOMe)Me	Me	<10	75
1c	Ph	C(=NOMe)Me	OMe	48	71
1d	Me	C(=NOMe)Me	OMe	50	69
1e	Ph	C(=NOMe)Me	NMe_2	35	48
1f	Me	C(=NOMe)Me	NMe_2	38	47
1g	Ph	Me	NMe_2	11	48

2.3.2. Decomposition under Physiological Conditions

HNO generation following decomposition of the synthesized **NHPY** donors under physiological conditions was explored. Presumably, upon deprotonation of oxygen, a nitrosocarbonyl intermediate and pyrazolone byproduct are formed (Scheme 2-3). As described above, the reactions of nitrosocarbonyls and pyrazolones can be efficient, and therefore there is a competition between the reverse reaction to produce the initial **NHPY** compound and hydrolysis of the nitrosocarbonyl intermediate to generate HNO.

Scheme 2-3. HNO Release Pathway from NHPY Donors

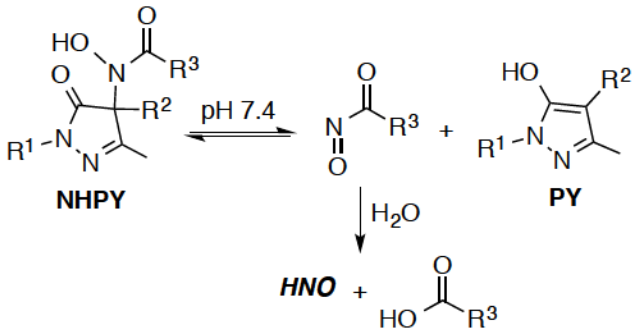

We have recently used ^{1}H NMR spectroscopy to measure half-lives of donor decomposition by quantifying donor and pyrazolone byproduct as a function of time.[15,16] Based on the distinctive chemical shifts of the methyl groups of the **NHPY** donors and the pyrazolone byproducts, the decomposition of the donors and release of byproducts is easily monitored. Utilizing this assay, the half-lives of **NHPY** donors were determined under physiologically relevant conditions (Table 2-2).

Table 2-2. Half-lives and HNO Yields for NHPY Donors

NHPY	R¹	R²	R³	$t_{1/2}$[a]	% HNO[c]
1a	Ph	C(=NOMe)Me	Me	5 days	82[d]
1b	Me	C(=NOMe)Me	Me	Stable[b]	-
1c	Ph	C(=NOMe)Me	OMe	2 days	104[d]
1d	Me	C(=NOMe)Me	OMe	4 days	94[d]
1e	Ph	C(=NOMe)Me	NMe_2	25 min	> 95[e]
1f	Me	C(=NOMe)Me	NMe_2	46 min	> 95[e]
1g	Ph	Me	NMe_2	Stable[b]	-

[a]Determined from ^{1}H NMR analysis of the decomposition of 5 mM of the donor in 10% DMSO-d_6, 10% D_2O, and 80% H_2O, phosphate buffer (0.25 M) with DTPA (0.2 mM), pH 7.4 at 37 °C under argon. [b] Less than 5% decomposition after 2 days. [c] Donors (0.1 mM) were incubated in phosphate buffer (0.25 M) with DTPA (0.2 mM), pH 7.4 at 37 °C under argon. HNO yields are measured either (d) at the half-life of the donor or (e) after complete decomposition of the donor and are reported relative to the standard HNO donor, Angeli's salt, as determined by N_2O headspace analysis (SEM ± 5%; n = 3).

Based on our previous studies of **HAPY** donors,[15a] we investigated the effect of the leaving group on **NHPY** donor half-life. As expected, we observe a substantial impact on half-life that is related to the pK_a values of the respective pyrazolone byproducts. For example, pyrazolone **2a** (R^1 = Ph, R^2 = C(=NOMe)Me) has a pK_a of 6, making it anionic under physiological conditions and consequently a better leaving group compared with pyrazolone **2c** (R^1 = Ph, R^2 = Me) which has a pK_a of 7.6.[15a] Accordingly, when R^2 is changed from an *O*-methyloxime group (donors **1e-f**) to a methyl group (donor **1g**) the observed half-life increases dramatically from tens of minutes to days (Table 2-2). Exchanging the R^1 group from phenyl to methyl also has a small effect on half-life, consistent with that previously reported for **HAPY** donors.[15a] Further exploration of **NHPY** derivatives revealed that the R^3 group has a surprisingly large effect on half-life (Table 2-2). The origin of this unexpected effect is examined in more detail below.

Dimerization of HNO and subsequent dehydration provides N_2O, which is a common benchmark for HNO production.[10] Using Angeli's salt as a standard, the relative amounts of N_2O released from the **NHPY** donors were measured via gas chromatography headspace analysis following incubation in pH 7.4 phosphate buffer solutions containing the metal chelator, diethylenetriaminepentaacetic acid (DTPA), at 37 ˚C under argon. In all examples (Table 2-2), we find that the **NHPY** compounds are excellent HNO donors, even for the very long-lived donors (**1a** and **1c-d**). HNO was confirmed as the source of N_2O from donor **1e** by membrane inlet mass spectrometry (MIMS), which is a useful technique to detect dissolved gases, including HNO, directly in aqueous solutions (Supporting Information).[51,52]

2.3.3. Mechanistic Studies

Pyrazolone **2c** has been shown to be an effective trap for HNO and nitrosocarbonyl intermediates under physiological conditions.[15] Our proposed mechanism for the decomposition of the **NHPY** class of HNO donors involves initial oxygen deprotonation followed by formation of a nitrosocarbonyl intermediate. Further hydrolysis of this reactive species generates HNO. Based on analogy with HNO and recent reports of nitroso aldol and nitrosocarbonyl aldol reactions,[15,16,37,39,40,44,46,48-50,53] we examined nitrosocarbonyl aldol reaction using pyrazolone **2c** as an efficient trap for nitrosocarbonyls (Scheme 2-4).

Donor **1e** was incubated in the presence of pyrazolone **2c** and the reaction was followed by ^{1}H NMR spectroscopy in pH 7.4 phosphate buffer at 37 °C (Supporting Information). Upon decomposition of donor **1e**, we observe efficient trapping of the nitrosocarbonyl intermediate by pyrazolone **2c** through an *N*-selective nitrosocarbonyl aldol reaction to generate **NHPY 1g**.

Scheme 2-4. Nitrosocarbonyl Trapping by Pyrazolone 2c

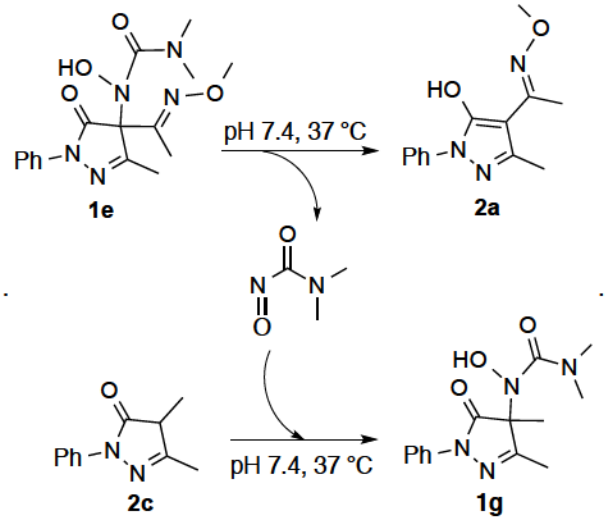

Although the above findings strongly suggest the formation of a nitrosocarbonyl intermediate, based on Glover's extensive reactivity studies of *bis*-heteroatom-substituted amides,[54] attack of pyrazolone **2c** at the amide nitrogen of the hydroxamic acid moiety of donor **1e** to form **NHPY 1g** directly may be possible. To eliminate this possibility, *O*-methylated **NHPY 1** was synthesized and its stability in the presence of pyrazolone **2c** was confirmed by ^{1}H NMR spectroscopy (Scheme 2-5).

Scheme 2-5. Possible Reaction of *O*-Methylated NHPY 1 with Pyrazolone 2c

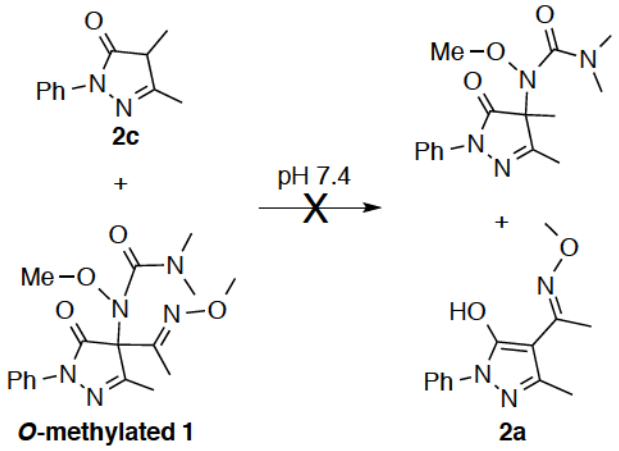

2.3.4. Stability Studies

As described previously, decomposition analysis of **NHPY** compounds revealed a surprisingly strong dependence of the R^3 group on donor stability. Donors **1a** (R^3 = Me), **1c** (R^3 = OMe), and **1e** (R^3 = NMe_2) all have the same pyrazolone leaving group, but decompose with dramatically different half-lives of 5 days, 2 days, and 25 min, respectively.

Our previous studies determined that **HAPY** decomposition rates are correlated with donor pK_a, confirming a very low barrier for decomposition once the oxyanion is formed.[15a,55] To determine if the R^3 group has an unexpected impact on the pK_a values of **NHPY** compounds, we evaluated the pK_a of donors **1a**, **1c**, and **1e**. Decomposition of donor **1e** was monitored by examining the growth of the anionic pyrazolone byproduct **2a** (λ = 265 nm) at pH 7.4 and 37 °C in phosphate buffer as a function of pH (Figure 2-2).[14,15a] The decomposition rate is pH-dependent, and based on the experimental kinetic data, the pK_a of donor **1e** is estimated to be 10.7. Under these conditions, donor **1c** decomposes slowly, and donor **1a** is observed to be stable for 1 h. Thus, we measured the pK_a values of donor **1a** (10.0) and **1c** (9.1) in 50% (v/v) aqueous ethanol by titration with NaOH solution. These measurements reveal that donors **1a**, **1c,** and **1e** have similar pK_a values. Interestingly, **HAPY** compounds with pK_a values near 10.5 have half-lives of approximately 30 min,[15a,55] consistent with our results for donor **1e**. In contrast to the **HAPY** compounds (and **1e** (R^3 = NMe_2)), the stability of **1a** (R^3 = Me) and **1c** (R^3 = OMe) suggests a barrier for the decomposition of these donors even after oxyanion formation.

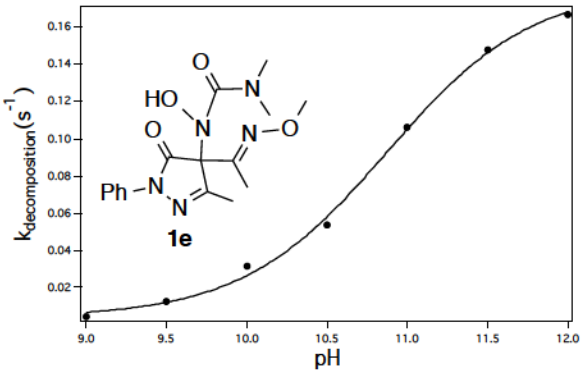

Figure 2-2. Plot of the observed decomposition rates of donor **1e** (20 μM) as a function of pH in 0.25 M phosphate buffer containing 0.2 mM DTPA at 25 °C determined by UV-vis analysis of the growth of the anionic pyrazolone byproduct **2a** (λ_{max} = 265 nm). The solid curve is the calculated best fit to a sigmoid function.

2.3.4.1. Structural Studies

To explore the origin of the R^3 group's impact on donor stability, we examined **NHPY** structural properties. Resonance structures **A**, **B**, and **C** (Figure 2-3) can be used as a guide to describe the structures of **NHPY** compounds. We assume that nitrosocarbonyl formation should be favored from structures **A** and **C**, but not from structure **B**.

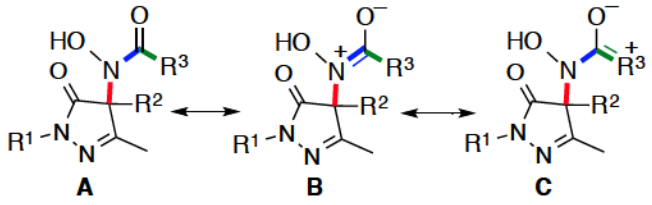

Figure 2-3. Important resonance structures for **NHPY** compounds.

2.3.4.2. X-ray Crystallographic Studies

For **NHPY** compounds **1a**, **1b**, **1d**, and **1g**, we were able to obtain suitable crystals for X-ray diffraction experiments. Distances for the C-N bond (red) between the pyrazolone ring and the hydroxamic acid nitrogen are similar in all cases; however, the N-C(O) bond (blue) distance depends on the electron donating ability of the R^3 group (Table 2-3). This bond is shortest for R^3 = Me and longest for R^3 = NMe_2. The C(O)-R^3 bond (green) lengths are similarly impacted by R^3. These bond lengths suggest that resonance structure **C** is most important for R^3 = NMe_2. The HO-N-C=O dihedral angle of **NHPY 1g** (R^3 = NMe_2) (139.4°) is also consistent with resonance structure **C**. On the other hand, the bond length and angles observed for **NHPY 1a** (R^3 = Me) and **1b** (R^3 = Me) suggest that resonance structure **B** is most important for these precursors. This resonance structure should not favor nitrosocarbonyl generation, and as a result, these donors decompose very slowly (**1a**) or are stable (**1b**) even after deprotonation.

Table 2-3. Selected X-ray Crystallographic Geometry Parameters for NHPY 1a, 1b, 1d, and 1g.

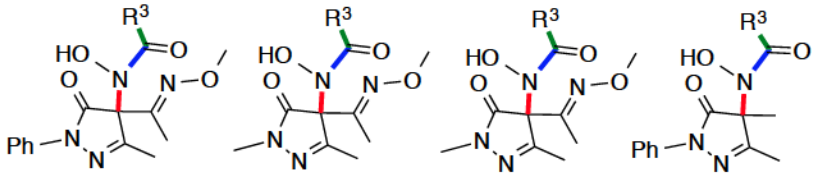

1a R^3 = Me **1b** R^3 = Me **1d** R^3 = OMe **1g** R^3 = $N(Me)_2$

NHPY	d_{C-N} (Å)	$d_{N-C(O)}$ (Å)	$d_{C(O)-R^3}$ (Å)	$d_{C=O}$ (Å)	< HO-N-C=O (°)
1a	1.459	1.355	1.500	1.229	157.7
1b	1.454	1.349	1.492	1.240	164.0
1d	1.455	1.385	1.335	1.209	157.2
1g	1.471	1.409	1.341	1.238	139.4

2.3.4.3. Computational Studies

To gain additional insight into the structural properties and further compare these with half-life measurements, we calculated the geometries of **NHPY** donors **1a** (R^3 = Me), **1c** (R^3 = OMe), and **1e** (R^3 = NMe_2). All calculations were performed with Spartan '14 at the B3LYP/6-31G(d) level;[56] optimized geometries and vibrational frequencies were calculated for each compound. Based on the calculated N-C(O) and C(O)-R^3 bond distances and the HO-N-C=O dihedral angles, the degree of pyramidalization at the amide nitrogen is markedly increased in donor **1e** compared with donors **1a** and **1c** (Table 2-4). This result, along with the observed half-lives, suggests that an analysis of the contributions of resonance structures **A** – **C** is a good indicator of the stability of the donors. Donor **1e** ($t_{1/2}$ = 25 min), with dominant resonance structure **C**, possesses a pyramidal amide nitrogen and is a much shorter-lived donor compared with donors **1a** ($t_{1/2}$ = 5 days) and **1c** ($t_{1/2}$ = 2 days). Resonance structure **B**, the major contributor for **NHPY 1a**, does not favor nitrosocarbonyl generation, consistent with the long half-life of this donor.

Table 2-4. Selected B3LYP/6-31G(d) Calculated Geometry Parameters for NHPY 1a, 1c, and 1e

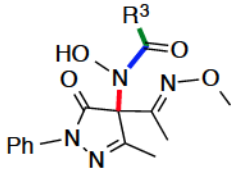

1a R^3 = Me
1c R^3 = OMe
1e R^3 = $N(Me)_2$

NHPY	d_{C-N} (Å)	$d_{N-C(O)}$ (Å)	$d_{C(O)-R^3}$ (Å)	$d_{C=O}$ (Å)	< HO-N-C=O (°)
1a	1.470	1.385	1.512	1.222	169.5
1c	1.466	1.394	1.343	1.215	154.7
1e	1.468	1.413	1.369	1.232	136.5

Deprotonation of hydroxyl group is expected to be the first step for decomposition of **NHPY** donors. As mentioned above, donors **1a** and **1c** are still relatively stable to dissociation even after deprotonation. This observation suggests a barrier to decomposition for the oxyanionic species. To gain insight into the stability of anionic **NHPY** compounds, we calculated barriers for dissociation upon deprotonation. Consistent with the results discussed earlier, these calculations indicate the lowest barrier of dissociation for deprotonated **1e** (R^3 = NMe_2) and highest for deprotonated **1a** (R^3 = Me) (Table 2-5), again consistent with the resonance structure discussion above.

Table 2-5. B3LYP/6-31G(d) Calculated Decomposition Barriers for Anionic Donors

NHPY	$\Delta G^{\ddagger}$ (kcal/mol)
1a	11.8
1c	7.9
1e	5.2

The relationship between resonance structures and donor decomposition was further studied by examining the barrier for rotation around HON-C(O) bonds in three model hydroxamic acid derivatives **3a – 3c** (Figure 2-4). The lowest barriers to rotation around the HON-C(O) bonds for these three model compounds were calculated to be 15, 11.2, and 5.1 kcal/mol, respectively (Supporting Information). This observed trend indicates a correlation between the nature of substituted carbonyl and the rotational barrier.[57] The highest barrier to rotation for compound **3a** with R = Me suggests a strong contribution from resonance structure **B** in Figure 2-3. On the other hand, the low barrier to rotation calculated for

compound **3c** with R = NMe_2 suggests a large contribution from resonance structure **C**.

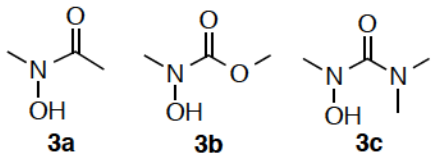

Figure 2-4. Model hydroxamic acid derivatives

2.3.5. Potential Synthetic Utility of NHPY Compounds.

Nitrosocarbonyl compounds have been utilized as versatile electrophiles in a range of synthetic procedures. Recently, mild oxidative pathways to generate nitrosocarbonyls have significantly expanded the scope of their applications. Diels-Alder reactions, ene reactions, and nitrosocarbonyl aldol reactions are examples of useful methodologies that involve nitrosocarbonyl intermediates.[33-46,48,50]

To demonstrate the potential synthetic utility of **NHPY** compounds, the reaction of donor **1e** with anionic pyrazolone **2d** was examined in organic solvent (dichloromethane) in the presence of 1 equiv of the non-nucleophilc base, diazabicycloundecene (DBU) (Scheme 2-6). After complete decomposition of **NHPY 1e**, ^{1}H NMR spectroscopy confirmed the formation of pyrazolone byproduct **2a** and a new *N*-substituted hydroxamic acid adduct **1i** in excellent yield (99%), which was independently synthesized and characterized (Supporting Information). The formation of pyrazolone **1i** is the result of nitrosocarbonyl formation and

subsequent trapping by pyrazolone byproduct **2d**, and can be thought of as a nitrosocarbonyl transfer reaction.

Scheme 2-6. Nitrosocarbonyl Generation from NHPY Compounds in Organic Solvent

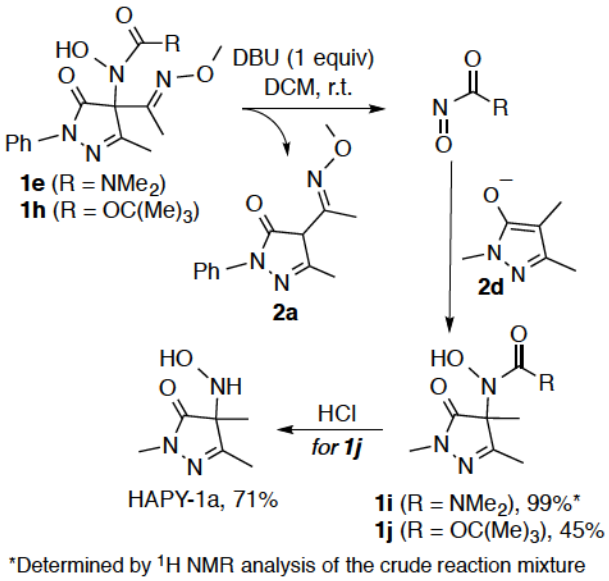

We also examined a hydroxamic acid derivative that can be further manipulated after completion of the reaction. Donor **1h** generates a nitrosocarbonyl intermediate under mild basic conditions, and in the presence of anionic pyrazolone **2d**, *N*-substituted hydroxamic acid adduct **1j** is formed in good yield (45%) (Scheme 2-6). Acid catalyzed deprotection of the Boc-group leads to the formation of **HAPY**-1a which has previously been reported.[16] These results demonstrate that **NHPY** compounds are efficient nitrosocarbonyl precursors that can be used under mild basic conditions in organic solvent without the need of metal-based catalysts. This non-oxidative protocol importantly avoids any problems associated with product overoxidation.

2.4. Conclusion

The **NHPY** class of nitrosocarbonyl precursors quantitatively generates nitrosocarbonyl intermediates (and ultimately HNO) under physiological conditions with tunable half-lives. The nitrosocarbonyl release rate is dependent on the nature of pyrazolone leaving groups and also significantly on the structural properties of the donors. Under these conditions, pyrazolones are demonstrated to be efficient nitrosocarbonyl traps through an *N*-selective nitrosocarbonyl aldol reaction. This trapping reaction has been used to provide evidence for the involvement of nitrosocarbonyl intermediates in the aqueous decomposition of **NHPY** compounds. Additionally, **NHPY** compounds are shown to release nitrosocarbonyls under mild basic conditions in organic solvent and may enjoy further synthetic applications.

2.5. Experimental

2.5.1. Method and Materials

All starting materials were of reagent grade and used without further purification. 4-(Acetyl-*O*-methoxyoxime)-*N*-phenyl-3-methyl-pyrazolone **2a**, 4-(acetyl-*O*-methoxyoxime)-1,3-dimethylpyrazolone **2b**, 3,4-methyl-*N*-phenylpyrazolone **2c**, 1,3,4-trimethylpyrazolone **2d**,[15a] brominated pyrazolones (Br-PY),[14] *C*-methoxycarbohydroxamic acid, and *N*-hydroxy-*N'*,*N'*-dimethylurea[58] were prepared according to literature procedures. Acetohydroxamic acid was purchased and used without further purification. NMR spectra were obtained on a 300 or 400 MHz FT-NMR spectrometer. All chemical shifts are reported in parts per million (ppm) relative to residual $CHCl_3$ (7.26 ppm for ^1H, 77.23 ppm for ^{13}C). High-resolution mass spectra were collected on a magnetic sector mass spectrometer working in fast atom bombardment (FAB) mode. Gas chromatography (GC) headspace analysis was performed on the instrument equipped with ECD detection and a packed column. UV-vis absorption spectra were collected using a diode array spectrophotometer.

Method A for the Synthesis of NHPY Compounds: Base (1 equiv) was added to a solution of Boc protected hydroxamic acids (1 equiv) in an appropriate solvent at room temperature and stirred for one hour. The solution was added dropwise to a solution of brominated pyrazolone and stirred for 3 h. The reaction was followed to completion by TLC. The organic solvent was then removed by rotary evaporation, and the **NHPY** product was purified either by column

chromatography (ethyl acetate/hexane) on silica gel or by recrystallization from dichloromethane and hexane.

Method B for the synthesis of NHPY Compounds: Hydroxamic acid (1 – 5 equiv) was added to a solution of pyrazolone (1 equiv) in 50% aqueous ethanol. The pH of the solution was adjusted to 7-8 using 0.2 equiv of potassium carbonate. Sodium periodate (0.5 – 5 equiv) was added to the solution and the reaction mixture was sonicated for 10 min and stirred at room temperature for 3 h until the reaction was complete as determined by TLC. The white solid was removed by filtration and the resulting filtrate concentrated under reduced pressure. Recrystallization from dichloromethane and hexane gave the desired **NHPY** compound.

***N*-Hydroxy-*N*-(4-(acetyl-*O*-methoxyoxime)-3-methyl-5-oxo-1-phenyl-4,5-dihydro-1*H*-pyrazol-4-yl)-*N*-acetamide (1a):** According to Method A, triethylamine (0.05 mL, 0.39 mmol) was added to a solution of *N*-(*t*-butoxycarbonyloxy)-acetamide (0.068 g, 0.39 mmol) in acetonitrile (4 mL) at room temperature and the reaction was stirred for 1 h. This solution was added dropwise to 4-(acetyl-*O*-methoxyoxime)-4-bromo-*N*-phenyl-5-methylpyrazolone (0.126 g, 0.39 mmol) and the reaction proceeded at room temperature for 3 h. The reaction was concentrated by rotary evaporation, and the resulting solid was redissolved in dichloromethane and washed with water. The organic phase was collected and concentrated via rotary evaporation. Without further purification, the compound was dissolved in methanol (3 mL), cooled to 0 °C, and acetyl chloride (0.2 mL) was added. The reaction was allowed warm to room temperature and stirred overnight.

The solution was concentrated via rotary evaporation and redissolved in dichloromethane, filtered, and the filtrate was concentrated *in vacuo*. Recrystallization from dichloromethane and hexane gave the title compound as white solid (9 mg, 7%).

According to method B, acetohydroxamic acid (0.161 g, 2.14 mmol) was added to a solution of pyrazolone byproduct **2a** (0.105 g, 0.43 mmol) in 50 % aqueous ethanol (7 mL), and potassium carbonate (0.012 g, 0.09 mmol) was added to adjust the pH to 7-8. Sodium periodate (0.458 g, 2.14 mmol) was added to the reaction mixture, sonicated for 10 min, and then stirred for 3 h at room temperature. The reaction mixture was diluted with ethanol (10 mL) and the solid was filtered. The filtrate was concentrated via rotary evaporation and the resulting solid was redissolved in ethyl acetate (50 mL) and washed three times with a saturated solution of ammonium chloride (30 mL). The organic phase was collected, dried over $MgSO_4$, filtered, and concentrated *in vacuo*. Recrystallization from dichloromethane and hexane gave the title compound as white solid (0.1 g, 73%).

^{1}H NMR (400 MHz, $CDCl_3$) δ: 7.86 (m, 2H), 7.51 (s, 1H), 7.42 (m, 2H), 7.22 (m, 1H), 3.95 (s, 3H), 2.25 (s, 3H), 2.19 (s, 3H), 2.01 (s, 3H). ^{13}C NMR (100 MHz, $CDCl_3$) δ: 167.8, 159.0, 157.0, 151.4, 137.8, 128.8, 125.8, 119.5, 76.3, 62.5, 21.0, 15.4, 11.4. HR-MS (FAB): found *m/z* = 319.14094 (MH^+); calcd for $C_{15}H_{18}N_4O_4$: 319.14063. Mp: 168-170 °C.

***N*-Hydroxy-*N*-(4-(acetyl-*O*-methoxyoxime)-1,3-dimethyl-5-oxo-4,5-dihydro-1*H*-pyrazol-4-yl)-*N*-acetamide (1b):** Following the methods described

above for the synthesis of **NHPY 1a** and using 4-(acetyl-*O*-methoxyoxime)-4-bromo-1,3-dimethyl-pyrazolone in method A and pyrazolone **2b** in method B, the title compound was obtained in 8% and 75% yields, respectively, as a white solid.

^{1}H NMR (400 MHz, $CDCl_3$) δ: 7.98 (s, 1H), 3.92 (s, 3H), 3.32 (s, 3H), 2.25 (s, 3H), 2.10 (s, 3H), 1.94 (s, 3H). ^{13}C NMR (100 MHz, $CDCl_3$): 169.9, 161.4, 157.0, 151.4, 75.0, 62.5, 31.9, 21.3, 15.5, 11.6. HR-MS (FAB): found *m/z* = 257.12526 (MH^+); calcd for $C_{10}H_{16}N_4O_4$: 257.12498. Mp: 171-173 °C.

***N*-Hydroxy-*N*-(4-(acetyl-*O*-methoxyoxime)-3-methyl-5-oxo-1-phenyl-4,5-dihydro-1*H*-pyrazol-4-yl)-*N*-methylcarbamate (1c):** According to method A, sodium hydride 60% (0.061 g, 1.52 mmol) was added to a solution of *N*-(*t*-butoxycarbonyloxy)-methylcarbamate (0.265 g, 1.38 mmol) in dimethylformamide (6 mL) at room temperature and the reaction was stirred for 1 h. This solution was added dropwise to 4-(acetyl-*O*-methoxyoxime)-4-bromo-*N*-phenyl-5-methylpyrazolone (0.447 g, 1.38 mmol) and the reaction proceeded at room temperature for 3 h. The reaction was diluted with ether (10 mL) and washed with ammonium chloride, water, and brine. The organic phase was collected and concentrated via rotary evaporation. Without further purification, the compound was dissolved in methanol (10 mL), cooled to 0 °C, and acetyl chloride (0.6 mL) was added. The reaction was allowed to warm to room temperature and stirred overnight. The solution was concentrated via rotary evaporation and redissolved in dichloromethane, filtered, and the filtrate was concentrated *in vacuo*. Recrystallization from dichloromethane and hexane gave the title compound as

white solid (0.221 g, 48%).

According to method B, to a solution of pyrazolone **2a** (0.245 g, 1 mmol) and *C*-methoxycarbohydroxamic acid (0.109 g, 1.2 mmol) in 50 % aqueous ethanol (5 mL), potassium carbonate (0.028 g, 0.2 mmol) was added to adjust the pH to 7-8. Sodium periodate (0.257 g, 1.2 mmol) was added to the reaction mixture and sonicated for 10 min, and then stirred for 3 h at room temperature. The reaction mixture was diluted with ethanol (10 mL) and the solid was filtered. The filtrate was concentrated via rotary evaporation, redissolved in ethyl acetate (50 mL), and washed three times with saturated solution of ammonium chloride (30 mL). The organic phase was collected, dried over $MgSO_4$, filtered, and concentrated *in vacuo*. Recrystallization from dichloromethane and hexane gave the title compound as white solid (0.237 g, 71%).

^{1}H NMR (400 MHz, $CDCl_3$) δ: 8.59 (s, 1H), 7.88 (m, 2H), 7.41 (m, 2H), 7.23 (m, 1H), 3.89 (s, 3H), 3.76 (s, 3H), 2.26 (s, 3H), 2.14 (s, 3H). ^{13}C NMR (100 MHz, $CDCl_3$) δ: 167.6, 158.3, 158.1, 152.2, 138.0, 128.9, 125.6, 119.6, 76.5, 62.6, 54.5, 16.0, 10.9. HR-MS (FAB): found *m/z* = 335.13550 (MH^+); calcd. for $C_{15}H_{18}N_4O_5$: 335.13554. Mp: 160-162 °C.

***N*-Hydroxy-*N*-(*4*-(acetyl-*O*-methoxyoxime)-1,3-dimethyl-5-oxo-4,5-dihydro-1*H*-pyrazol-4-yl)-*N*-methylcarbamate (1d):** Following the methods described above for the synthesis of **NHPY 1c** and using brominated pyrazolone 4-(acetyl-*O*-methoxyoxime)-4-bromo-1,3-dimethylpyrazolone in method A and pyrazolone **2b** in method B, the title compound was obtained in 50% and 69%

yields, respectively, as a white solid.

^{1}H NMR (400 MHz, $CDCl_3$) δ: 7.05 (s, 1H), 3.89 (s, 3H), 3.82 (s, 3H), 3.30 (s, 3H), 2.13 (s, 3H), 2.04 (s, 3H). ^{13}C NMR (100 MHz, $CDCl_3$) δ: 169.4, 157.9, 157.5, 152.0, 75.4, 62.5, 54.3, 31.9, 15.7, 11.0. HR-MS (FAB): found *m/z* = 273.11964 (MH^+); calcd. for $C_{10}H_{16}O_5N_4$: 273.11989. Mp: 162-164 °C.

***N'*,*N'*-Dimethyl-*N*-hydroxy-*N*-(*4*-(acetyl-*O*-methoxyoxime)-3-methyl-5-oxo-1-phenyl-4,5-dihydro-1*H*-pyrazol-4-yl)-urea (1e):** According to Method A, triethylamine (0.07 mL, 0.5 mmol) was added to a solution of *N*-(*t*-butoxycarbonyloxy)-*N'*,*N'*-dimethylurea (0.102 g, 0.5 mmol) in acetonitrile (6 mL) at room temperature and the reaction stirred for one hour. This solution was added dropwise to 4-(acetyl-*O*-methoxyoxime)-4-bromo-*N*-phenyl-5-methyl-pyrazolone (0.161 g, 0.5 mmol) and the reaction proceeded at room temperature for 3 h. The reaction was concentrated by rotary evaporation, redissolved in dichloromethane, and washed with water. The organic phase was collected and concentrated via rotary evaporation. Without further purification, the compound was dissolved in methanol (7 mL), cooled to 0 °C and acetyl chloride (0.3 mL) was added. The reaction was allowed warm to room temperature and stirred overnight. The solution was concentrated via rotary evaporation, redissolved in dichloromethane, filtered, and the filtrate was concentrated *in vacuo*. Recrystallization from dichloromethane and hexane gave the title compound as white solid (61 mg, 35%).

According to method B, to a solution of pyrazolone byproduct **2a** (0.711 g, 2.9 mmol) and *N*-hydroxy-*N'*,*N'*-dimethylurea (0.302 g, 2.9 mmol) in 50 % aqueous

ethanol (15 mL), potassium carbonate (0.08 g, 0.58 mmol) was added to adjust the pH to 7-8. Sodium periodate (0.299 g, 1.4 mmol) was added to the reaction mixture, sonicated for 10 min, and stirred for 3 h at room temperature. The reaction mixture was diluted with ethanol (5 mL) and the solid was filtered. The filtrate was concentrated via rotary evaporation, redissolved in ethylacetate (40 mL), and washed three times with saturated solution of ammonium chloride (20 mL). The organic phase was collected, dried over $MgSO_4$, filtered, and concentrated *in vacuo*. Recrystallization from dichloromethane and hexane gave the title compound as white solid (0.483 g, 48%).

^{1}H NMR (400 MHz, $CDCl_3$) δ: 7.88 (m, 2H), 7.44 (m, 2H), 7.40 (s, 1H), 7.22 (m, 1H), 3.89 (s, 3H), 3.00 (s, 6H), 2.22 (s, 3H), 2.08 (s, 3H). ^{13}C NMR (100 MHz, $CDCl_3$) δ: 171.9, 161.1, 157.0, 152.6, 138.0, 128.8, 125.3, 119.3, 76.2, 62.5, 37.9, 15.56, 11.4. HR-MS (FAB): found *m/z* = 348.16732 (MH^+); calcd for $C_{16}H_{22}N_5O_4$: 348.16718. Mp: 140-142 °C.

***N'*,*N'*-Dimethyl-*N*-hydroxy-*N*-(*4*-(acetyl-*O*-methoxyoxime)-1,3-dimethyl-5-oxo-4,5-dihydro-1*H*-pyrazol-4-yl)-urea (1f):** Following the methods described above for the synthesis of **NHPY 1e** and using brominated 4-(acetyl-*O*-methoxyoxime)-4-bromo-1,3-dimethylpyrazolone in method A and pyrazolone **2b** in method B the title compound was obtained in 38% and 47% yields, respectively, as a white solid.

^{1}H NMR (400 MHz, $CDCl_3$) δ: 7.35 (s, 1H), 3.92 (s, 3H), 3.35 (s, 3H), 3.02 (s, 6H), 2.09 (s, 3H), 2.01 (s, 3H). ^{13}C NMR (100 MHz, $CDCl_3$) δ: 172.7, 161.5, 157.8,

152.8, 75.2, 62.8, 38.2, 31.8, 16.1, 10.7. HR-MS (FAB): found *m/z* = 286.15192 (MH^+); calcd for $C_{11}H_{19}N_5O_4$: 286.15153. Mp: 144-146 °C.

***N'*,*N'*-dimethyl-*N*-hydroxy-*N*-(3,4-dimethyl-5-oxo-1-phenyl-4,5-dihydro-1*H*-pyrazol-4-yl)-urea (1g):** Following the methods described above for the synthesis of **NHPY 1e** and using 4-bromo-4,5-dimethyl-*N*-phenylpyrazolone in Method A and pyrazolone **2c** in Method B, the title compound was obtained in 11% and 48% yields, respectively, as a white solid.

^{1}H NMR (400 MHz, $CDCl_3$) δ: 7.89 (m, 2H), 7.38 (m, 2H), 7.25 (s, 1H), 7.17 (m, 1H), 3.00 (s, 6H), 2.10 (s, 3H), 1.70 (s, 3H). ^{13}C NMR (100 MHz, $CDCl_3$) δ: 175.7, 162.8, 161.6, 138.1, 128.8, 124.9, 119.0, 69.6, 38.1, 20.1, 12.7. HR-MS (FAB): found *m/z* = 291.14536 (MH^+); calcd for $C_{14}H_{19}O_3N_4$: 291.14572. Mp: 162-164 °C.

***N*-Hydroxy-*N*-(4-(acetyl-*O*-methoxyoxime)-3-methyl-5-oxo-1-phenyl-4,5-dihydro-1*H*-pyrazol-4-yl)-*t*-butylcarbamate (1h):** According to Method B, to a solution of pyrazolone **2a** (0.135 g, 0.55 mmol) and *t*-butylhydroxycarbamate (0.088 g, 0.66 mmol) in 50 % aqueous ethanol (3 mL), potassium carbonate (0.018 g, 0.13 mmol) was added to adjust the pH to 7-8. Sodium periodate (0.141 g, 0.66 mmol) was added to the reaction mixture, sonicated for 10 min, and then stirred for 3 h at room temperature. The reaction mixture was diluted with ethanol (6 mL) and the solid was filtered. The filtrate was concentrated via rotary evaporation, redissolved in ethylacetate (50 mL), and washed three times with saturated solution of ammonium chloride (30 mL). The organic phase was collected, dried over $MgSO_4$, filtered, and concentrated *in vacuo*. Recrystallization from dichloromethand and

hexane gave the title compound as white solid. (0.142 g, 69%)

^{1}H NMR (300 MHz, $CDCl_3$): 7.92 (m, 2H), 7.40 (m, 2H), 7.19 (m, 1H), 3.87 (s, 3H), 2.26 (s, 3H), 2.13 (s, 3H), 1.38 (s, 9H). ^{13}C NMR (100 MHz, $CDCl_3$) δ: 166.86, 158.6, 156.9, 152.5, 138.7, 129.0, 124.6, 118.3, 85.7, 76.0, 62.4, 28.2, 15.8, 10.9. HR-MS (FAB): found *m/z* = 377.18193 (MH^+); calcd for $C_{18}H_{24}O_5N_4$: 377.18250.

***N'*,*N'*-Dimethyl-*N*-hydroxy-*N*-(1,3,4-trimethyl-5-oxo-4,5-dihydro-1*H*-pyrazol-4-yl)-urea (1i):** A solution of pyrazolone **2d** (0.023 g, 0.18 mmol) and 1,8-diazabicycloundec-7-ene (0.027 mL, 0.18 mmol) in 1 mL dichloromethane was stirred for 30 min. The mixture was added to a solution of **NHPY 1e** (0.062 g, 0.18 mmol) in dichloromethane (1 mL). To this solution, diazabicycloundec-7-ene (0.027 mL, 0.18 mmol) was added dropwise and stirred for 4 h at room temperature. The reaction mixture was diluted with 5 mL dichloromethane and washed with HCl 1 N solution. The organic phase was collected, dried over $MgSO_4$, and the solvent was removed by rotary evaporation (99% conversion).

According to method B, to a solution of pyrazolone **2d** (0.063 g, 0.5 mmol) and *N*-hydroxy-*N'*,*N'*-dimethylurea (0.052 g, 0.5 mmol) in 50 % aqueous ethanol (5 mL), potassium carbonate (0.014 g, 0.1 mmol) was added to adjust the pH to 7-8. Sodium periodate (0.053 g, 0.25 mmol) was added to the reaction mixture, sonicated for 10 min, and then stirred for 3 h at room temperature. The reaction mixture was diluted with ethanol (5 mL) and the solid was filtered. The filtrate was concentrated via rotary evaporation, redissolved in ethyl acetate (40 mL), and washed three times with saturated solution of ammonium chloride (20 mL). The

organic phase was collected, dried over $MgSO_4$, filtered, and concentrated *in vacuo*. Recrystallization from dichloromethane and hexane gave the title compound as white solid (0.055 g, 48%).

^{1}H NMR (300 MHz, $CDCl_3$) δ: 8.36 (s, 1H), 3.29 (s, 3H), 2.97 (s, 6H), 2.00 (s, 3H), 1.53 (s, 3H). ^{13}C NMR (100 MHz, $CDCl_3$) δ: 177.0, 162.1, 161.4, 68.4, 38.0, 31.4, 19.5, 13.4. HR-MS (FAB): found *m/z* = 229.13012 (MH^+); calcd for $C_9H_{16}O_3N_4$: 229.13007. Mp: 125-127 °C.

***N*-Hydroxy-*N*-(1,3,4-trimethyl-5-oxo-4,5-dihydro-1*H*-pyrazol-4-yl)-*t*-butylcarbamate (1j):** A solution of pyrazolone **2d** (0.035 g, 0.28 mmol) and 1,8-diazabicycloundec-7-ene (0.042 mL, 0.28 mmol) in 2 mL dichloromethane was stirred for 30 min. The mixture was added to a solution of **NHPY 1h** (0.105 g, 0.28 mmol) in dicholoromethane (2 mL). To this solution, diazabicycloundec-7-ene (0.042 mL, 0.28 mmol) was added dropwise and stirred for 4 h at room temperature. The reaction mixture was diluted with 10 mL dichloromethane and washed with HCl 1 N solution. The organic phase was collected, dried over $MgSO_4$, filtered, and the solvent was removed by rotary evaporation. The residue was purified by column chromatography (20% ethyl acetate/hexane) on silica gel to obtain the title compound as white solid. (0.032 g, 45%)

According to method B, to a solution of pyrazolone **2d** (0.052 g, 0.41 mmol) and *N*-Boc-hydroxylamine (0.065 g, 0.49 mmol) in 50 % aqueous ethanol (2 mL), potassium carbonate (0.011 g, 0.08 mmol) was added to adjust the pH to 7-8. Sodium periodate (0.105 g, 0.49 mmol) was added to the reaction mixture,

sonicated for 10 min, and then stirred for 3 h at room temperature. The reaction mixture was diluted with ethanol (6 mL) and the solid was filtered. The filtrate was concentrated via rotary evaporation, redissolved in ethylacetate (30 mL), and washed three times with saturated solution of ammonium chloride (20 mL). The organic phase was collected, dried over $MgSO_4$, and concentrated *in vacuo*. Recrystallization from dichloromethane and hexane gave the title compound as white solid. (0.068 g, 65%)

^{1}H NMR (300 MHz, $CDCl_3$) δ: 7.81 (s, 1H), 3.32 (s, 3H), 2.07 (s, 3H), 1.60 (s, 3H), 1.43 (s, 9H). ^{13}C NMR (100 MHz, $CDCl_3$) δ: 175.4, 161.5, 155.1, 77.4, 69.0, 32.0, 28.3, 19.6, 13.1. HR-MS (FAB): found *m/z* = 258.14549 (MH^+); calcd for $C_{11}H_{19}N_3O_4$: 258.14538. Mp: 130-132 °C.

***N'*,*N'*-Dimethyl-*N*-methoxy-*N*-(4-(acetyl-*O*-methoxyoxime)-3-methyl-5-oxo-1-phenyl-4,5-dihydro-1*H*-pyrazol-4-yl)-urea (compound 1):** According to the method A, sodium hydride 60% (0.016 g, 0.4 mmol) was added to a solution of *N*-methoxy-*N'*,*N'*-dimethylurea (0.042 g, 0.36 mmol) in dimethylformamide (5 mL) at room temperature and the reaction stirred for 1 h. This solution was added dropwise to 4-(acetyl-*O*-methoxyoxime)-4-bromo-*N*-phenyl-5-methyl-pyrazolone (0.116 g, 0.36 mmol) and the reaction proceeded at room temperature for 3 h. The reaction was diluted with ether (8 mL) and washed with ammonium chloride, water, and brine. The organic phase was collected and concentrated by rotary evaporation. The residue was purified by column chromatography (20% ethyl acetate/hexane) on silica gel to obtain the title compound as yellowish oil (0.099 g, 76%).

^{1}H NMR (400 MHz, $CDCl_3$) δ: 7.89 (m, 2H), 7.38 (m, 2H), 7.17 (m, 1H), 3.90 (s, 3H), 3.78 (s, 3H), 3.01 (s, 6H), 2.31 (s, 3H), 2.12 (s, 3H). ^{13}C NMR (100 MHz, $CDCl_3$) δ: 168.6, 158.9, 158.4, 152.1, 138.3, 128.8, 125.0, 119.3, 76.7, 64.0, 62.4, 38.1, 17.3, 12.5. HR-MS (FAB): found *m/z* = 362.18259 (MH^+); calcd for $C_{17}H_{23}N_5O_4$: 362.18283.

4-(*N*-Hydroxylamino)-4-methyl-N-methyl-3-methylpyrazolone (HAPY-1a): Compound **1j** (32 mg, 0.13 mmol) was dissolved in methanol (3 mL) at 0 °C and acetyl chloride (0.2 mL) was added. The reaction was allowed to warm to room temperature, and stirring was continued overnight. The reaction was concentrated *in vacuo*, redissolved in dichloromethane, filtered, and the filtrate was concentrated via rotary evaporation to give the title compound (71 %, 14 mg), whose characterization was consistent with that previously reported.[15]

^{1}H NMR (400 MHz, DMSO-d_6) δ: 7.51 (d, 1H), 6.25 (d, 1H), 3.10 (s, 3H), 1.98 (s, 3H), 1.00 (s, 3H). ^{13}C NMR (100 MHz, DMSO-d_6) δ: 175.3, 161.9, 69.0, 30.7, 16.0, 12.7.

***N*-(*t*-Butoxycarbonyloxy)-*N'*,*N'*-dimethylurea:** For this synthesis, we modified a procedure that was previously reported.[59] *N*-Hydroxy-*N'*,*N'*-dimethylurea (2.73 mmol, 0.284 g, 1 equiv) and triethylamine (2.73 mmol, 0.38 mL, 1 equiv) in 15 mL acetonitrile were stirred for 1 h at room temperature. Di-*t*-butyl dicarbonate (2.73 mmol, 0.595 g, 1.0 equiv) was added dropwise to the reaction mixture and stirred for 3 h. The reaction was diluted with dichloromethane and washed twice with 1 N HCl solution. The organic phase was dried over $MgSO_4$, filtered, and the organic solvent was removed by rotary evaporation, which gave the

title compound as a white solid (0.407 g, 73%).

^{1}H NMR (400 MHz, $CDCl_3$) d: 7.71 (s, 1H), 2.98 (s, 6H), 1.56 (s, 9H). ^{13}C NMR (100 MHz, $CDCl_3$) δ: 158.0, 154.6, 85.3, 36.2, 27.8. HR-MS (FAB): found *m/z* = 205.11902 (MH^+); calcd for $C_8H_{16}N_2O_4$: 205. 11883.

***N*-(*t*-Butoxycarbonyloxy)-methylcarbamate:** The synthetic procedure is the same as described above using *C*-methoxycarbohydroxamic acid (0.354 g, 68%).

^{1}H NMR (400 MHz, $CDCl_3$) d: 7.87 (s, 1H), 3.84 (s, 3H), 9.15 (s, 9H). ^{13}C NMR (400 MHz, $CDCl_3$) δ: 157.5, 153.6, 86.4, 53.9, 27.8. HR-MS (FAB): found *m/z* = 192.08716 (MH^+); calcd for $C_7H_{13}NO_5$: 192.08720.

***N*-(*t*-Butoxycarbonyloxy)-acetamide:** For this synthesis, we modified a procedure that was previously reported.[59] Di-*t*-butyl dicarbonate (9.3 mmol, 2.03 g, 1.0 equiv) was added to a suspension of acetohydroxamic acid (9.3 mmol, 0.7 g, 1.0 equiv) in 50 mL of dichloromethane at room temperature. Sodium *t*-butoxide (5.6 mmol, 0.54 g, 0.6 equiv) was added dropwise to the reaction mixture and allowed to stir overnight. The reaction was diluted with dichloromethane and washed twice with saturated NH_4Cl solution. The organic phase was dried over $MgSO_4$, filtered, and the organic solvent was removed by rotary evaporation. The resulting solid, without further purification, was used for the synthesis of **NHPY** donors using Method A.

^{1}H NMR (400 MHz, $CDCl_3$) d: 9.87 (s, 1H), 1.52 (s, 9H), 1.45 (s, 3H). ^{13}C NMR (100 MHz, $CDCl_3$) δ: 158.2, 155,7, 86.2, 31.1, 29.8. HR-MS (FAB): found *m/z* =

176.09325 (MH^+); calcd for $C_7H_{13}NO_4$: 176.09228.

***N*-Methoxy-*N'*,*N'*-dimethylurea:** To a solution of *O*-methylhydroxylamine hydrochloride (46 mmol, 3.84 g, 1 equiv) and potassium carbonate (41.6 mmol, 5.75 g, 0.9 equiv) in 2 mL water and 100 mL ethyl acetate at 0 °C was added (37.2 mmol, 4 g, 0.8 equiv) of dimethylcarbamyl chloride. The reaction mixture was stirred overnight. The solid was filtered off and washed with boiling ethyl acetate. The organic solution was dried over $MgSO_4$, filtered, and the organic solvent was removed by rotary evaporation, which gave the title compound as colorless oil (3.80 g, 86%).

^1H NMR (400 MHz, $CDCl_3$) δ: 7.41 (s, 1H), 3.66 (s, 3H), 2.92 (s, 6H). ^{13}C NMR (100 MHz, $CDCl_3$) δ: 160.5, 63.3, 35.7. HR-MS (FAB): found *m/z* = 119.08228 (MH^+); calcd for $C_4H_{10}N_2O_2$: 119.08205.

2.6. References

(1) Paolocci, N.; Saavedra, W. F.; Miranda, K. M.; Martignani, C.; Isoda, T.; Hare, J. M.; Espey, M. G.; Fukuto, J. M.; Feelisch, M.; Wink, D. A.; Kass, D. A. *Proc. Natl. Acad. Sci. U.S.A.* **2001**, *98*, 10463–10468.

(2) Paolocci, N.; Katori, T.; Champion, H. C.; St. John, M. E.; Miranda, K. M.; Fukuto, J. M.; Wink, D. A.; Kass, D. A. *Proc. Natl. Acad. Sci. U.S.A.* **2003**, *100*, 5537–5542.

(3) Dai, T.; Tian, Y.; Tocchetti, C. G.; Katori, T.; Murphy, A. M.; Kass, D. A.; Paolocci, N.; Gao, W. D. *J. Physiol.* **2007**, *580*, 951–960.

(4) Tocchetti, C. G.; Wang, W.; Froehlich, J. P.; Huke, S.; Aon, M. A.; Wilson, G. M.; Di Benedetto, G.; O'Rourke, B.; Gao, W. D.; Wink, D. A.; Toscano, J. P.; Zaccolo, M.; Bers, D. M.; Valdivia, H. H.; Cheng, H.; Kass, D. A.; Paolocci, N. *Circ. Res.* **2007**, *100*, 96–104.

(5) Tocchetti, C. G.; Stanley, B. A.; Murray, C. I.; Sivakumaran, V.; Donzelli, S.; Mancardi, D.; Pagliaro, P.; Gao, W. D.; Van Eyk, J.; Kass, D. A.; Wink, D. A.; Paolocci, N. *Antioxid. Redox Signal.* **2011**, *14*, 1687–1698.

(6) Sabbah, H. N.; Tocchetti, C. G.; Wang, M.; Daya, S.; Gupta, R. C.; Tunin, R. S.; Mazhari, R.; Takimoto, E.; Paolocci, N.; Cowart, D.; Colucci, W. S.; Kass, D. A. *Circ. Hear. Fail.* **2013**, *6*, 1250–1258.

(7) Arcaro, A.; Lembo, G.; Tocchetti, C. G. *Curr. Heart Fail. Rep.* **2014**, *11*, 227–235.

(8) Kemp-Harper, B. K. *Antioxid. Redox Signal.* **2011**, *14*, 1609– 1613.

(9) Flores-Santana, W.; Salmon, D. J.; Donzelli, S.; Switzer, C. H.; Basudhar, D.;

Ridnour, L.; Cheng, R.; Glynn, S. A.; Paolocci, N.; Fukuto, J. M.; Miranda, K. M.; Wink, D. A. *Antioxid. Redox Signal.* **2011**, *14*, 1659–1674.

(10) Shafirovich, V.; Lymar, S. V. *Proc. Natl. Acad. Sci. U.S.A.* **2002**, *99*, 7340–7345.

(11) Hughes, M. N.; Cammack, R. *Methods Enzymol.* **1999**, *301*, 279–287.

(12) (a) Porcheddu, A.; De Luca, L.; Giacomelli, G. *Synlett* **2009**, *13*, 2149–2153. (b) Sirsalmath, K.; Suárez, S. A.; Bikiel, D. E.; Doctorovich, F. *J. Inorg. Biochem.* **2013**, *118*, 134–139. (c) Toscano, J. P.; Brookfield, F. A.; Cohen, A. D.; Courtney, S. M.; Frost, L. M.; Kalish, V. J. U.S. Patent 8,030,356, 2011.

(13) (a) Sha, X.; Isbell, T. S.; Patel, R. P.; Day, C. S.; King, S. B. *J. Am. Chem. Soc.* **2006**, *128*, 9687–9692. (b) Shoman, M. E.; DuMond, J. F.; Isbell, T. S.; Crawford, J. H.; Brandon, A.; Honovar, J.; Vitturi, D. A.; White, C. R.; Patel, R. P.; King, S. B. *J. Med. Chem.* **2011**, *54*, 1059–1070.

(14) Guthrie, D. A.; Kim, N. Y.; Siegler, M. A.; Moore, C. D.; Toscano, J. P. *J. Am. Chem. Soc.* **2012**, *134*, 1962–1965.

(15) (a) Guthrie, D. A.; Ho, A.; Takahashi, C. G.; Collins, A.; Morris, M.; Toscano, J. P. *J. Org. Chem.* **2015**, *80*, 1338–1348. (b) Nourian, S.; Lesko, R. P.; Guthrie, D. A.; Toscano, J. P. *Tetrahedron* **2016**, *72*, 6037–6042.

(16) Guthrie, D. A.; Nourian, S.; Takahashi, C. G.; Toscano, J. P. *J. Org. Chem.* **2015**, *80*, 1349–1356.

(17) Sutton, A. D.; Williamson, M.; Weismiller, H.; Toscano, J. P. *Org. Lett.* **2012**, *14*, 472–475.

(18) Nakagawa, H. *J. Inorg. Biochem.* **2013**, *118*, 187–190.

(19) Miao, Z.; King, B. *Nitric Oxide* **2016**, *57*, 1–14.

(20) Atkinson, R. N.; Storey, B. M.; King, S. B. *Tetrahedron Lett.* **1996**, *37*, 9287–9290.

(21) Kirby G. W., Sweeny J. G. *J. Chem. Soc. Perkin Trans. I.* **1981**, 3250–3254.

(22) Corrie J. E. T., Kirby G. W., Mackinnon J. W. M. *J. Chem. Soc. Perkin Trans. I.* **1985**, 883–886.

(23) Zeng, B. B.; Huang, J.; Wright, M. W.; King, S. B. *Bioorg. Med. Chem.* **2004**, *14*, 5565–5568.

(24) Quadrelli, P.; Mella, M.; Caramella, P. *Tetrahedron Lett.* **1999**, *40*, 797–800.

(25) O'Bannon, P. E.; William, D. P. *Tetrahedron Lett.* **1988**, *29*, 5719–5722.

(26) O'Bannon, P. E.; Dailey, W. P. *J. Org. Chem.* **1989**, *54*, 3096–3101.

(27) Chemagin, A. V.; Yashin, N. V.; Grishin, Y. K.; Kuznetsova, T. S.; Zefirov, N. S. *Synthesis* **2010**, 259–266.

(28) So, S. S.; Mattson, A. E. *J. Am. Chem. Soc.* **2012**, *134*, 8798–8801.

(29) Nagasawa, H. T.; Lee, M. J. C.; Kwon, C. H.; Shirota, F. N.; DeMaster, E. G. *Alcohol* **1992**, *9*, 349–353.

(30) Ritter, A. R.; Miller, M. J. *J. Org. Chem.* **1994**, *59*, 4602–4611.

(31) Streith, J.; Defoin, A. *Synthesis* **1994**, 1107–1117.

(32) Vogt, P. F.; Miller, M. J. *Tetrahedron* **1998**, *54*, 1317–1348.

(33) Frazier, C. P.; Engelking, J. R.; Read de Alaniz, J. *J. Am. Chem. Soc.* **2011**, *133*, 10430–10433.

(34) Fakhruddin, A.; Iwasa, S.; Nishiyama, H.; Tsutsumi, K. *Tetrahedron Lett.* **2004**, *45*, 9323–9326.

(35) Yamamoto, Y.; Yamamoto, H. *Eur. J. Org. Chem.* **2006**, *2006*, 2031–2043.

(36) Chaiyaveij, D.; Cleary, L.; Batsanov, A. S.; Marder, T. B.; Shea, K. J.; Whiting, A. *Org. Lett.* **2011**, *13*, 3442–3445.

(37) Sandoval, D.; Frazier, C. P.; Bugarin, A.; Read de Alaniz, J. *J. Am. Chem. Soc.* **2012**, *134*, 18948–18951.

(38) Baidya, M.; Griffin, K. A.; Yamamoto, H. *J. Am. Chem. Soc.* **2012**, *134*, 18566–18569.

(39) Selig, P. *Angew. Chemie Int. Ed.* **2013**, *52*, 7080–7082.

(40) Palmer, L.; Frazier, C. P.; Read de Alaniz, J. *Synthesis.* **2013**, *46*, 269–280.

(41) Baidya, M.; Yamamoto, H. *Synthesis.* **2013**, *45*, 1931–1938.

(42) Frazier, C. P.; Sandoval, D.; Palmer, L. I.; Read de Alaniz, J. *Chem. Sci.* **2013**, *4*, 3857–3862.

(43) Yang, W.; Huang, L.; Yu, Y.; Pflasterer, D.; Rominger, F.; Hashmi, A. S. K. *Chem. Eur. J.* **2014**, *20*, 3927–3931.

(44) Yu, C.; Song, A.; Zhang, F. Wang, W. *ChemCatChem.* **2014**, *6*, 1863–1865.

(45) Sandoval, D.; Samoshin, A. V; Read de Alaniz, J. *Org. Lett.* **2015**, *17*, 4514–4517.

(46) Ramakrishna, I.; Grandhi, G. S.; Sahoo, H.; Baidya, M. *Chem. Commun.* **2015**, *51*, 13976–13979.

(47) Maji, B.; Yamamoto, H. *Angew. Chem.* **2014**, *126*, 14700–14703.

(48) Maji, B.; Yamamoto, H. *Bull. Chem. Soc. Jpn.* **2015**, *88*, 753–762.

(49) Xu, C.; Zhang, L.; Luo, S. *Angew. Chem. Int. Ed.* **2014**, *53*, 4149–4153.

(50) Merino, P.; Tejero, T.; Delso, I.; Matute, R. *Synthesis* **2016**, *48*, 653–676.

(51) Cline, M. R.; Tu, C.; Silverman, D. N.; Toscano, J. P. *Free Radic. Biol. Med.* **2011**,

50, 1274–1279.

(52) Chavez, T. A.; Toscano, J. P. "Detection of HNO by Membrane Inlet Mass Spectrometry." In *The Chemistry and Biology of Azanone (HNO)*; Marti, M.A.; Doctorovich, F.; Farmer, P., Ed.; Elsevier, 2016, 255–267.

(53) (a) Momiyama, N.; Yamamoto, H. *J. Am. Chem. Soc.* **2004**, 126, 5360–5361. (b) Momiyama, N.; Yamamoto, H. *J. Am. Chem. Soc.* **2005**, 127, 1080–1081. (c) Guo, H.-M.; Cheng, L.; Cun, L.-F.; Gong, L.-Z.; Mi, A.-Q.; Jiang, Y. Z. *Chem. Commun.* **2006**, 429–431. (d) Kano, T.; Ueda, M.; Takai, J.; Maruoka, K. *J. Am. Chem. Soc.* **2006**, *128*, 6046–6047. (e) Palomo,C.; Vera,S.; Velilla, I.; Mielgo, A.; Gońez- Bengoa, E. *Angew. Chem., Int. Ed.* **2007**, *46*, 8054–8056. (f) Lopez-Cantarero, J.; Cid, M. B.; Poulsen, T. B.; Bella, M.; Ruano, J. L. G.; Jørgensen, K. A. *J. Org. Chem.* **2007**, *72*, 7062–7065. (g) Shen, K.; Liu, X.; Wang, G.; Lin, L.; Feng, X. Angew. Chem., Int. Ed. **2011**, *50*, 4684–4688. (h) Yanagisawa, A.; Fujinami, T.; Oyokawa, Y.; Sugita, T.; Yoshida, K. *Org. Lett.* **2012**, *14*, 2434–2437.

(54) Glover, S. A. In *The Chemistry of Hydroxylamines, Oximes, and Hydroxamic Acids, Part 2*; Rappoport, Z., Liebman, J. F., Eds.; John Wiley & Sons: Chichester, West Sussex, 2009, p 839–923.

(55) Guthrie, D. A.; Nourian, S.; Toscano, J. P. "Hydroxylamines with Organic-Based Leaving Groups as HNO Donors." In *The Chemistry and Biology of Azanone (HNO)*; Marti, M.A., Doctorovich, F., Farmer, P., Ed.; Elsevier, 2016, 37–51.

(56) Shao, Y.; Molnar, L. F.; Jung, Y.; Kussmann, J.; Ochsenfeld, C.; Brown, S. T.; Gilbert, A. T. B.; Slipchenko, L. V.; Levchenko, S. V.; O'Neill, D. P.; DiStasio, R.

A., Jr.; Lochan, R. C.; Wang, T.; Beran, G. J. O.; Besley, N. A.; Herbert, J. M.; Lin, C. Y.; Van Voorhis, T.; Chien, S. H.; Sodt, A.; Steele, R. P.; Rassolov, V. A.; Maslen, P. E.; Korambath, P. P.; Adamson, R. D.; Austin, B.; Baker, J.; Byrd, E. F. C.; Dachsel, H.; Doerksen, R. J.; Dreuw, A.; Dunietz, B. D.; Dutoi, A. D.; Furlani, T. R.; Gwaltney, S. R.; Heyden, A.; Hirata, S.; Hsu, C.-P.; Kedziora, G.; Khalliulin, R. Z.; Klunzinger, P.; Lee, A. M.; Lee, M. S.; Liang, W. Z.; Lotan, I.; Nair, N.; Peters, B.; Proynov, E. I.; Pieniazek, P. A.; Rhee, Y. M.; Ritchie, J.; Rosta, E.; Sherrill, C. D.; Simmonett, A. C.; Subotnik, J. E.; Woodcock, H. L., III; Zhang, W.; Bell, A. T.; Chakraborty, A. K.; Chipman, D. M.; Keil, F. J.; Warshel, A.; Hehre, W. J.; Schaefer, H. F.; Kong, J.; Krylov, A. I.; Gill, P. M. W.; Head-Gordon, M. *Phys. Chem. Chem. Phys.* **2006**, *8*, 3172–3191.

(57) Rablen, P. R.; Bentrup, K. H. *J. Am. Chem. Soc.* **2003**, *125*, 2142–2147.

(58) Defoin, A.; Fritz, H.; Schmidlin, C.; Streith, J. *Helv. Chim. Acta* **1987**, *70*, 554–569.

(59) Guimond, N.; Gorelsky, S. I.; Fagnou, K. *J. Am. Chem. Soc.* **2011**, *133*, 6449–6457.

2.7. Supporting Information

2.7.1. Analysis of Nitrous Oxide (N_2O) by Headspace Gas Chromatography.

A gas chromatography instrument equipped with a 1041 injector, electron capture detector, and 2 m x 2 mm x 1/8 in ShinCarbon ST packed column was applied for the analysis of nitrous oxide (N_2O). Grade 5.0 nitrogen was used as both the carrier (8 mL/min) and the make-up (22 mL/min) gas. For all the measurements, the column oven temperature was kept constant at 150 °C, and the injector oven and the detector oven were held at 200 °C and 300 °C, respectively. A 100 µL gastight syringe with a sample-lock was used for all gas injections. Samples were prepared in 6 mL headspace vials with volumes pre-measured for sample uniformity (actual vial volume ranges from 5.8 - 6.3 mL). Vials were charged with 3 mL of phosphate buffer containing the metal chelator, diethylenetriaminepentaacetic acid (DTPA), and fit with rubber septa and 20 mm aluminum seals. The vials were purged with argon and equilibrated for at least 10 minutes at 37 °C in a dry block heater. A 10 mM stock solution of Angeli's salt (AS) was prepared in 10 mM sodium hydroxide, and HNO donors **1a-g** (10 mM) were prepared in acetonitrile and used immediately after preparation. 30 µL of the stock solutions was transferred into vials using a gastight syringe, yielding final concentrations of 0.1 mM. Substrates were then incubated long enough to ensure complete decomposition and equilibration of N_2O with the headspace. For each sample, 60 µL of the headspace was sampled and injected three times using a gastight syringe with a sample lock. The N_2O yield was averaged and reported

relative to the standard, Angeli's salt.

2.7.2. X-ray Crystallographic Data

All reflection intensities were measured at 110(2) K using a diffractometer with either enhance graphite-monochromated Mo *K*α radiation (λ = 0.71073 Å) or Cu *K*α radiation (λ = 1.54178 Å) equipped with mirror optics. The program CrysAlisPro was used to refine the cell dimensions and for data reduction. The structure was solved with the program SHELXS-2013/SHELXS-2014/7 and was refined on F^2 with SHELXL-2013/SHELXL-2014/7. Empirical absorption correction using spherical harmonics or analytical numeric absorption corrections based on a multifaceted crystal model were applied using CrysAlisPro. The temperature of the data collection was controlled using the system Cryojet. The H atoms were placed at calculated positions (unless otherwise specified) using the instructions AFIX 43 or AFIX 137 with isotropic displacement parameters having values 1.2 or 1.5 times *U*eq of the attached C atoms. For **NHPY 1a**, the H atoms attached to O2 and O1W (lattice water molecule) were found from difference Fourier maps. Their coordinates and isotropic temperature factors were refined freely. For **NHPY 1b** and **NHPY 1d**, the H atoms attached to O3 were found from difference Fourier maps. Their coordinates and isotropic temperature factor were refined freely. For **NHPY 1g**, the H atoms attached to O2A and O2B were found from difference Fourier maps, and the coordinates were refined freely.

NHPY 1a. Fw = 336.35, colorless block, 0.43 × 0.37 × 0.30 mm³, monoclinic, $P2_1/c$ (no. 14), a = 12.2766(2), b = 11.1657(3), c = 12.4961(3) Å, β = 99.727(2)°, V = 1688.30(7) Å³, Z = 4, D_x = 1.323 g cm⁻³, μ = 0.101 mm⁻¹, abs. corr. range: 0.968–0.977. 12780 Reflections were measured up to a resolution of $(\sin \theta/\lambda)_{max}$ = 0.62 Å⁻¹. 3409 Reflections were unique (R_{int} = 0.0374), of which 2931 were observed [$I > 2\ \sigma(I)$]. 233 Parameters were refined. $R1/wR2$ [$I > 2\ \sigma(I)$]: 0.0437/0.1157. $R1/wR2$ [all refl.]: 0.0509/0.1199. S = 1.070. Residual electron density found between –0.26 and 0.53 e Å⁻³. Displacement ellisoids are given at the 50% probability level.

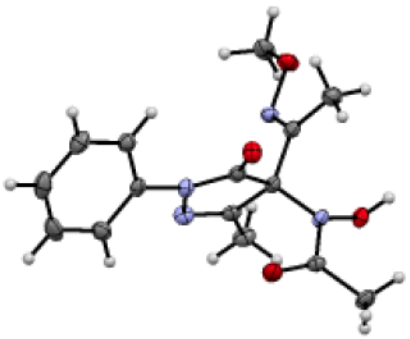

NHPY 1b. Fw = 256.27, irregular colorless lath, 0.43 × 0.12 × 0.08 mm³, orthorhombic, $Pna2_1$ (no. 33), a = 9.49728(11), b = 21.3932(2), c = 6.35861(9) Å, V = 1291.92(3) Å³, Z = 4, D_x = 1.318 g cm⁻³, μ = 0.872 mm⁻¹, abs. corr. range: 0.774–0.947. 8608 Reflections were measured up to a resolution of $(\sin \theta/\lambda)_{max}$ = 0.62 Å⁻¹. 2408 Reflections were unique (R_{int} = 0.0208), of which 2358 were observed [$I > 2\sigma(I)$]. 172 Parameters were refined using 1 restraint. $R1/wR2$ [$I > 2\sigma(I)$]: 0.0283/0.0757. $R1/wR2$ [all refl.]: 0.0289/0.0763. S = 1.046. Residual electron density found between –0.15 and 0.23 e Å⁻³. Displacement ellisoids are given at the 50% probability level

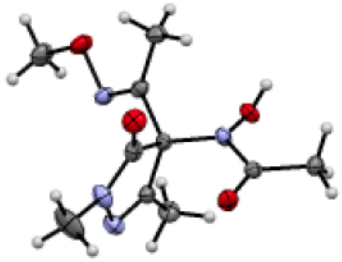

NHPY 1d. Fw = 272.27, colorless rod, 0.46 × 0.08 × 0.06 mm³, monoclinic, $P2_1$ (no. 4), a = 9.44384(14), b = 6.72231(9), c = 10.34284(17) Å, β = 96.4986(14)°, V = 652.390(17) Å³, Z = 2, D_x = 1.386 g cm⁻³, μ = 0.957 mm⁻¹, abs. corr. range: 0.796–0.956. 7685 Reflections were measured up to a resolution of $(\sin \theta/\lambda)_{max}$ = 0.62 Å⁻¹. 2562 Reflections were unique (R_{int} = 0.0258), of which 2500 were observed [$I > 2\sigma(I)$]. 182 Parameters were refined using 1 restraint. $R1/wR2$ [$I > 2\sigma(I)$]: 0.0251/0.0648. $R1/wR2$ [all refl.]: 0.0259/0.0657. S = 1.052. Residual electron density found between –0.15 and 0.19 e Å⁻³. Displacement ellisoids are given at the 50% probability level.

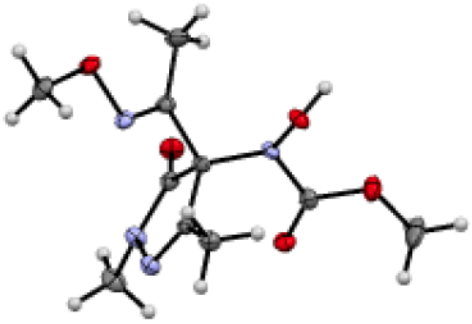

NHPY 1g. Fw = 290.32, colorless needle, 0.45 × 0.05 × 0.05 mm³, triclinic, P-1 (no. 2), a = 10.8050(3), b = 11.4659(3), c = 13.3709(4) Å, α = 111.885(3), β = 90.695(2), γ = 93.750(2)°, V = 1532.65(8) Å³, Z = 4, D_x = 1.258 g cm⁻³, μ = 0.750 mm⁻¹, abs. corr. range: 0.54–1.00. 17989 Reflections were measured up to a resolution of $(\sin \theta/\lambda)_{max}$ = 0.62 Å⁻¹. 5960 Reflections were unique (R_{int} = 0.0338), of which 5119 were observed [$I > 2\sigma(I)$]. 393 Parameters were refined. $R1/wR2$ [$I > 2\sigma(I)$]: 0.0404/0.1071. $R1/wR2$ [all refl.]: 0.0470/0.1125. S = 1.042. Residual electron density found between –0.26 and 0.32 e Å⁻³. Displacement ellisoids are given at the 50% probability level

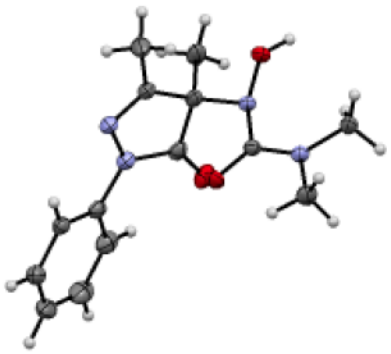

2.7.3. Membrane Inlet Mass Spectrometry (MIMS) Experiment:

HNO was detected using a MIMS system that consists of a sample cell and membrane probe that has been optimized to detect gases dissolved in aqueous solution. The cell contains rotary blades with an imbedded magnet for efficient stirring past the silastic membrane. The sample cell is also fitted with a heating/cooling jacket for temperature regulation. Both the sample cell and the stock solutions are purged with argon for 10 minutes before the experiment. Injection of 100 μM of **NHPY** donor **1e** into the MIMS sample cell containing 0.1 M phosphate buffered saline containing 0.1 mM DTPA results in an increase in the *m/z* 31 (HNO^+) signal.

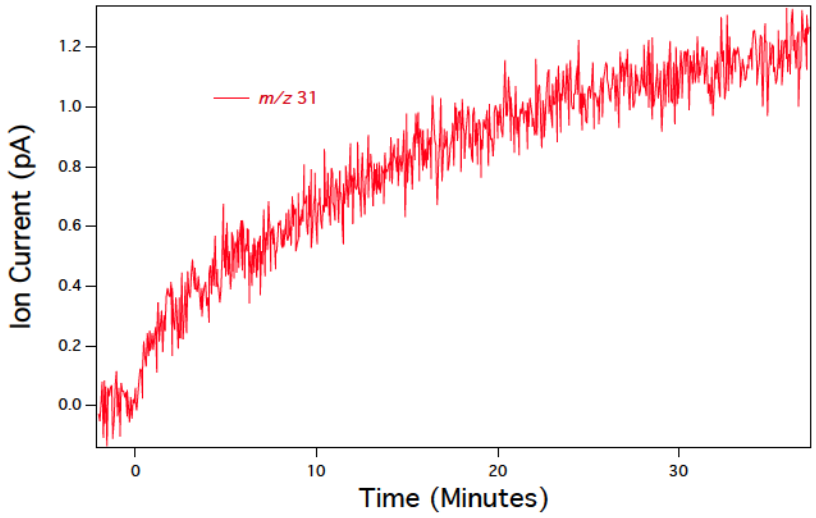

Figure 2-5. MIMS signal obesreved at *m/z* 31 after injection of 100 μM of **NHPY** donor **1e** to an argon-purged 0.1 M PBS solution pH 7.4 at 37 °C with 0.1 mM DTPA.

Scheme 2-7. ^{1}H NMR Spectroscopy Analysis of Nitrosocarbonyl Trapping by Pyrazolone 2c

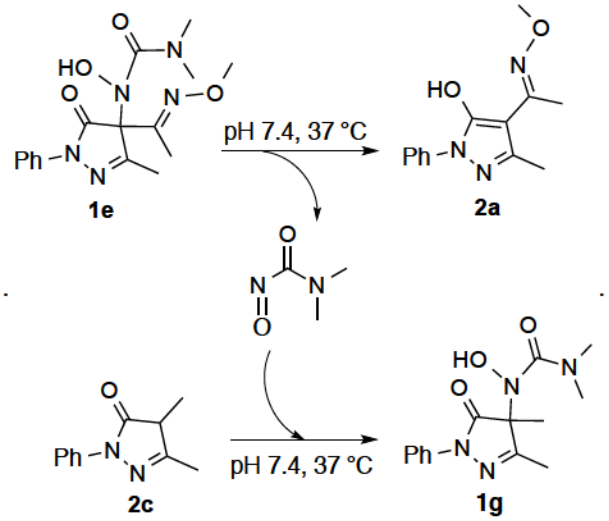

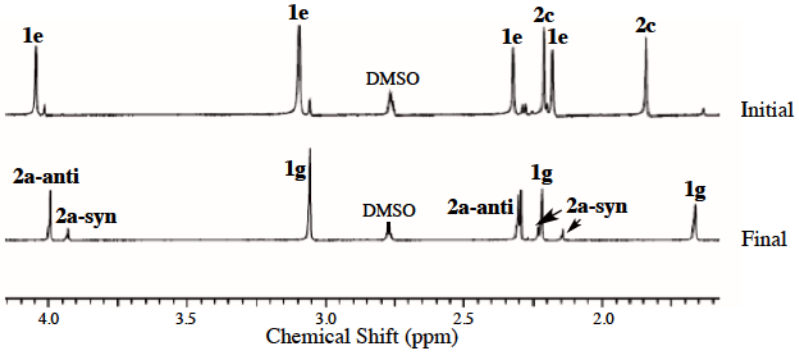

The decomposition of 5 mM of donor **1e** was examined by ^{1}H NMR spectroscopy in presence of 5 mM of pyrazolone **2c** in 0.25 M phosphate buffer with 0.2 mM DTPA at pH 7.4, 80% H_2O, 10% D_2O, and 10% DMSO-d_6 at 37 °C under argon. Spectra were collected at the start of the experiment and after complete decomposition.

2.7.4. Density Functional Theory (DFT) Calculations

All calculations were performed at the B3LYP/6-31G(d) level using Spartan '14 modeling software.[2] Geometries were fully optimized and vibrational frequencies were also calculated to verify minimum energy structures (no imaginary frequencies) or transition states (one imaginary frequency) and to provide zero-point vibrational energy corrections.

For neutral and anionic model hydroxamic acid derivatives **3a-b** (Figure S1a), the lowest energy ground states for the *syn* and *anti* conformers (GS1 and GS2, respectively) were calculated. Two transition states, one of which has the nitrogen lone pair *anti* to the carbonyl oxygen (TS1) and the other with the lone pair *syn* (TS2), were examined. For hydroxamic acid **3c** (Figure S2a), three transition states (TS1, TS2, and TS3) were identified that connect the *syn* (GS1) and *anti* (GS2 and GS3) minima. Previous computational investigations of urea derivative have similarly identified three ground states and transition states. For anionic hydroxamic acid derivatives **3a-c** (Figure S1b and S2b), *syn* and *anti* conformers (GS1 and GS2, respectively) and two transition states were calculated (TS1 and TS2).

We also examined the B3LYP/6-31G(d) calculated lowest energy geometries and vibrational frequencies for neutral and anionic NHPY donors **1a**, **1c**, and **1e**. The transition states for nitrosocarbonyl formation from these anionic donors were also calculated.

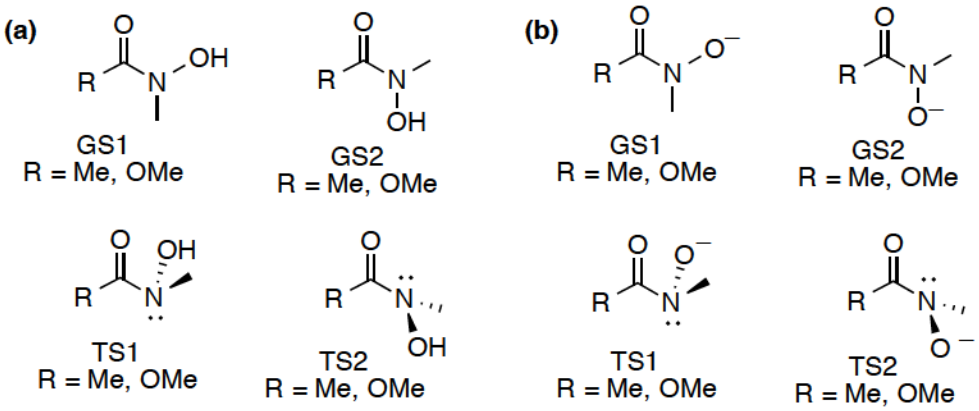

Figure 2-6. The lowest energy geometries of (a) neutral and (b) anionic hydroxamic acid derivatives **3a** (R = Me) and **3b** (R = OMe) and transition states for C(O)-N bond rotation.

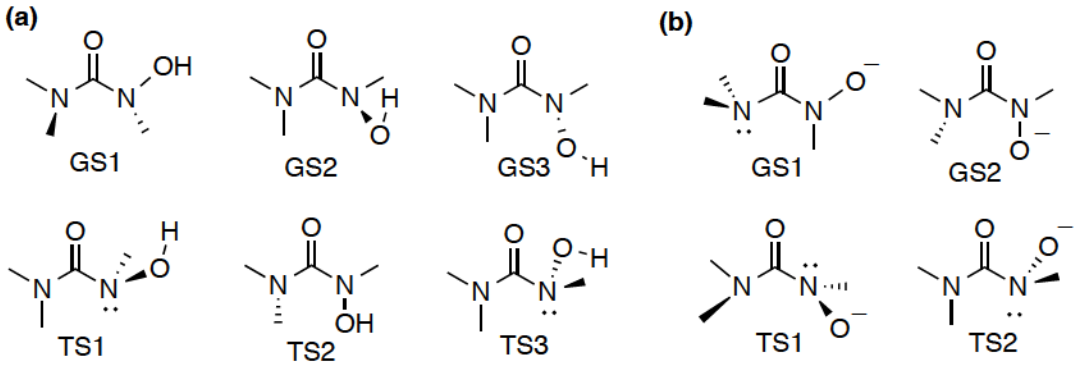

Figure 2-7. The lowest energy geometries of (a) neutral and (b) anionic hydroxamic acid derivative **3c** and transition states for C(O)-N bond rotation.

Table 2-6. B3LYP/6-31G(d) Optimized Geometries, Energies, ZPE and Temperature Corrections for *N*-hydroxy-*N*-methylacetamide (3a, GS1):

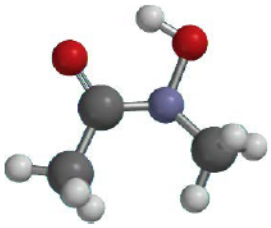

B3LYP/6-31G(d) Energy (E): -323.682931 hartrees

ZPE: 279.3172 kJ/mol

Temp. Correction: 298.9793 kJ/mol

G° = E + ZPE + "Temp. Correction": -202975.8884 kcal/mol

	Atomic	Cartesian Coordinates (Angstroms)		
	Number	X	Y	Z
1	C2	0.7239598	-0.1989052	-0.0169590
2	C3	1.6820838	0.9745635	-0.0289737
3	H5	1.6370652	1.5286163	0.9162305
4	H6	1.4728393	1.6735174	-0.8445657
5	H7	2.6896644	0.5740363	-0.1490820
6	O1	1.0968026	-1.3722089	0.0936361
7	N1	-0.6048689	0.0598945	-0.1847683
8	C4	-1.3301915	1.2777573	0.0953432
9	H8	-1.6842832	1.2982462	1.1344908
10	H9	-2.1941570	1.3375045	-0.5727126
11	H10	-0.6815028	2.1349170	-0.0891680
12	O2	-1.4353650	-1.0668825	-0.0275603
13	H11	-0.7521566	-1.7738616	0.0731155

Table 2-7. B3LYP/6-31G(d) Calculated IR Frequencies (cm^{-1}, uncorrected) and Intensities for *N*-hydroxy-*N*-methylacetamide (3a, GS1):

	cm^{-1}	Intensity		cm^{-1}	Intensity		cm^{-1}	Intensity
1	104	0.09	12	983	30.19	23	1516	6.91
2	108	4.74	13	1030	12.16	24	1535	56.97
3	139	0.89	14	1062	7.42	25	1586	42.44
4	243	6.60	15	1161	13.68	26	1729	241.13
5	296	6.19	16	1183	12.45	27	3046	44.92
6	407	23.67	17	1238	61.42	28	3063	5.85
7	455	4.04	18	1402	92.21	29	3119	19.81
8	480	71.03	19	1434	97.22	30	3127	9.34
9	609	33.94	20	1473	3.32	31	3173	10.63
10	621	19.78	21	1493	16.92	32	3177	5.22
11	742	15.82	22	1503	32.38	33	3460	76.83

Table 2-8. B3LYP/6-31G(d) Optimized Geometries, Energies, ZPE and Temperature Corrections for *N*-hydroxy-*N*-methylacetamide (3a, GS2):

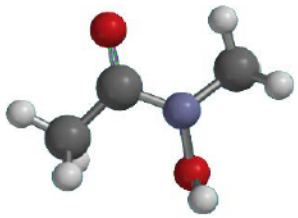

B3LYP/6-31G(d) Energy (E): -323.681788 hartrees

ZPE: 278.6126 kJ/mol

Temp. Correction: 298.6464 kJ/mol

G° = E + ZPE + "Temp. Correction": -202975.4191 kcal/mol

	Atomic	Cartesian Coordinates (Angstroms)		
	Number	X	Y	Z
1	C2	0.6908628	-0.3573148	0.0371970
2	C3	1.7855324	0.6887276	-0.0458733
3	H5	1.7404161	1.3901430	0.7934103
4	H6	1.6875508	1.2772178	-0.9637293
5	H7	2.7447562	0.1692036	-0.0414910
6	O1	0.9052973	-1.5598144	0.0009249
7	N1	-0.5994860	0.1252884	0.2211921
8	C4	-1.7562416	-0.7047956	-0.0742486
9	H8	-2.0507770	-0.6113056	-1.1271043
10	H9	-2.5947908	-0.4051322	0.5616937
11	H10	-1.4801762	-1.7373877	0.1389229
12	O2	-0.8002107	1.4797862	-0.1401100
13	H11	-1.0121911	1.9207644	0.7009832

Table 2-9. B3LYP/6-31G(d) Calculated IR Frequencies (cm^{-1}, uncorrected) and Intensities for *N*-hydroxy-*N*-methylacetamide (3a, GS2):

	cm^{-1}	Intensity		cm^{-1}	Intensity		cm^{-1}	Intensity
1	117	2.50	12	954	5.68	23	1506	7.60
2	138	0.60	13	1013	18.40	24	1514	12.61
3	141	3.32	14	1063	6.95	25	1540	10.61
4	238	6.89	15	1157	24.84	26	1785	213.15
5	286	5.69	16	1168	13.33	27	3050	42.82
6	382	100.70	17	1203	70.46	28	3070	4.64
7	389	18.35	18	1374	76.62	29	3116	31.13
8	489	15.39	19	1418	32.54	30	3134	9.86
9	580	4.00	20	1426	115.37	31	3177	8.43
10	591	10.09	21	1456	31.51	32	3189	1.55
11	733	13.78	22	1495	10.67	33	3689	24.90

Table 2-10. B3LYP/6-31G(d) Optimized Geometries, Energies, ZPE and Temperature Corrections for *N*-hydroxy-*N*-methylacetamide (3a, TS2):

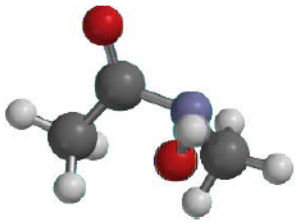

B3LYP/6-31G(d) Energy (E): -323.656483 hartrees

ZPE: 276.6488 kJ/mol

Temp. Correction: 296.7526 kJ/mol

G° = E + ZPE + "Temp. Correction": -202960.462 kcal/mol

	Atomic	Cartesian Coordinates (Angstroms)		
	Number	X	Y	Z
1	C2	0.7779790	-0.1061065	-0.1852166
2	C3	1.1861109	1.0858436	0.6549626
3	H5	0.6279339	1.0922462	1.5967822
4	H6	0.9661704	2.0240308	0.1318571
5	H7	2.2577495	1.0348918	0.8534240
6	O1	1.5657357	-0.8787507	-0.6721910
7	N1	-0.6601149	-0.3597083	-0.3712624
8	C4	-1.4772213	0.8266867	-0.6032533
9	H8	-1.4561258	1.5499450	0.2245187
10	H9	-2.5095618	0.5034272	-0.7596634
11	H10	-1.1212631	1.3102741	-1.5197335
12	O2	-1.0568117	-0.8726123	0.9364179
13	H11	-1.1367033	-1.8244964	0.7588799

Table 2-11. B3LYP/6-31G(d) Calculated IR Frequencies (cm^{-1}, uncorrected) and Intensities for *N*-hydroxy-*N*-methylacetamide (3a, TS2):

	cm^{-1}	Intensity		cm^{-1}	Intensity		cm^{-1}	Intensity
1	-77	3.19	12	887	21.44	23	1499	5.64
2	193	0.29	13	992	22.64	24	1513	16.72
3	234	0.10	14	1046	19.36	25	1535	3.16
4	271	0.71	15	1107	5.86	26	1849	209.39
5	289	2.62	16	1153	61.66	27	3027	35.57
6	377	74.91	17	1156	6.71	28	3064	3.29
7	386	33.78	18	1259	65.42	29	3106	23.54
8	479	9.16	19	1374	54.86	30	3129	5.03

9	570	6.78	20	1406	37.53	31	3144	18.51
10	610	3.97	21	1457	0.19	32	3174	7.60
11	733	18.32	22	1495	11.81	33	3736	49.25

Table 2-12. B3LYP/6-31G(d) Optimized Geometries, Energies, ZPE and Temperature Corrections for *N*-hydroxy-*N*-methylacetamide (3a, TS1):

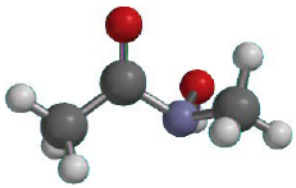

B3LYP/6-31G(d) Energy (E): -323.656757 hartrees

ZPE: 276.3121 kJ/mol

Temp. Correction: 296.6113 kJ/mol

G° = E + ZPE + "Temp. Correction": -202960.7482 kcal/mol

	Atomic	Cartesian Coordinates (Angstroms)		
	Number	X	Y	Z
1	C2	-0.7194683	-0.0896141	0.1828935
2	C3	-1.8940165	0.1828863	-0.7201923
3	H5	-1.7923299	-0.3919099	-1.6484517
4	H6	-1.8903550	1.2409246	-1.0087954
5	H7	-2.8313288	-0.0656472	-0.2188862
6	O1	-0.7991516	-0.4725114	1.3228725
7	N1	0.5768895	0.1713736	-0.4828306
8	C4	1.4318900	-1.0182414	-0.4136196
9	H8	1.5867596	-1.3551767	0.6190867
10	H9	2.3924216	-0.7784468	-0.8759968
11	H10	0.9529201	-1.8185281	-0.9901719

12	O2	1.2102658	1.1747692	0.3617937
13	H11	1.3443408	1.9009222	-0.2687894

Table 2-13. B3LYP/6-31G(d) Calculated IR Frequencies (cm^{-1}, uncorrected) and Intensities for *N*-hydroxy-*N*-methylacetamide (3a, TS1):

	cm^{-1}	Intensity		cm^{-1}	Intensity		cm^{-1}	Intensity
1	-110	1.70	12	895	20.10	23	1498	10.67
2	183	0.32	13	1001	14.11	24	1504	6.12
3	246	1.13	14	1026	30.23	25	1528	8.92
4	257	2.54	15	1095	6.10	26	1846	150.33
5	293	2.00	16	1158	15.30	27	3042	27.52
6	328	62.25	17	1180	61.61	28	3057	1.02
7	352	38.33	18	1243	93.72	29	3112	19.21
8	464	2.96	19	1378	55.95	30	3115	7.26
9	605	1.98	20	1416	32.98	31	3146	20.96
10	632	26.63	21	1457	0.79	32	3171	12.27
11	744	13.80	22	1488	13.78	33	3732	32.34

Table 2-14. B3LYP/6-31G(d) Optimized Geometries, Energies, ZPE and Temperature Corrections for *N*-methyl-*N*-hydroxy-methylcarbamate (3b, TS2):

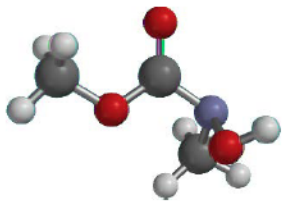

B3LYP/6-31G(d) Energy (E): -398.883941 hartrees

ZPE: 292.3093 kJ/mol

Temp. Correction: 313.9885 kJ/mol

G° = E + ZPE + "Temp. Correction": -250158.5418 kcal/mol

	Atomic	Cartesian Coordinates (Angstroms)		
	Number	X	Y	Z
1	C1	-0.2746898	0.4725827	-0.1682392
2	O2	-0.8411466	1.4888061	-0.4872776
3	O3	-0.8910904	-0.6729908	0.1700789
4	C2	-2.3272935	-0.6182950	0.1806819
5	H3	-2.6746139	0.1215916	0.9070736
6	H4	-2.6550532	-1.6185583	0.4659353
7	H5	-2.7074492	-0.3537482	-0.8097915
8	N1	1.1682745	-0.3595667	-0.1115332
9	C3	1.6889669	-0.7365604	-0.9323253
10	H6	1.3255811	-1.7189648	-0.6067430
11	H7	2.7799458	-0.7104853	-0.8774753
12	H8	1.3840975	-0.5556448	-1.9688931
13	O4	1.4717235	0.0313141	1.2705566
14	H9	1.9317758	0.8354446	1.5630583

Table 2-15. B3LYP/6-31G(d) Calculated IR Frequencies (cm^{-1}, uncorrected) and Intensities for compound 3b (TS2):

	cm^{-1}	Intensity		cm^{-1}	Intensity		cm^{-1}	Intensity
1	-71	1.11	13	839	17.79	25	1506	5.80
2	131	3.07	14	919	20.06	26	1514	6.39
3	159	0.43	15	1034	21.30	27	1523	8.54
4	219	6.45	16	1096	10.86	28	1536	8.77
5	275	1.44	17	1165	21.95	29	1845	286.14
6	311	2.66	18	1185	169.50	30	3048	26.84
7	333	12.68	19	1187	4.07	31	3075	28.55

8	370	78.76	20	1227	45.64	32	3122	19.99
9	385	24.71	21	1291	240.03	33	3149	20.63
10	568	5.84	22	1389	54.87	34	3151	20.36
11	639	4.36	23	1463	2.11	35	3183	15.86
12	811	20.09	24	1492	6.56	36	3730	41.06

Table 2-16. B3LYP/6-31G(d) Optimized Geometries, Energies, ZPE and Temperature Corrections for *N*-methyl-*N*-hydroxy-methylcarbamate (3b, TS1):

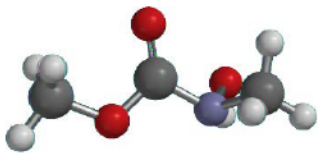

B3LYP/6-31G(d) Energy (E): -398.884152 hartrees

ZPE: 292.0982 kJ/mol

Temp. Correction: 313.9673 kJ/mol

G° = E + ZPE + "Temp. Correction": -250158.7297 kcal/mol

	Atomic	Cartesian Coordinates (Angstroms)		
	Number	X	Y	Z
1	C1	-0.2694872	-0.0161145	-0.1813712
2	O2	-0.4367793	-0.0487380	-1.3762377
3	O3	-1.2498194	0.0260772	0.7329219
4	C2	-2.5822266	0.0437331	0.1884001
5	H3	-2.7153718	0.9079760	-0.4680009
6	H4	-3.2472977	0.1057645	1.0503011
7	H5	-2.7713378	-0.8695877	-0.3821694
8	N1	1.0108127	-0.0081132	0.5064043
9	C3	1.8132013	1.1416815	0.0766548

10	H6	1.9732399	1.1507352	-1.0090552
11	H7	2.7737413	1.0962513	0.5942931
12	H8	1.2887977	2.0544094	0.3800089
13	O4	1.6946335	-1.1890868	0.0133582
14	H9	1.7893366	-1.7105769	0.8273513

Table 2-17. B3LYP/6-31G(d) Calculated IR Frequencies (cm^{-1}, uncorrected) and Intensities for *N*-methyl-*N*-hydroxy-methylcarbamate (3b, TS1):

	cm^{-1}	Intensity		cm^{-1}	Intensity		cm^{-1}	Intensity
1	-84	1.24	13	853	19.43	25	1506	6.47
2	135	0.45	14	922	20.07	26	1512	7.04
3	165	1.98	15	1027	16.58	27	1523	9.27
4	227	6.34	16	1090	8.57	28	1528	9.06
5	274	2.60	17	1163	8.25	29	1834	229.45
6	306	1.99	18	1187	1.50	30	3044	27.58
7	324	67.79	19	1204	61.67	31	3075	25.68
8	340	48.74	20	1233	35.43	32	3119	18.95
9	365	0.31	21	1290	462.82	33	3152	18.82
10	529	7.91	22	1392	50.93	34	3155	19.02
11	680	6.87	23	1459	1.72	35	3183	16.10
12	812	17.03	24	1491	11.18	36	3734	37.51

Table 2-18. B3LYP/6-31G(d) Optimized Geometries, Energies, ZPE and Temperature Corrections for *N*-methyl-*N*-hydroxy-methylcarbamate (3b, GS2):

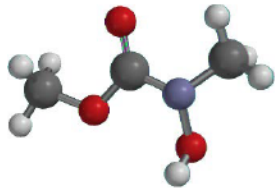

B3LYP/6-31G(d) Energy (E): -398.90247 hartrees

ZPE: 292.9144 kJ/mol

Temp. Correction: 315.0936 kJ/mol

G° = E + ZPE + "Temp. Correction": -250169.7602 kcal/mol

	Atomic	Cartesian Coordinates (Angstroms)		
	Number	X	Y	Z
1	C1	0.2496925	-0.3543167	0.0569280
2	O2	0.5064796	-1.5426216	0.0012979
3	O3	1.1665214	0.6361034	0.0412838
4	C2	2.5235351	0.1823228	-0.0682982
5	H3	2.7918910	-0.4471520	0.7845151
6	H4	3.1295647	-1.0890277	-0.0813579
7	H5	2.6681769	-0.3874483	-0.9900314
8	N1	-1.0304624	0.1465357	0.2539143
9	C3	-2.1702137	-0.6907013	-0.0849785
10	H6	-2.3857822	-0.6599658	-1.1610532
11	H7	-3.0430190	-0.3344081	0.4674786
12	H8	-1.9356361	-1.7134850	0.2090523
13	O4	-1.2402655	1.4809488	-0.1745945
14	H9	-1.0919271	2.0084077	0.6281918

Table 2-19. B3LYP/6-31G(d) Calculated IR Frequencies (cm^{-1}, uncorrected) and Intensities for *N*-methyl-*N*-hydroxy-methylcarbamate (3b, GS2):

	cm^{-1}	Intensity		cm^{-1}	Intensity		cm^{-1}	Intensity
1	107	0.65	13	844	20.81	25	1512	4.93
2	116	5.81	14	970	4.57	26	1513	9.34
3	136	0.24	15	1065	30.40	27	1528	5.31
4	174	3.22	16	1161	47.74	28	1542	14.63
5	199	33.72	17	1185	37.18	29	1806	258.04
6	260	71.22	18	1189	1.14	30	3048	45.59
7	271	7.68	19	1212	21.61	31	3074	33.05
8	355	43.30	20	1238	199.70	32	3130	24.88
9	384	1.88	21	1393	354.39	33	3149	23.05
10	549	5.04	22	1436	76.86	34	3178	18.18
11	605	3.65	23	1460	15.08	35	3192	3.59
12	771	26.46	24	1500	50.91	36	3720	33.57

Table 2-20. B3LYP/6-31G(d) Optimized Geometries, Energies, ZPE and Temperature Corrections for *N*-methyl-*N*-hydroxy-methylcarbamate (3b, GS1):

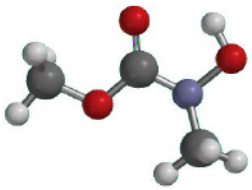

B3LYP/6-31G(d) Energy (E):	-398.903703 hartrees
ZPE:	293.4614 kJ/mol
Temp. Correction:	315.3582 kJ/mol
G° = E + ZPE + "Temp. Correction":	-250170.3399 kcal/mol

	Atomic	Cartesian Coordinates (Angstroms)		
	Number	X	Y	Z
1	C1	0.2557244	-0.3122274	-0.0387635
2	O2	0.5336673	-1.5004613	0.0826430
3	O3	1.1496505	0.6979565	-0.0543208
4	C2	2.5232594	0.2830858	0.0254954
5	H3	2.7051155	-0.2735279	0.9481556
6	H4	3.1022806	1.2070189	0.0142755
7	H5	2.7859944	-0.3442691	-0.8302777
8	N1	-1.0254317	0.1209117	-0.2475802
9	C3	-1.5313038	1.4311569	0.1095209
10	H6	-1.7809818	1.4865599	1.1773565
11	H7	-2.4318419	1.6272542	-0.4781568
12	H8	-0.7702114	2.1713074	-0.1354619
13	O4	-1.9941307	-0.8788541	0.0184918
14	H9	-1.4319106	-1.6819447	0.0851418

Table 2-21. B3LYP/6-31G(d) Calculated IR Frequencies (cm^{-1}, uncorrected) and Intensities for *N*-methyl-*N*-hydroxy-methylcarbamate (3b, GS1):

	cm^{-1}	Intensity		cm^{-1}	Intensity		cm^{-1}	Intensity
1	104	7.01	13	839	1.86	25	1512	6.14
2	121	0.03	14	991	7.90	26	1527	9.61
3	136	7.17	15	1080	29.77	27	1531	47.17
4	161	3.49	16	1163	44.38	28	1580	37.24
5	221	0.98	17	1188	0.68	29	1774	293.35
6	256	13.13	18	1203	17.00	30	3046	49.20
7	340	32.53	19	1224	184.85	31	3078	33.32

8	355	64.91	20	1237	63.6	32	3129	20.62
9	410	37.42	21	1388	404.36	33	3155	20.63
10	529	7.99	22	1471	9.09	34	3182	16.02
11	628	15.20	23	1500	41.73	35	3192	4.71
12	745	47.08	24	1505	22.62	36	3561	71.86

Table 2-22. B3LYP/6-31G(d) Optimized Geometries, Energies, ZPE and Temperature Corrections for *N*-hydroxy-*N*, *N'*, *N'*-trimethylurea (3c, TS1):

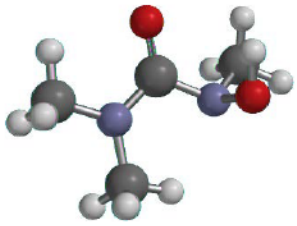

B3LYP/6-31G(d) Energy (E): -418.337917 hartrees

ZPE: 399.1888 kJ/mol

Temp. Correction: 424.0615 kJ/mol

G° = E + ZPE + "Temp. Correction": -262314.2432 kcal/mol

	Atomic	Cartesian Coordinates (Angstroms)		
	Number	X	Y	Z
1	C2	-0.0020036	0.4731751	-0.0234923
2	O1	0.1779011	1.6678954	0.1898195
3	N1	-1.2204878	-0.1173595	-0.1326769
4	C3	-1.4332246	-1.5491273	-0.2989345
5	H5	-1.8454832	-1.9866225	0.6204407
6	H6	-0.4865460	-2.0302292	-0.5325574
7	H7	-2.1494371	-1.7201945	-1.1124475
8	C4	-2.4136572	0.6891205	0.0836072

9	H8	-2.9297074	0.3768758	1.0014965
10	H9	-3.1038917	0.5660347	-0.7596791
11	H10	-2.1211561	1.7344328	0.1706006
12	N2	1.1215061	-0.4513129	-0.1648170
13	C1	2.2453974	0.1527180	-0.8756162
14	H1	2.5702977	1.1024519	-0.4266525
15	H3	1.9400359	0.3417993	-1.9100921
16	H4	3.0657059	-0.5681019	-0.8702695
17	O2	1.5276721	-0.7389460	1.1860777
18	H2	1.7293954	0.1373482	1.5810548

Table 2-23. B3LYP/6-31G(d) Calculated IR Frequencies (cm^{-1}, uncorrected) and Intensities for *N*-hydroxy-*N*, *N'*, *N'*-trimethylurea (3c, TS1):

	cm^{-1}	Intensity		cm^{-1}	Intensity		cm^{-1}	Intensity
1	-65	11.06	17	902	14.55	33	1519	6.92
2	81	0.23	18	987	3.33	34	1523	11.03
3	115	0.07	19	1084	5.11	35	1525	15.7
4	155	0.08	20	1099	5.16	36	1533	13.55
5	220	3.76	21	1137	0.78	37	1562	31.94
6	228	5.11	22	1150	74.43	38	1770	372.56
7	273	0.29	23	1186	37.69	39	3027	43.5
8	310	9.34	24	1191	14.97	40	3031	24.27
9	336	1.79	25	1243	48.74	41	3039	81.76
10	377	21.8	26	1289	52.97	42	3081	39.13
11	434	4.21	27	1424	46.12	43	3089	28.05
12	518	51.86	28	1443	77.56	44	3111	20.69
13	572	88.02	29	1449	22.07	45	3158	14.92
14	615	16.00	30	1459	17.23	46	3193	1.12
15	753	12.59	31	1483	39.62	47	3209	0.83
16	804	3.24	32	1511	19.03	48	3542	2.54

Table 2-24. B3LYP/6-31G(d) Optimized Geometries, Energies, ZPE and Temperature Corrections for compound 3c (GS2):

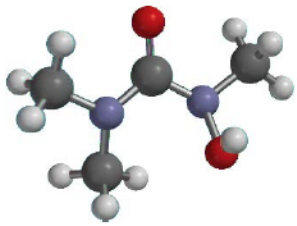

B3LYP/6-31G(d) Energy (E): -418.341575 hartrees

ZPE: 399.4399 kJ/mol

Temp. Correction: 424.7096 kJ/mol

G° = E + ZPE + "Temp. Correction": -262316.3237 kcal/mol

	Atomic	Cartesian Coordinates (Angstroms)		
	Number	X	Y	Z
1	C2	0.0243511	0.5655762	-0.0680072
2	O1	0.1360799	1.7874231	-0.0172034
3	N1	-1.1743240	-0.0949483	0.0145745
4	C3	-1.4089880	-1.4453511	-0.4855047
5	H5	-1.6237152	-2.1478055	0.3289743
6	H6	-0.5403534	-1.8053716	-1.0332170
7	H7	-2.2718646	-1.4258915	-1.1640225
8	C4	-2.3625604	0.6965587	0.2961425
9	H8	-3.0206545	0.1411425	0.9747602
10	H9	-2.9221820	0.9212476	-0.6234009
11	H10	-2.0652133	1.6371401	0.7583184
12	N2	1.1687329	-0.2544683	-0.2483752
13	C1	2.4537895	0.4280058	-0.2185597
14	H1	2.6851912	0.8449997	0.7745062
15	H3	2.4323276	1.2494469	-0.9350365

16	H4	3.2211680	-0.2949589	-0.5027389
17	O2	1.1946137	-1.4184885	0.5699678
18	H2	1.2593327	-1.0942482	1.4919217

Table 2-25. B3LYP/6-31G(d) Calculated IR Frequencies (cm^{-1}, uncorrected) and Intensities for *N*-hydroxy-*N*, *N'*, *N'*-trimethylurea (3c, GS2):

	cm^{-1}	Intensity		cm^{-1}	Intensity		cm^{-1}	Intensity
1	81	4.18	17	913	10.55	33	1516	6.79
2	107	2.66	18	1022	3.9	34	1518	12.83
3	119	0.82	19	1097	7.86	35	1527	11.51
4	150	0.48	20	1135	27.15	36	1535	11.27
5	188	6.74	21	1146	3.47	37	1562	50.57
6	215	1.13	22	1154	73.96	38	1759	322.24
7	253	5.29	23	1182	11.57	39	3012	65.54
8	295	23.51	24	1201	21.11	40	3027	42.12
9	351	4.59	25	1285	20.59	41	3039	76.35
10	374	2.74	26	1303	93.37	42	3085	63.58
11	397	56.02	27	1418	60.32	43	3089	11.37
12	432	68.72	28	1441	142.58	44	3131	21.68
13	553	0.91	29	1461	18.48	45	3185	5.64
14	583	29.06	30	1466	30.65	46	3186	3.23
15	732	5.64	31	1497	36.54	47	3194	4.89
16	779	11.45	32	1515	13.45	48	3572	3.03

Table 2-26. B3LYP/6-31G(d) Optimized Geometries, Energies, ZPE and Temperature Corrections for *N*-hydroxy-*N*, *N'*, *N'*-trimethylurea (3c, TS3):

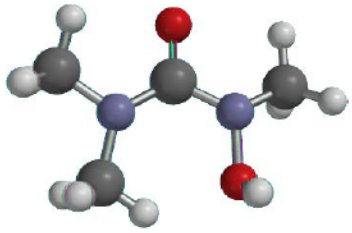

B3LYP/6-31G(d) Energy (E): -418.336455 hartrees

ZPE: 399.1928 kJ/mol

Temp. Correction: 424.4896 kJ/mol

G° = E + ZPE + "Temp. Correction": -262313.2225 kcal/mol

	Atomic	Cartesian Coordinates (Angstroms)		
	Number	X	Y	Z
1	C2	-0.0179120	0.5585954	-0.0442936
2	O1	-0.0736696	1.7861786	0.0301933
3	N1	1.1906063	-0.1058341	-0.0576009
4	C3	1.4989329	-1.5114173	0.1903312
5	H5	2.0487539	-1.9341642	-0.6630536
6	H6	0.5989694	-2.0880687	0.3646780
7	H7	2.1477832	-1.5897322	1.0744383
8	C4	2.3819570	-0.7388833	0.0634610
9	H8	3.1209102	-0.3087899	0.7510625
10	H9	2.8347638	0.7935884	0.9374282
11	H10	2.1159853	1.7436703	-0.3845942
12	N2	-1.2381942	-0.1171116	-0.2786602
13	C1	-2.4580693	0.5377330	0.1864752
14	H1	-3.3051264	0.1066588	-0.3545317
15	H3	-2.3783369	1.5999428	-0.0336482

16	H4	-2.6101026	0.3936445	1.2646640
17	O2	-1.3250061	-1.5131141	-0.0086673
18	H2	-1.4805307	-1.9009918	-0.8870097

Table 2-27. B3LYP/6-31G(d) Calculated IR Frequencies (cm^{-1}, uncorrected) and Intensities for *N*-hydroxy-*N*, *N'*, *N'*-trimethylurea (3c, TS3):

	cm^{-1}	Intensity		cm^{-1}	Intensity		cm^{-1}	Intensity
1	-70	0.57	17	909	13.23	33	1522	8.8
2	82	1.11	18	1026	11.13	34	1532	9.97
3	101	4.77	19	1085	10.77	35	1537	7.4
4	136	1.88	20	1133	49.37	36	1544	14.19
5	166	0.39	21	1146	27.15	37	1565	48.63
6	252	6.93	22	1152	99.04	38	1728	283.74
7	268	2.39	23	1188	2.51	39	3017	43.53
8	285	6.17	24	1193	72.06	40	3027	106.65
9	336	12.2	25	1267	7.48	41	3044	49.61
10	387	105.01	26	1314	79.91	42	3056	50.69
11	410	0.92	27	1399	49.52	43	3078	36.67
12	439	16.47	28	1426	185.73	44	3120	33.38
13	555	1.77	29	1451	59.4	45	3202	1.36
14	586	19.94	30	1455	7.02	46	3209	1.6
15	713	5.77	31	1493	88.18	47	3256	5.07
16	737	28.13	32	1519	8.49	48	3695	30.09

Table 2-28. B3LYP/6-31G(d) Optimized Geometries, Energies, ZPE and Temperature Corrections for *N*-hydroxy-*N*, *N'*, *N'*-trimethylurea (3c, GS3):

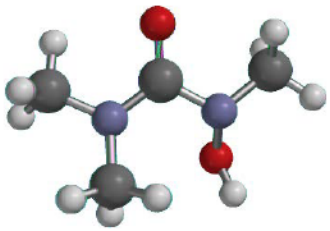

B3LYP/6-31G(d) Energy (E): -418.342619 hartrees

ZPE: 399.7424 kJ/mol

Temp. Correction: 424.9626 kJ/mol

G° = E + ZPE + "Temp. Correction": -262316.8461 kcal/mol

	Atomic	Cartesian Coordinates (Angstroms)		
	Number	X	Y	Z
1	C2	-0.0248288	0.5751105	-0.0758145
2	O1	-0.1401850	1.7948729	-0.0166037
3	N1	1.1807267	-0.0752127	-0.0404268
4	C3	1.3885917	-1.4575767	-0.4392854
5	H5	2.3553332	-1.5313804	-0.9507737
6	H6	0.6153890	-1.7693779	-1.1452105
7	H7	1.3928783	-2.1444741	0.4160459
8	C4	2.3691997	0.6938782	0.2938051
9	H8	3.0266593	0.8063335	-0.5797164
10	H9	2.9333927	0.1908740	1.0893981
11	H10	2.0626612	1.6831376	0.6306482
12	N2	-1.1700088	-0.2528473	-0.2582415
13	C1	-2.4448760	0.4564608	-0.1750519
14	H1	-3.2393586	-0.2520574	-0.4237236

15	H3	-2.4378120	1.2676397	-0.9037096
16	H4	-2.6209804	0.8752163	0.8229823
17	O2	-1.1821351	-1.3345738	0.6893119
18	H2	-1.3131466	-2.1191215	0.1311518

Table 2-29. B3LYP/6-31G(d) Calculated IR Frequencies (cm^{-1}, uncorrected) and Intensities for *N*-hydroxy-*N*, *N'*, *N'*-trimethylurea (3c, GS3):

	cm^{-1}	Intensity		cm^{-1}	Intensity		cm^{-1}	Intensity
1	78	0.14	17	910	12.41	33	1519	15.6
2	95	1.22	18	1014	6.17	34	1526	3.45
3	109	4.84	19	1096	9.62	35	1526	11.22
4	153	1.85	20	1120	25.28	36	1537	10.84
5	184	1.67	21	1139	2.8	37	1557	49.63
6	205	4.37	22	1152	80.98	38	1765	329.77
7	260	3.08	23	1178	5.62	39	3028	56.3
8	311	1.23	24	1189	39.27	40	3042	65.96
9	362	5.17	25	1284	45.74	41	3057	37.16
10	384	65.55	26	1303	56.4	42	3077	47.38
11	395	77.88	27	1397	59.65	43	3095	25.66
12	417	1.42	28	1433	194.46	44	3130	27.95
13	554	0.85	29	1460	9.16	45	3141	20.98
14	582	16.15	30	1464	14.03	46	3179	9.08
15	732	9.6	31	1494	46.32	47	3192	1.29
16	781	19.36	32	1508	8.36	48	3715	21.06

Table 2-30. B3LYP/6-31G(d) Optimized Geometries, Energies, ZPE and Temperature Corrections for *N*-hydroxy-*N*, *N'*, *N'*-trimethylurea (3c, TS2):

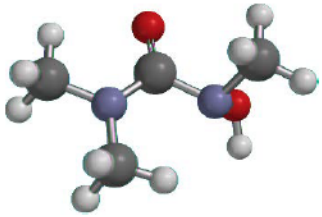

B3LYP/6-31G(d) Energy (E): -418.333735 hartrees

ZPE: 398.6948 kJ/mol

Temp. Correction: 424.227 kJ/mol

G° = E + ZPE + "Temp. Correction": -262311.6975 kcal/mol

	Atomic	Cartesian Coordinates (Angstroms)		
	Number	X	Y	Z
1	C2	0.0144728	-0.4757280	-0.0260063
2	O1	-0.1221771	-1.6869877	-0.0257530
3	N1	1.2240587	0.1616330	0.0056491
4	C3	1.4245150	1.6016062	-0.0525286
5	H5	1.9589495	1.9490994	0.8422301
6	H6	0.4601633	2.1010357	-0.1123735
7	H7	2.0300848	1.8645846	-0.9310070
8	C4	2.4342134	-0.6459999	0.0620981
9	H8	3.0433782	-0.3583265	0.9289252
10	H9	3.0363091	-0.4998959	-0.8448042
11	H10	2.1515086	-1.6944351	0.1426908
12	N2	-1.1289787	0.4482102	-0.0316898
13	C1	-1.9459166	0.2277364	1.1662109
14	H1	-2.8065608	0.8996858	1.1249291
15	H3	-1.3394910	0.4775837	2.0442032

16	H4	-2.2840361	-0.8131204	1.2391697
17	O2	-1.9443024	0.028451	-1.1547452
18	H2	-1.9477385	0.827485	-1.7063375

Table 2-31. B3LYP/6-31G(d) Calculated IR Frequencies (cm^{-1}, uncorrected) and Intensities for *N*-hydroxy-*N*, *N'*, *N'*-trimethylurea (3c, TS2):

	cm^{-1}	Intensity		cm^{-1}	Intensity		cm^{-1}	Intensity
1	-55	0.91	17	898	18.37	33	1523	0.72
2	79	0.60	18	985	12.22	34	1528	17.25
3	137	0.28	19	1078	14.70	35	1530	11.12
4	170	0.52	20	1083	7.18	36	1536	15.28
5	225	2.12	21	1144	8.39	37	1564	22.37
6	243	1.14	22	1145	110.17	38	1791	357.09
7	270	1.63	23	1174	60.75	39	3025	43.24
8	285	70.47	24	1194	9.20	40	3036	84.13
9	309	22.93	25	1238	42.58	41	3047	26.23
10	340	5.73	26	1290	51.42	42	3069	47.72
11	377	12.86	27	1389	62.22	43	3081	26.77
12	434	5.73	28	1432	109.87	44	3119	19.63
13	537	7.56	29	1452	12.46	45	3148	23.38
14	621	14.49	30	1460	11.61	46	3194	0.83
15	767	4.66	31	1481	23.37	47	3201	2.25
16	791	6.03	32	1505	4.77	48	3730	25.56

Table 2-32. B3LYP/6-31G(d) Optimized Geometries, Energies, ZPE and Temperature Corrections for *N*-hydroxy-*N*, *N'*, *N'*-trimethylurea (3c, GS1):

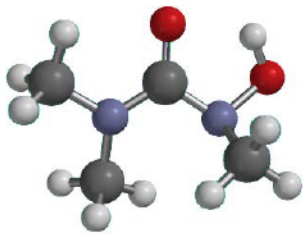

B3LYP/6-31G(d) Energy (E): -418.344388 hartrees

ZPE: 400.8163 kJ/mol

Temp. Correction: 425.6998 kJ/mol

G° = E + ZPE + "Temp. Correction": -262317.5233 kcal/mol

	Atomic	Cartesian Coordinates (Angstroms)		
	Number	X	Y	Z
1	C2	0.0186957	0.5195060	-0.0490905
2	O1	0.1548202	1.7358448	0.0989570
3	N1	-1.1856543	-0.1225820	-0.0150919
4	C3	-1.4129017	-1.4486794	-0.5729710
5	H5	-1.6415854	-2.1855056	0.2090391
6	H6	-0.5307936	-1.7710790	-1.1266112
7	H7	-2.2655257	-1.4101338	-1.2626589
8	C4	-2.3704549	0.6414664	0.3501387
9	H8	-2.9780817	0.0685626	1.0608717
10	H9	-2.9837665	0.8618509	-0.5343627
11	H10	-2.0599316	1.5806856	0.8054634
12	N2	1.1532913	-0.3079882	-0.2817218
13	C1	1.4946843	-1.2307245	0.8111210

14	H1	2.3497740	-1.8297428	0.4918792
15	H3	0.6516035	-1.8954641	1.0122695
16	H4	1.7604086	-0.6869132	1.7285417
17	O2	2.2888279	0.5147035	-0.5205728
18	H2	1.9951134	1.3879323	-0.1689996

Table 2-33. B3LYP/6-31G(d) Calculated IR Frequencies (cm^{-1}, uncorrected) and Intensities for *N*-hydroxy-*N*, *N'*, *N'*-trimethylurea (3c, GS1):

	cm^{-1}	Intensity		cm^{-1}	Intensity		cm^{-1}	Intensity
1	83	1.24	17	936	8.30	33	1520	13.57
2	112	1.19	18	1026	12.51	34	1527	8.12
3	117	0.76	19	1094	4.68	35	1539	15.21
4	192	4.54	20	1111	120.48	36	1541	3.63
5	211	1.04	21	1146	1.19	37	1565	60.46
6	238	5.06	22	1156	36.44	38	1752	280.28
7	260	0.83	23	1169	31.19	39	3030	34.65
8	297	7.69	24	1186	13.17	40	3034	59.41
9	373	5.46	25	1273	30.93	41	3038	62.84
10	398	42.58	26	1296	86.33	42	3080	47.75
11	443	17.22	27	1435	147.68	43	3089	23.10
12	474	72.89	28	1461	9.60	44	3129	21.83
13	545	5.66	29	1472	19.39	45	3166	18.84
14	603	3.78	30	1492	33.72	46	3174	0.87
15	759	17.13	31	1499	83.02	47	3192	1.41
16	783	24.53	32	1510	75.40	48	3482	75.03

Table 2-34. B3LYP/6-31G(d) Optimized Geometries, Energies, ZPE and Temperature Corrections for compound Anionic 3a (TS1):

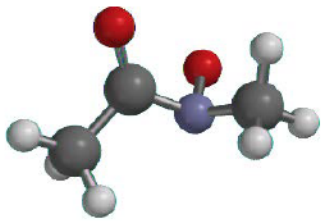

B3LYP/6-31G(d) Energy (E): -323.037961 hartrees

ZPE: 238.3478 kJ/mol

Temp. Correction: 257.6948 kJ/mol

G° = E + ZPE + "Temp. Correction": -202590.8227 kcal/mol

	Atomic	Cartesian Coordinates (Angstroms)		
	Number	X	Y	Z
1	C1	0.6501063	-0.1274599	0.1531125
2	C2	1.8047527	0.6782130	-0.4422528
3	H2	2.7550837	0.4496280	0.0554651
4	H4	1.5863129	1.7526985	-0.3780759
5	H5	1.8885596	0.4422501	-1.5110506
6	O1	0.8680894	-1.0444368	0.9373907
7	N1	-0.6143138	0.2804808	-0.4111596
8	C3	-1.4944090	0.7997815	0.6325870
9	H1	-1.6904461	0.0375486	1.4111482
10	H6	-2.4504868	1.0468143	0.1522990
11	H7	-1.0842459	1.7123689	1.1057972
12	O2	-1.1764994	-0.8940483	-0.9396589

Table 2-35. B3LYP/6-31G(d) Calculated IR Frequencies (cm^{-1}, uncorrected) and Intensities for compound Anionic 3a (TS1):

	cm^{-1}	Intensity		cm^{-1}	Intensity		cm^{-1}	Intensity
1	-208	4.6	11	894	31.2	21	1484	9.79
2	188	1.7	12	976	28.18	22	1505	7.56
3	235	14.09	13	1004	23.74	23	1525	3.01
4	271	2.33	14	1034	8.18	24	1731	258.78
5	325	8.95	15	1141	39.03	25	2919	167.82
6	347	7.91	16	1157	44.8	26	2969	123.96
7	452	9.31	17	1251	98.85	27	3022	48.49
8	533	2.24	18	1379	15.87	28	3054	75.5
9	617	18.91	19	1420	8.46	29	3087	32.18
10	749	5.31	20	1476	1.06	30	3102	58.4

Table 2-36. B3LYP/6-31G(d) Optimized Geometries, Energies, ZPE and Temperature Corrections for compound Anionic 3a (GS1):

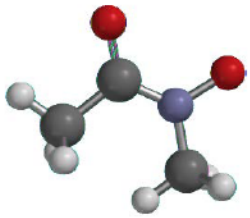

B3LYP/6-31G(d) Energy (E):	-323.072464 hartrees
ZPE:	242.9482 kJ/mol
Temp. Correction:	261.8235 kJ/mol
G° = E + ZPE + "Temp. Correction":	-202610.3874 kcal/mol

	Atomic	Cartesian Coordinates (Angstroms)		
	Number	X	Y	Z
1	C1	0.6985093	-0.2424118	-0.0006617
2	C2	1.5438219	1.0554560	0.0001220
3	H2	2.5879974	0.7311961	-0.0027410
4	H4	1.3859803	1.6884173	0.8864923
5	H5	1.3820037	1.6935678	-0.8816886
6	O1	1.3059449	-1.3363637	0.0000480
7	N1	-0.6457949	-0.1071082	-0.0001194
8	C3	-1.3310793	1.1693598	-0.0000644
9	H1	-1.9873834	1.2169244	0.8838358
10	H6	-1.9878973	1.2168064	-0.8835424
11	H7	-0.6686459	2.0435394	-0.0002963
12	O2	-1.5133200	-1.1305260	0.0002521

Table 2-37. B3LYP/6-31G(d) Calculated IR Frequencies (cm^{-1}, uncorrected) and Intensities for compound Anionic 3a (GS1):

	cm^{-1}	Intensity		cm^{-1}	Intensity		cm^{-1}	Intensity
1	97	0.00	11	955	116.64	21	1508	37.76
2	152	0.21	12	1006	1.68	22	1525	1.01
3	180	0.88	13	1038	4.73	23	1546	14.81
4	313	1.01	14	1147	40.00	24	1707	399.35
5	330	1.09	15	1156	0.01	25	2975	178.10
6	424	7.43	16	1215	53.18	26	2999	64.65
7	463	2.09	17	1385	0.88	27	3001	109.52
8	537	0.41	18	1436	2.09	28	3044	60.53
9	593	24.57	19	1455	23.25	29	3076	101.03
10	741	7.24	20	1486	0.40	30	3128	33.46

Table 2-38. B3LYP/6-31G(d) Optimized Geometries, Energies, ZPE and Temperature Corrections for compound Anionic 3a (TS2):

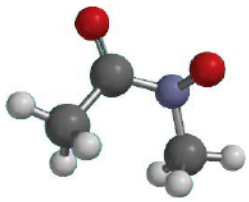

B3LYP/6-31G(d) Energy (E): -323.043055 hartrees

ZPE: 239.4306 kJ/mol

Temp. Correction: 258.6135 kJ/mol

G° = E + ZPE + "Temp. Correction": -202593.5409 kcal/mol

	Atomic	Cartesian Coordinates (Angstroms)		
	Number	X	Y	Z
1	C1	0.7168333	-0.1162168	-0.1738646
2	C2	1.1381454	1.2181913	0.4577436
3	H2	0.6187630	1.3149220	1.4215295
4	H4	0.8590910	2.0843775	-0.1546851
5	H5	2.2201119	1.2235570	0.6185978
6	O1	1.5791574	-0.9502324	-0.4335822
7	N1	-0.6551887	-0.3450071	-0.3711022
8	C3	-1.5245961	0.8110992	-0.3761184
9	H1	-1.5605354	1.3317819	0.6039235
10	H6	-2.5377880	0.4382044	-0.5718796
11	H7	-1.2584451	1.5350334	-1.1692480
12	O2	-1.0463039	-1.1736762	0.7339464

Table 2-39. B3LYP/6-31G(d) Calculated IR Frequencies (cm^{-1}, uncorrected) and Intensities for compound Anionic 3a (TS2):

	cm^{-1}	Intensity		cm^{-1}	Intensity		cm^{-1}	Intensity
1	-249	6.10	11	888	26.12	21	1496	5.94
2	204	1.21	12	964	41.45	22	1515	3.43
3	237	5.05	13	1031	7.86	23	1535	2.40
4	320	0.20	14	1074	11.60	24	1755	350.11
5	328	1.21	15	1139	52.78	25	2883	179.72
6	396	17.13	16	1150	11.91	26	2957	143.92
7	418	3.87	17	1306	83.37	27	3026	30.86
8	527	7.52	18	1371	41.48	28	3065	73.77
9	571	16.92	19	1438	12.39	29	3090	33.21
10	744	5.23	20	1477	6.88	30	3125	47.94

Table 2-40. B3LYP/6-31G(d) Optimized Geometries, Energies, ZPE and Temperature Corrections for compound Anionic 3a (GS2):

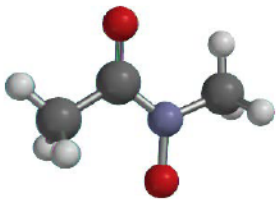

B3LYP/6-31G(d) Energy (E):	-323.091848 hartrees
ZPE:	243.3784 kJ/mol
Temp. Correction:	262.4243 kJ/mol
G° = E + ZPE + "Temp. Correction":	-202622.3046 kcal/mol

	Atomic	Cartesian Coordinates (Angstroms)		
	Number	X	Y	Z
1	C1	0.6404043	-0.3440664	0.0006704
2	C2	1.7449703	0.7063536	-0.0024691
3	H2	1.6400266	1.3759161	-0.8649493
4	H4	2.7157692	0.1991732	-0.0218411
5	H5	1.6681482	1.3543507	0.8796637
6	O1	0.8880717	-1.5825233	0.0018389
7	N1	-0.5864315	0.2080450	0.0016258
8	C3	-1.7659325	-0.6260195	-0.0021362
9	H1	-2.3771601	-0.3929535	-0.8886676
10	H6	-2.3802987	-0.3977961	0.8834212
11	H7	-1.4759145	-1.6802318	-0.0045909
12	O2	-0.8133470	1.5409759	0.0018102

Table 2-41. B3LYP/6-31G(d) Calculated IR Frequencies (cm^{-1}, uncorrected) and Intensities for compound Anionic 3a (GS2):

	cm^{-1}	Intensity		cm^{-1}	Intensity		cm^{-1}	Intensity
1	87	1.30	11	948	23.59	21	1490	25.12
2	166	11.02	12	1032	7.33	22	1504	1.14
3	190	0.01	13	1036	3.50	23	1543	13.87
4	284	25.21	14	1156	34.61	24	1684	239.15
5	300	4.49	15	1157	0.50	25	2984	187.77
6	379	0.93	16	1231	170.46	26	3009	107.50
7	503	28.53	17	1385	5.12	27	3030	47.88
8	552	1.99	18	1407	9.55	28	3087	38.74
9	597	1.31	19	1457	83.98	29	3117	37.63
10	759	4.85	20	1486	1.34	30	3130	26.45

Table 2-42. B3LYP/6-31G(d) Optimized Geometries, Energies, ZPE and Temperature Corrections for compound Anionic 3b (GS1):

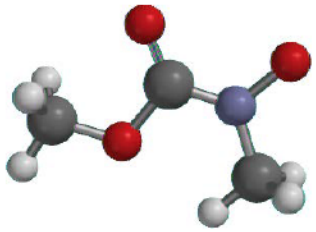

B3LYP/6-31G(d) Energy (E): -398.297861 hartrees

ZPE: 255.6549 kJ/mol

Temp. Correction: 276.7056 kJ/mol

G° = E + ZPE + "Temp. Correction": -249808.4424 kcal/mol

	Atomic	Cartesian Coordinates (Angstroms)		
	Number	X	Y	Z
1	C1	0.2005045	-0.4011461	-0.0003128
2	O1	0.6703298	-1.5453781	0.0000167
3	N1	-1.0805083	-0.0172081	-0.0003235
4	C3	-1.5068576	1.3663940	0.0005558
5	H1	-2.1399333	1.5345536	0.8861406
6	H6	-2.1434889	1.5346860	-0.8824434
7	H7	-0.6743077	2.0744965	-0.0010221
8	O2	-2.1087479	-0.8902216	0.0002121
9	O3	1.0914332	0.7260898	-0.0017791
10	C2	2.4469121	0.3464999	0.0009252
11	H2	3.0247897	1.2800952	-0.0084717
12	H3	2.7136158	-0.2576815	-0.8769920
13	H4	2.7154078	-0.2401010	0.8904457

Table 2-43. B3LYP/6-31G(d) Calculated IR Frequencies (cm^{-1}, uncorrected) and Intensities for compound Anionic 3b (GS1):

	cm^{-1}	Intensity		cm^{-1}	Intensity		cm^{-1}	Intensity
1	54	1.20	12	769	61.96	23	1494	0.77
2	112	1.50	13	987	146.50	24	1501	0.06
3	141	0.38	14	1093	13.31	25	1540	19.81
4	151	1.76	15	1146	287.98	26	1543	24.02
5	242	2.73	16	1159	0.04	27	1792	520.02
6	297	2.69	17	1188	0.20	28	2985	207.73
7	361	8.06	18	1196	53.75	29	3009	103.34
8	411	7.02	19	1226	37.89	30	3010	107.43
9	507	9.27	20	1409	18.87	31	3061	76.71
10	608	8.55	21	1440	18.93	32	3080	71.43
11	612	17.30	22	1493	2.35	33	3125	47.12

Table 2-44. B3LYP/6-31G(d) Optimized Geometries, Energies, ZPE and Temperature Corrections for compound Anionic 3b (TS2):

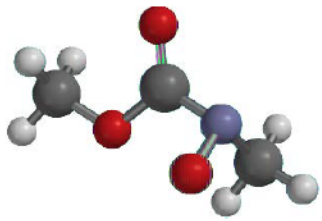

B3LYP/6-31G(d) Energy (E): -398.268593 hartrees

ZPE: 253.4696 kJ/mol

Temp. Correction: 274.3995 kJ/mol

G° = E + ZPE + "Temp. Correction": -249791.15 kcal/mol

	Atomic	Cartesian Coordinates (Angstroms)		
	Number	X	Y	Z
1	C1	-0.1933961	-0.4653194	-0.1261565
2	O1	-0.8162686	-1.4977001	-0.3403819
3	N1	1.2006061	-0.2969207	-0.2571585
4	C3	1.8440650	-0.0235311	1.0245517
5	H1	1.4995113	0.9323443	1.4635889
6	H6	2.9187009	0.0738546	0.8216708
7	H7	1.6873802	-0.8444079	1.7467880
8	O2	1.3683417	0.8096367	-1.1135400
9	O3	-0.8864729	0.6894390	0.2253747
10	C2	-2.2897076	0.5452060	0.2427419
11	H2	-2.6952073	1.5241984	0.5260918
12	H3	-2.6237166	-0.2137896	0.9653617
13	H4	-2.6814804	0.2571069	-0.7418356

Table 2-45. B3LYP/6-31G(d) Calculated IR Frequencies (cm^{-1}, uncorrected) and Intensities for compound Anionic 3b (TS2):

	cm^{-1}	Intensity		cm^{-1}	Intensity		cm^{-1}	Intensity
1	-138	6.54	12	814	16.64	23	1486	1.78
2	110	4.34	13	924	82.93	24	1507	0.36
3	181	1.13	14	990	41.40	25	1531	6.81
4	232	1.30	15	1100	8.48	26	1535	1.01
5	272	20.06	16	1127	384.68	27	1747	400.88
6	311	4.30	17	1158	43.19	28	2928	148.98
7	339	22.52	18	1186	0.34	29	2988	127.05
8	373	4.79	19	1209	16.08	30	3009	108.30

9	565	6.86	20	1275	118.23	31	3059	71.79
10	632	6.62	21	1428	11.52	32	3062	73.09
11	729	4.07	22	1479	1.62	33	3092	66.84

Table 2-46. B3LYP/6-31G(d) Optimized Geometries, Energies, ZPE and Temperature Corrections for compound Anionic 3b (GS2):

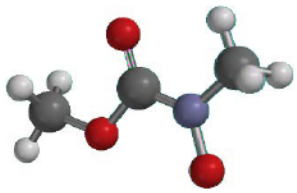

B3LYP/6-31G(d) Energy (E): -398.302795 hartrees

ZPE: 256.7936 kJ/mol

Temp. Correction: 277.728 kJ/mol

G° = E + ZPE + "Temp. Correction": -249811.0221 kcal/mol

	Atomic	Cartesian Coordinates (Angstroms)		
	Number	X	Y	Z
1	C1	0.2009868	-0.3018268	-0.0004237
2	O1	0.5241775	-1.5134476	-0.0004973
3	N1	-1.0297102	0.2210470	-0.0002004
4	C3	-2.1629303	-0.6772161	0.0005938
5	H1	-2.7844068	-0.4697998	-0.8849820
6	H6	-2.7836205	-0.4673330	0.8859941
7	H7	-1.8412748	-1.7222177	0.0015463
8	O2	-1.3452150	1.5329589	-0.0001727
9	O3	1.1812591	0.6967567	-0.0005995
10	C2	2.4916514	0.1802544	0.0007758
11	H2	3.1576306	1.0520637	0.0152879

12	H3	2.7054331	-0.4275154	-0.8900309
13	H4	2.6941886	-0.4499397	0.8780679

Table 2-47. B3LYP/6-31G(d) Calculated IR Frequencies (cm^{-1}, uncorrected) and Intensities for compound Anionic 3b (GS2):

	cm^{-1}	Intensity		cm^{-1}	Intensity		cm^{-1}	Intensity
1	89	0.86	12	811	32.16	23	1501	1.03
2	125	10.08	13	975	15.30	24	1503	0.57
3	162	1.50	14	1100	82.47	25	1538	7.97
4	193	0.62	15	1160	0.02	26	1544	19.59
5	228	9.67	16	1188	3.60	27	1733	316.16
6	292	2.62	17	1191	221.72	28	2986	213.70
7	372	28.30	18	1205	227.01	29	3009	90.59
8	386	4.30	19	1222	62.34	30	3012	103.61
9	563	15.65	20	1410	100.36	31	3055	83.06
10	599	8.04	21	1428	79.74	32	3085	73.86
11	643	11.39	22	1498	36.16	33	3128	30.86

Table 2-48. B3LYP/6-31G(d) Optimized Geometries, Energies, ZPE and Temperature Corrections for compound Anionic 3b (TS1):

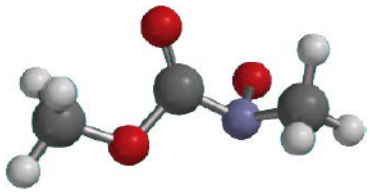

B3LYP/6-31G(d) Energy (E): -398.26669 hartrees

ZPE: 253.3854 kJ/mol

Temp. Correction: 274.2658 kJ/mol

G° = E + ZPE + "Temp. Correction": -249790.0079 kcal/mol

	Atomic	Cartesian Coordinates (Angstroms)		
	Number	X	Y	Z
1	C1	-0.1902721	-0.1343545	-0.1280617
2	O1	-0.4685672	-0.8632790	-1.0676982
3	N1	1.0520956	0.2001342	0.4651483
4	C3	1.8640151	0.9764643	-0.4686455
5	H1	2.0659214	0.4107487	-1.3985669
6	H6	2.8248013	1.1584162	0.0295156
7	H7	1.3954295	1.9468094	-0.7156837
8	O2	1.6836889	-1.0412678	0.6952244
9	O3	-1.2145604	0.4848769	0.5857899
10	C2	-2.5172081	0.1785677	0.1159212
11	H2	-3.2134373	0.7073569	0.7768840
12	H3	-2.7139923	-0.8995441	0.1509054
13	H4	-2.6670910	0.5085684	-0.9209058

Table 2-49. B3LYP/6-31G(d) Calculated IR Frequencies (cm^{-1}, uncorrected) and Intensities for compound Anionic 3b (TS1):

	cm^{-1}	Intensity		cm^{-1}	Intensity		cm^{-1}	Intensity
1	-144	5.14	12	832	44.57	23	1481	1.64
2	117	0.49	13	916	43.87	24	1503	0.64
3	147	4.40	14	997	30.84	25	1529	3.27
4	246	1.43	15	1071	5.23	26	1531	6.51
5	283	19.74	16	1132	402.71	27	1748	279.63
6	324	3.50	17	1159	92.71	28	2926	160.29
7	343	16.82	18	1181	0.98	29	2981	127.71
8	374	6.37	19	1206	29.99	30	3023	87.51

9	518	9.86	20	1252	137.42	31	3065	66.95
10	664	3.37	21	1425	7.23	32	3082	61.91
11	722	5.36	22	1478	3.59	33	3107	60.02

Table 2-50. B3LYP/6-31G(d) Optimized Geometries, Energies, ZPE and Temperature Corrections for compound Anionic 3c (GS1):

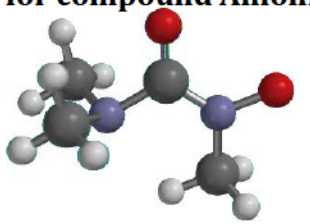

B3LYP/6-31G(d) Energy (E): -417.731271 hartrees

ZPE: 362.8821 kJ/mol

Temp. Correction: 387.1761 kJ/mol

G° = E + ZPE + "Temp. Correction": -261951.0604 kcal/mol

	Atomic	Cartesian Coordinates (Angstroms)		
	Number	X	Y	Z
1	C1	0.0838105	-0.5187155	0.0031933
2	O1	-0.1700421	-1.7402052	0.0265423
3	N1	1.3044732	0.0449862	-0.0025074
4	C3	1.5394762	1.4791562	-0.0402735
5	H1	2.1553204	1.7019490	-0.9252102
6	H6	2.1406323	1.7533201	0.8404457
7	H7	0.6115872	2.0531990	-0.0644282
8	O2	2.4365902	-0.6613782	0.0168763
9	N2	-1.0401813	0.4597376	-0.0147736
10	C2	-1.8745745	0.2143444	-1.1886450
11	H2	-2.7076178	0.9329629	-1.2100611
12	H4	-2.2860639	-0.8100550	-1.2123537

13	H5	-1.2725969	0.3587726	-2.0932463
14	C4	-1.8337247	0.3034270	1.2013942
15	H3	-2.6775742	1.0095155	1.1895283
16	H8	-1.2066482	0.5313492	2.0710588
17	H9	-2.2293919	-0.7206852	1.3238715

Table 2-51. B3LYP/6-31G(d) Calculated IR Frequencies (cm^{-1}, uncorrected) and Intensities for compound Anionic 3c (GS1):

	cm^{-1}	Intensity		cm^{-1}	Intensity		cm^{-1}	Intensity
1	36	0.58	16	949	3.52	31	1502	1.39
2	99	3.78	17	1013	113.62	32	1511	10.24
3	207	3.52	18	1058	12.87	33	1533	2.45
4	212	1.74	19	1104	98.92	34	1537	35.83
5	237	0.33	20	1115	2.18	35	1547	7.00
6	264	0.20	21	1161	0.18	36	1731	399.76
7	272	2.53	22	1199	2.24	37	2964	70.13
8	330	7.16	23	1218	17.60	38	2977	177.32
9	374	8.17	24	1222	94.80	39	2990	148.34
10	378	0.07	25	1276	20.15	40	3017	87.75
11	444	3.29	26	1404	7.32	41	3030	7.51
12	522	9.89	27	1421	11.07	42	3034	153.87
13	614	23.85	28	1439	4.66	43	3093	52.63
14	674	0.03	29	1483	0.81	44	3096	47.22
15	739	10.76	30	1499	1.59	45	3142	31.98

Table 2-52. B3LYP/6-31G(d) Optimized Geometries, Energies, ZPE and Temperature Corrections for compound Anionic 3c (TS2):

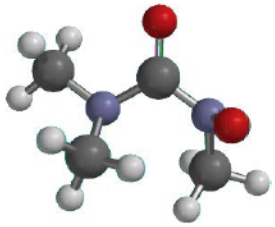

B3LYP/6-31G(d) Energy (E): -417.71183 hartrees

ZPE: 361.3775 kJ/mol

Temp. Correction: 385.7142 kJ/mol

G° = E + ZPE + "Temp. Correction": -261939.57 kcal/mol

	Atomic	Cartesian Coordinates (Angstroms)		
	Number	X	Y	Z
1	C1	-0.0642150	0.7075924	-0.1073951
2	O1	-0.4739237	1.8584209	0.0537432
3	N1	1.2737033	0.3469729	-0.2208823
4	C3	1.6556592	-0.7827702	-1.0347520
5	H1	1.5532875	-1.7676741	-0.5337597
6	H6	2.7257794	-0.6606345	-1.2567551
7	H7	1.0977267	-0.8079103	-1.9838138
8	O2	1.9495235	0.3320400	1.0208347
9	N2	-0.9857728	-0.3767608	-0.1938135
10	C2	-0.7058185	-1.4360989	0.7786490
11	H2	-0.8228828	-2.4409640	0.3425087
12	H4	-1.3966461	-1.3601735	1.6374909
13	H5	0.3149528	-1.2987053	1.1626551
14	C4	-2.3870904	-0.0216830	-0.3077972
15	H3	-2.9647654	-0.8970266	-0.6408634

16	H8	-2.4992451	0.7826902	-1.0386416
17	H9	-2.8197312	0.3329839	0.6451985

Table 2-53. B3LYP/6-31G(d) Calculated IR Frequencies (cm^{-1}, uncorrected) and Intensities for compound Anionic 3c (TS2):

	cm^{-1}	Intensity		cm^{-1}	Intensity		cm^{-1}	Intensity
1	-154	5.85	16	907	28.38	31	1508	4.18
2	124	3.66	17	991	35.52	32	1530	4.28
3	177	2.21	18	1082	131.85	33	1537	4.27
4	229	0.62	19	1103	23.87	34	1548	9.93
5	239	6.76	20	1121	80.61	35	1564	6.43
6	273	9.11	21	1144	2.07	36	1735	416.09
7	305	1.88	22	1157	6.01	37	2899	161.56
8	326	6.33	23	1180	11.18	38	2954	100.57
9	329	0.39	24	1253	10.43	39	2967	194.96
10	373	14.04	25	1309	15.53	40	3002	138.25
11	412	3.61	26	1355	164.68	41	3003	81.11
12	534	20.55	27	1445	13.27	42	3026	98.65
13	581	13.69	28	1457	0.52	43	3046	77.88
14	740	3.21	29	1480	7.93	44	3056	18.18
15	782	12.56	30	1498	14.83	45	3138	25.97

Table 2-54. B3LYP/6-31G(d) Optimized Geometries, Energies, ZPE and Temperature Corrections for compound Anionic 3c (GS2):

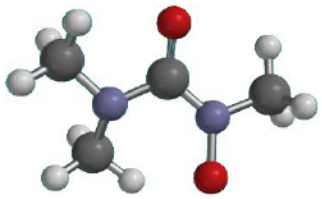

B3LYP/6-31G(d) Energy (E): -417.750439 hartrees

ZPE: 363.2809 kJ/mol

Temp. Correction: 387.4416 kJ/mol

G° = E + ZPE + "Temp. Correction": -261962.9297 kcal/mol

	Atomic	Cartesian Coordinates (Angstroms)		
	Number	X	Y	Z
1	C1	-0.0514048	0.5400347	-0.0333643
2	O1	-0.0114078	1.7896372	0.1271666
3	N1	-1.1927298	-0.1810241	-0.0742567
4	C3	-2.4492744	0.4793502	0.1903526
5	H1	-2.9802201	-0.0709146	0.9829873
6	H6	-3.0842629	0.4422932	-0.7097192
7	H7	-2.2831107	1.5176625	0.4858142
8	O2	-1.3216812	-1.4971410	-0.4111288
9	N2	1.1630997	-0.1856773	-0.2256802
10	C2	1.3277953	-1.4628330	0.4516272
11	H2	1.6420621	-1.3356620	1.5089244
12	H4	2.1110319	-2.0505653	-0.0533502
13	H5	0.3610098	-1.9811145	0.3869545
14	C4	2.3529062	0.6351686	-0.2095482
15	H3	2.6877625	0.9041497	0.8128673

16	H8	2.1633830	1.5662801	-0.7447944
17	H9	3.1743335	0.0844880	-0.6928312

Table 2-55. B3LYP/6-31G(d) Calculated IR Frequencies (cm^{-1}, uncorrected) and Intensities for compound Anionic 3c (GS2):

	cm^{-1}	Intensity		cm^{-1}	Intensity		cm^{-1}	Intensity
1	95	2.02	16	940	10.69	31	1506	18.59
2	119	6.88	17	1025	52.81	32	1528	8.10
3	155	1.84	18	1096	9.74	33	1539	10.31
4	161	1.20	19	1141	10.80	34	1556	3.32
5	236	2.46	20	1152	65.43	35	1561	23.45
6	263	0.72	21	1159	48.36	36	1674	261.29
7	288	13.12	22	1193	63.70	37	2894	147.49
8	335	6.89	23	1205	151.60	38	2919	242.37
9	373	23.46	24	1270	8.10	39	2982	231.86
10	398	14.43	25	1339	16.56	40	2991	107.15
11	414	1.93	26	1415	15.81	41	3008	106.64
12	559	5.96	27	1430	138.05	42	3019	121.68
13	585	30.97	28	1441	2.79	43	3053	22.60
14	692	8.24	29	1477	185.58	44	3141	21.90
15	742	7.65	30	1504	0.99	45	3160	19.19

Table 2-56. B3LYP/6-31G(d) Optimized Geometries, Energies, ZPE and Temperature Corrections for compound Anionic 3c (TS1):

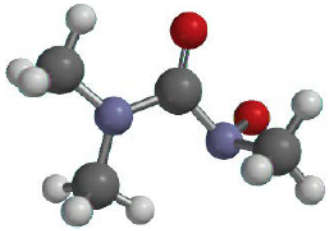

B3LYP/6-31G(d) Energy (E): -417.71223 hartrees

ZPE: 358.9498 kJ/mol

Temp. Correction: 383.4 kJ/mol

G° = E + ZPE + "Temp. Correction": -261940.9543 kcal/mol

	Atomic	Cartesian Coordinates (Angstroms)		
	Number	X	Y	Z
1	C1	0.0508571	0.4890355	0.0076525
2	O1	0.0786728	1.7133817	0.1266288
3	N1	1.1677955	-0.4004943	-0.1762510
4	C3	1.9526895	-0.4466296	1.0582648
5	H1	2.3691001	0.5494784	1.2983132
6	H6	2.7917710	-1.1301432	0.8760393
7	H7	1.3612736	-0.8199931	1.9159416
8	O2	1.9664538	0.1347281	-1.1963583
9	N2	-1.1892288	-0.1764054	-0.0011516
10	C2	-1.3374690	-1.6000591	-0.1898587
11	H2	-1.9969738	-1.8171441	-1.0495164
12	H4	-1.7862790	-2.0854436	0.6958516
13	H5	-0.3368137	-2.0001853	-0.3658038
14	C4	-2.4056691	0.5878827	0.1201196
15	H3	-3.0572996	0.4455651	-0.7592291

16	H8	-2.1298547	1.6397854	0.2017544
17	H9	-2.9883539	0.2901221	1.0092326

Table 2-57. B3LYP/6-31G(d) Calculated IR Frequencies (cm^{-1}, uncorrected) and Intensities for compound Anionic 3c (TS1):

	cm^{-1}	Intensity		cm^{-1}	Intensity		cm^{-1}	Intensity
1	-116	3.60	16	917	20.16	31	1521	13.03
2	74	1.13	17	968	19.03	32	1525	23.22
3	124	2.37	18	1027	17.67	33	1525	1.29
4	185	2.06	19	1072	14.37	34	1535	6.74
5	231	2.93	20	1099	341.44	35	1558	1.78
6	253	1.92	21	1145	0.89	36	1716	303.22
7	279	7.94	22	1156	28.75	37	2925	180.84
8	309	8.70	23	1191	3.88	38	2945	106.18
9	342	14.82	24	1238	72.35	39	2969	228.95
10	389	4.22	25	1307	47.19	40	2971	120.86
11	422	8.53	26	1372	117.40	41	2977	128.53
12	530	12.59	27	1410	44.12	42	2989	84.99
13	608	4.99	28	1423	11.23	43	3061	73.90
14	725	2.08	29	1442	29.67	44	3140	12.00
15	768	8.53	30	1479	0.49	45	3166	5.29

Table 2-58. B3LYP/6-31G(d) Optimized Geometries, Energies, ZPE and Temperature Corrections for *N*-hydroxy-*N*-(4-(methoxyiminoethyl)-3-methyl-5-oxo-1-phenyl-4,5-dihydro-1*H*-pyrazol-4-yl)-*N*-acetamide (1a):

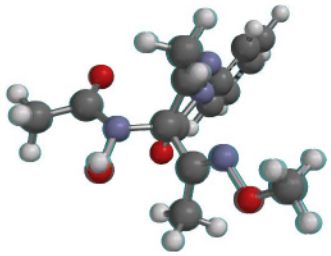

B3LYP/6-31G(d) Energy (E):	-1102.203696 hartrees
ZPE:	851.3509 kJ/mol
Temp. Correction:	902.8418 kJ/mol
G° = E + ZPE + "Temp. Correction":	-691223.9952 kcal/mol

	Atomic	Cartesian Coordinates (Angstroms)		
	Number	X	Y	Z
1	C7	-0.3221715	0.4444090	0.6459756
2	C2	1.0508052	0.2415914	-0.0756404
3	C3	0.5564202	-0.1931578	-1.4494729
4	N1	-0.7094613	-0.4012104	-1.4725757
5	N2	-1.2526225	-0.0970571	-0.2151291
6	O1	-0.4894411	0.9037248	1.7605355
7	C4	1.3934496	-0.3248903	-2.6765096
8	H5	2.2156696	-1.0270241	-2.5093477
9	H6	1.8219871	0.6467701	-2.9533020
10	H7	0.7739667	-0.6768841	-3.5051886
11	C5	-2.6538098	-0.2307714	-0.0351182
12	C6	-5.4177496	-0.5524043	0.2910739
13	C8	-3.4139945	-0.8436064	-1.0417681
14	C9	-3.2773639	0.2229271	1.1370865
15	C10	-4.6534671	0.0559900	1.2869396
16	C11	-4.7875894	-0.9988289	-0.8715190
17	H8	-2.9232784	-1.1857048	-1.9438251
18	H9	-2.6899299	0.6987221	1.9097769
19	H10	-5.1283894	0.4122762	2.1973422
20	H11	-5.3668939	-1.4745646	-1.6585920
21	H12	-6.4896100	-0.6761895	0.4181636
22	C12	1.7978026	-0.8706600	0.6709259
23	C13	2.0288719	-0.7831326	2.1543235

24	H13	3.1023516	-0.8261268	2.3630268
25	H14	1.5686975	-1.6474217	2.6467727
26	H15	1.6081226	0.1307975	2.5698818
27	N3	2.1532867	-1.8649585	-0.0602856
28	N4	1.8660999	1.4636084	-0.1151071
29	O3	3.0781711	1.4577760	0.5975661
30	C14	1.2714473	2.6911611	-0.3546898
31	O4	0.1317587	2.7155500	-0.7957029
32	H21	3.7474427	1.1955339	-0.0599639
33	O2	2.7893421	-2.8504048	0.6919545
34	C15	3.1074964	-3.9514719	-0.1568450
35	H16	3.5959346	-4.6827411	0.4910231
36	H17	3.7914402	-3.6474437	-0.9578461
37	H18	2.2016943	-4.3849979	-0.5944922
38	C1	2.1108738	3.9192667	-0.0851828
39	H2	2.3321798	4.0019920	0.9836290
40	H3	1.5441690	4.7911828	-0.4141471
41	H4	3.0685530	3.8774492	-0.6135297

Table 2-59. B3LYP/6-31G(d) Calculated IR Frequencies (cm^{-1}, uncorrected) and Intensities for *N*-hydroxy-*N*-(4-(methoxyiminoethyl)-3-methyl-5-oxo-1-phenyl-4,5-dihydro-1*H*-pyrazol-4-yl)-*N*-acetamide (1a):

	cm^{-1}	Intensity		cm^{-1}	Intensity		cm^{-1}	Intensity
1	21	1.36	40	662	33.85	79	1423	42.12
2	26	1.34	41	678	1.59	80	1430	14.59
3	34	0.12	42	707	13.91	81	1434	45.28
4	50	1.52	43	730	5.10	82	1442	98.52
5	67	1.90	44	754	5.04	83	1485	5.43
6	92	3.45	45	774	47.15	84	1494	3.04
7	110	0.25	46	840	27.12	85	1496	21.29
8	117	1.01	47	859	0.10	86	1501	3.15
9	122	0.48	48	874	28.24	87	1505	5.45
10	145	0.22	49	926	5.72	88	1508	6.21
11	149	3.89	50	937	45.91	89	1508	5.04
12	152	0.56	51	961	15.32	90	1513	5.85
13	154	1.98	52	976	0.05	91	1515	6.65
14	157	2.09	53	998	1.42	92	1535	24.44
15	179	0.37	54	1015	6.21	93	1548	149.44
16	197	1.04	55	1017	0.31	94	1643	3.70
17	212	6.17	56	1022	10.58	95	1662	74.54
18	239	1.48	57	1036	9.89	96	1695	4.68
19	249	3.21	58	1061	1.16	97	1708	7.64
20	265	5.98	59	1063	6.57	98	1771	201.43
21	274	2.48	60	1067	13.22	99	1801	197.84
22	307	3.33	61	1068	22.50	100	3046	74.09

23	325	7.67	62	1071	17.79	101	3054	20.56
24	343	2.51	63	1098	199.54	102	3068	4.47
25	351	1.33	64	1103	56.07	103	3073	4.11
26	371	8.83	65	1114	6.55	104	3116	34.04
27	390	0.10	66	1140	25.33	105	3118	8.61
28	404	135.15	67	1176	17.17	106	3123	8.05
29	420	0.08	68	1184	0.69	107	3137	6.62
30	437	6.64	69	1194	0.40	108	3157	6.18
31	469	13.98	70	1201	4.82	109	3160	19.46
32	508	31.67	71	1217	10.40	110	3181	5.64
33	525	4.13	72	1221	17.38	111	3184	0.77
34	534	4.42	73	1276	19.35	112	3193	24.80
35	581	2.32	74	1312	111.33	113	3199	0.53
36	588	10.71	75	1353	91.31	114	3210	37.86
37	593	15.62	76	1356	109.89	115	3251	0.86
38	625	7.71	77	1371	13.87	116	3270	3.17
39	633	0.26	78	1397	149.74	117	3672	25.43

Table 2-60. B3LYP/6-31G(d) Optimized Geometries, Energies, ZPE and Temperature Corrections for *N*-hydroxy-*N*-(4-(methoxyiminoethyl)-3-methyl-5-oxo-1-phenyl-4,5-dihydro-1*H*-pyrazol-4-yl)-*N*-methylcarbamate (1c):

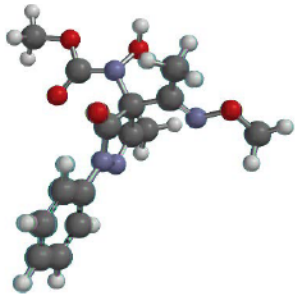

B3LYP/6-31G(d) Energy (E):	-1177.426718 hartrees
ZPE:	863.6825 kJ/mol
Temp. Correction:	918.2394 kJ/mol
G° = E + ZPE + "Temp. Correction":	-738420.5264 kcal/mol

	Atomic	Cartesian Coordinates (Angstroms)		
	Number	X	Y	Z
1	C7	-0.3617286	0.0496930	0.7944898
2	C2	1.0094787	-0.0858400	0.0551330
3	C3	0.5276289	-0.2536713	-1.3777989
4	N1	-0.7511968	-0.3173796	-1.4600681
5	N2	-1.3080669	-0.1999477	-0.1771313
6	O1	-0.5194892	0.2430542	1.9848301
7	C4	1.4027719	-0.3035295	-2.5839029
8	H5	2.0747132	-1.1655915	-2.5238397
9	H6	2.0275351	0.5955033	-2.6525500
10	H7	0.7868341	-0.3794006	-3.4834691
11	C5	-2.7216771	-0.1967930	-0.0536404
12	C6	-5.5171024	-0.2107232	0.1426107
13	C8	-3.5061198	-0.4182446	-1.1949136
14	C9	-3.3371352	0.0162642	1.1893216
15	C10	-4.7288436	0.0069517	1.2727663
16	C11	-4.8948598	-0.4224835	-1.0884853
17	H8	-3.0213418	-0.5782231	-2.1491000
18	H9	-2.7316058	0.1917608	2.0673494
19	H10	-5.1967323	0.1753732	2.2392751
20	H11	-5.4920135	-0.5931875	-1.9805165
21	H12	-6.6008053	-0.2147512	0.2198455
22	C12	1.7086853	-1.3169501	0.6263037
23	C13	2.2185275	-1.2833157	2.0407872
24	H13	3.3146587	-1.2276175	2.0463953

25	H14	1.9456491	-2.2102914	2.5526747
26	H15	1.8017579	-0.4335632	2.5826052
27	N3	1.7673903	-2.3303575	-0.1569594
28	N4	1.8497632	1.0890415	0.3053439
29	O3	3.1955896	0.8812540	-0.0782716
30	C14	1.3362506	2.3529363	0.0206938
31	O4	0.1500579	2.5634348	-0.1375656
32	H21	3.6988061	1.0320589	0.7407077
33	O2	2.3791552	-3.4216284	0.4579597
34	C15	2.3798670	-4.5232878	-0.4473962
35	H16	2.8601262	-5.3412428	0.0945197
36	H17	2.9520095	-4.2887461	-1.3524372
37	H18	1.3582145	-4.8063991	-0.7235845
38	O5	2.3021815	3.2860503	0.0291630
39	C16	1.8295889	4.6303863	-0.1708265
40	H19	1.3088624	4.7162433	-1.1275964
41	H20	2.7252864	5.2517156	-0.1632857
42	H22	1.1508640	4.9211864	0.6349319

Table 2-61. B3LYP/6-31G(d) Calculated IR Frequencies (cm^{-1}, uncorrected) and Intensities for *N*-hydroxy-*N*-(4-(methoxyiminoethyl)-3-methyl-5-oxo-1-phenyl-4,5-dihydro-1*H*-pyrazol-4-yl)-*N*-methylcarbamate (1c):

	cm^{-1}	Intensity		cm^{-1}	Intensity		cm^{-1}	Intensity
1	2	0.05	41	676	19.63	81	1398	159.23
2	26	0.20	42	706	16.15	82	1430	7.60
3	38	0.28	43	734	4.12	83	1431	74.23
4	50	1.38	44	744	3.00	84	1441	40.11
5	61	1.50	45	767	15.49	85	1484	6.53
6	91	0.83	46	774	45.73	86	1497	53.16
7	97	1.66	47	788	16.67	87	1498	1.60
8	106	1.09	48	845	30.28	88	1506	5.29
9	111	2.78	49	858	0.02	89	1507	2.82
10	118	0.54	50	892	26.18	90	1510	4.54
11	135	0.36	51	925	6.06	91	1511	8.78
12	145	3.60	52	935	89.99	92	1512	4.20
13	153	1.21	53	975	0.04	93	1516	6.82
14	154	7.21	54	977	4.73	94	1525	7.91
15	162	1.40	55	996	1.30	95	1534	22.03
16	166	0.13	56	1012	13.17	96	1546	155.34
17	185	3.00	57	1017	0.57	97	1642	3.66
18	206	1.47	58	1035	22.98	98	1662	76.36
19	223	2.77	59	1043	24.69	99	1708	7.67
20	248	1.21	60	1058	10.51	100	1712	4.85
21	265	5.23	61	1064	19.55	101	1797	304.81
22	279	0.60	62	1075	21.95	102	1808	163.07
23	305	15.29	63	1082	21.68	103	3047	74.00

24	319	0.67	64	1097	160.87	104	3056	13.84
25	328	64.59	65	1102	103.83	105	3057	11.78
26	338	11.72	66	1134	14.69	106	3079	33.24
27	351	3.73	67	1151	41.21	107	3117	33.80
28	364	55.11	68	1181	36.76	108	3118	7.48
29	379	28.84	69	1185	1.17	109	3125	4.89
30	395	9.20	70	1187	0.29	110	3156	7.28
31	418	0.03	71	1193	0.48	111	3157	16.13
32	433	35.69	72	1201	3.62	112	3159	21.11
33	480	3.73	73	1217	4.03	113	3180	0.75
34	522	7.20	74	1221	8.10	114	3184	0.46
35	524	2.90	75	1227	71.18	115	3186	16.59
36	535	3.48	76	1287	25.97	116	3194	25.04
37	579	6.02	77	1312	181.54	117	3209	38.53
38	606	2.86	78	1354	8.86	118	3254	0.77
39	632	0.33	79	1368	28.61	119	3271	3.12
40	662	34.06	80	1374	595.19	120	3708	40.90

Table 2-62. B3LYP/6-31G(d) Optimized Geometries, Energies, ZPE and Temperature Corrections for *N'*,*N'*-dimethyl-*N*-hydroxy-*N*-(*4*-(methoxyiminoethyl)-3-methyl-5-oxo-1-phenyl-4,5-dihydro-1*H*-pyrazol-4-yl)-urea (1e):

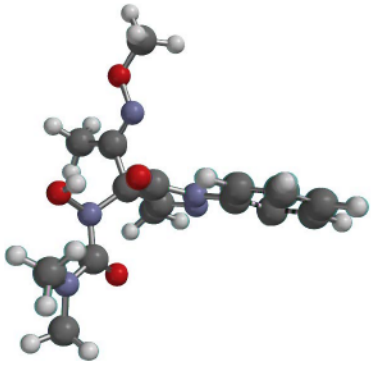

B3LYP/6-31G(d) Energy (E): -1196.86653 hartrees

ZPE: 972.4043 kJ/mol

Temp. Correction: 1029.5846 kJ/mol

G° = E + ZPE + "Temp. Correction": -750566.5953 kcal/mol

	Atomic	Cartesian Coordinates (Angstroms)		
	Number	X	Y	Z
1	C7	0.3257691	-0.1215717	-0.5312182
2	C2	-0.8981283	-0.5423706	0.3117883
3	C3	-0.3372081	-0.3455985	1.7171676
4	N1	0.9125939	-0.0478228	1.6960673
5	N2	1.3321316	0.1226719	0.3574230
6	O1	0.3080634	0.0490909	-1.7502539
7	C4	-1.0439202	-0.6327777	2.9999146
8	H5	-1.3037153	-1.6956059	3.0794033
9	H6	-1.9598503	-0.0405033	3.0593481
10	H7	-0.3897060	-0.3729633	3.8356782
11	C5	2.6649018	0.5470640	0.1138513
12	C6	5.3048550	1.3661447	-0.3247703

13	C8	3.5250546	0.7503598	1.2015853
14	C9	3.1235332	0.7525111	-1.1961296
15	C10	4.4407433	1.1608116	-1.4007305
16	C11	4.8375018	1.1581098	0.9736539
17	H8	3.1582679	0.5866755	2.2064366
18	H9	2.4564051	0.5958481	-2.0325585
19	H10	4.7893520	1.3187337	-2.4179107
20	H11	5.4973612	1.3133739	1.8230617
21	H12	6.3293819	1.6843919	-0.4958522
22	N4	-2.0495843	0.2711887	-0.0982129
23	O3	-2.4591425	-0.0927920	-1.4005785
24	C14	-2.1693926	1.6146773	0.3217679
25	O4	-1.8882382	1.8737709	1.4928260
26	H21	-1.6323285	-0.0488184	-1.9370445
27	N5	-2.7091031	2.5370642	-0.5339342
28	C16	-2.5204739	2.5646140	-1.9886910
29	H19	-2.5091816	3.6134504	-2.2994345
30	H20	-3.3223114	2.0460326	-2.5214677
31	H22	-1.5590333	2.1345996	-2.2773297
32	C17	-3.1312349	3.7976878	0.0740672
33	H23	-3.4267241	3.6207315	1.1072722
34	H24	-3.9836730	4.1922782	-0.4882010
35	H25	-2.3251111	4.5444634	0.0687246
36	C12	-1.2471902	-2.0196690	0.1141913
37	N3	-0.3037856	-2.7236909	-0.3930510
38	O2	-0.6579504	-4.0676453	-0.4889187

39	C13	-2.5868735	-2.5436951	0.5467928
40	H13	-2.4602020	-3.4001098	1.2173495
41	H14	-3.1404699	-2.8963895	-0.3301489
42	H15	-3.1755224	-1.7665185	1.0363366
43	C15	0.4173228	-4.7876964	-1.0898379
44	H16	1.3272573	-4.7120102	-0.4842814
45	H17	0.6198452	-4.4183909	-2.1011457
46	H18	0.0807713	-5.8261488	-1.1312963

Table 2-63. B3LYP/6-31G(d) Calculated IR Frequencies (cm^{-1}, uncorrected) and Intensities for *N'*,*N'*-dimethyl-*N*-hydroxy-*N*-(*4*-(methoxyiminoethyl)-3-methyl-5-oxo-1-phenyl-4,5-dihydro-1*H*-pyrazol-4-yl)-urea (1e):

	cm^{-1}	Intensity		cm^{-1}	Intensity		cm^{-1}	Intensity
1	20	0.35	45	706	11.74	89	1436	81.68
2	29	0.15	46	721	42.65	90	1462	3.94
3	32	1.52	47	734	3.72	91	1486	6.94
4	39	0.51	48	744	10.16	92	1491	4.20
5	44	2.53	49	767	144.20	93	1502	6.42
6	78	0.44	50	775	73.16	94	1504	39.43
7	90	0.37	51	818	13.61	95	1507	5.66
8	102	3.61	52	858	0.10	96	1508	5.54
9	109	1.50	53	860	26.47	97	1510	4.25
10	113	2.64	54	927	0.33	98	1516	10.98
11	118	0.95	55	929	60.78	99	1520	4.60
12	127	0.02	56	975	0.01	100	1524	92.99
13	136	0.59	57	990	7.69	101	1534	21.69
14	148	1.28	58	994	18.38	102	1537	23.12
15	161	1.81	59	998	1.65	103	1541	7.68
16	171	0.66	60	1017	0.20	104	1547	123.40
17	186	1.81	61	1025	8.44	105	1557	75.63
18	200	2.57	62	1035	1.14	106	1643	2.78
19	213	4.35	63	1052	10.80	107	1661	66.47
20	226	3.25	64	1062	6.09	108	1692	14.10
21	242	6.29	65	1064	15.52	109	1710	16.85
22	261	4.37	66	1077	8.42	110	1729	225.08
23	271	10.48	67	1091	50.96	111	1751	297.89

24	285	1.23	68	1094	112.98	112	3036	57.12
25	308	1.32	69	1102	129.23	113	3049	67.13
26	335	14.16	70	1122	45.27	114	3059	15.71
27	347	4.46	71	1134	22.60	115	3067	6.56
28	356	7.50	72	1144	3.11	116	3068	40.83
29	374	13.86	73	1161	5.92	117	3103	34.39
30	381	19.41	74	1169	7.20	118	3119	32.32
31	397	9.33	75	1185	0.64	119	3124	5.46
32	418	0.01	76	1194	0.50	120	3132	6.27
33	425	16.34	77	1204	21.92	121	3135	19.31
34	447	26.66	78	1219	20.09	122	3149	15.55
35	473	0.21	79	1227	5.31	123	3160	21.39
36	518	0.04	80	1271	110.39	124	3166	3.97
37	528	5.96	81	1289	34.15	125	3171	5.21
38	548	4.71	82	1294	84.16	126	3186	0.31
39	565	4.33	83	1310	68.69	127	3187	4.16
40	600	11.83	84	1354	7.70	128	3195	22.67
41	632	0.27	85	1369	12.67	129	3210	34.62
42	661	17.64	86	1406	317.44	130	3254	0.41
43	667	13.22	87	1419	185.13	131	3266	2.46
44	702	3.40	88	1428	9.67	132	3466	129.31

Table 2-64. B3LYP/6-31G(d) Optimized Geometries, Energies, ZPE and Temperature Corrections for compound Anionic 1a (GS):

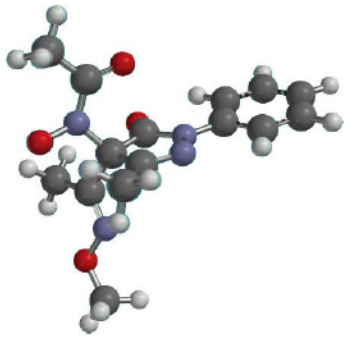

B3LYP/6-31G(d) Energy (E):	-1101.655352 hartrees
ZPE:	814.3522 kJ/mol
Temp. Correction:	866.095 kJ/mol
G° = E + ZPE + "Temp. Correction":	-690897.5297 kcal/mol

	Atomic	Cartesian Coordinates (Angstroms)		
	Number	X	Y	Z
1	C7	-0.2635357	0.1848330	0.7519384
2	C2	1.0840099	0.2539997	-0.0148590
3	C3	0.6128709	-0.0325204	-1.4213853
4	N1	-0.6628766	-0.1873243	-1.5189948
5	N2	-1.2093696	-0.1442473	-0.2208932
6	O1	-0.4312810	0.2013195	1.9609585
7	C4	1.5261003	0.0246143	-2.5972603
8	H5	2.0917042	-0.9119781	-2.6755032
9	H6	2.2605193	0.8223821	-2.4209718
10	H7	0.9627675	0.1848166	-3.5223376
11	C5	-2.5928436	-0.2990928	-0.0712766
12	C6	-5.3763260	-0.6538091	0.1861986
13	C8	-3.3705709	-0.6844796	-1.1791195
14	C9	-3.2245604	-0.0893145	1.1694379
15	C10	-4.6013779	-0.2686554	1.2823199
16	C11	-4.7453815	-0.8571322	-1.0429831
17	H8	-2.8789429	-0.8351401	-2.1316984
18	H9	-2.6273269	0.2094609	2.0195396
19	H10	-5.0731256	-0.0985641	2.2481273
20	H11	-5.3281210	-1.1541464	-1.9129109
21	H12	-6.4504125	-0.7909532	0.2874885
22	C12	2.0455638	-0.7621664	0.5904846
23	C13	2.7388342	-0.3792927	1.8621894
24	H13	3.4419317	0.4203392	1.6017198

25	H14	3.2546863	-1.2310373	2.3063837
26	H15	1.9972352	0.0249114	2.5589082
27	N3	2.1221380	-1.8774287	-0.0371919
28	N4	1.7329290	1.5793011	-0.0001528
29	O3	3.0350767	1.5973822	-0.3597766
30	C14	0.9599074	2.6871185	0.0564743
31	O4	-0.2820836	2.6485946	0.1904487
32	O2	2.9802513	-2.8034429	0.6114888
33	C15	2.9913406	-3.9893846	-0.1571151
34	H16	3.6574096	-4.6802095	0.3703485
35	H17	3.3757769	-3.8113521	-1.1708956
36	H18	1.9885884	-4.4315729	-0.2339585
37	C1	1.7466368	3.9779596	-0.0537421
38	H2	2.6038703	3.9700215	0.6268973
39	H3	1.0810634	4.8184087	0.1605153
40	H4	2.1629152	4.0756163	-1.0637914

Table 2-65. B3LYP/6-31G(d) Calculated IR Frequencies (cm^{-1}, uncorrected) and Intensities for compound Anionic 1a (GS):

	cm^{-1}	Intensity		cm^{-1}	Intensity		cm^{-1}	Intensity
1	23	0.96	39	664	37.91	77	1402	32.47
2	26	0.11	40	669	3.17	78	1406	10.4
3	40	0.3	41	705	14.37	79	1439	35.6
4	63	0.19	42	724	6.88	80	1448	140.74
5	77	3.36	43	754	22	81	1484	11.77
6	87	0.63	44	763	38.05	82	1485	6.64
7	98	0.09	45	844	32.88	83	1490	14.24
8	108	1.95	46	850	0.24	84	1494	7.73
9	126	1.5	47	867	84.98	85	1502	1.91
10	137	1.25	48	903	10.68	86	1502	2.61
11	154	0.87	49	914	37.63	87	1504	2.68
12	166	5.35	50	964	0.26	88	1522	14
13	177	0.58	51	975	10.55	89	1525	6.2
14	190	1.56	52	980	1.94	90	1541	29.84
15	202	13.01	53	999	13.13	91	1547	246.29
16	217	12.53	54	1013	9	92	1630	8.02
17	231	9.26	55	1017	53.51	93	1661	190.15
18	233	3.12	56	1038	26.7	94	1667	97.96
19	257	6.39	57	1053	6.09	95	1694	149.9
20	278	8.92	58	1061	14.12	96	1719	22.24
21	293	4.44	59	1070	105.38	97	1776	220.44
22	321	0.95	60	1083	4.36	98	3016	110.75
23	340	2.22	61	1087	5.19	99	3027	53.08
24	346	10.58	62	1096	18.52	100	3051	38.53

25	349	14.93	63	1105	44.96	101	3059	18.28
26	377	4.12	64	1109	159.38	102	3072	57.48
27	388	2.19	65	1135	17.42	103	3092	13.72
28	421	0.76	66	1177	50.23	104	3112	21.39
29	426	9.77	67	1185	2.71	105	3120	48.04
30	479	10.5	68	1187	0.28	106	3126	18.52
31	487	22.38	69	1188	10.84	107	3128	2.48
32	511	20.15	70	1207	8.74	108	3148	23.11
33	527	5.19	71	1224	15.4	109	3161	2.85
34	573	0.57	72	1301	49.71	110	3171	47.95
35	582	18.97	73	1322	133.72	111	3177	9.78
36	596	7.68	74	1350	11.57	112	3191	74.3
37	633	0.52	75	1367	6.61	113	3249	1.75
38	660	20.24	76	1392	252.32	114	3266	4.54

Table 2-66. B3LYP/6-31G(d) Optimized Geometries, Energies, ZPE and Temperature Corrections for compound Anionic 1a (TS):

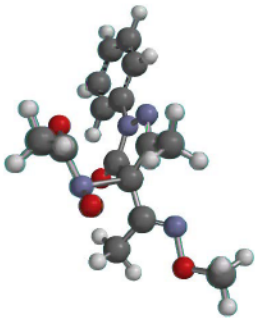

B3LYP/6-31G(d) Energy (E): -1101.632193 hartrees

ZPE: 808.3613 kJ/mol

Temp. Correction: 860.7744 kJ/mol

G° = E + ZPE + "Temp. Correction": -690885.7007 kcal/mol

	Atomic	Cartesian Coordinates (Angstroms)		
	Number	X	Y	Z
1	C7	-0.3864436	-0.5601887	0.7698960
2	C2	0.9028822	-0.2119736	0.1180202
3	C3	0.5257070	0.0786483	-1.2593213
4	N1	-0.7643118	0.0236761	-1.4521853
5	N2	-1.3369098	-0.4055142	-0.2477620
6	O1	-0.6131426	-0.9526202	1.9170749
7	C4	1.4395265	0.5405152	-2.3485021
8	H5	2.0553538	-0.2841069	-2.7218364
9	H6	2.1320177	1.2921968	-1.9467329
10	H7	0.8517589	0.9620487	-3.1707799
11	C5	-2.7278581	-0.5331105	-0.1733751
12	C6	-5.5327389	-0.8176131	-0.0930625
13	C8	-3.5054973	-0.3039313	-1.3246331
14	C9	-3.3724401	-0.9056276	1.0223516
15	C10	-4.7590374	-1.0417139	1.0475746
16	C11	-4.8892995	-0.4464760	-1.2761353
17	H8	-3.0023451	-0.0113904	-2.2372748
18	H9	-2.7734914	-1.0784708	1.9056299
19	H10	-5.2392297	-1.3280058	1.9815995
20	H11	-5.4705234	-0.2615269	-2.1778807
21	H12	-6.6144111	-0.9274950	-0.0604902
22	C12	2.1417653	-0.8931736	0.5264238
23	C13	2.4784760	-0.9876364	1.9895498
24	H13	3.1055046	-0.1237402	2.2401254

25	H14	3.0413005	-1.9001039	2.2017671
26	H15	1.5646610	-0.9486229	2.5830452
27	N3	2.9041138	-1.3133551	-0.4264094
28	N4	1.4989297	1.6166654	0.7851447
29	O3	2.6721439	1.8782040	0.3530280
30	C14	0.4691735	2.5520931	0.4417336
31	O4	-0.7220348	2.3179663	0.5916159
32	O2	4.1001448	-1.8881790	0.0794809
33	C15	4.8844501	-2.2886139	-1.0242538
34	H16	5.7853632	-2.7467680	-0.6021155
35	H17	5.1682026	-1.4313856	-1.6501221
36	H18	4.3585784	-3.0227758	-1.6511238
37	C1	0.9990655	3.9371623	0.1000083
38	H2	1.5149675	4.3798095	0.9599944
39	H3	0.1619916	4.5742747	-0.1945020
40	H4	1.7442716	3.8526264	-0.6980632

Table 2-67. B3LYP/6-31G(d) Calculated IR Frequencies (cm^{-1}, uncorrected) and Intensities for compound Anionic 1a (TS):

	cm^{-1}	Intensity		cm^{-1}	Intensity		cm^{-1}	Intensity
1	-175	100.89	39	648	12.79	77	1396	320.60
2	27	0.41	40	665	45.65	78	1408	11.82
3	31	0.02	41	702	6.80	79	1423	47.16
4	39	0.38	42	706	14.53	80	1455	24.66
5	58	3.35	43	745	33.45	81	1483	6.29
6	61	0.10	44	763	37.23	82	1484	18.50
7	89	7.85	45	777	2.61	83	1497	2.14
8	93	0.34	46	796	24.41	84	1500	5.68
9	104	3.35	47	851	76.13	85	1503	4.44
10	116	2.05	48	853	0.12	86	1504	4.62
11	131	2.42	49	901	137.70	87	1511	21.74
12	134	0.48	50	902	10.14	88	1515	21.66
13	138	0.98	51	963	74.13	89	1526	8.25
14	160	7.32	52	966	0.32	90	1541	32.20
15	168	8.60	53	983	2.63	91	1550	230.41
16	184	3.14	54	1010	21.09	92	1614	72.16
17	202	8.05	55	1013	9.21	93	1636	17.28
18	219	1.00	56	1034	53.17	94	1660	189.68
19	241	3.69	57	1041	9.53	95	1672	10.14
20	254	7.86	58	1053	23.38	96	1730	254.76
21	284	10.43	59	1066	4.86	97	1753	205.44
22	305	2.16	60	1080	5.93	98	3013	139.02
23	338	10.81	61	1088	1.83	99	3036	31.05
24	342	1.64	62	1094	30.32	100	3056	23.79

25	352	36.37	63	1098	18.09	101	3065	14.99
26	375	6.91	64	1115	256.96	102	3067	57.85
27	387	1.70	65	1145	17.56	103	3104	9.63
28	406	9.32	66	1178	247.39	104	3116	51.77
29	424	0.04	67	1185	1.05	105	3117	13.37
30	445	15.29	68	1188	3.06	106	3128	18.77
31	479	19.39	69	1198	24.65	107	3133	17.80
32	521	25.53	70	1206	7.05	108	3157	15.98
33	529	17.12	71	1233	14.81	109	3158	1.37
34	542	8.31	72	1308	357.41	110	3169	53.00
35	556	38.33	73	1347	55.09	111	3181	1.06
36	600	4.93	74	1353	19.34	112	3188	84.45
37	604	8.95	75	1366	13.25	113	3249	1.77
38	633	0.54	76	1388	24.34	114	3268	7.22

Table 2-68. B3LYP/6-31G(d) Optimized Geometries, Energies, ZPE and Temperature Corrections for compound Anionic 1c (GS):

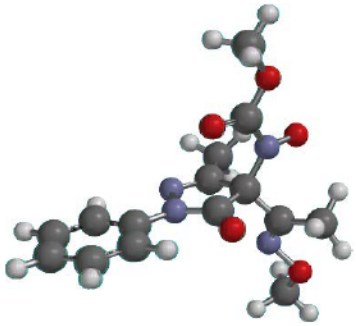

B3LYP/6-31G(d) Energy (E): -1176.866643 hartrees

ZPE: 827.839 kJ/mol

Temp. Correction: 881.3944 kJ/mol

G° = E + ZPE + "Temp. Correction": -738086.4469

	Atomic	Cartesian Coordinates (Angstroms)		
	Number	X	Y	Z
1	C7	-0.2873222	-0.0909803	0.7676999
2	C2	1.0590699	-0.0205186	0.0024215
3	C3	0.5819677	-0.2439237	-1.4121928
4	N1	-0.6994955	-0.3495001	-1.5163342
5	N2	-1.2430960	-0.3420006	-0.2119924
6	O1	-0.4528535	-0.0872463	1.9772562
7	C4	1.5002535	-0.1663995	-2.5811081
8	H5	2.0421322	-1.1136258	-2.6924679
9	H6	2.2568163	0.6022110	-2.3617662
10	H7	0.9461237	0.0438768	-3.5020018
11	C5	-2.6338426	-0.4367800	-0.0687352
12	C6	-5.4328032	-0.6563705	0.1670256
13	C8	-3.4331605	-0.6461910	-1.2076317
14	C9	-3.2508949	-0.3371979	1.1929034
15	C10	-4.6360231	-0.4473979	1.2945933
16	C11	-4.8156442	-0.7529080	-1.0819429
17	H8	-2.9512086	-0.7130587	-2.1743517
18	H9	-2.6366149	-0.1704038	2.0667656
19	H10	-5.0960855	-0.3646081	2.2773145
20	H11	-5.4154665	-0.9125505	-1.9759572
21	H12	-6.5130998	-0.7406010	0.2596619
22	C12	2.0004154	-1.0762217	0.5753210
23	C13	2.7320894	-0.7337000	1.8374243
24	H13	3.4267466	0.0725619	1.5754812

25	H14	3.2593594	-1.5991125	2.2395512
26	H15	2.0147294	-0.3505854	2.5709740
27	N3	2.0208615	-2.1844004	-0.0684974
28	N4	1.7549128	1.2827497	0.0596345
29	O3	3.0405145	1.2474029	-0.3591307
30	C14	0.9947902	2.4026471	0.0729477
31	O4	-0.2348972	2.4427855	0.2205925
32	O2	2.8544226	-3.1524575	0.5493705
33	C15	2.8146738	-4.3219012	-0.2431199
34	H16	3.4645879	-5.0453816	0.2602118
35	H17	3.1904701	-4.1360204	-1.2587178
36	H18	1.7966175	-4.7289533	-0.3140261
37	O5	1.7587203	3.5366886	-0.0435255
38	C16	1.0042732	4.7352918	0.0523041
39	H19	0.2198803	4.7822706	-0.7114291
40	H20	1.7226764	5.5468964	-0.0967386
41	H22	0.5257486	4.8370685	1.0338584

Table 2-69. B3LYP/6-31G(d) Calculated IR Frequencies (cm^{-1}, uncorrected) and Intensities for compound Anionic 1c (GS):

	cm^{-1}	Intensity		cm^{-1}	Intensity		cm^{-1}	Intensity
1	17	0.05	40	665	28.3	79	1392	242.4
2	22	0.69	41	690	20.72	80	1402	103.16
3	37	0.88	42	705	15.41	81	1413	405.99
4	49	1.46	43	726	3.58	82	1443	25.24
5	75	0.65	44	738	12.68	83	1484	11.93
6	79	2.82	45	764	39.23	84	1485	4.21
7	101	1.16	46	783	5.73	85	1499	53.03
8	106	0.58	47	845	31.85	86	1502	39.59
9	119	0.36	48	853	0.02	87	1502	5.34
10	131	1.88	49	871	122.34	88	1504	2.51
11	143	0.68	50	905	10.99	89	1507	6.21
12	146	3.96	51	916	53.02	90	1525	14.09
13	166	5.64	52	966	0.12	91	1527	9.2
14	174	1.19	53	977	11.73	92	1535	3.81
15	186	1.1	54	983	2.18	93	1542	30.66
16	202	10.18	55	1008	64.46	94	1547	233.34
17	211	6.28	56	1013	4.77	95	1631	8.47
18	228	9.72	57	1038	19.08	96	1660	173.34
19	247	3.08	58	1048	44.69	97	1675	62.42
20	270	2.59	59	1060	23.75	98	1715	151.25
21	275	8.05	60	1082	22.08	99	1723	106.41
22	286	0.95	61	1084	40.97	100	1779	220.26
23	317	5.29	62	1086	13.03	101	3012	52.84
24	327	2.88	63	1101	4.63	102	3016	125.34

25	340	2.72	64	1108	223.36	103	3040	87.32
26	351	9.87	65	1127	14.56	104	3058	18.99
27	373	26.84	66	1148	49.1	105	3072	57.36
28	379	5.87	67	1170	224.85	106	3085	16.05
29	391	23.77	68	1186	1.44	107	3101	43.96
30	422	0.27	69	1188	0.54	108	3119	50.07
31	427	17.88	70	1188	2.3	109	3122	20.51
32	480	8.22	71	1191	3.07	110	3127	3.39
33	500	2.78	72	1207	8.06	111	3129	51.2
34	520	11.89	73	1216	114.09	112	3163	0.81
35	529	4.76	74	1224	33.75	113	3173	48.37
36	590	5.12	75	1301	82.89	114	3177	10.39
37	606	4.66	76	1321	143.65	115	3191	73.94
38	632	0.45	77	1350	11.15	116	3251	1.42
39	660	25.67	78	1365	6.36	117	3267	5.04

Table 2-70. B3LYP/6-31G(d) Optimized Geometries, Energies, ZPE and Temperature Corrections for compound Anionic 1c (TS):

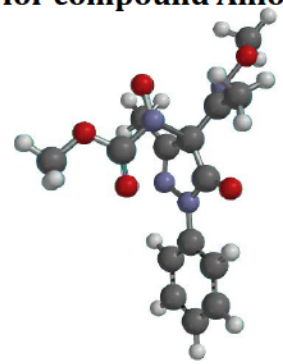

B3LYP/6-31G(d) Energy (E): -1176.851434 hartrees

ZPE: 824.1969 kJ/mol

Temp. Correction: 878.2288 kJ/mol

G° = E + ZPE + "Temp. Correction": -738078.5302 kcal/mol

	Atomic	Cartesian Coordinates (Angstroms)		
	Number	X	Y	Z
1	C7	-0.3226350	-0.6921466	0.7973842
2	C2	0.9590910	-0.2727111	0.1555812
3	C3	0.5705638	-0.0179801	-1.2333283
4	N1	-0.7128383	-0.1419465	-1.4336484
5	N2	-1.2707594	-0.5937636	-0.2264243
6	O1	-0.5290166	-1.0887078	1.9453721
7	C4	1.4744285	0.5063088	-2.3000362
8	H5	2.1622511	-0.2714421	-2.6477828
9	H6	2.0926242	1.3100731	-1.8734350
10	H7	0.8821091	0.8776901	-3.1429318
11	C5	-2.6535751	-0.7961938	-0.1610617
12	C6	-5.4401755	-1.2230091	-0.0957654
13	C8	-3.4329197	-0.6234848	-1.3210270
14	C9	-3.2865700	-1.1856687	1.0353561
15	C10	-4.6645347	-1.3921758	1.0531577
16	C11	-4.8080266	-0.8361873	-1.2798299
17	H8	-2.9382028	-0.3186511	-2.2342676
18	H9	-2.6862698	-1.3166305	1.9249384
19	H10	-5.1364993	-1.6900639	1.9876910
20	H11	-5.3913029	-0.6947114	-2.1881008
21	H12	-6.5150538	-1.3873783	-0.0687759
22	C12	2.1916430	-1.0026439	0.5426751
23	C13	2.6035264	-1.0027851	1.9880460
24	H13	3.2031205	-0.1007404	2.1566465

25	H14	3.2046921	-1.8829761	2.2249370
26	H15	1.7155680	-0.9582731	2.6206181
27	N3	2.8442938	-1.5597941	-0.4176930
28	N4	1.5032386	1.4574234	0.7802860
29	O3	2.6595543	1.7519376	0.3111836
30	C14	0.4283632	2.3407911	0.4428959
31	O4	-0.7492614	2.1415174	0.6896370
32	O2	4.0252652	-2.1958637	0.0494448
33	C15	4.6703856	-2.7778811	-1.0643782
34	H16	5.5614406	-3.2761933	-0.6676669
35	H17	4.9725853	-2.0189153	-1.7995304
36	H18	4.0286670	-3.5168926	-1.5645755
37	O5	0.8952892	3.5547665	0.0236269
38	C16	-0.1227038	4.5416085	-0.1155990
39	H19	-0.8657557	4.2430174	-0.8630050
40	H20	0.3897935	5.4532336	-0.4344077
41	H22	-0.6431208	4.7111744	0.8334696

Table 2-71. B3LYP/6-31G(d) Calculated IR Frequencies (cm^{-1}, uncorrected) and Intensities for compound Anionic 1c (TS):

	cm^{-1}	Intensity		cm^{-1}	Intensity		cm^{-1}	Intensity
1	-212	135.68	40	664	36.59	79	1389	274.86
2	29	0.20	41	677	39.68	80	1402	87.25
3	36	0.69	42	706	12.47	81	1419	21.40
4	41	0.22	43	716	2.33	82	1454	20.37
5	46	2.19	44	735	31.24	83	1482	17.37
6	71	0.40	45	761	20.47	84	1487	4.12
7	94	0.81	46	763	38.18	85	1497	2.43
8	104	7.34	47	790	0.74	86	1504	6.05
9	108	3.79	48	849	48.18	87	1504	0.90
10	129	1.33	49	853	0.03	88	1509	11.63
11	135	1.40	50	862	43.43	89	1510	2.56
12	143	1.39	51	899	135.23	90	1522	19.44
13	157	0.45	52	903	6.65	91	1523	8.87
14	166	0.69	53	966	0.13	92	1530	9.66
15	174	2.38	54	983	2.06	93	1540	29.91
16	178	8.05	55	1004	8.41	94	1550	236.65
17	194	4.78	56	1013	10.93	95	1618	64.07
18	211	6.90	57	1038	65.29	96	1637	23.88
19	235	9.01	58	1048	22.65	97	1660	181.02
20	253	7.44	59	1063	20.25	98	1687	10.97
21	279	2.86	60	1068	4.27	99	1735	212.63
22	283	14.05	61	1084	10.87	100	1759	225.73
23	292	1.89	62	1089	9.13	101	3012	130.41
24	305	1.15	63	1095	28.22	102	3024	33.67

25	343	5.81	64	1098	11.54	103	3050	71.53
26	358	22.81	65	1111	291.09	104	3068	57.29
27	369	13.73	66	1143	25.74	105	3069	13.40
28	375	27.82	67	1178	839.41	106	3100	12.23
29	394	1.02	68	1186	1.50	107	3116	31.18
30	423	18.53	69	1188	2.52	108	3117	52.68
31	424	0.13	70	1190	70.64	109	3129	19.36
32	460	35.78	71	1197	12.88	110	3141	43.31
33	479	17.47	72	1206	6.71	111	3141	12.37
34	523	3.78	73	1215	5.97	112	3158	1.00
35	529	7.77	74	1231	11.80	113	3169	52.18
36	579	1.65	75	1287	365.68	114	3176	2.75
37	603	9.29	76	1340	49.29	115	3188	82.13
38	631	23.36	77	1353	22.72	116	3249	1.65
39	634	6.85	78	1366	21.17	117	3267	6.80

Table 2-72. B3LYP/6-31G(d) Optimized Geometries, Energies, ZPE and Temperature Corrections for compound Anionic 1e (GS):

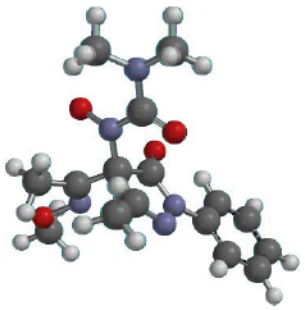

B3LYP/6-31G(d) Energy (E):	-1196.299145 hartrees
ZPE:	934.8819 kJ/mol
Temp. Correction:	991.828 kJ/mol
G° = E + ZPE + "Temp. Correction":	-750228.5479 kcal/mol

	Atomic	Cartesian Coordinates (Angstroms)		
	Number	X	Y	Z
1	C7	-0.4450546	-0.0350475	0.6583269
2	C2	0.7918996	-0.4402869	-0.1940928
3	C3	0.2944699	-0.0100102	-1.5704756
4	N1	-0.9457381	0.3256567	-1.5909594
5	N2	-1.4288866	0.3162210	-0.2735329
6	O1	-0.5549024	-0.0123062	1.8663466
7	C4	1.1021819	-0.0185696	-2.8254235
8	H5	1.4722944	-1.0218943	-3.0680004
9	H6	1.9696450	0.6391244	-2.7057816
10	H7	0.4894877	0.3448042	-3.6554812
11	C5	-2.7489543	0.7316742	-0.0450273
12	C6	-5.4176866	1.5376264	0.3626437
13	C8	-3.5706480	1.0645531	-1.1378761
14	C9	-3.2767698	0.8090988	1.2580456
15	C10	-4.5985889	1.2084854	1.4444791
16	C11	-4.8882034	1.4619110	-0.9273133
17	H8	-3.1567061	1.0076000	-2.1363440
18	H9	-2.6413711	0.5620584	2.0970904
19	H10	-4.9894750	1.2641662	2.4585055
20	H11	-5.5061658	1.7157247	-1.7865222
21	H12	-6.4475669	1.8486123	0.5215611
22	N4	2.0485002	0.1297785	0.2712096
23	O3	2.7238880	-0.6771892	1.1517000

24	C14	2.1942978	1.4755078	0.1414996
25	O4	1.3185290	2.1697236	-0.4304652
26	N5	3.3582512	2.0640915	0.6530334
27	C16	4.6205583	1.3430060	0.6920384
28	H19	5.2439528	1.7432481	1.5044790
29	H20	5.1866777	1.4627430	-0.2523415
30	H22	4.3918759	0.2875921	0.8775130
31	C17	3.4798917	3.4909573	0.4425383
32	H23	2.4928035	3.9507410	0.4885330
33	H24	3.9260040	3.7427171	-0.5382133
34	H25	4.1274252	3.9145362	1.2227167
35	C1	0.9788084	-1.9623395	-0.1899521
36	N3	-0.0221267	-2.6293301	0.2553278
37	O2	0.1846460	-4.0252447	0.1117839
38	C12	2.1976780	-2.5807254	-0.8197213
39	H1	1.9126937	-3.1350887	-1.7261231
40	H3	2.6362598	-3.2963584	-0.1205510
41	H4	2.9419246	-1.8212904	-1.0476654
42	C13	-0.8853687	-4.6869258	0.7598996
43	H2	-1.8538662	-4.4061558	0.3247830
44	H13	-0.9045883	-4.4638041	1.8345901
45	H14	-0.7096573	-5.7573571	0.6092439

Table 2-73. B3LYP/6-31G(d) Calculated IR Frequencies (cm^{-1}, uncorrected) and Intensities for Anionic 1e (GS):

	cm^{-1}	Intensity		cm^{-1}	Intensity		cm^{-1}	Intensity
1	24	0.49	44	702	12.92	87	1441	183.82
2	27	0.87	45	707	13.56	88	1443	63.85
3	40	0.02	46	712	2.37	89	1450	0.93
4	46	0.74	47	734	4.69	90	1483	36.82
5	54	2.28	48	741	9.04	91	1486	8.9
6	82	0.74	49	766	38.94	92	1488	315.67
7	98	0.94	50	825	56.93	93	1502	1.57
8	106	0.51	51	854	7.87	94	1504	4.81
9	109	0.75	52	855	30.73	95	1506	4.23
10	122	3.96	53	903	98.98	96	1510	2.67
11	139	0.16	54	908	10.91	97	1514	13
12	153	3.34	55	967	0.11	98	1515	17.55
13	161	0.91	56	970	12.26	99	1531	6.33
14	172	2.92	57	987	2.5	100	1540	19.87
15	175	3.89	58	1011	39.17	101	1547	222.32
16	193	1.17	59	1013	8.33	102	1557	12.99
17	211	3.62	60	1016	78.17	103	1563	70.19
18	229	1.8	61	1037	2.56	104	1632	7.19
19	235	5.72	62	1057	10.16	105	1645	196.03
20	240	4.35	63	1059	20.51	106	1661	164.33
21	254	1.86	64	1064	30.63	107	1696	18.18
22	270	5.53	65	1079	9.9	108	1708	37.33
23	285	14.63	66	1095	3.57	109	1816	174.38
24	307	5.07	67	1097	20.96	110	2931	159.23

25	317	8.5	68	1103	264.9	111	2951	211.63
26	323	4.42	69	1131	10.83	112	3022	131.09
27	337	5.51	70	1139	105.61	113	3023	143.19
28	357	16.64	71	1146	53.57	114	3025	24.21
29	370	0.3	72	1150	6.25	115	3044	106.22
30	384	52.14	73	1186	9.49	116	3053	34.95
31	388	22.34	74	1188	5.23	117	3082	50.47
32	416	14.82	75	1189	1.7	118	3089	32.58
33	422	0.25	76	1197	39.24	119	3115	13.95
34	445	32.65	77	1208	9.76	120	3121	46.7
35	472	0.15	78	1221	16.66	121	3131	10.64
36	508	12.4	79	1281	9.51	122	3141	17.05
37	526	10.81	80	1287	70.04	123	3162	2.49
38	542	27.32	81	1299	95.28	124	3170	8.83
39	572	5.76	82	1335	31.87	125	3173	46.56
40	600	8.86	83	1352	16.97	126	3191	72.43
41	633	0.73	84	1366	11.73	127	3204	5.69
42	655	2.89	85	1391	260.85	128	3250	1.78
43	665	34.92	86	1425	10.63	129	3267	5.8

Table 2-74. B3LYP/6-31G(d) Optimized Geometries, Energies, ZPE and Temperature Corrections for compound Anionic 1e (TS):

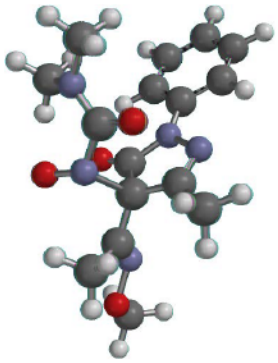

B3LYP/6-31G(d) Energy (E):	-1196.287079 hartrees
ZPE:	929.6539 kJ/mol
Temp. Correction:	987.2558 kJ/mol
G° = E + ZPE + "Temp. Correction":	-750223.3187 kcal/mol

	Atomic	Cartesian Coordinates (Angstroms)		
	Number	X	Y	Z
1	C7	-0.1568911	-0.5474637	-0.4910702
2	C2	-1.2442264	0.0531074	0.3208273
3	C3	-0.7285144	-0.0644738	1.6919178
4	N1	0.4946856	-0.5057922	1.7463555
5	N2	0.8984980	-0.7570127	0.4352090
6	O1	-0.1107054	-0.7506673	-1.7004798
7	C4	-1.4544050	0.3243738	2.9365280
8	H5	-2.4122370	-0.2042876	3.0291087
9	H6	-1.6501668	1.4018389	2.9084337
10	H7	-0.8379780	0.0983516	3.8116929
11	C5	2.1870209	-1.2483352	0.2023256
12	C6	4.7950090	-2.2348551	-0.2221786
13	C8	3.0650985	-1.4439511	1.2865900
14	C9	2.6314798	-1.5510428	-1.1005072
15	C10	3.9226413	-2.0378891	-1.2949990
16	C11	4.3502085	-1.9317317	1.0672053
17	H8	2.7177174	-1.2041961	2.2836408
18	H9	1.9526247	-1.4035577	-1.9295052
19	H10	4.2475844	-2.2663841	-2.3083899
20	H11	5.0123326	-2.0744599	1.9194907
21	H12	5.8006096	-2.6150591	-0.3867355
22	N4	-1.2695870	1.7936151	-0.2634745
23	O3	-1.5239748	1.8527151	-1.5252550
24	C14	-0.0262826	2.4175913	0.2150068

25	O4	0.0762025	2.6357949	1.4254581
26	N5	0.8533553	2.9778385	-0.6897445
27	C16	1.1703251	2.3853491	-1.9850492
28	H19	2.0923550	1.7864086	-1.9199256
29	H20	1.3351149	3.1875529	-2.7193119
30	H22	0.3364560	1.7628197	-2.3054007
31	C17	1.8809027	3.8456595	-0.1434533
32	H23	1.4910130	4.3610872	0.7345420
33	H24	2.1764977	4.5758536	-0.9088163
34	H25	2.7795856	3.2850727	0.1612337
35	C1	-2.6678827	-0.3525615	0.0493471
36	N3	-2.8140739	-1.5966356	-0.2368144
37	O2	-4.1741855	-1.9453447	-0.4603891
38	C12	-3.7736397	0.6622264	0.1423107
39	H1	-4.7504736	0.1785705	0.1827594
40	H3	-3.6967646	1.3101980	-0.7384624
41	H4	-3.6245643	1.3033725	1.0159104
42	C13	-4.2076456	-3.3107806	-0.8270205
43	H2	-3.8009148	-3.9536632	-0.0337204
44	H13	-3.6427242	-3.4936233	-1.7505357
45	H14	-5.2640974	-3.5513092	-0.9880835

Table 2-75. B3LYP/6-31G(d) Calculated IR Frequencies (cm^{-1}, uncorrected) and Intensities for compound Anionic 1e (TS):

	cm^{-1}	Intensity		cm^{-1}	Intensity		cm^{-1}	Intensity
1	-227	114.80	44	696	25.99	87	1413	44.50
2	21	0.23	45	703	2.68	88	1440	33.64
3	27	0.06	46	706	9.64	89	1449	3.11
4	44	0.06	47	710	13.63	90	1467	18.30
5	51	1.76	48	740	13.45	91	1483	10.58
6	60	1.73	49	755	21.08	92	1493	6.58
7	83	7.89	50	761	34.39	93	1501	8.27
8	90	0.42	51	792	3.94	94	1503	1.82
9	104	2.09	52	846	51.64	95	1505	2.13
10	112	1.60	53	856	0.15	96	1511	12.47
11	123	3.65	54	891	143.09	97	1515	0.38
12	131	1.17	55	903	7.77	98	1521	9.66
13	139	2.29	56	968	0.22	99	1530	5.70
14	160	1.28	57	984	21.66	100	1542	25.81
15	167	0.42	58	987	1.65	101	1545	86.11
16	186	1.03	59	1002	23.70	102	1549	172.18
17	193	0.86	60	1011	12.86	103	1556	12.93
18	197	1.36	61	1032	59.90	104	1621	28.73
19	209	1.25	62	1042	51.90	105	1639	22.28
20	218	12.75	63	1056	2.97	106	1660	196.06
21	235	1.48	64	1070	9.82	107	1698	9.43
22	254	0.86	65	1080	68.91	108	1707	231.58
23	268	1.51	66	1087	12.95	109	1748	193.63
24	288	2.24	67	1088	10.38	110	2993	37.75

25	299	7.99	68	1096	10.56	111	3001	145.78
26	332	0.95	69	1105	225.53	112	3018	120.51
27	340	5.88	70	1134	252.38	113	3040	53.40
28	345	32.35	71	1139	90.56	114	3042	81.45
29	365	25.07	72	1142	71.89	115	3056	77.13
30	370	5.03	73	1186	1.32	116	3063	17.50
31	388	2.61	74	1189	2.94	117	3077	54.72
32	420	6.24	75	1190	19.95	118	3106	12.48
33	423	0.09	76	1194	6.27	119	3117	48.46
34	441	13.92	77	1205	3.66	120	3129	10.04
35	458	14.36	78	1229	25.08	121	3137	15.83
36	475	21.71	79	1263	206.93	122	3158	3.21
37	519	3.33	80	1290	135.75	123	3168	8.24
38	529	2.49	81	1333	16.57	124	3169	49.82
39	572	16.34	82	1351	46.60	125	3172	17.83
40	605	10.72	83	1362	115.26	126	3180	31.43
41	633	1.04	84	1368	39.07	127	3188	76.09
42	641	16.02	85	1389	101.10	128	3248	1.60
43	668	31.71	86	1395	200.26	129	3260	6.19

2.7.5. ^{1}H NMR and ^{13}C NMR Spectra: **NHPY** compounds were synthesized using Methods **A** and/or **B**, as indicated in the manuscript. NMR spectra of the donors including the synthetic method are provided below.

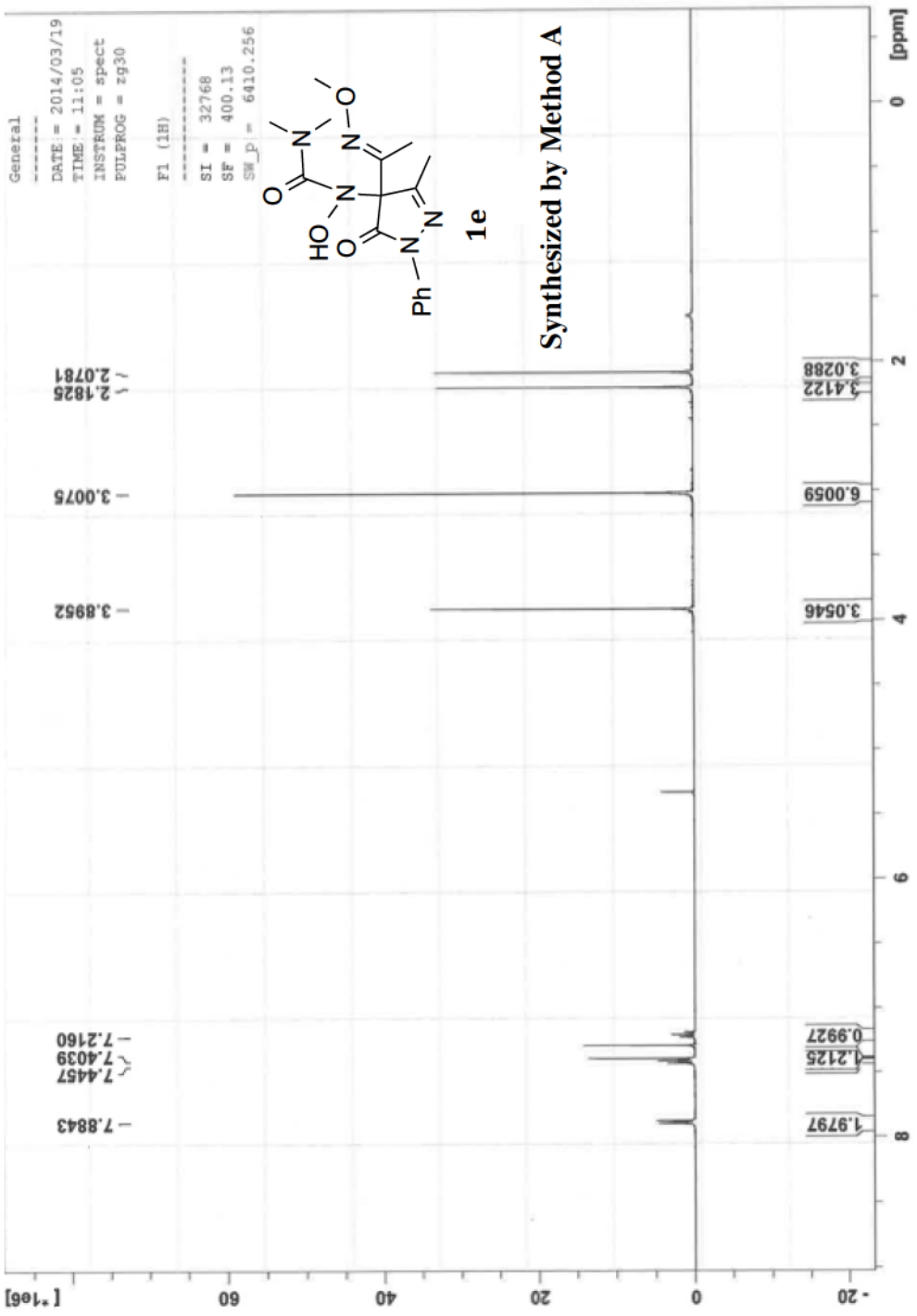

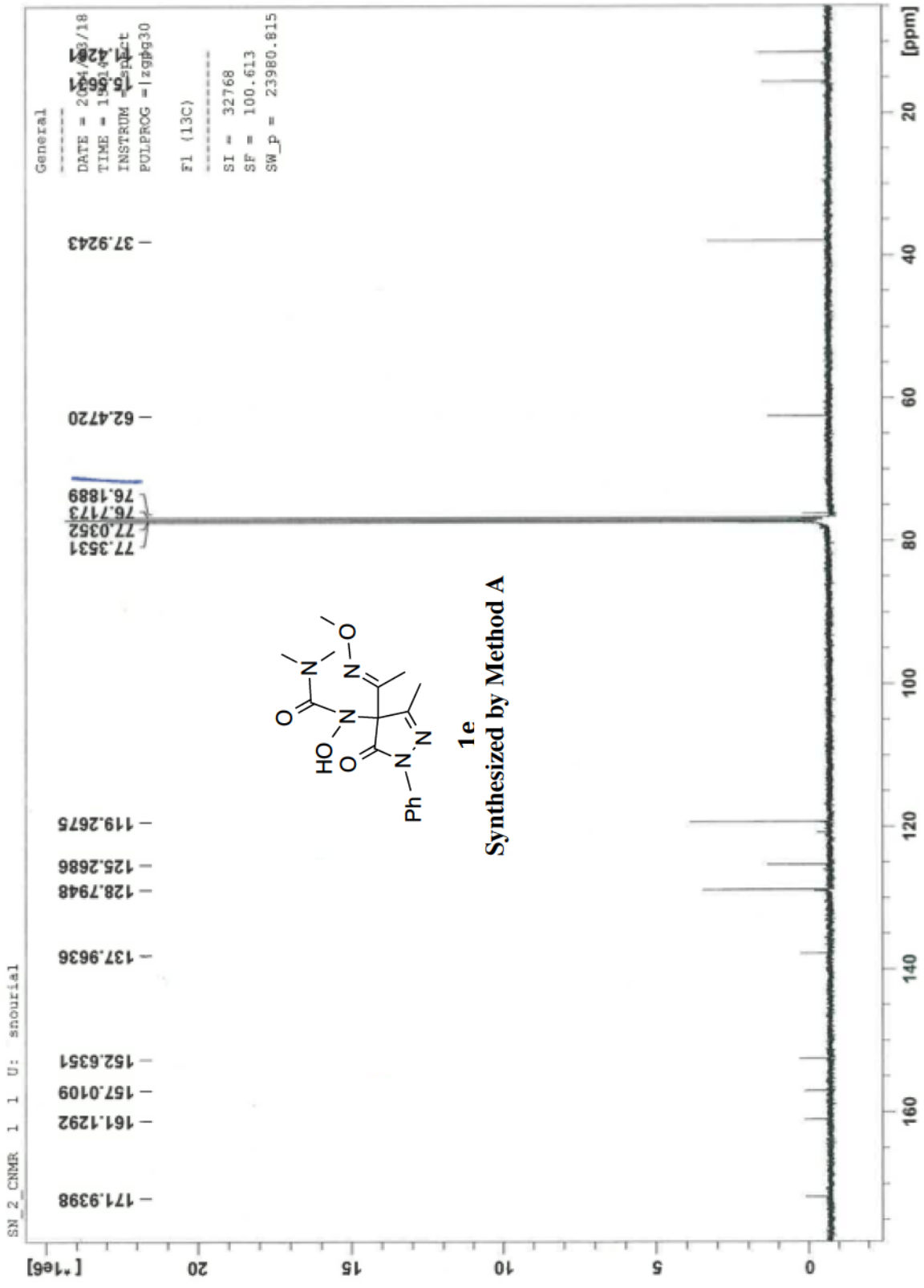
SN_2_CNMR 1 1 U: snouvial
General
DATE = 20/03/18
TIME = 15:01:04
INSTRUM = spect
PULPROG = zgpg30
F1 (13C)
SI = 32768
SF = 100.613
SW_p = 23980.815
171.9398
161.1292
157.0109
152.6351
137.9636
128.7948
125.2686
119.2675
77.3531
77.0352
76.7173
76.1889
62.4720
37.9243
15.5631
14.4281
[ppm]
[*1e6]
1e
Synthesized by Method A

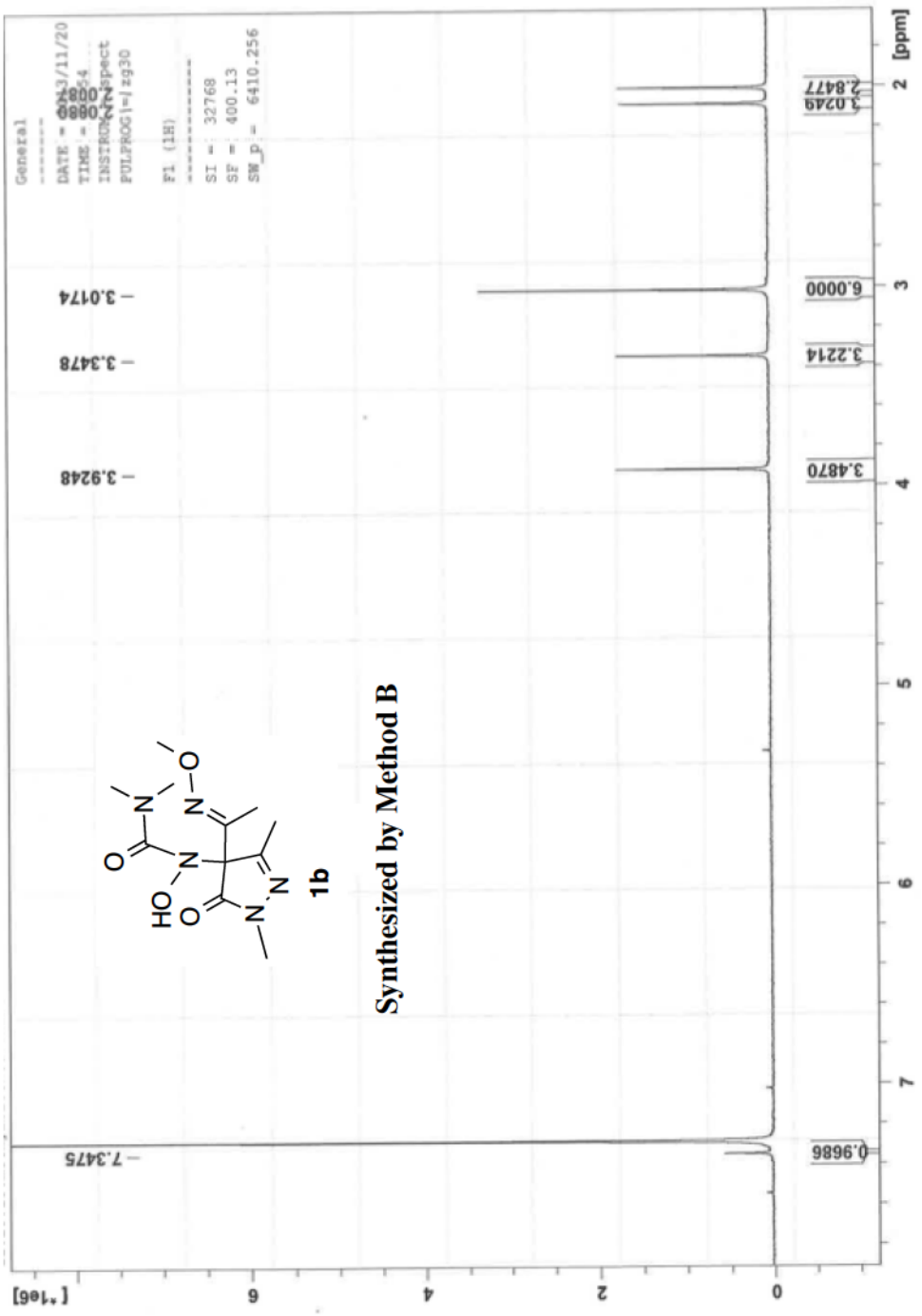
Synthesized by Method B
1b
7.3475
3.9248
3.3478
3.0174
0.9686
3.4870
3.2214
6.0000
3.0249
2.8477
[ppm]
[*10e6]

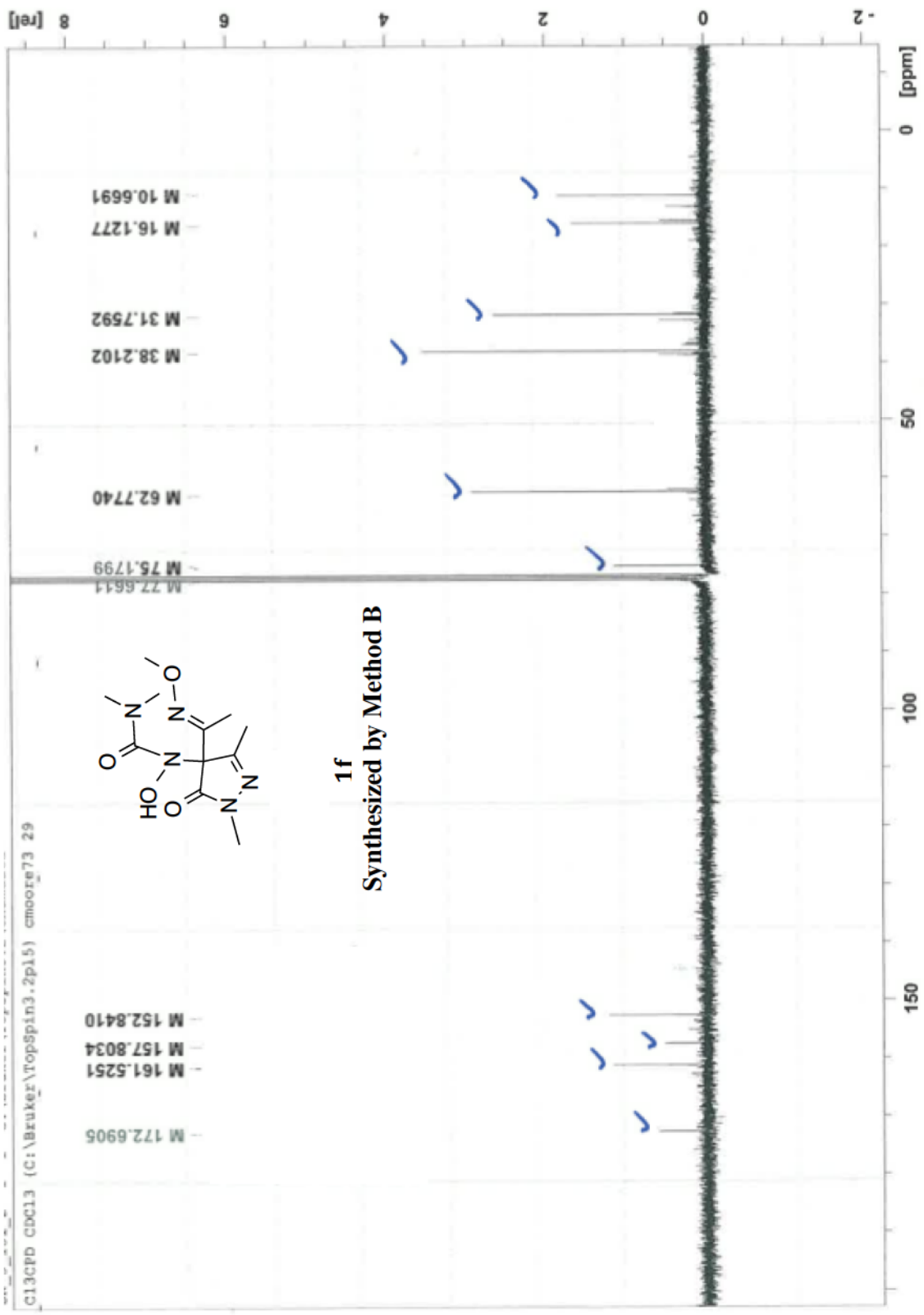

1f
Synthesized by Method B

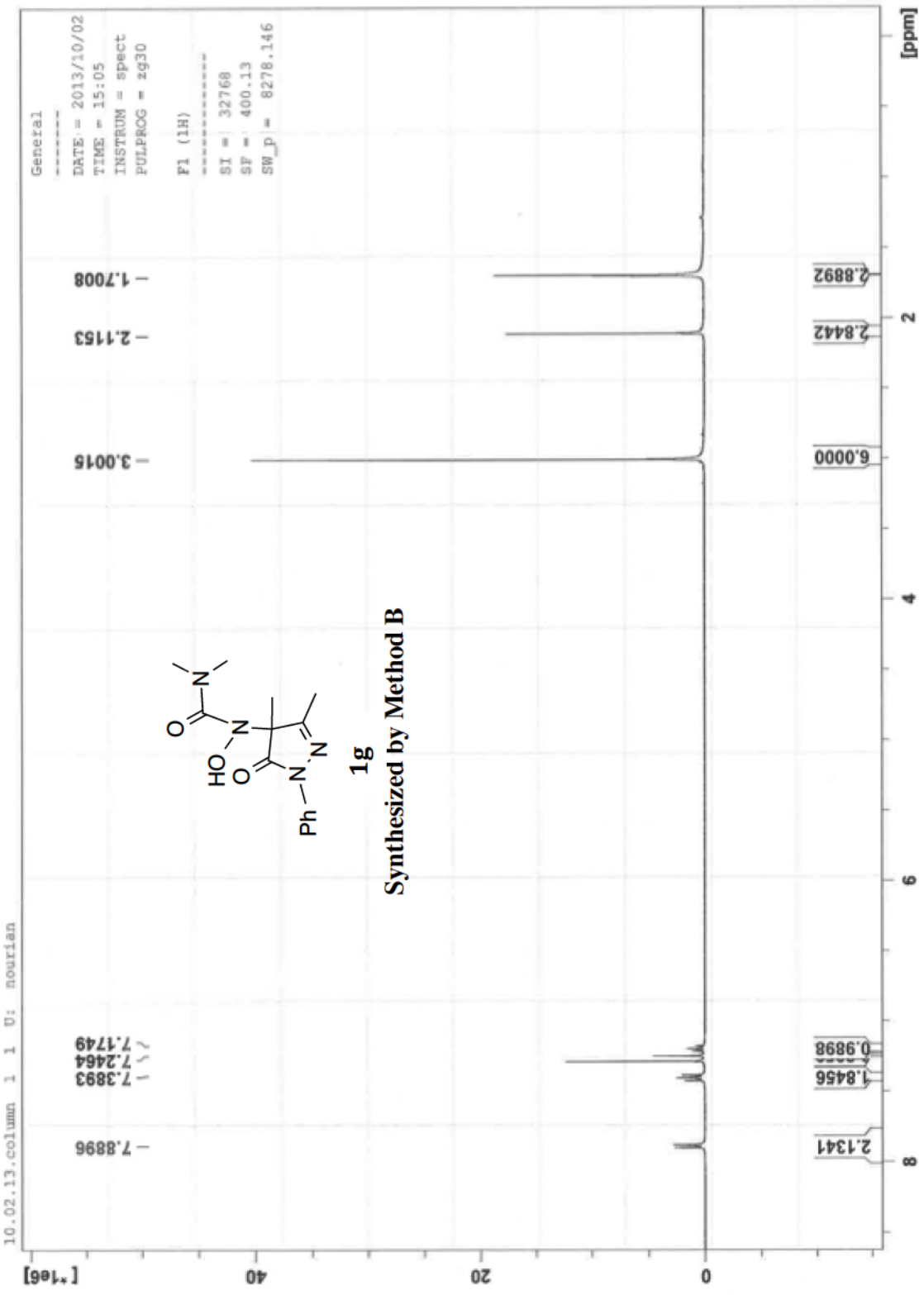

1g

Synthesized by Method B

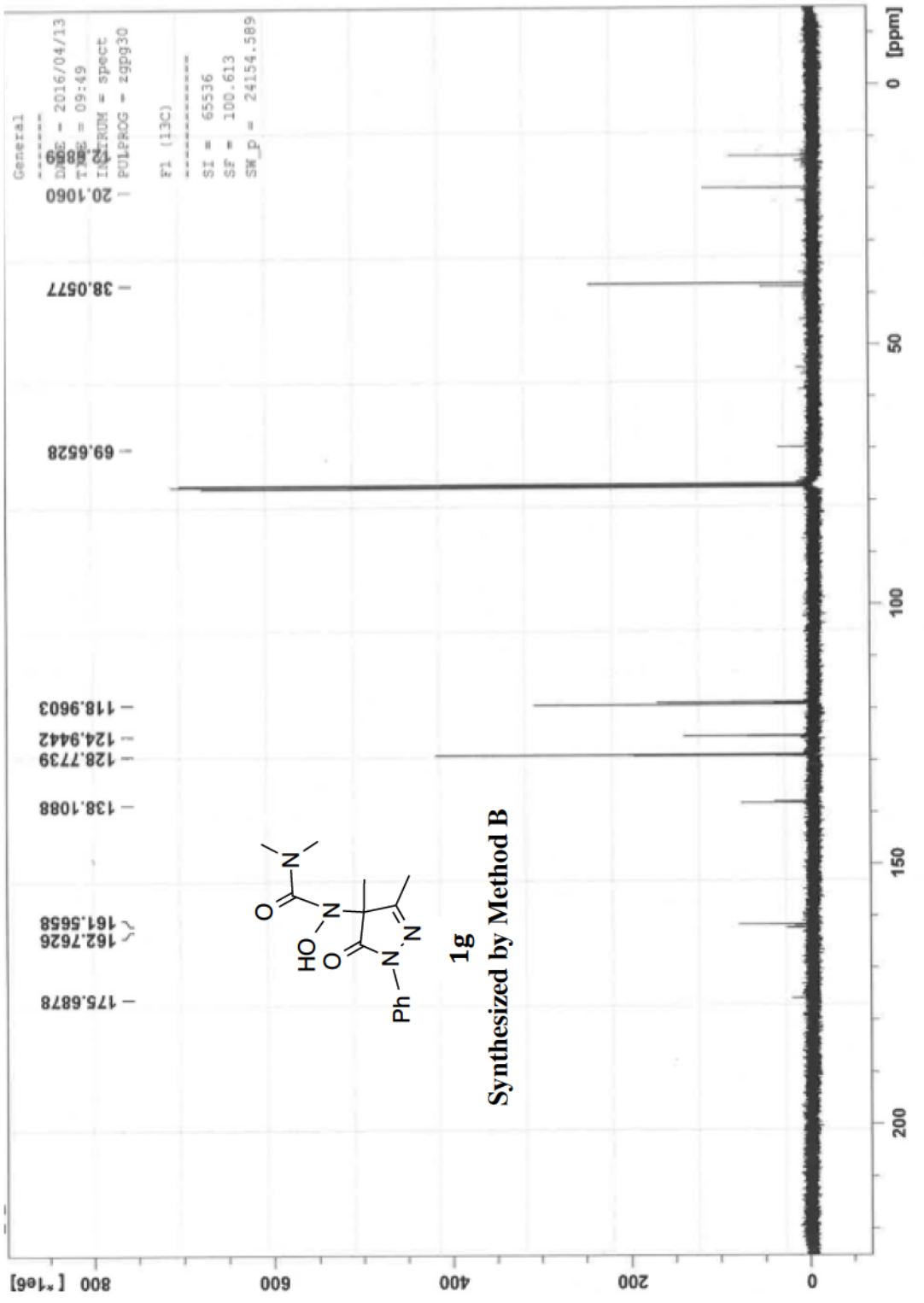
General
DATE = 2016/04/13
TIME = 09:49
INSTRUM = spect
PULPROG = zgpg30
F1 (13C)
SI = 65536
SF = 100.613
SW_p = 24154.589
20.1060
38.0577
69.6528
118.9603
124.9442
128.7739
138.1088
162.7626
161.5658
175.6878
[ppm]
[*10e6]
1g
Synthesized by Method B

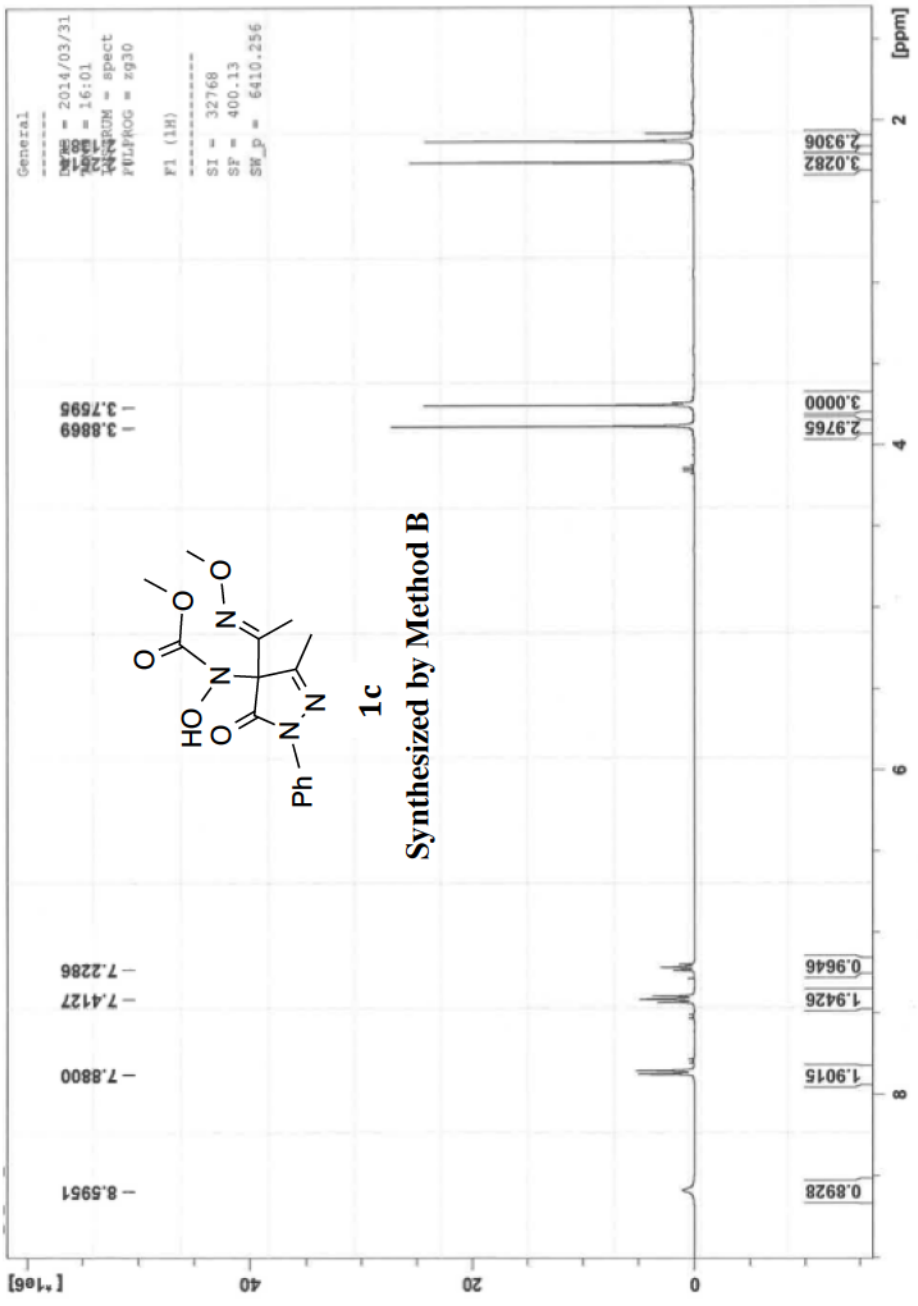

1c

Synthesized by Method B

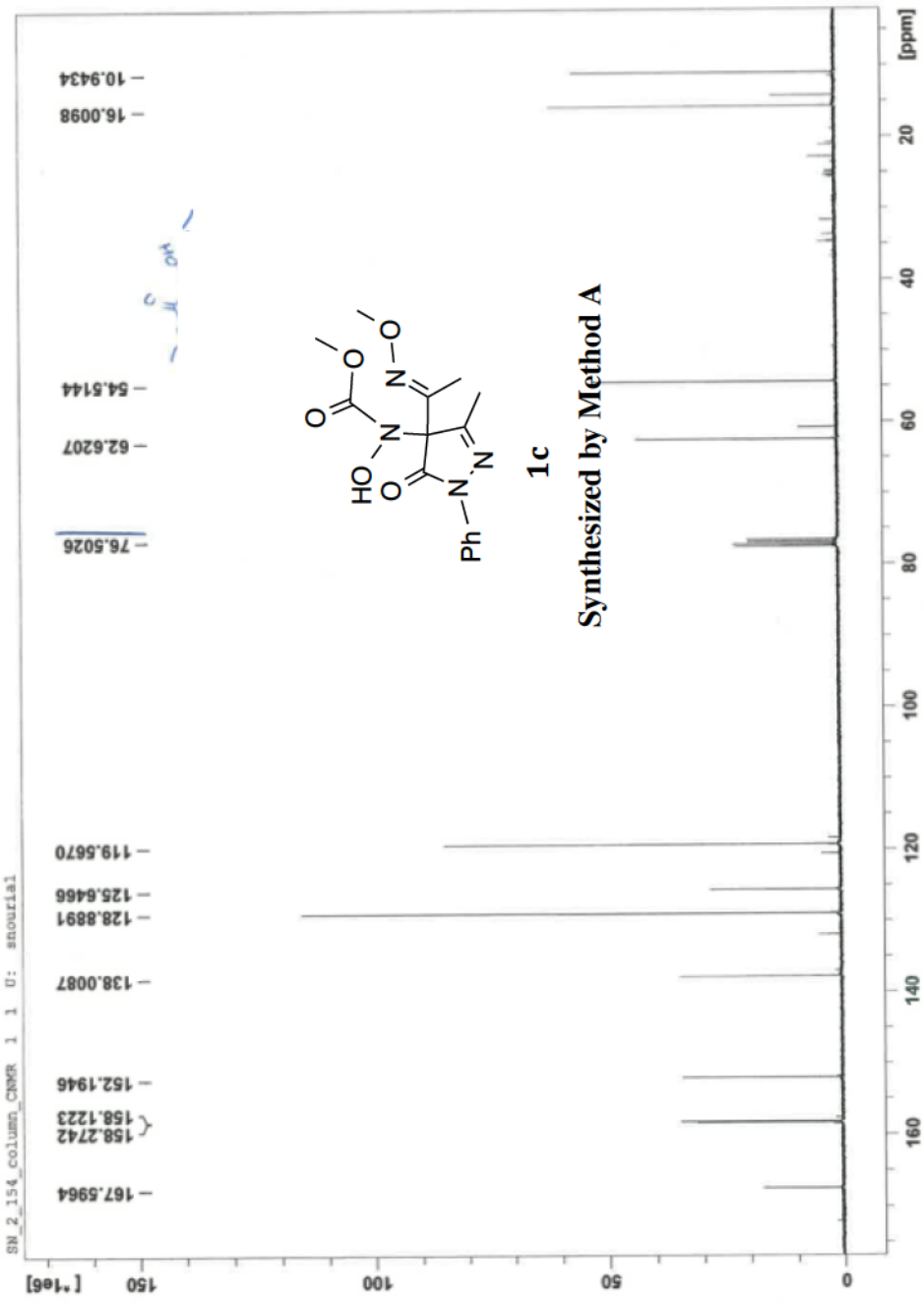
10.9434
16.0098
54.5144
62.6207
76.5026
119.5670
125.6466
128.8891
138.0087
152.1946
158.2742
158.1223
167.5964
[ppm]
[*1e6]
SN_2_154_column_CNMR 1 1 U: snourial
Ph
HO
1c
Synthesized by Method A

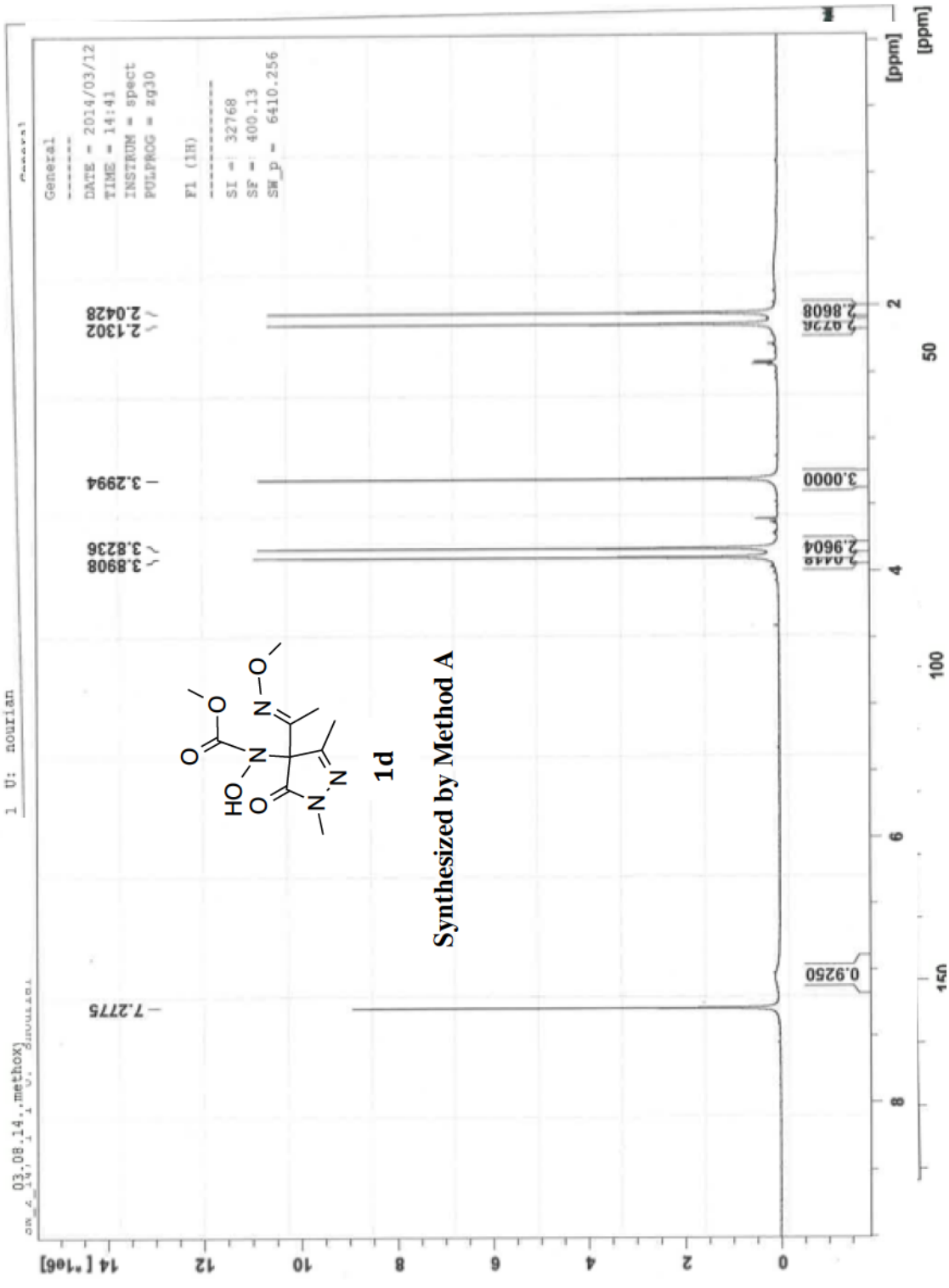
1d
Synthesized by Method A
7.2775
3.8908
3.8236
3.2994
2.1302
2.0428
0.9250
3.0000
2.9604
2.8608
[ppm]
[ppm]

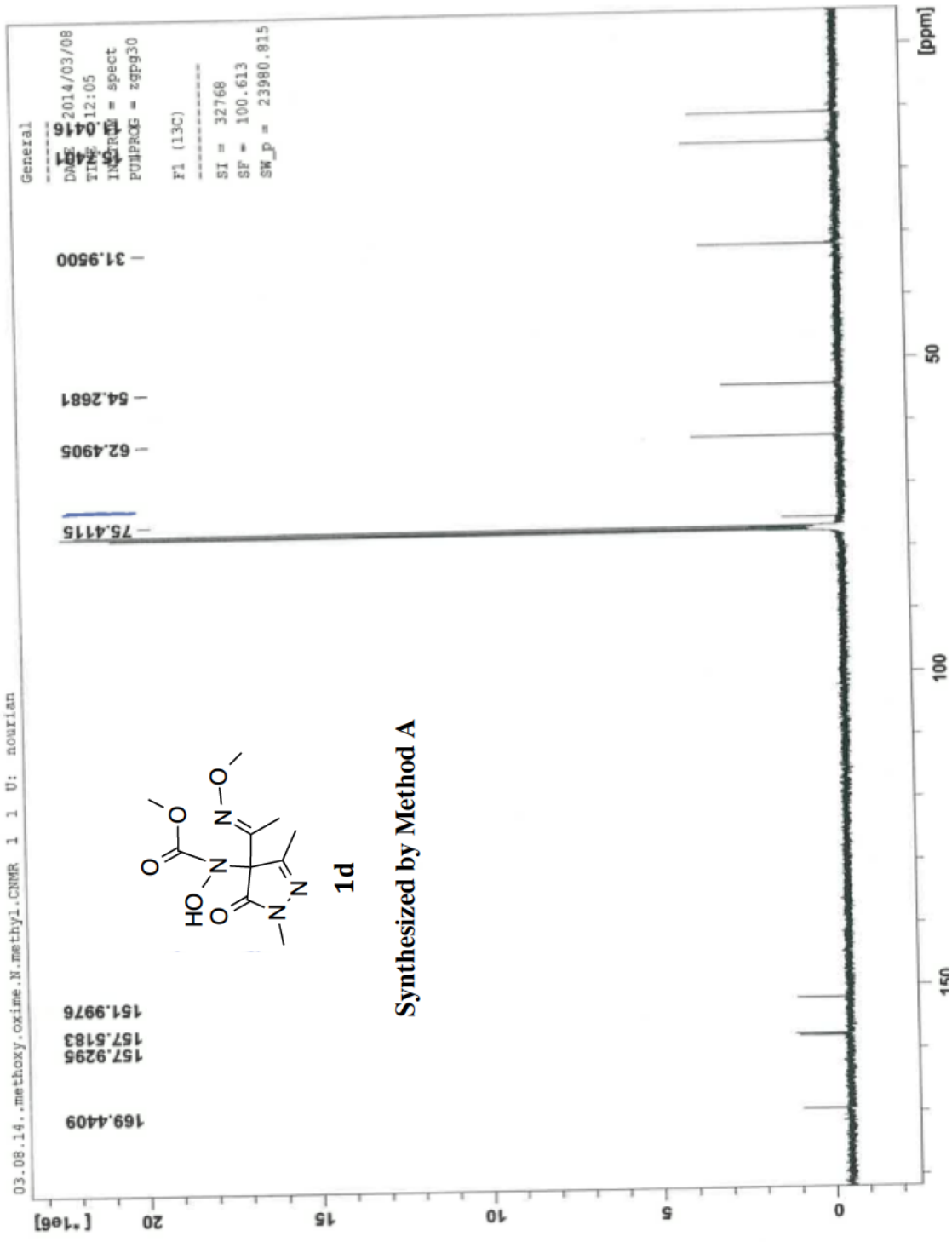
03.08.14..methoxy.oxime.N.methyl.CNMR 1 1 U: nourian
General
DATE 2014/03/08
TIME 12:05
INSTRU = spect
PULPROG = zgpg30
F1 (13C)
SI = 32768
SF = 100.613
SW_p = 23980.815
169.4409
157.9295
157.5183
151.9976
75.4115
62.4905
54.2681
31.9500
[ppm]
[*10e6]
1d
Synthesized by Method A

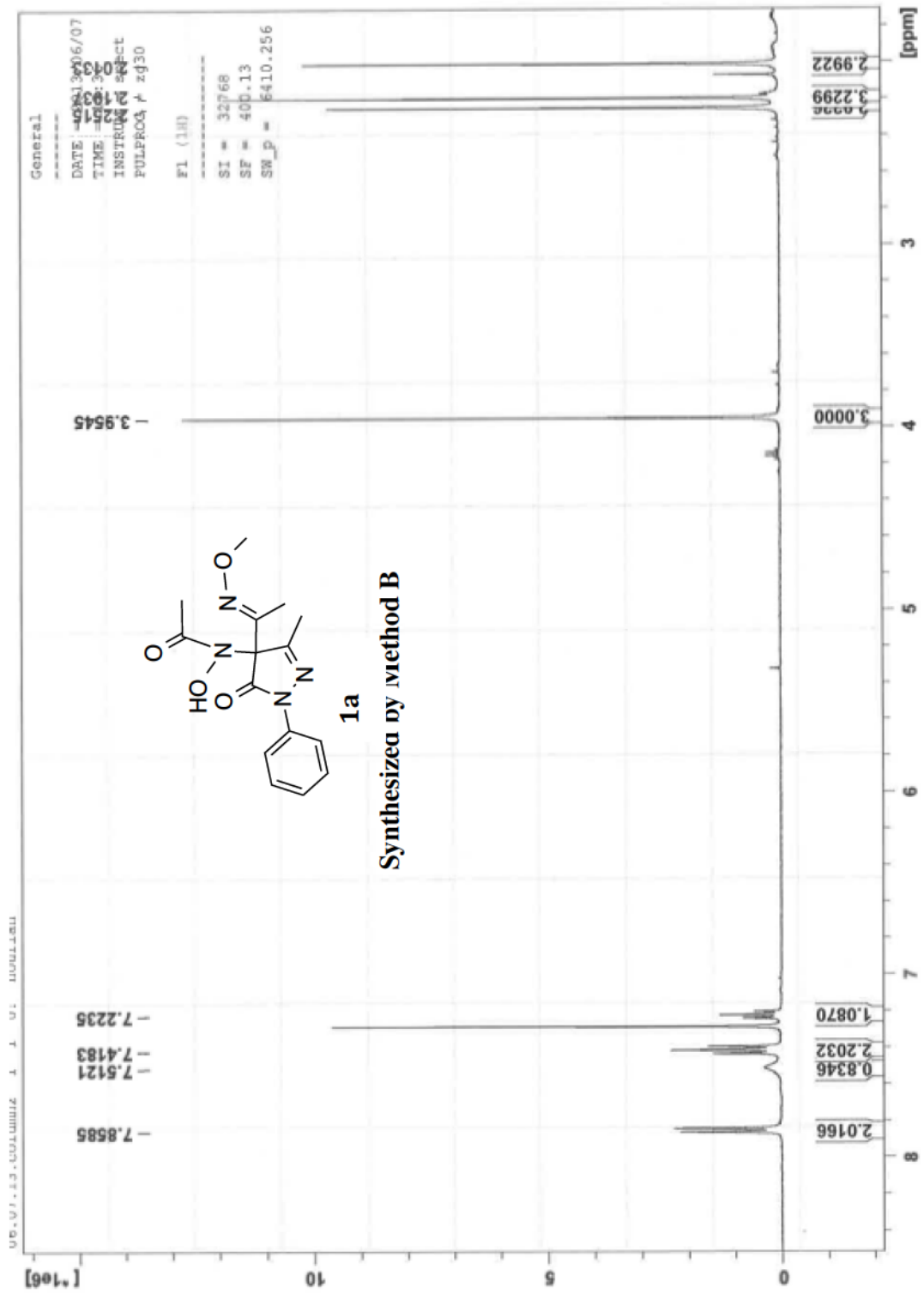
1a
Synthesized by method B
[ppm]
[*10e6]
3.9545
7.8585
7.6121
7.4183
7.2235
2.9922
3.2299
3.0000
2.0166
0.8346
2.2032
1.0870

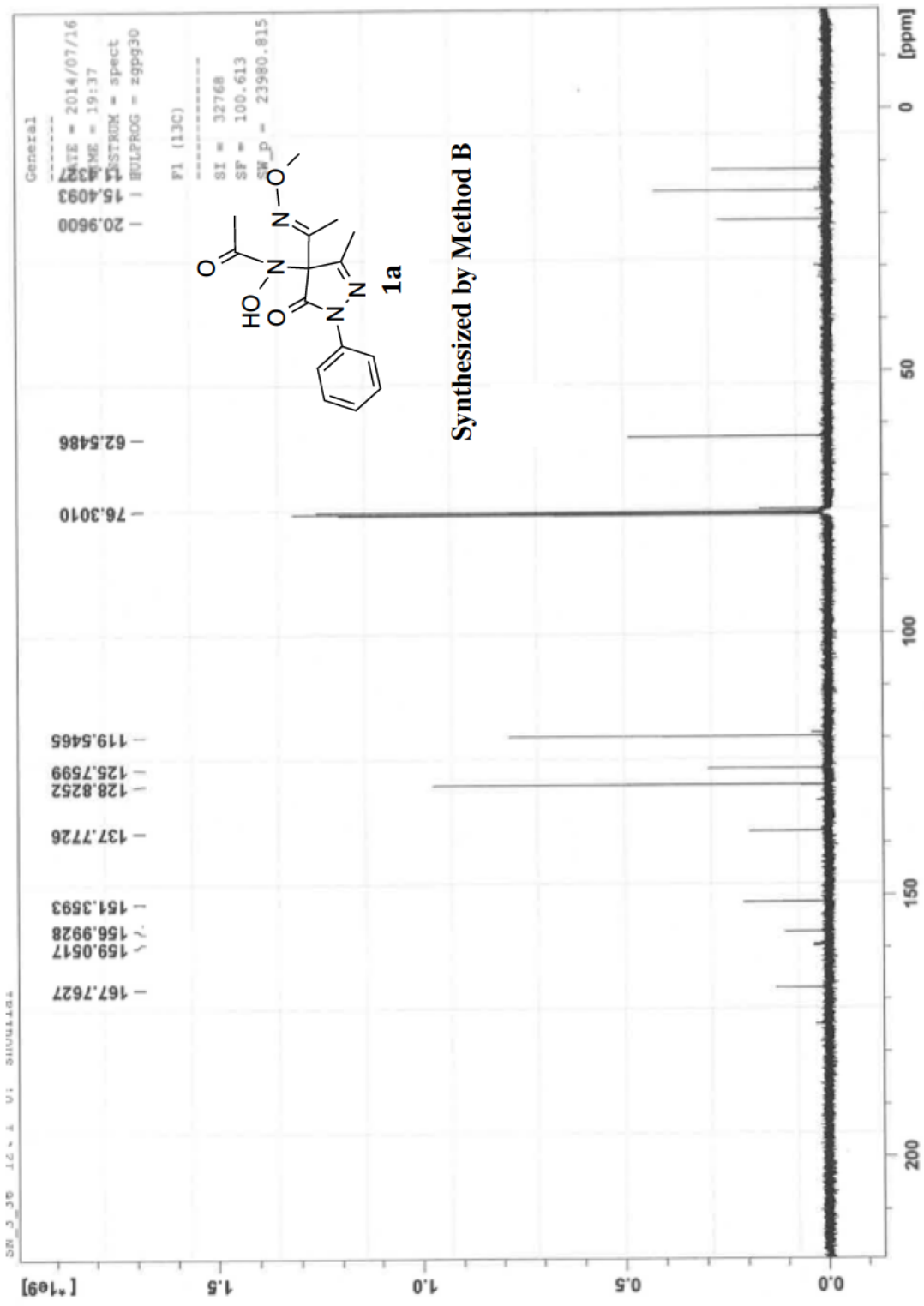
Synthesized by Method B
1a
[ppm]
0
50
100
150
200
0.0
0.5
1.0
1.5
[*10^9]
167.7627
159.0517
156.9928
151.3593
137.7726
128.8252
125.7599
119.5465
76.3010
62.5486
20.9600
15.4093
General
SI = 32768
SF = 100.613
F1 (13C)

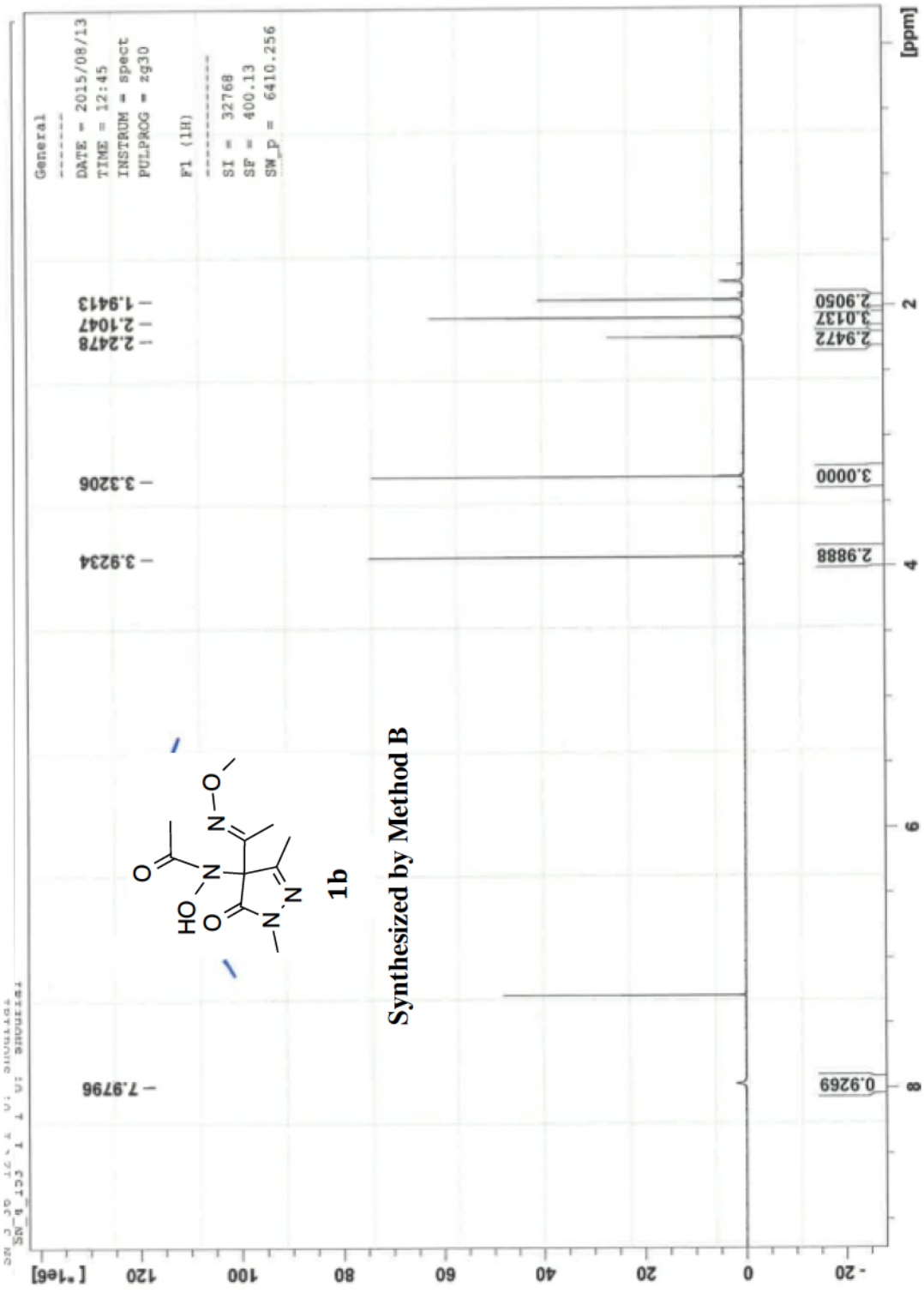

1b

Synthesized by Method B

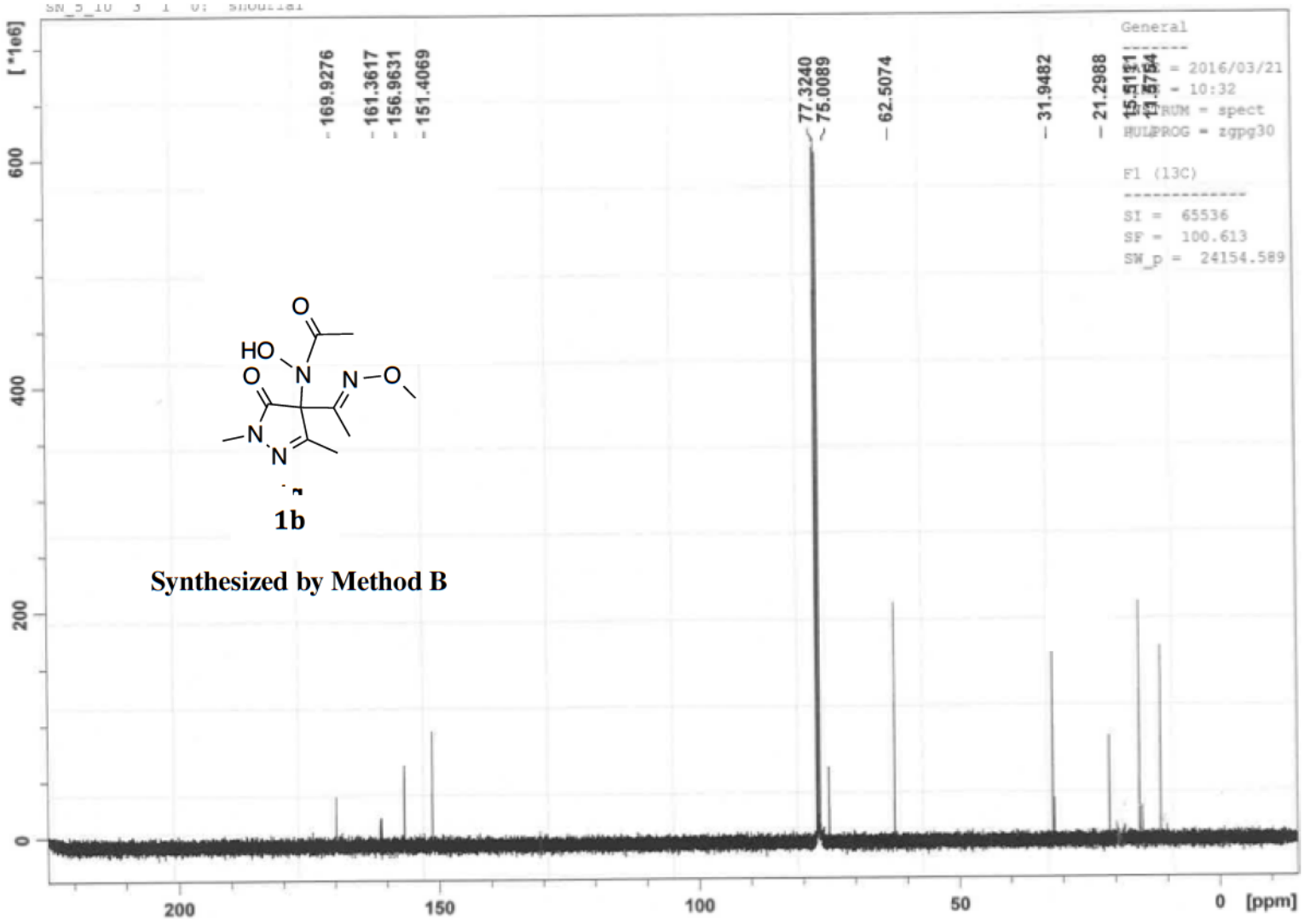

1b

Synthesized by Method B

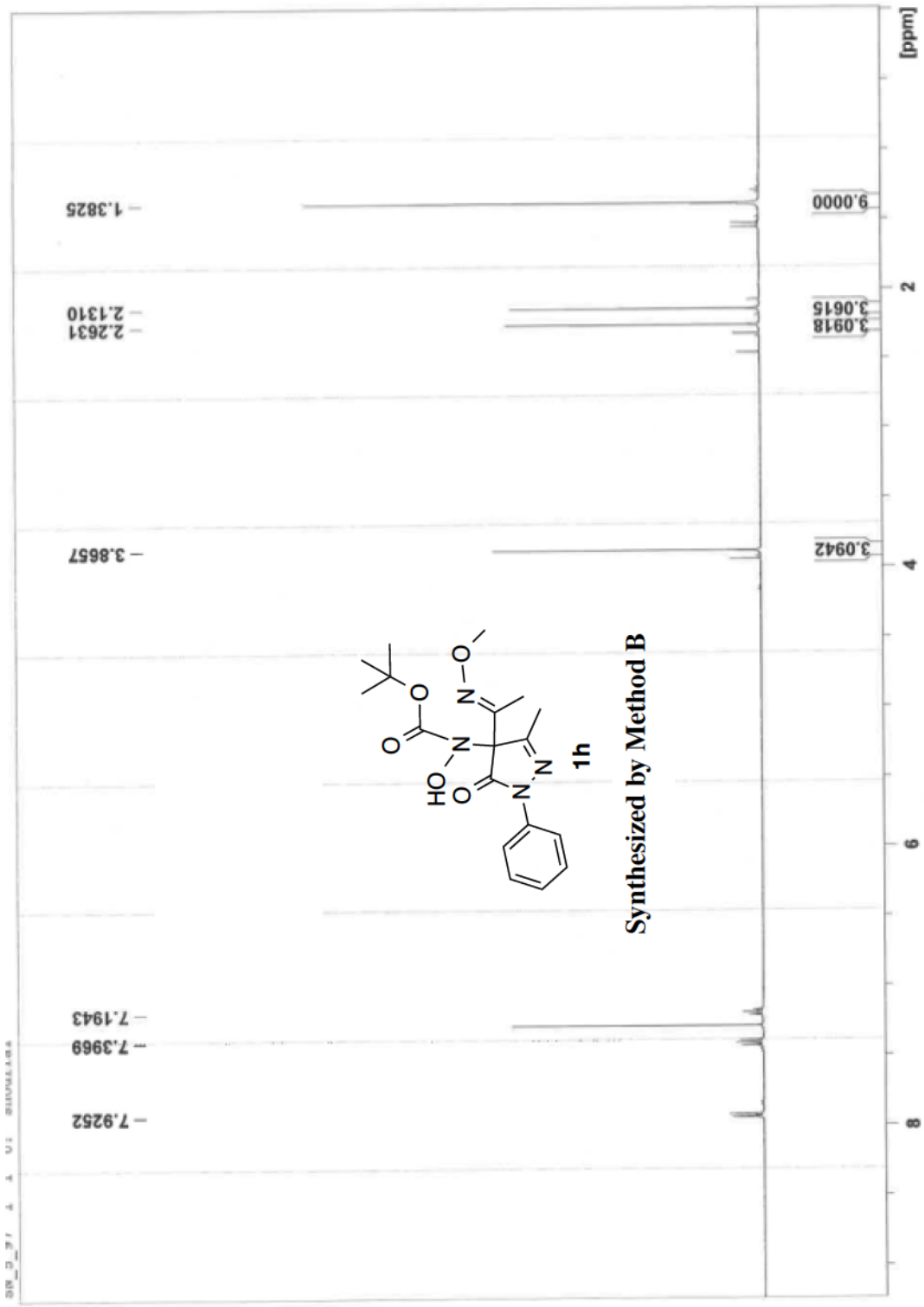
1.3825
2.1310
2.2631
3.8657
7.1943
7.3969
7.9252
9.0000
3.0615
3.0918
3.0942
2
4
6
8
[ppm]
1h
Synthesized by Method B

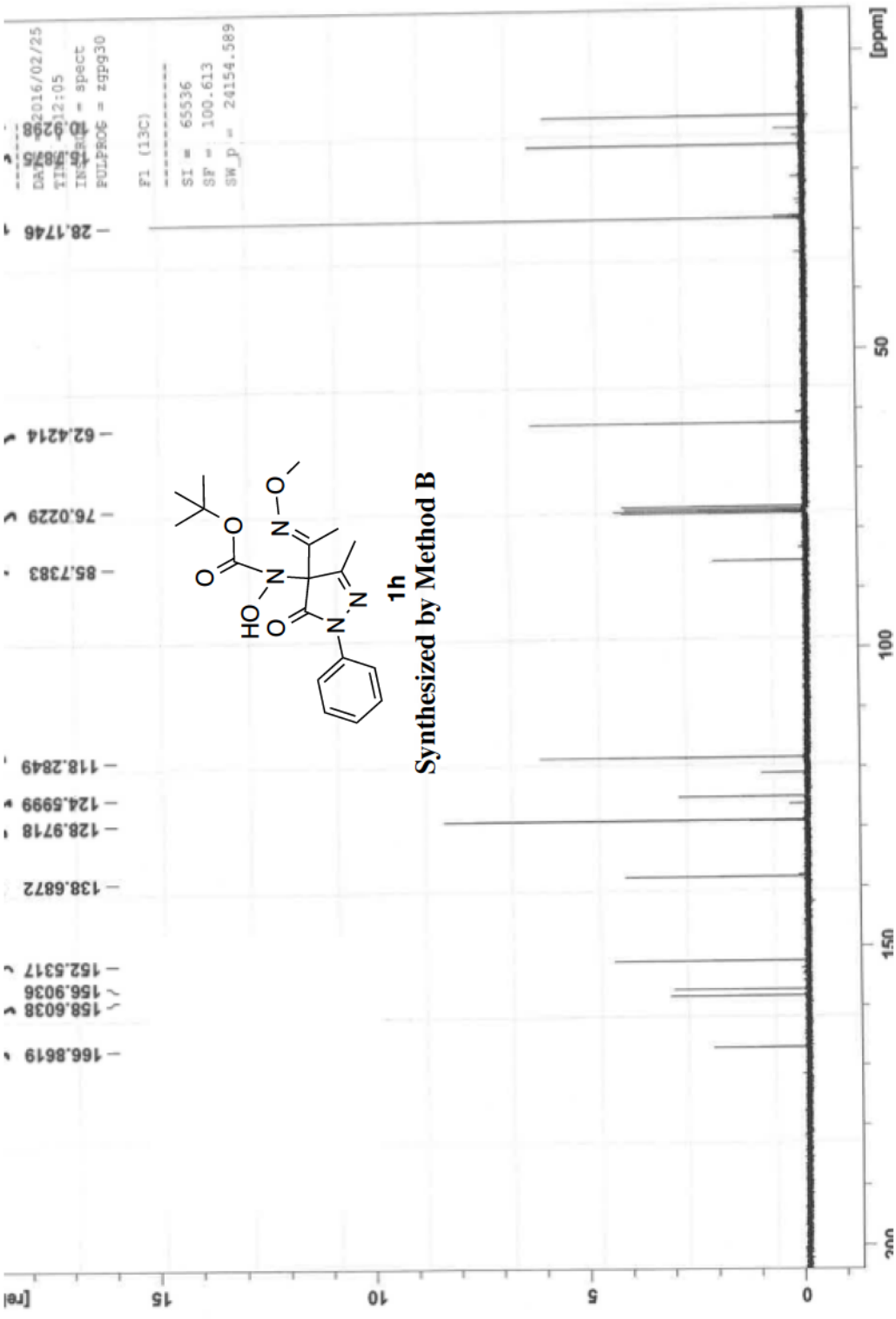

1h

Synthesized by Method B

Chapter 3.

Nitrosocarbonyl Release from *O*-Substituted Hydroxamic Acids with Pyrazolone Leaving Groups

3.1. Abstract

A new class of nitrosocarbonyl precursors, *O*-substituted hydroxamic acids with pyrazolone leaving groups (**OHPY**), is described. These compounds generate nitrosocarbonyl intermediates, which upon hydrolysis release nitroxyl (azanone, HNO) under physiologically relevant conditions. Pyrazolones have been used to confirm the generation of nitrosocarbonyls by competitive trapping to form isomeric *N*-substituted hydroxamic acids (**NHPY**) via an *N*-selective nitrosocarbonyl

aldol reaction. The rate of nitrosocarbonyl release from **OHPY** donors is impacted by donor substituents, including the pyrazolone leaving group.

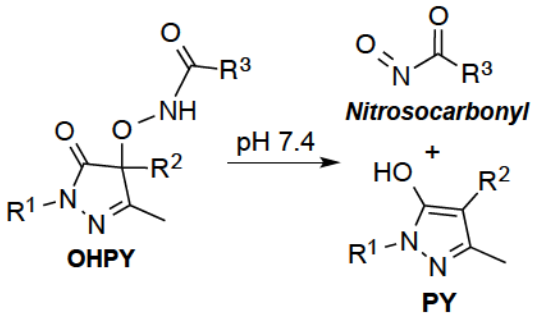

3.2. Introduction

Nitroxyl (azanone, HNO), the one-electron reduced and protonated form of nitric oxide, has been shown to improve both vasorelaxation and myocardial contractility, making HNO donors ideal candidates for drug development.[1-9] HNO is a reactive molecule that spontaneously dimerizes to produce hyponitrous acid (HON=NOH), which then dehydrates to give nitrous oxide (N_2O).[10] Due to this inherent reactivity, HNO must be generated *in situ* through the use of donor compounds.

Angeli's salt ($Na_2N_2O_3$, **AS**, Figure 3-1) is a well-known donor that generates HNO under physiological conditions with a short half-life.[11] Derivatization of this inorganic salt has been unsuccessful to date, thus preventing modification for tunable HNO release. Piloty's acid (**PA**) derivatives and acyloxy nitroso compounds (**AcON**) represent other types of HNO donors that have been developed with tunable half-lives.[12-17] Our group has recently reported two new series of HNO

donors with half-lives that can be varied from minutes to hours under physiological conditions: (hydroxylamino)pyrazolone (**HAPY**) and (hydroxylamino)barbituric acid (**HABA**) derivatives.[18-20] In addition to these examples, the continued development of efficient HNO donors is important to expand the research tools available to understand the potential role of HNO in biological processes.

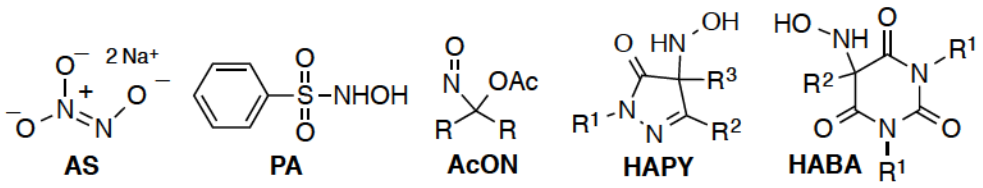

Figure 3-1. Some previously reported HNO donors.

Another strategy to release HNO is based on the hydrolysis of nitrosocarbonyl intermediates.[21-22] Nitrosocarbonyls are highly reactive species that can react with nucleophiles including water to generate HNO. Oxidation of hydroxamic acids and thermal decomposition of 9,10-dimethylanthracene adducts represent common approaches to nitrosocarbonyl generation.[23-25] The photolysis of nitrodiazo compounds, nitronates with alpha leaving groups, and 1,2,4-oxadiazole-4-oxides have also been shown to generate nitrosocarbonyls efficiently.[26-28] Recently, the aerobic oxidation of hydroxamic acids by metal catalysts under mild conditions has been developed as an efficient strategy for nitrosocarbonyl generation.[29-46] In general, however, the above methods are not suitable for HNO generation under physiological conditions.

Herein, we report a novel class of nitrosocarbonyl donors that upon deprotonation and loss of the leaving group (Scheme 1, HX = pyrazolone) irreversibly generate nitrosocarbonyl intermediates that can hydrolyze to release HNO under physiological conditions. As has been demonstrated in recent reports,[33,35,36,40-42,45] nitrosocarbonyls can react with nucleophiles through an *N*-selective nitrosocarbonyl aldol reaction to produce *N*-substituted hydroxamic acid adducts. We have recently found that pyrazolones are efficient traps for nitrosocarbonyl intermediates to generate *N*-substituted hydroxamic acid derivatives with pyrazolone leaving groups (**NHPY**) in a reversible manner.[47] In the current work, we observe this same reactivity upon **OHPY** decomposition to generate nitrosocarbonyls which further react with pyrazolones to produce **NHPY** compounds (Scheme 3-1). We have synthesized and studied **NHPY** compounds independently, and as discussed in Chapter 2, have demonstrated the efficient formation of nitrosocarbonyl intermediates upon decomposition of these compounds.[47]

Scheme 3-1. Reactivity of OHPY nitrosocarbonyl precursors

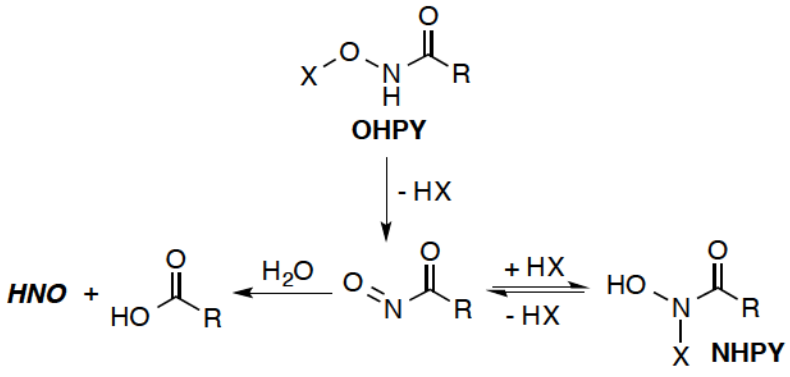

3.3. Results and Discussion

3.3.1. Synthesis

OHPY compounds **1** have been synthesized by formation of the corresponding bromide (Br-PY) followed by reaction with hydroxamic acids (Scheme 3-2). Initially, **OHPY 1a** was synthesized without the need for chromatographic purification, and its structure was confirmed by X-ray crystallography. The other precursors were purified using column chromatography.

Scheme 3-2. Synthesis of OHPY derivatives

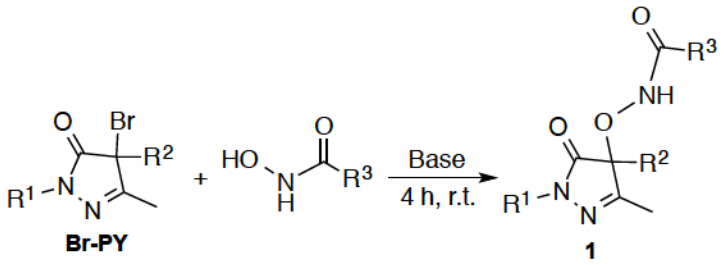

The **OHPY** and **NHPY** isomers can obviously be distinguished by X-ray crystallography. An analysis of ^{13}C NMR data and available crystal structures (Supporting Information), reveal that **OHPY** and **NHPY** compounds have distinctive chemical shifts for their quaternary carbons (δ = 87.6 – 90.2 ppm for **OHPY** vs. δ = 68.4 – 76.5 ppm for **NHPY**). Thus, ^{13}C NMR spectroscopy conveniently allows the two isomers to be distinguished if crystal structures cannot be obtained.

3.3.2. Decomposition of OHPY compounds

Nitrosocarbonyl formation following **OHPY** decomposition under physiological conditions was studied. As described above, the reaction of nitrosocarbonyls and pyrazolones to produce **NHPY** compounds can be efficient. Upon nitrosocarbonyl generation from **OHPY** precursors **1**, therefore, a competition exits between hydrolysis to generate HNO and carboxylic acid **4** (Scheme 3-3, *Path A*) and trapping by the pyrazolone byproduct **2** to produce **NHPY** compounds **3** (Scheme 3-3, *Path B*). **NHPY** compounds subsequently can also release nitrosocarbonyl intermediates with half-lives that depend on R^1, R^2, and R^3 (Scheme 3.3, *Path C*).[47]

Scheme 3-3. Reactivity of OHPY donors 1

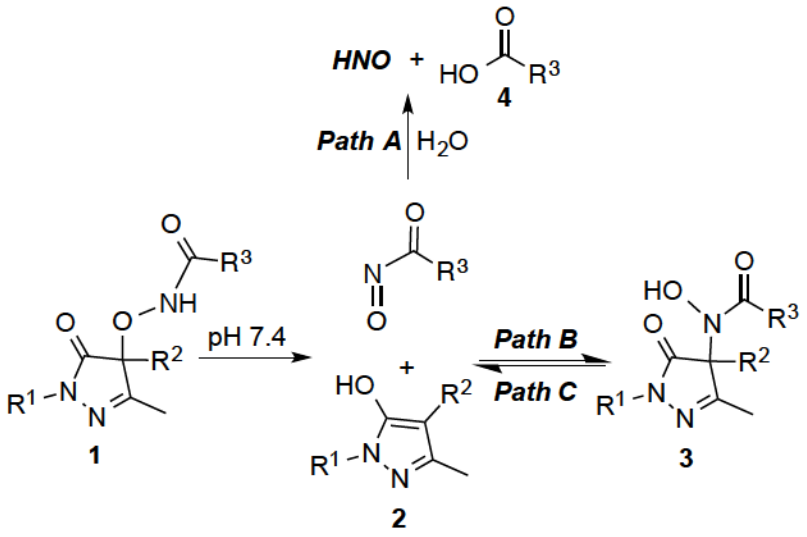

^{1}H NMR spectroscopy was used to examine the decomposition of **OHPY** donors and measure relative product yields in aqueous solution (Table 3-1).[19,20] Pyrazolone **2**, **NHPY** **3**, and carboxylic acid **4** are cleanly formed as the only observable organic products. Because **NHPY** compounds **3a**, **3c**, and **3d** all have

half-lives on the order of days,[47] *Path C* in Scheme 3-3 does not contribute to the obser

ved chemistry for **OHPY** donors **1a**, **1c**, and **1d**. Thus, the relative yields of pyrazolone **2** and carboxylic acid **4** compared with that for **NHPY** compound **3** in Table 3-1 reflect the competition between *Path A* and *Path B* for these donors.

Table 3-1. Product yields and half-lives for OHPY donors

OHPY	R^1	R^2	R^3	%2[a]	%3[a]	%4[a]	$t_{1/2}$ (min)[b]
1a	Ph	C(=NOMe)Me	Me	74	26	73	25
1b	Ph	Me	Me				Stable[c]
1c	Ph	C(=NOMe)Me	MeO	28	72	27	0.6
1d	Me	C(=NOMe)Me	MeO	14	86	14	1.2
1e	Ph	C(=NOMe)Me	*t*-BuO	*d*	*d*	*d*	*d*

[a]Relative yields determined from ^{1}H NMR analysis of the complete decomposition of 0.5 mM of the **OHPY** donor in 10% DMSO-d_6, 10% D_2O, and 80% H_2O, phosphate buffer (0.25 M) containing 0.2 mM of the metal chelator, diethylenetriaminepentaacetic acid (DTPA), pH 7.4 at 37 °C under argon. [b]Determined by UV-vis spectroscopy. [c]Less than 5% decomposition after 2 days. [d]Not Determined due to low solubility.

OHPY decomposition was also monitored by UV-vis spectroscopy to measure donor half-lives at pH 7.4 and 37 °C (Table 3-1). Based on the chemistry of related HNO donors,[19,20] we propose that the first step of decomposition is deprotonation which leads to release of nitrosocarbonyl plus pyrazolone. If the barrier to dissociation from anionic **OHPY** is very small, observed half-lives should correlate with donor pK_a and the pyrazolone leaving group.[19,20] Pyrazolone **2a** (R^1 = Ph, R^2 =

(C(=NOMe)Me, pK_a = 6) is a better leaving group than pyrazolone **2b** (R^1 = Ph, R^2 = Me, pK_a = 7.6),[19] consistent with the much shorter half-life for **OHPY 1a** ($t_{1/2}$ = 25 min) compared with **1b** (stable). Exchanging the R^1 group from phenyl to methyl (**OHPY 1c** vs. **1d**) increases the half-life by a factor of two, consistent with that previously reported for analogous **HAPY** and **NHPY** donors.[19,47] A comparison of the known pK_a values of the related compounds, PhC(O)NHOH (8.8) and PhOC(O)NHOH (10.0),[48] indicates that the pK_a of **OHPY 1a** is likely lower than that of **OHPY 1c**.

Although these two donors have the same pyrazolone leaving group, the longer half-life for **OHPY 1a** ($t_{1/2}$ = 25 min) compared with **1c** ($t_{1/2}$ = 0.6 min) suggests that the barrier to dissociation may also affect the observed half-lives. In the case of **NHYP** donors, the dissociation barrier was found to be strongly dependent on the R^3 group.[47] The origin and impact of the R^3 group on **OHPY** dissociation requires further investigation.

HNO generation was examined by gas chromatographic (GC) headspace analysis to quantify the amount of its dimerization product, N_2O, formed following decomposition of **OHPY** donors in pH 7.4 phosphate buffer solutions at 37 °C (Table 3-2). The amount of HNO release was measured relative to standard HNO donor, Angeli's salt. As expected, HNO yields from **OHPY** donors are consistent with the corresponding yields of pyrazolone **2** and carboxylic acid **4** observed under the same conditions.

Table 3-2. HNO yields for OHPY donors at different concentrations

OHPY	% HNO[a]		
	500 μM	100 μM	20 μM
1a	70	75	91
1b	*b*	*b*	*b*
1c	20	29	41
1d	8	17	29
1e	*c*	26	35[d]

[a] HNO yields are measured after complete decomposition of the donor and are reported relative to the standard HNO donor, Angeli's salt, as determined by N_2O headspace analysis (SEM ± 5%; *n*=3). [b] Stable. [c] Not determined due to low solubility. [d] $t_{1/2}$ = 3.2 min (measured using UV-vis spectroscopy).

The competition between nitrosocarbonyl hydrolysis to HNO (*Path* A) and pyrazolone trapping (*Path* B) depends on the relative concentration of pyrazolone. Lower concentrations of pyrazolone **2** following decomposition of lower concentrations of **OHPY 1** will disfavor **NHPY** formation and correspondingly increase the yield of HNO. Determination of HNO yields at different concentrations of donors (Table 3-2), confirms that the yield of HNO is impacted as expected.

3.3.3. Mechanistic Studies

Our proposed mechanism for **OHPY** decomposition involves deprotonation followed by initial formation of a nitrosocarbonyl intermediate. Pyrazolone **2b** has recently been demonstrated to be an efficient trap for nitrosocarbonyls under physiological conditions.[47] To confirm the formation of nitrosocarbonyls upon **OHPY** decomposition, we incubated **OHPY 1a** (0.5 mM) in presence of pyrazolone **2b** (0.5 mM) in pH 7.4 phosphate buffer at 37 °C (Scheme 3-4). Upon decomposition

of donor **1a** under these conditions, we observe quantitative formation of **NHPY 3b** (Supporting Information), strong evidence for nitrosocarbonyl formation.

Scheme 3-4. Reactivity of OHPY 1a in the presence of pyrazolone 2b

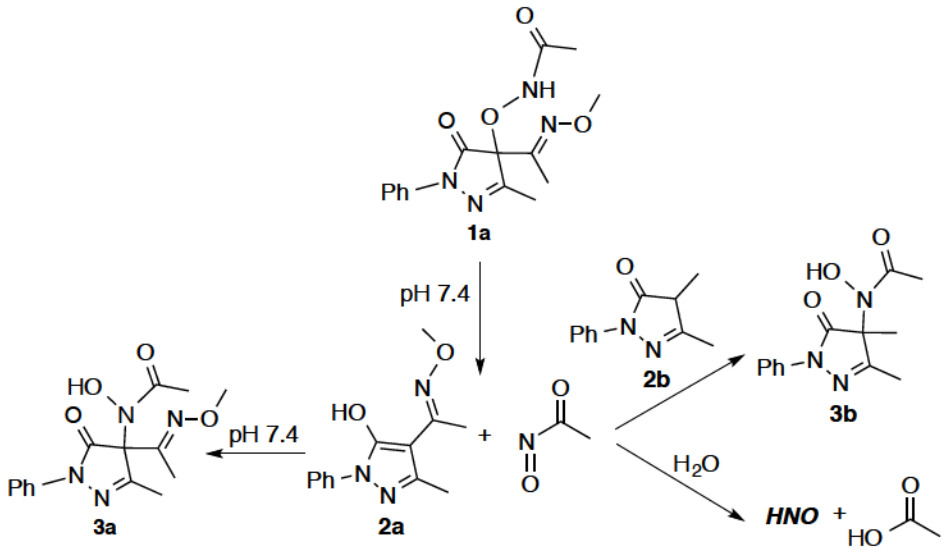

In the absence of pyrazalone **2b**, the decomposition of **OHPY 1a** provides **NHPY 3a** (26%) (which has a half-life of 5 days), and HNO (70%) and acetate (73%) (Scheme 3-4 and Tables 3-1, 3-2). The stability of **NHPY 3a**, along with the observation that it is not formed in the presence of pyrazolone **2b**, also argues against the possibility of a direct intramolecular rearrangement from anionic **OHPY 1a** to NHPY **3a** without involvement of a nitrosocarbonyl intermediate.

Based on reactivity studies of *bis*-heteroatom-substituted amides,[49] the formation of **NHPY 3b** may be possible through the direct attack of pyrazolone **2b** on the amide nitrogen of the hydroxamic acid moiety of **NHPY 3a** (Scheme 3-5). To examine this possibility, **NHPY 3a** was incubated with pyrazolone **2b** and its stability was confirmed by ^{1}H NMR spectroscopy at pH 7.4 and 10. The pK_a of **NHPY**

3a has recently been measured to be 10.0 and its stability at or above pH 10 suggests a relatively high barrier for nitrosocarbonyl formation from this **NHPY** donor even when deprotonated.[47]

Scheme 3-5. The possible reaction of NHPY 3a with pyrazolone 2b

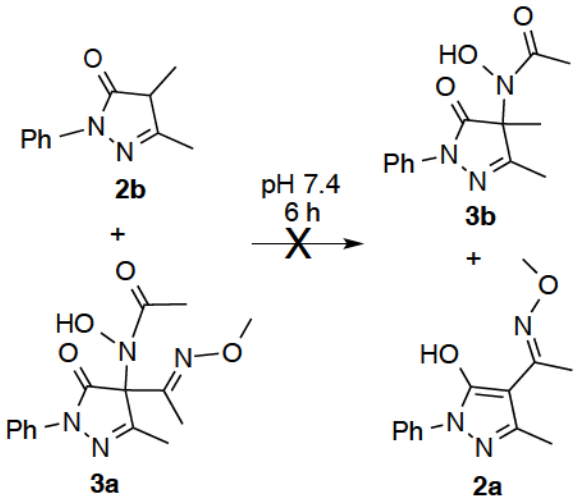

3.4. Conclusions

The **OHPY** class of nitrosocarbonyl precursors efficiently generates these intermediates under physiological conditions following deprotonation and loss of pyrazolone. The nitrosocarbonyl produced is subsequently hydrolyzed to HNO in competition with trapping by the pyrazolone byproduct via an *N*-selective nitrosocarbonyl aldol reaction to form an isomeric **NHPY** compound. The rate of nitrosocarbonyl release from **OHPY** compounds in aqueous solution is dependent on the pyrazolone leaving group. This rate is also influenced by the R^3 substituent, an effect that is under current investigation.

3.5. Experimental Section

3.5.1. Method and Materials

All starting materials were of reagent grade and used without further purification. *N*-hydroxy-*N*-(4-(acetyl-*O*-methoxyoxime)-3-methyl-5-oxo-1-phenyl-4,5-dihydro-1*H*-pyrazol-4-yl)-*N*-acetamide (**NHPY 3a**), *N*-hydroxy-*N*-(4-(acetyl-*O*-methoxy-oxime)-3-methyl-5-oxo-1-phenyl-4,5-dihydro-1*H*-pyrazol-4-yl)-*N*-methylcarbamate (**NHPY 3c**), *N*-hydroxy-*N*-(*4*-(acetyl-*O*-methoxyoxime)-1,3-dimethyl-5-oxo-4,5-dihydro-1*H*-pyrazol-4-yl)-*N*-methylcarbamate (**NHPY 3d**),[47] 4-(acetyl-*O*-methoxy-oxime)-3-methyl-1-phenyl-pyrazolone **2a**, 3,4-dimethyl-1-phenyl-pyrazolone **2b**, 4-(acetyl-*O*-methoxyoxime)-1,3-dimethylpyrazolone **2c**,[19] 4-(acetyl-*O*-methoxy-oxime)-4-bromo-3-methyl-1-phenyl-pyrazolone , 4-bromo-3,4-dimethyl-1-phenyl-pyrazolone, 4-(acetyl-*O*-methoxyoxime)-4-bromo-1,3-dimethyl-pyrazolone,[18] *C*-methoxycarbohydroxamic acid, and *tert*-butylhydroxycarbamate[50] were prepared according to literature procedures. Acetohydroxamic acid was purchased and used without further purification. NMR spectra were obtained on a 400 MHz FT-NMR spectrometer. All chemical shifts are reported in parts per million (ppm) relative to residual $CHCl_3$ (7.26 ppm for ^1H, 77.23 ppm for ^{13}C). High-resolution mass spectra were collected on a magnetic sector mass spectrometer working in fast atom bombardment (FAB) mode. Gas chromatography (GC) headspace analysis was performed on the instrument equipped with ECD detection and a molecular sieve packed column. Ultraviolet-visible (UV-vis) absorption spectra were collected using a diode array spectrophotometer.

3.5.2. Synthesis

*General procedure for the synthesis of N-((4-(acetyl-O-methoxyoxime)-3-methyl-5-oxo-1-phenyl-4,5-dihydro-1H-pyrazol-4-yl)oxy)-acetamide (**OHPY 1a**) and N-((3,4-dimethyl-5-oxo-1-phenyl-4,5-dihydro-1H-pyrazol-4-yl)oxy)-acetamide (**OHPY 1b**):* To a solution of acetohydroxamic acid (1 mmol) in dimethylformamide (3 mL) at room temperature was added sodium hydride, 60 % (1.1 mmol), and the reaction stirred for one hour. This solution was added to a solution of 1 mmol of brominated pyrazolone (4-(acetyl-*O*-methoxyoxime)-4-bromo-3-methyl-1-phenylpyrazolone for the synthesis of **OHPY 1a** and 4-bromo-3,4-dimethyl-1-phenylpyrazolone for the synthesis of **OHPY 1b**) in dimethylformamide (2 mL), and the reaction proceeded at room temperature for 3 hours. The reaction was diluted with ether (20 mL) and washed with ammonium chloride, water, and brine. The organic phase was collected, dried over magnesium sulfate ($MgSO_4$), and concentrated *in vacuo*. Recrystallization from dichloromethane and hexane gave **OHPY 1a** and, following purification by flash chromatography (30% ethyl acetate/hexane) on silica gel, gave **OHPY 1b**.

*General procedure for the synthesis of N-((4-(acetyl-O-methoxyoxime)-3-methyl-5-oxo-1-phenyl-4,5-dihydro-1H-pyrazol-4-yl)oxy)-methylcarbamate (**OHPY 1c**), N-((4-(acetyl-O-methoxyoxime)-1,3-dimethyl-5-oxo-4,5-dihydro-1H-pyrazol-4-yl)oxy)-methylcarbamate (**OHPY 1d**), and N-(4-(acetyl-O-methoxyoxime)-3-methyl-5-oxo-1-phenyl-4,5-dihydro-1H-pyrazol-4-yl)oxy)-tert-butylcarbamate (**OHPY 1e**):* To a solution of 1 mmol of hydroxamic acid (*C*-methoxycarbohydroxamic acid for the

synthesis **OHPY 1c** and **1d**, and *tert*-butylhydroxycarbamate for the synthesis of **OHPY 1e**) in acetonitrile (3 mL) at room temperature was added triethylamine (1 mmol), and the reaction stirred for one hour. This solution was added to a solution of 1 mmol of brominated pyrazolone 4-(acetyl-*O*-methoxyoxime)-4-bromo-3-methyl-1-phenyl-pyrazolone for the synthesis of **OHPY 1c** and **1e**, and 4-(acetyl-*O*-methoxyoxime)-4-bromo-1,3-dimethyl-pyrazolone for the synthesis of **OHPY 1d**) in acetonitrile (2 mL), and the reaction proceeded at room temperature for 3 hours. The reaction mixture was concentrated via rotary evaporation, redissolved in dichloromethane, and washed with water and brine. The organic phase was collected, dried over $MgSO_4$, and concentrated *in vacuo*. The compound was purified by flash chromatography (20% ethylacetate/hexane) on silica gel to give **OHPY 1c**, **1d**, and **1e**.

*Synthesis of N-hydroxy-N-(3,4-dimethyl-5-oxo-1-phenyl-4,5-dihydro-1H-pyrazol-4-yl)-N-acetamide (**NHPY 3b**):* To a solution of acetohydroxamic acid (210 mg, 2.80 mmol) and pyrazolone **2b** (105 mg, 0.56 mmol) in 50% aqueous ethanol (7 mL), was added potassium carbonate (12 mg, 0.09 mmol) to adjust the pH to 7-8. Sodium periodate (599 mg, 2.80 mmol) was added to the reaction mixture, which was sonicated for 10 min, and then stirred for 3 h at room temperature. The reaction mixture was diluted with ethanol (12 mL) and the solid was filtered. The filtrate was concentrated via rotary evaporation and the resulting solid was redissolved in ethylacetate (50 mL) and washed three times with a saturated solution of ammonium chloride (30 mL). The organic phase was collected, dried

over $MgSO_4$, and concentrated *in vacuo*. Recrystallization from dichloromethane and hexane gave the title compound.

3.5.3. Compound Characterization

***N*-((4-(Acetyl-*O*-methoxyoxime)-3-methyl-5-oxo-1-phenyl-4,5-dihydro-1*H*-pyrazol-4-yl)oxy)-acetamide (OHPY 1a):** Colorless crystals, yield 79 mg (25%), m.p. 143-145 °C. ^{1}H NMR (400 MHz, $CDCl_3$) δ: 8.96 (1H, s, OH), 7.85-7.83 (2H, m, arom), 7.41-7.38 (2H, m, arom), 7.22-7.20 (1H, m, arom), 3.90 (3H, s, Me), 2.34 (3H, s, Me), 2.06 (3H, s, Me), 1.92 (3H, s, Me). ^{13}C NMR (100 MHz, $CDCl_3$) δ: 167.5, 158.1, 156.7, 150.8, 137.8, 129.1, 125.7, 119.1, 90.2, 62.5, 20.0, 16.4, 10.2. HR-MS (FAB): found *m/z* = 319.14094 (MH^+); calc. for $C_{15}H_{19}N_4O_4$: 319.14063.

***N*-((3,4-Dimethyl-5-oxo-1-phenyl-4,5-dihydro-1*H*-pyrazol-4-yl)oxy)-acetamide (OHPY 1b):** White solid, 73 mg (28%), m.p. 142-144 °C. ^{1}H NMR (400 MHz, $CDCl_3$) δ: 9.07 (1H, s, OH), 7.90-7.88 (2H, m, arom), 7.44-7.41 (2H, m, arom), 7.23-7.25 (1H, m, arom), 2.34 (3H, s, Me), 1.92 (3H, s, Me), 1.56 (3H, s, Me). ^{13}C NMR (100 MHz, $CDCl_3$) δ: 170.6, 161.3, 158.1, 137.5, 129.1, 125.6, 118.4, 87.6, 20.4, 18.5, 13.2. HR-MS (FAB): found *m/z* = 262.11949 (MH^+); calc. for $C_{13}H_{15}N_3O_3$: 262.11917.

***N*-((4-(Acetyl-*O*-methoxyoxime)-3-methyl-5-oxo-1-phenyl-4,5-dihydro-1*H*-pyrazol-4-yl)oxy)-methylcarbamate (OHPY 1c):** White solid, yield 113 mg (34%), m.p. 128-130 °C. ^{1}H NMR (400 MHz, $CDCl_3$) δ: 7.92-7.90 (2H, m, arom), 7.50 (1H, s, OH), 7.41-7.44 (2H, m, arom), 7.20-7.22 (1H, m, arom), 3.90 (3H, s, Me), 3.77 (3H, s, Me), 2.38 (3H, s, Me), 2.08 (3H, s, Me). ^{13}C NMR (100 MHz, $CDCl_3$) δ: 166.8,

158.8, 157.3, 151.3, 137.4, 129.2, 125.3, 118.7, 89.8, 62.8, 53.8, 14.9, 10.0. HR-MS (FAB): found *m/z* = 335.13496 (MH^+); calc. for $C_{15}H_{19}N_4O_5$: 335.13554.

***N*-((4-(Acetyl-*O*-methoxyoxime)-1,3-dimethyl-5-oxo-4,5-dihydro-1*H*-pyrazol-4-yl)oxy)-methylcarbamate (OHPY 1d):** White solid, yield 76 mg (28%), ^1H NMR (400 MHz, $CDCl_3$) δ : 7.52 (1H, s, OH), 3.89 (3H, s, Me), 3.79 (3H, s, Me), 3.28 (3H, s, Me), 2.27 (3H, s, Me), 2.03 (3H, s, Me). ^{13}C NMR (100 MHz, $CDCl_3$) δ: 168.6, 158.3, 157.6, 151.1, 88.9, 62.5, 53.3, 31.4, 15.0, 10.3. HR-MS (FAB): found *m/z* = 273.12013 (MH^+); calc. for $C_{10}H_{17}N_4O_5$: 273.11989.

***N*-((4-(Acetyl-*O*-methoxyoxime)-3-methyl-5-oxo-1-phenyl-4,5-dihydro-1*H*-pyrazol-4-yl)oxy)-*tert*-butylcarbamate (OHPY 1e):** White solid, yield 139 mg (37%), m.p. 102-104 °C. ^1H NMR (400 MHz, $CDCl_3$) δ: 7.94-7.92 (2H, m, arom), 7.43-7.40 (2H, m, arom), 7.31 (1H, s, OH), 7.23-7.21 (1H, m, arom), 3.91 (3H, s, Me), 2.36 (3H, s, Me), 2.06 (3H, s, Me), 1.46 (1H, s, $C(Me)_3$). ^{13}C NMR (100 MHz, $CDCl_3$) δ: 167.3, 159.4, 156.1, 151.2, 137.8, 129.2, 125.3, 118.4, 89.8, 82.9, 62.4, 28.0, 15.1, 10.2. HR-MS (FAB): found *m/z* = 377.18180 (MH^+); calc. for $C_{18}H_{25}N_4O_5$: 377.18250.

***N*-Hydroxy-*N*-(3,4-dimethyl-5-oxo-1-phenyl-4,5-dihydro-1*H*-pyrazol-4-yl)-*N*-acetamide (NHPY 3b):** White solid, yield 107 mg (73%). ^1H NMR (400 MHz, $CDCl_3$) δ: 9.08 (1H, s, OH), 7.87-7.85 (2H, m, arom), 7.45-7.43 (2H, m, arom), 7.24-7.22 (1H, m, arom), 2.18 (3H, s, Me), 2.10 (3H, s, Me), 1.68 (3H, s, Me). ^{13}C NMR (100 MHz, $CDCl_3$) δ: 167.8, 159.0, 157.2, 137.5, 127.9, 125.8, 119.5, 72.3, 22.5, 19.2, 12.4. HR-MS (FAB): found *m/z* = 262.11917 (MH^+); calc. for $C_{13}H_{15}N_3O_3$: 262.11981.

3.6. References

(1) Paolocci, N.; Saavedra, W. F.; Miranda, K. M.; Martignani, C.; Isoda, T.; Hare, J. M.; Espey, M. G.; Fukuto, J. M.; Feelisch, M.; Wink, D. A.; Kass, D. A. *Proc. Natl. Acad. Sci. U.S.A.* **2001**, *98*, 10463–10468.

(2) Paolocci, N.; Katori, T.; Champion, H. C.; St. John, M. E.; Miranda, K. M.; Fukuto, J. M.; Wink, D. A.; Kass, D. A. *Proc. Natl. Acad. Sci. U.S.A.* **2003**, *100*, 5537–5542.

(3) Dai, T.; Tian, Y.; Tocchetti, C. G.; Katori, T.; Murphy, A. M.; Kass, D. A.; Paolocci, N.; Gao, W. D. *J. Physiol.* **2007**, *580*, 951–960.

(4) Tocchetti, C. G.; Wang, W.; Froehlich, J. P.; Huke, S.; Aon, M. A.; Wilson, G. M.; Di Benedetto, G.; O'Rourke, B.; Gao, W. D.; Wink, D. A.; Toscano, J. P.; Zaccolo, M.; Bers, D. M.; Valdivia, H. H.; Cheng, H.; Kass, D. A.; Paolocci, N. *Circ. Res.* **2007**, *100*, 96–104.

(5) Tocchetti, C. G.; Stanley, B. A.; Murray, C. I.; Sivakumaran, V.; Donzelli, S.; Mancardi, D.; Pagliaro, P.; Gao, W. D.; van Eyk, J.; Kass, D. A.; Wink, D. A.; Paolocci, N. *Antioxid. Redox Signal.* **2011**, *14*, 1687–1698.

(6) Kemp-Harper, B. K. *Antioxid. Redox Signal.* **2011**, *14*, 1609–1616.

(7) Flores-Santana, W.; Salmon, D. J.; Donzelli, S.; Switzer, C. H.; Basudhar, D.; Ridnour, L.; Cheng, R.; Glynn, S. A.; Paolocci, N.; Fukuto, J. M.; Miranda, K. M.; Wink, D. A. *Antioxid. Redox Signal.* **2011**, *14*, 1659–1674.

(8) Sabbah, H. N.; Tocchetti, C. G.; Wang, M.; Daya, S.; Gupta, R. C.; Tunin, R. S.; Mazhari, R.; Takimoto, E.; Paolocci, N.; Cowart, D.; Colucci, W. S.; Kass, D. A. *Circ. Hear. Fail.* **2013**, *6*, 1250–1258.

(9) Arcaro, A.; Lembo, G.; Tocchetti, C. G. *Curr. Heart Fail. Rep.* **2014**, *11*, 227–235.

(10) Shafirovich, V.; Lymar, S. V. *Proc. Natl. Acad. Sci. U.S.A.* **2002**, *99*, 7340–7345.

(11) Hughes, M. N.; Cammack, R. *Methods Enzymol.* **1999**, *301*, 279–287.

(12) Porcheddu, A.; De Luca, L.; Giacomelli, G. *Synlett* **2009**, *13*, 2149–2153.

(13) Sirsalmath, K.; Suárez, S. A.; Bikiel, D. E.; Doctorovich, F. *J. Inorg. Biochem.* **2013**, *118*, 134–139.

(14) Toscano, J. P.; Brookfield, F. A.; Cohen, A. D.; Courtney, S. M.; Frost, L. M.; Kalish, V. J. U.S. Patent 8,030,356, 2011.

(15) Sutton, A. D.; Williamson, M.; Weismiller, H.; Toscano, J. P. *Org. Lett*. **2012**, *14*, 472–475.

(16) Sha, X.; Isbell, T. S.; Patel, R. P.; Day, C. S.; King, S. B. *J. Am. Chem. Soc.* **2006**, *128*, 9687–9692.

(17) Shoman, M. E.; DuMond, J. F.; Isbell, T. S.; Crawford, J. H.; Brandon, A.; Honovar, J.; Vitturi, D. A.; White, C. R.; Patel, R. P.; King, S. B. *J. Med. Chem.* **2011**, *54*, 1059–1070.

(18) Guthrie, D. A.; Kim, N. Y.; Siegler, M. A.; Moore, C. D.; Toscano, J. P. *J. Am. Chem. Soc.* **2012**, *134*, 1962–1965.

(19) Guthrie, D. A.; Ho, A.; Takahashi, C. G.; Collins, A.; Morris, M.; Toscano, J. P. *J. Org. Chem.* **2015**, *80*, 1338–1348.

(20) Guthrie, D. A.; Nourian, S.; Takahashi, C. G.; Toscano, J. P. *J. Org. Chem.* **2015**, *80*, 1349–1356.

(21) Atkinson, R. N.; Storey, B. M.; King, S. B. *Tetrahedron Lett.* **1996**, *37*,

9287–9290.

(22) Miao, Z.; King, S. B. *Nitric Oxide* **2016**, *57*, 1–14.

(23) Kirby G. W., Sweeny J. G. *J. Chem. Soc. Perkin Trans. I.* **1981**, 3250–3254.

(24) Corrie J. E. T., Kirby G. W., Mackinnon J. W. M. *J. Chem. Soc. Perkin Trans. I.* **1985**, 883–886.

(25) Zeng, B. B.; Huang, J.; Wright, M. W.; King, S. B. *Bioorg. Med. Chem.* **2004**, *14*, 5565–5568.

(26) Quadrelli, P.; Mella, M.; Caramella, P. *Tetrahedron Lett.* **1999**, *40*, 797–800.

(27) O'Bannon, P. E.; William, D. P. *Tetrahedron Lett.* **1988**, *29*, 5719–5722.

(28) Evans, A. S; Cohen, A. D.; Gurard-Levin, Z. A.; Kebede, N.; Celius T. C.; Miceli, A. P.; Toscano, J. P. *Can. J. Chem.* **2011**, *89*, 130–138.

(29) Frazier, C. P.; Engelking, J. R.; Read de Alaniz, J. *J. Am. Chem. Soc.* **2011**, *133*, 10430–10433.

(30) Fakhruddin, A.; Iwasa, S.; Nishiyama, H.; Tsutsumi, K. *Tetrahedron Lett.* **2004**, *45*, 9323–9326.

(31) Yamamoto, Y.; Yamamoto, H. *European J. Org. Chem.* **2006**, *2006*, 2031–2043.

(32) Chaiyaveij, D.; Cleary, L.; Batsanov, A. S.; Marder, T. B.; Shea, K. J.; Whiting, A. *Org. Lett.* **2011**, *13*, 3442–3445.

(33) Sandoval, D.; Frazier, C. P.; Bugarin, A.; Read de Alaniz, J. *J. Am. Chem. Soc.* **2012**, *134*, 18948–18951.

(34) Baidya, M.; Griffin, K. A.; Yamamoto, H. *J. Am. Chem. Soc.* **2012**, *134*, 18566–18569.

(35) Selig, P. *Angew. Chemie Int. Ed.* **2013**, *52*, 7080–7082.

(36) Palmer, L.; Frazier, C. P.; Read de Alaniz, J. *Synthesis.* **2013**, *46*, 269–280.

(37) Baidya, M.; Yamamoto, H. *Synthesis.* **2013**, *45*, 1931–1938.

(38) Frazier, C. P.; Sandoval, D.; Palmer, L. I.; Read de Alaniz, J. *Chem. Sci.* **2013**, *4*, 3857–3862.

(39) Yang, W.; Huang, L.; Yu, Y.; Pflasterer, D.; Rominger, F.; Hashmi, S. K. *Chem. Eur. J.* **2014**, *20*, 3927–3931.

(40) Yu, C.; Song, A.; Zhang, F. Wang, W. *ChemCatChem.* **2014**, *6*, 1863–1865.

(41) Sandoval, D.; Samoshin, A. V; Read de Alaniz, J. *Org. Lett.* **2015**, *17*, 4514–4517.

(42) Ramakrishna, I.; Grandhi, G. S.; Sahoo, H.; Baidya, M. *Chem. Commun.* **2015**, *51*, 13976–13979.

(43) Maji, B.; Yamamoto, H. *Angew. Chem.* **2014**, *126*, 14700–14703.

(44) Maji, B.; Yamamoto, H. *Bull. Chem. Soc. Jpn.* **2015**, *88*, 753–762.

(45) Xu, C.; Zhang, L.; Luo, S. *Angew. Chem. Int. Ed.* **2014**, *53*, 4149–4153.

(46) Merino, P.; Tejero, T.; Delso, I.; Matute, R. *Synthesis* **2016**, *48*, 653–676.

(47) Nourian, S.; Zilber, Z. A.; Toscano, J. P. J. Org. CHem. **2016**, *81*, 9138–9146.

(48) Steinberg, G. M.; Bolger, J. *J. Org. Chem.* **1956**, *21*, 660-662.

(49) Glover, S. A. In *The Chemistry of Hydroxylamines, Oximes, and Hydroxamic Acids, Part 2*; Rappoport, Z., Liebman, J. F., Eds.; John Wiley & Sons: Chichester, West Sussex, 2009, p 839-923.

(50) Defoin, A.; Fritz, H.; Schmidlin, C.; Streith, J. *Helv. Chim. Acta* **1987**, *70*, 554-569.

3.7. Supporting Information

3.7.1. Analysis of Nitrous Oxide (N_2O) by Headspace Gas Chromatography.

A Varian CP-3800 instrument equipped with a 1041 injector, electron capture detector, and a 25 m 5Å molecular sieve capillary column was applied for the analysis of nitrous oxide (N_2O). Grade 5.0 nitrogen was used as both the carrier (8 mL/min) and the make-up (22mL/min) gas. For all the measurements, the column oven temperature was kept constant at 150 °C, and the injector oven and the detector oven were held at 200 °C and 300 °C, respectively. A 100 µL gastight syringe with a sample-lock was used for all gas injections. Samples were prepared in 6 mL Wheaton Clr headspace vials with volumes pre-measured for sample uniformity (actual vial volume ranges from 5.8 - 6.3 mL). Vials were charged with 3 mL of phosphate buffer containing the metal chelator, diethylenetriaminepentaacetic acid (DTPA), and fit with rubber septa and 20 mm aluminum seals. The vials were purged with argon and equilibrated for at least 10 minutes at 37 °C in a dry block heater. Stock solutions of Angeli's salt (**AS**) were prepared in 10 mM sodium hydroxide, and **OHPY** donors **1a-e** were prepared in acetonitrile and used immediately after preparation. 30 µL of the stock solutions was transferred into vials using a gastight syringe, yielding final concentrations of 0.5, 0.1, 0.02 mM. Substrates were then incubated long enough to ensure complete decomposition and equilibration of N_2O with the headspace. Depending on the concentration of the donor, 60 or 20 µL of the headspace was sampled and injected three times using a gastight syringe with a sample lock. The N_2O yield was averaged

and reported relative to the AS standard.

3.7.2. Characterization of Compounds:

Pyrazolones, brominated pyrazolones, and *N*-substituted hydroxamic acids with pyrazolone leaving groups (**NHPY** compounds) were synthesized by previously reported methods.

4-(Acetyl-*O*-methoxyoxime)-3-methyl-1-phenylpyrazolone (PY-2a) ^{1}H NMR (400 MHz, CDCl3) δ: 7.85 (m, 2H), 7.44 (m, 2H), 7.26 (m, 1H), 3.92 (s, 3H), 2.43 (s, 3H), 2.29 (s, 3H).

3,4-Dimethyl-1-phenylpyrazolone (PY-2b): ^{1}H NMR (400 MHz, $CDCl_3$) δ: 7.91 (m, 2H), 7.44 (m, 2H), 7.21 (m, 1H), 2.23 (s, 3H), 1.47 (s, 3H).

4-(Acetyl-O-methoxyoxime)-1,3-dimethylpyrazolone (PY-2c): ^{1}H NMR (400 MHz, $CDCl_3$) δ: 3.85 (s, 3H), 3.56 (s, 3H), 2.29 (s, 3H), 2.19 (s, 3H).

4-(Acetyl-*O*-methoxyoxime)-4-bromo-3-methy-1-phenylpyrazolone (PYBr-a): ^{1}H NMR (400 MHz, $CDCl_3$) δ: 7.87 (m, 2H), 7.39 (m, 2H), 7.22 (m, 1H), 3.90 (s, 3H), 2.44 (s, 3H), 2.22 (s, 3H). ^{13}C NMR (100 MHz, $CDCl_3$) δ: 167.1, 157.2, 151.3, 137.7, 129.1, 125.8, 119.1, 62.7, 56.6, 15.7, 11.7.

4-Bromo-4-methyl-3-methyl-1-phenylpyrazolone (PYBr-b): ^{1}H NMR (400 MHz, $CDCl_3$) δ: 7.87 (m, 2H), 7.40 (m, 2H), 7.23 (m, 1H), 2.29 (s, 3H), 1.89 (s, 3H). ^{13}C NMR (100 MHz, $CDCl_3$) δ: 169.1, 156.3, 150.7, 138.9, 128.7, 125.6, 120.0, 59.1, 19.1, 11.5.

4-(Acetyl-*O*-methoxyoxime)-4-bromo-1,3-dimethyl-pyrazolone (PYBr-c): ^{1}H NMR (400 MHz, $CDCl_3$) δ: 3.85 (s, 3H), 3.32 (s, 3H), 2.25 (s, 3H), 2.18 (s, 3H). ^{13}C NMR (100 MHz, $CDCl_3$) δ: 168.7, 156.6, 151.1, 62.1, 55.2, 31.8, 15.2, 11.2.

***N*-Hydroxy-*N*-(4-(acetyl-*O*-methoxyoxime)-3-methyl-5-oxo-1-phenyl-4,5-dihydro-1*H*-pyrazol-4-yl)-*N*-acetamide (NHPY 3a):** ^{1}H NMR (400 MHz, $CDCl_3$) δ: 7.86 (m, 2H), 7.51 (s, 1H), 7.42 (m, 2H), 7.22 (m, 1H), 3.95 (s, 3H), 2.25 (s, 3H), 2.19 (s, 3H), 2.01 (s, 3H). ^{13}C NMR (100 MHz, $CDCl_3$) δ: 167.8, 159.0, 157.0, 151.4, 137.8, 128.8, 125.8, 119.5, 76.3, 62.5, 21.0, 15.4, 11.4.

***N*-Hydroxy-*N*-(4-(acetyl-*O*-methoxyoxime)-3-methyl-5-oxo-1-phenyl-4,5-dihydro-1*H*-pyrazol-4-yl)-*N*-methylcarbamate (NHPY 3c):** ^{1}H NMR (400 MHz, $CDCl_3$) δ: 8.59 (s, 1H), 7.88 (m, 2H), 7.41 (m, 2H), 7.23 (m, 1H), 3.89 (s, 3H), 3.76 (s, 3H), 2.26 (s, 3H), 2.14 (s, 3H). ^{13}C NMR (100 MHz, $CDCl_3$) δ: 167.6, 158.3, 158.1, 152.2, 138.0, 128.9, 125.6, 119.6, 76.5, 62.6, 54.5, 16.0, 10.9.

***N*-Hydroxy-*N*-(*4*-(acetyl-*O*-methoxyoxime)-1,3-dimethyl-5-oxo-4,5-dihydro-1*H*-pyrazol-4-yl)-*N*-methylcarbamate (NHPY 3d):** ^{1}H NMR (400 MHz, $CDCl_3$) δ: 7.05 (s, 1H), 3.89 (s, 3H), 3.82 (s, 3H), 3.30 (s, 3H), 2.13 (s, 3H), 2.04 (s, 3H). ^{13}C NMR (100 MHz, $CDCl_3$) δ: 169.4, 157.9, 157.5, 152.0, 75.4, 62.5, 54.3, 31.9, 15.7, 11.0.

***N*-Hydroxy-*N*-(4-(acetyl-*O*-methoxyoxime)-3-methyl-5-oxo-1-phenyl-4,5-dihydro-1*H*-pyrazol-4-yl)-*t*-butylcarbamate (NHPY 3e):** ^{1}H NMR (300 MHz, $CDCl_3$) δ: 7.92 (m, 2H), 7.40 (m, 2H), 7.19 (m, 1H), 3.87 (s, 3H), 2.26 (s, 3H), 2.13 (s,

3H), 1.38 (s, 9H). ^{13}C NMR (100 MHz, $CDCl_3$) δ: 166.86, 158.6, 156.9, 152.5, 138.7, 129.0, 124.6, 118.3, 85.7, 76.0, 62.4, 28.2, 15.8, 10.9.

Table 3-3. Comparison of ^{13}C NMR Chemical Shifts of the Quaternary Carbons in OHPY and NHPY Compounds

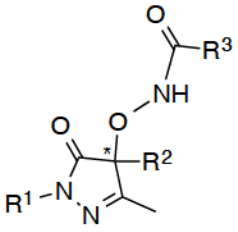

OHPY	R^1	R^2	R^3	δ (ppm)[a]
1	Ph	C(=NOMe)Me	Me	90.2
2	Ph	Me	Me	87.6
3	Ph	C(=NOMe)Me	MeO	89.8
4	Me	C(=NOMe)Me	MeO	88.9
5	Ph	C(=NOMe)Me	*t*-BuO	89.8

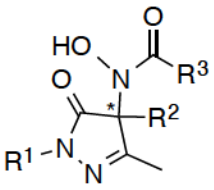

NHPY	R^1	R^2	R^3	δ (ppm)[a]
1	Ph	C(=NOMe)Me	Me	76.3
2	Me	C(=NOMe)Me	Me	75.0
3	Ph	Me	Me	72.3
4	Ph	C(=NOMe)Me	MeO	76.5
5	Me	C(=NOMe)Me	MeO	75.4
6	Ph	C(=NOMe)Me	*t*-BuO	76.0
7	Me	Me	*t*-BuO	69.0
8	Ph	C(=NOMe)Me	NMe_2	76.2
9	Me	C(=NOMe)Me	NMe_2	75.2
10	Ph	Me	NMe_2	69.6
11	Me	Me	NMe_2	68.4

[a] ^{13}C NMR Chemical shift of the carbon with an asterisk.

3.7.3. X-ray Crystallographic Data

All reflection intensities were measured at 110(2) K using a KM4/Xcalibur (detector: Sapphire 3) with enhance graphite-monochromated Mo *K*α radiation (λ = 0.71073 Å) under the program CrysAlisPro (Version 1.171.36.24 Agilent Technologies, 2012). The program CrysAlisPro (Version 1.171.36.24 Agilent Technologies, 2012) was used to refine the cell dimensions. Data reduction was done using the program CrysAlisPro (Version 1.171.36.24 Agilent Technologies, 2012). The structure was solved with the program SHELXS-2013 (Sheldrick, 2013) and was refined on F^2 with SHELXL-2013 (Sheldrick, 2013). Analytical numeric absorption corrections based on a multifaceted crystal model were applied using CrysAlisPro (Version 1.171.36.24 Agilent Technologies, 2012). The temperature of the data collection was controlled using the system Cryojet (manufactured by Oxford Instruments). The H atoms were placed at calculated positions (unless otherwise specified) using the instructions AFIX 43 or AFIX 137 with isotropic displacement parameters having values 1.2 or 1.5 times *U*eq of the attached C atoms.

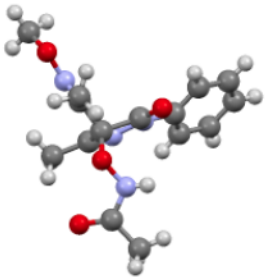

OHPY 1a. Fw = 318.33, colorless block, 0.59 × 0.43 × 0.38 mm³, monoclinic, *Pc* (no. 9), a = 14.9994(5), b = 12.1027(4), c = 9.3258(3) Å, β = 106.778(3)°, V = 1620.87(10) Å³, Z = 4, D_x = 1.304 g cm⁻³, μ = 0.097 mm⁻¹, abs. corr. range: 0.961–0.973. 7785 Reflections were measured up to a resolution of $(\sin \theta/\lambda)_{max}$ = 0.65 Å⁻¹. 3537 Reflections were unique (R_{int} = 0.0392), of which 3362 were observed [$I > 2\sigma(I)$]. 216 Parameters were refined using 2 restraints. $R1/wR2$

[$I > 2\sigma(I)$]: 0.0315/0.0813. $R1/wR2$ [all refl.]: 0.0340/0.0829. S = 1.056. Residual electron density found between –0.17 and 0.17 e Å^{-3}.

NHPY 3b. Fw = 261.28, colorless irregular shaped crystal, 0.23 × 0.09 × 0.08 mm^3, orthorhombic, $Pna2_1$ (no. 33), a = 10.0574(8), b = 11.5181(9), c = 11.6390(10) Å, V = 1348.29(19) Å^3, Z = 4, D_x = 1.287 g cm^{-3}, μ = 0.774 mm^{-1},

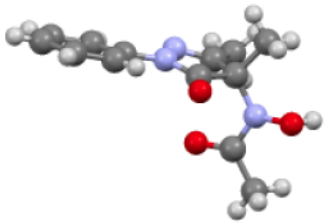

abs. corr. range: 0.893–0.961. 8035 Reflections were measured up to a resolution of $(\sin\theta/\lambda)_{max}$ = 0.62 Å^{-1}. 2530 Reflections were unique (R_{int} = 0.0310), of which 2346 were observed [$I > 2\sigma(I)$]. 177 Parameters were refined using 1 restraint. $R1/wR2$ [$I > 2\sigma(I)$]: 0.0561/0.1561. $R1/wR2$ [all refl.]: 0.0597/0.1603. S = 1.090. Residual electron density found between –0.22 and 0.33 e Å^{-3}.

3.7.4. ^{1}H NMR Spectroscopic Analysis of Nitrosocarbonyl Trapping by Pyrazolone 2b

The decomposition of 0.5 mM of donor **1a** was examined by ^{1}H NMR spectroscopy in presence of 0.5 mM of pyrazolone **2b** in 0.25 M phosphate buffer containing 0.2 mM of the metal chelator, diethylenetriaminepentaacetic acid (DTPA), at pH 7.4, 80% H_2O, 10% D_2O, and 10% DMSO-d_6 at 37 °C under argon. Spectra were collected at the start of the experiment and after complete decomposition.

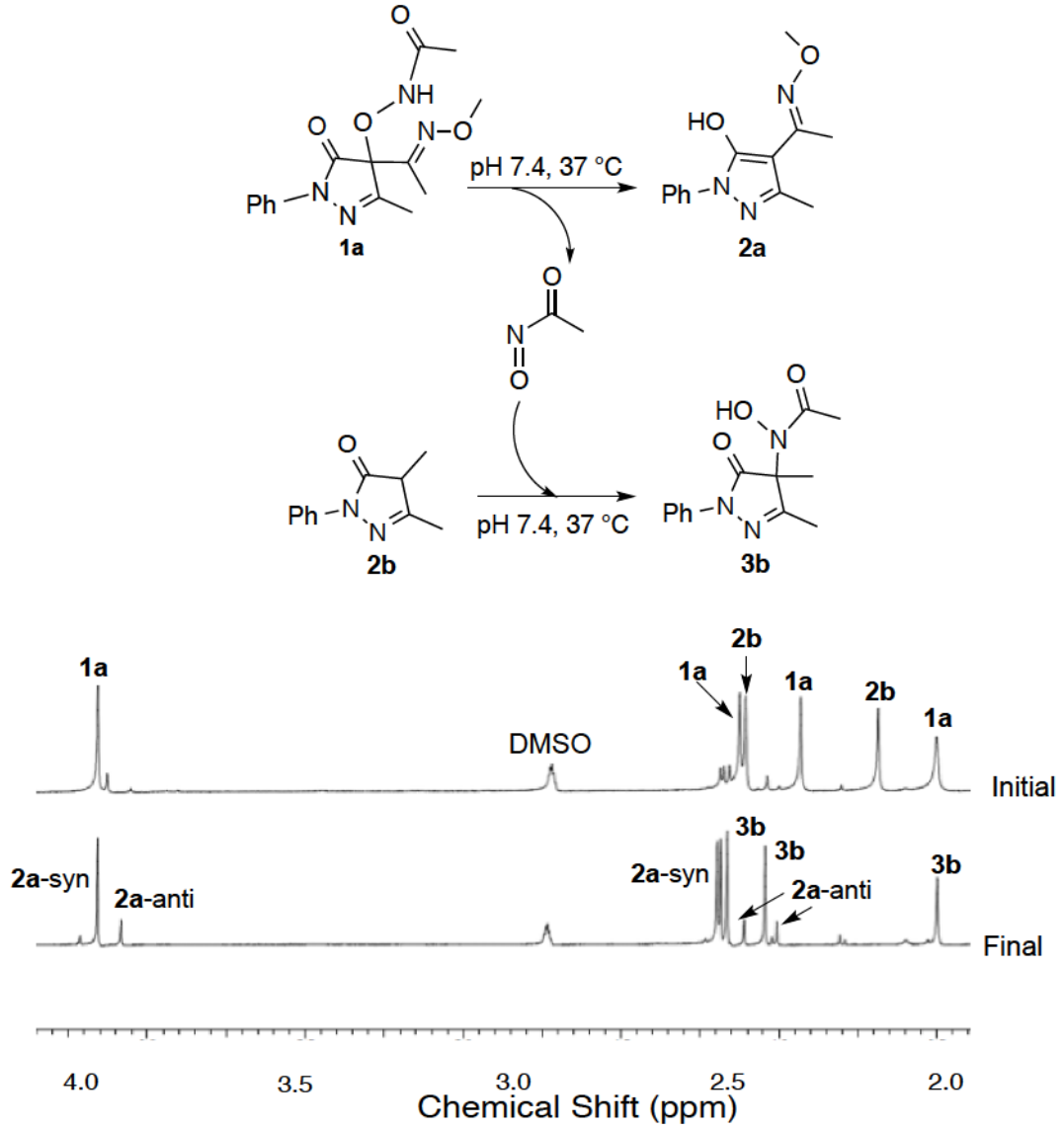

3.7.5. ^{1}H and ^{13}C NMR Spectra:

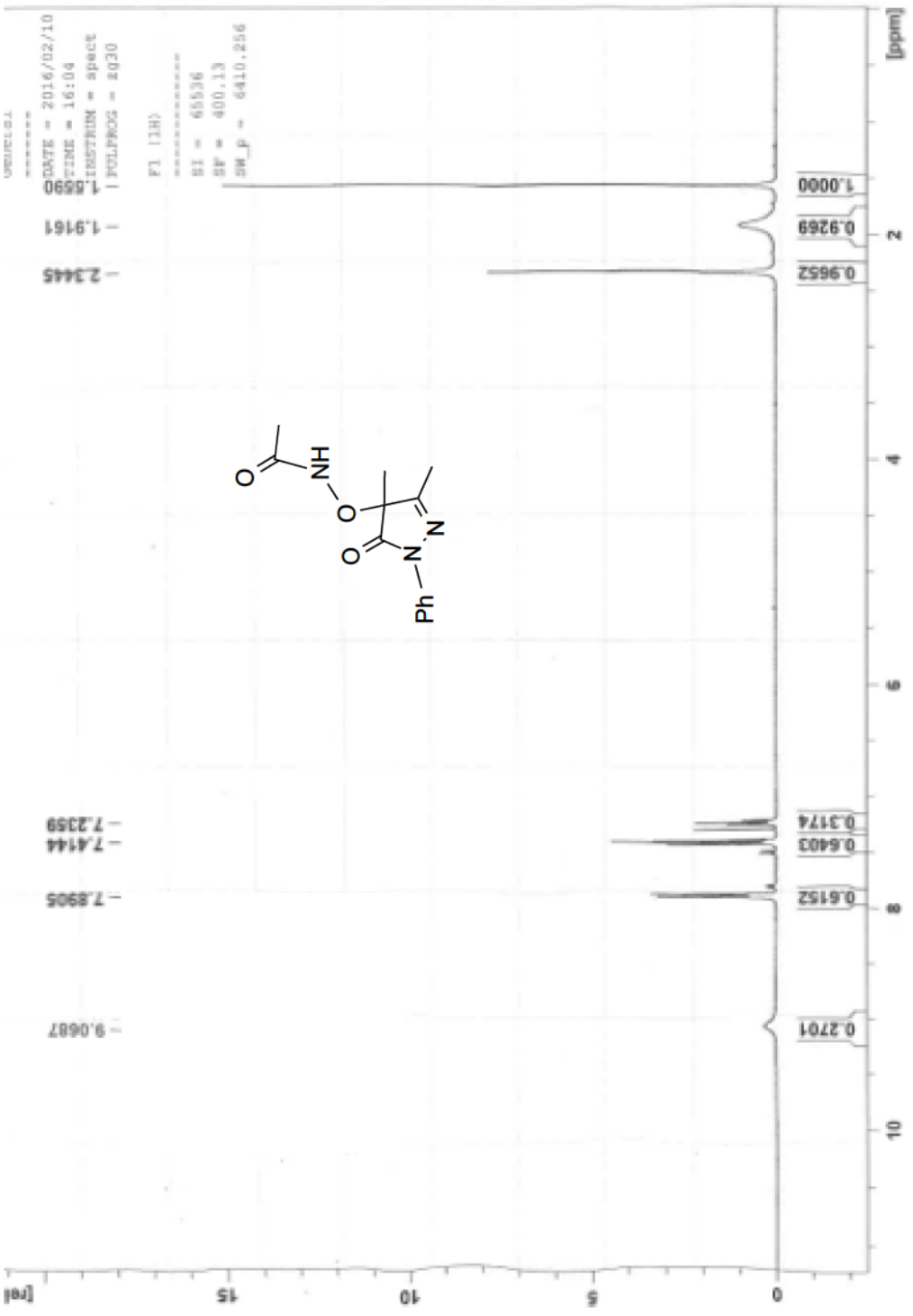

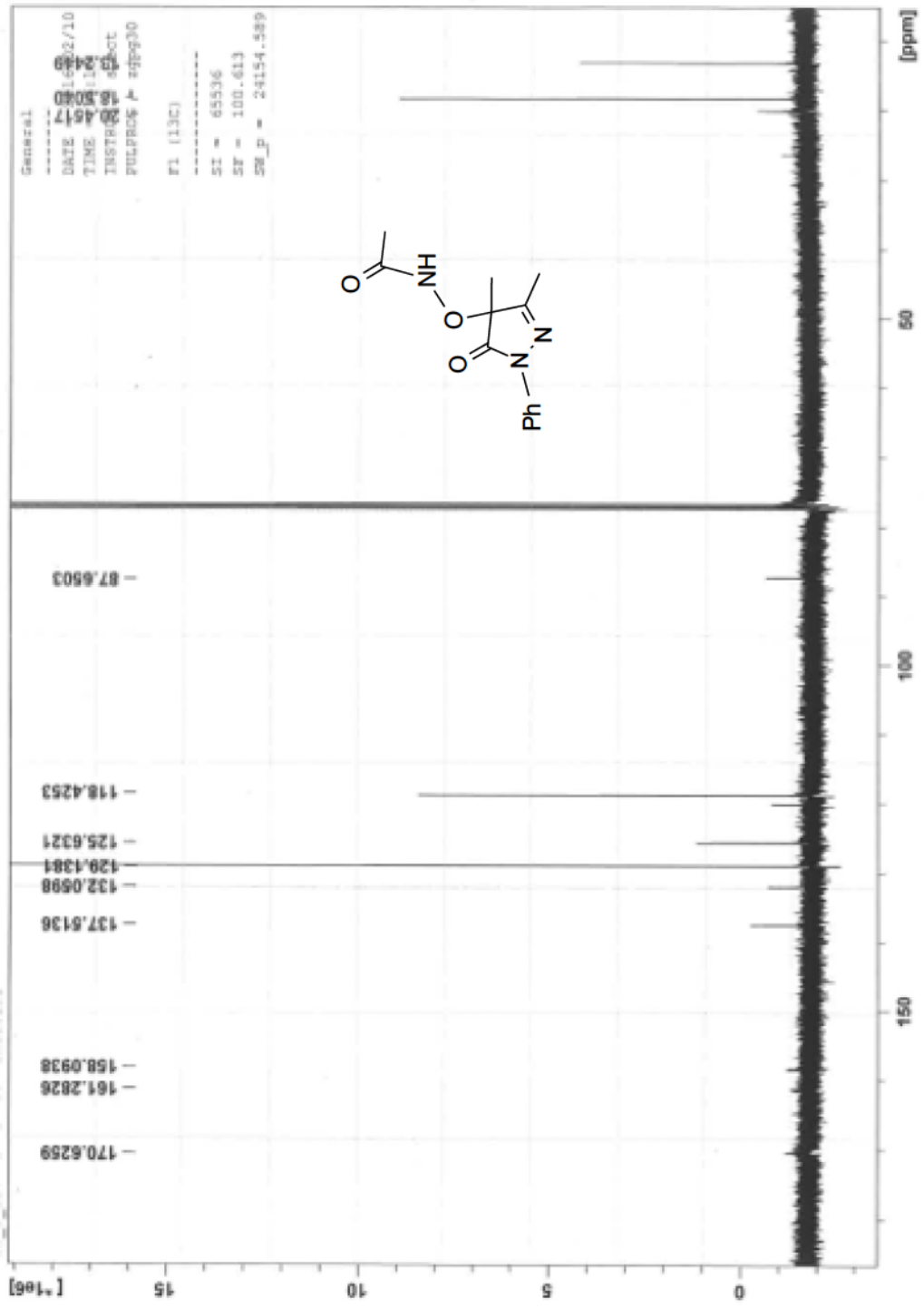
General
DATE 16
TIME
INSTR
PULPROG
F1 (13C)
SI = 65536
SF = 100.613
SW_p = 24154.589
170.6259
161.2826
158.0938
137.6136
132.0698
129.1381
125.6321
118.4253
87.6503
[ppm]
50
100
150
0
5
10
15
[*10^6]
O
NH
O
O
N
N
Ph

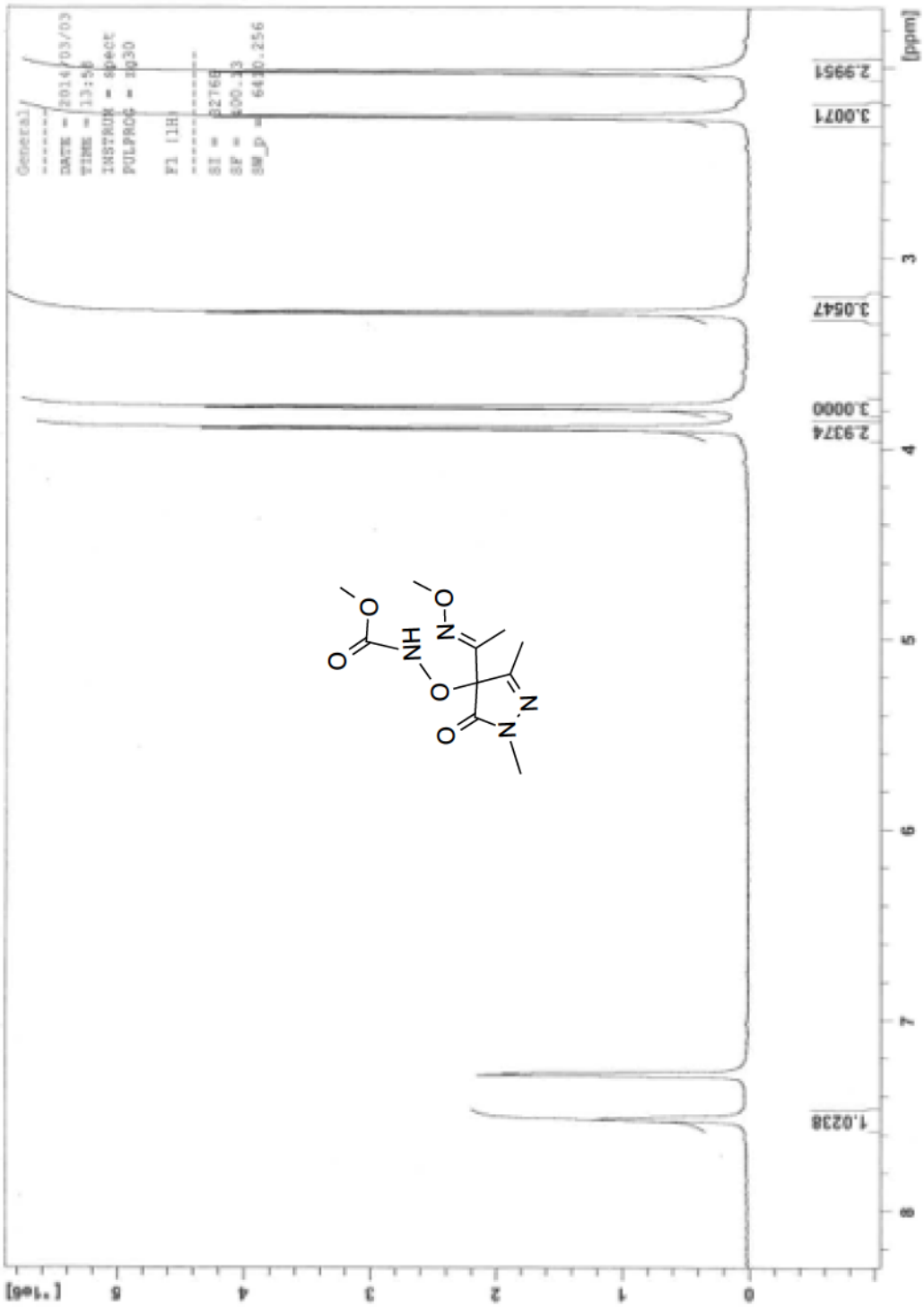
General
DATE = 2014/03/03
TIME = 13:58
INSTRUM = spect
PULPROG = zg30
F1 [1H]
SI = 32768
SF = 600.13
SW_p = 6410.256
2.9951
3.0071
3.0547
3.0000
2.9374
1.0238
[ppm]
[ppm]

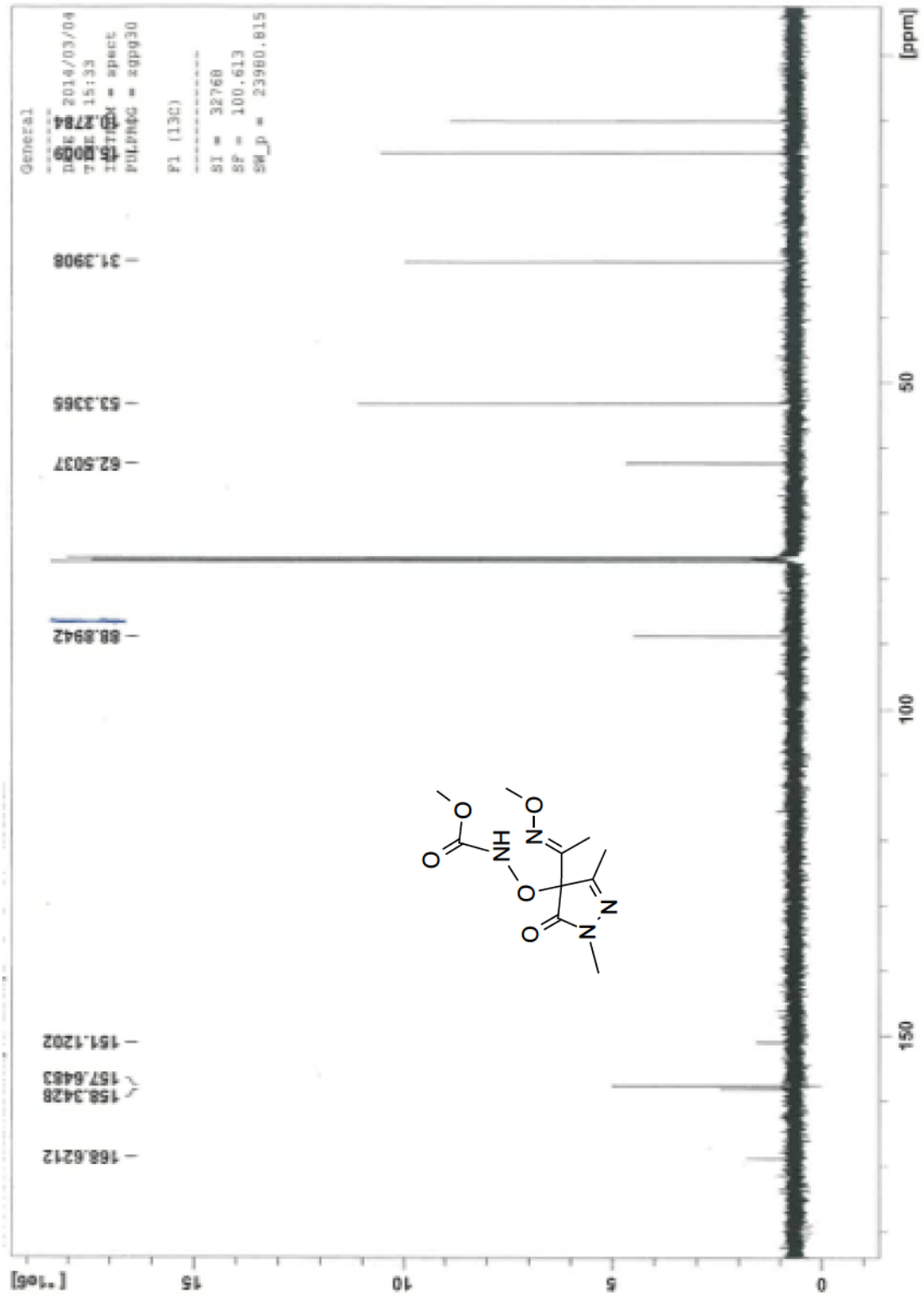
General
SI = 32768
SF = 100.613
SW_p = 23980.815
F1 (13C)
31.3908
52.3365
62.5037
88.8942
151.1202
157.6483
158.3428
168.6212
[ppm]
[ppm]
0
5
10
15
50
100
150

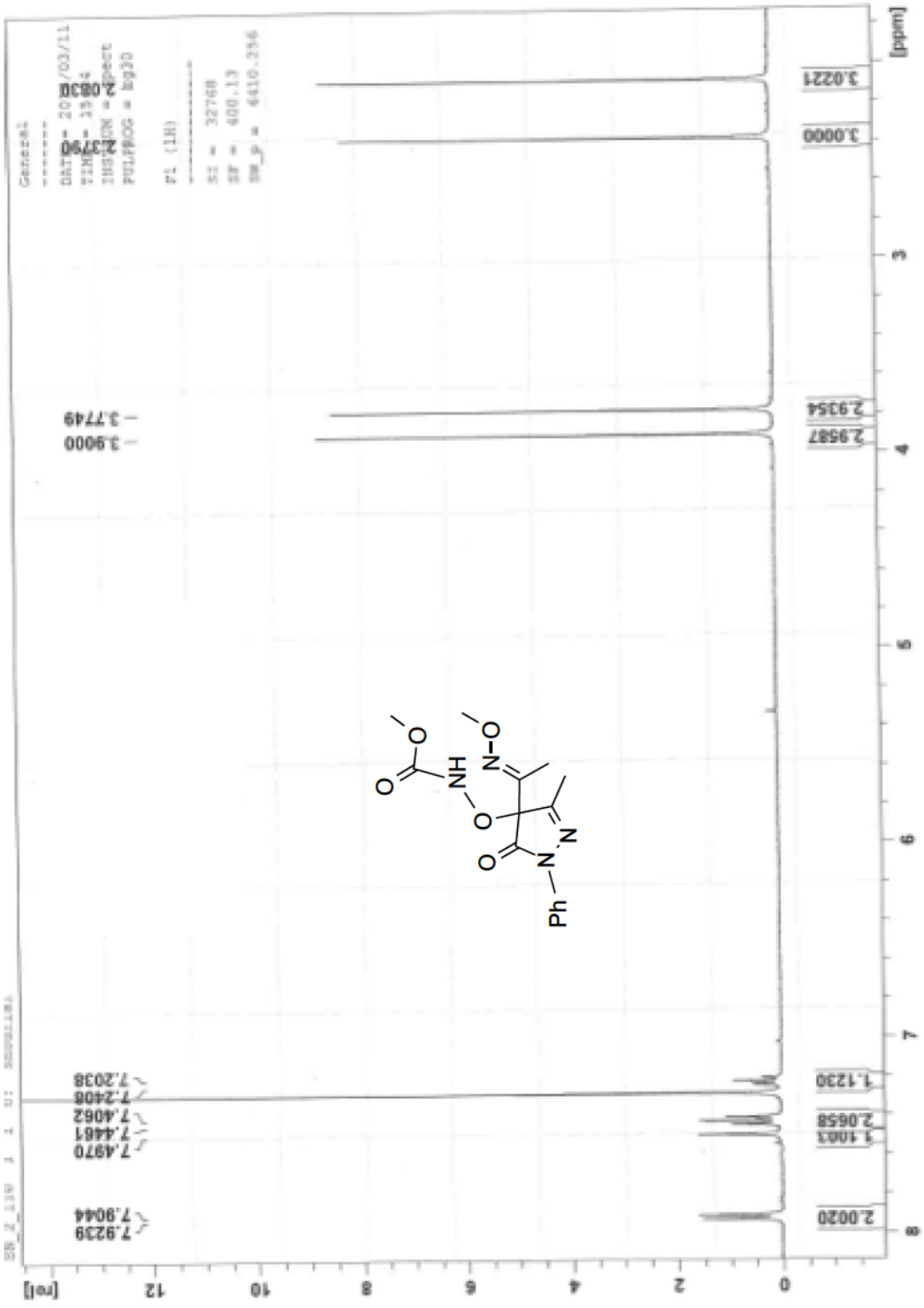
3.0221
3.0000
2.9354
2.9587
3.9000
3.7749
1.1230
2.0658
1.1003
2.0020
7.2038
7.2408
7.4062
7.4481
7.4970
7.9044
7.9239
[ppm]
O
NH
O
N
O
O
N
N
Ph

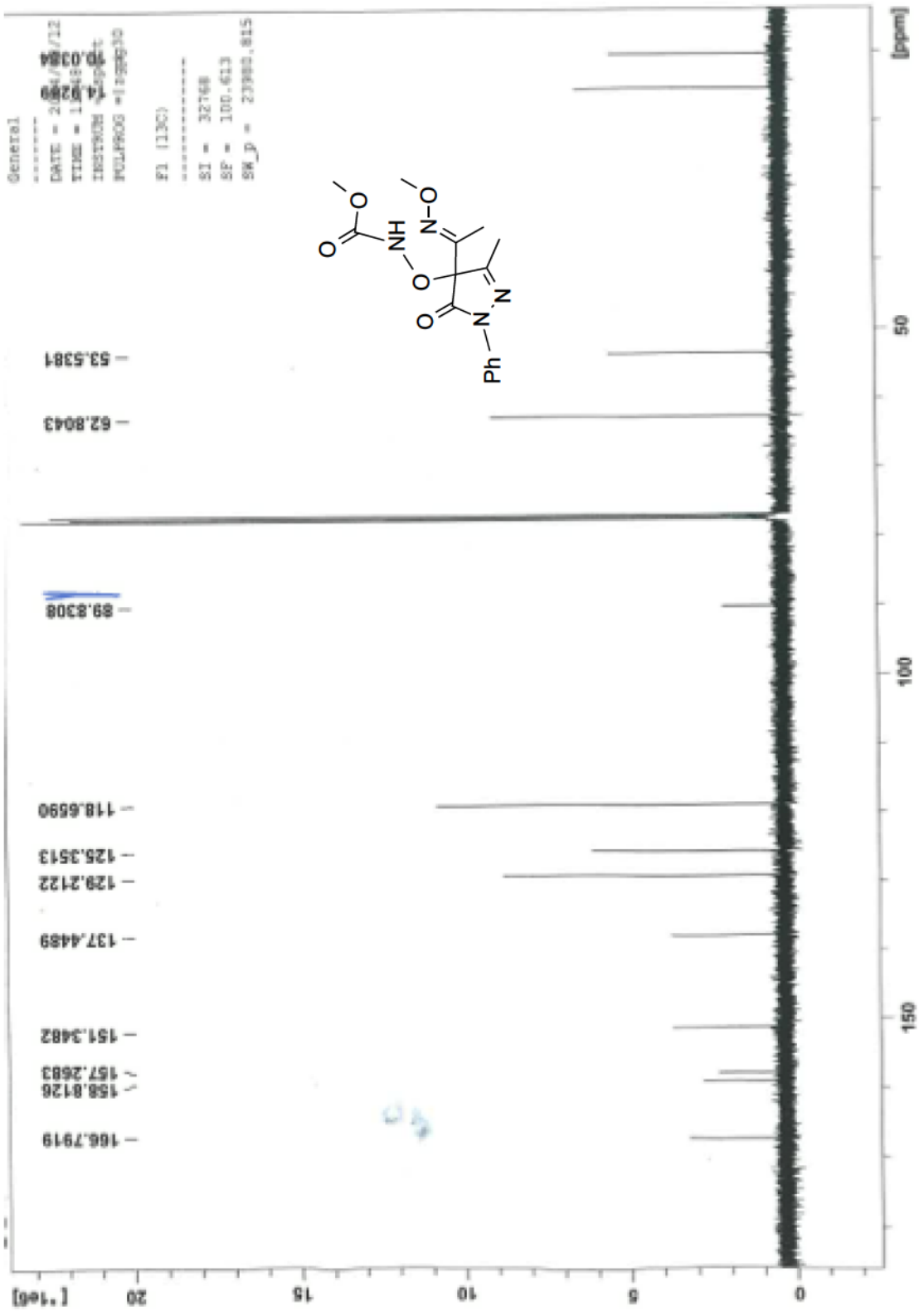
General
SI = 32768
SF = 100.613
SW_p = 23980.815
F1 (13C)
53.5381
62.8043
89.8308
118.6590
125.3513
129.2122
137.4489
151.3482
157.2683
158.8126
166.7919
[ppm]
[*10^6]
Ph

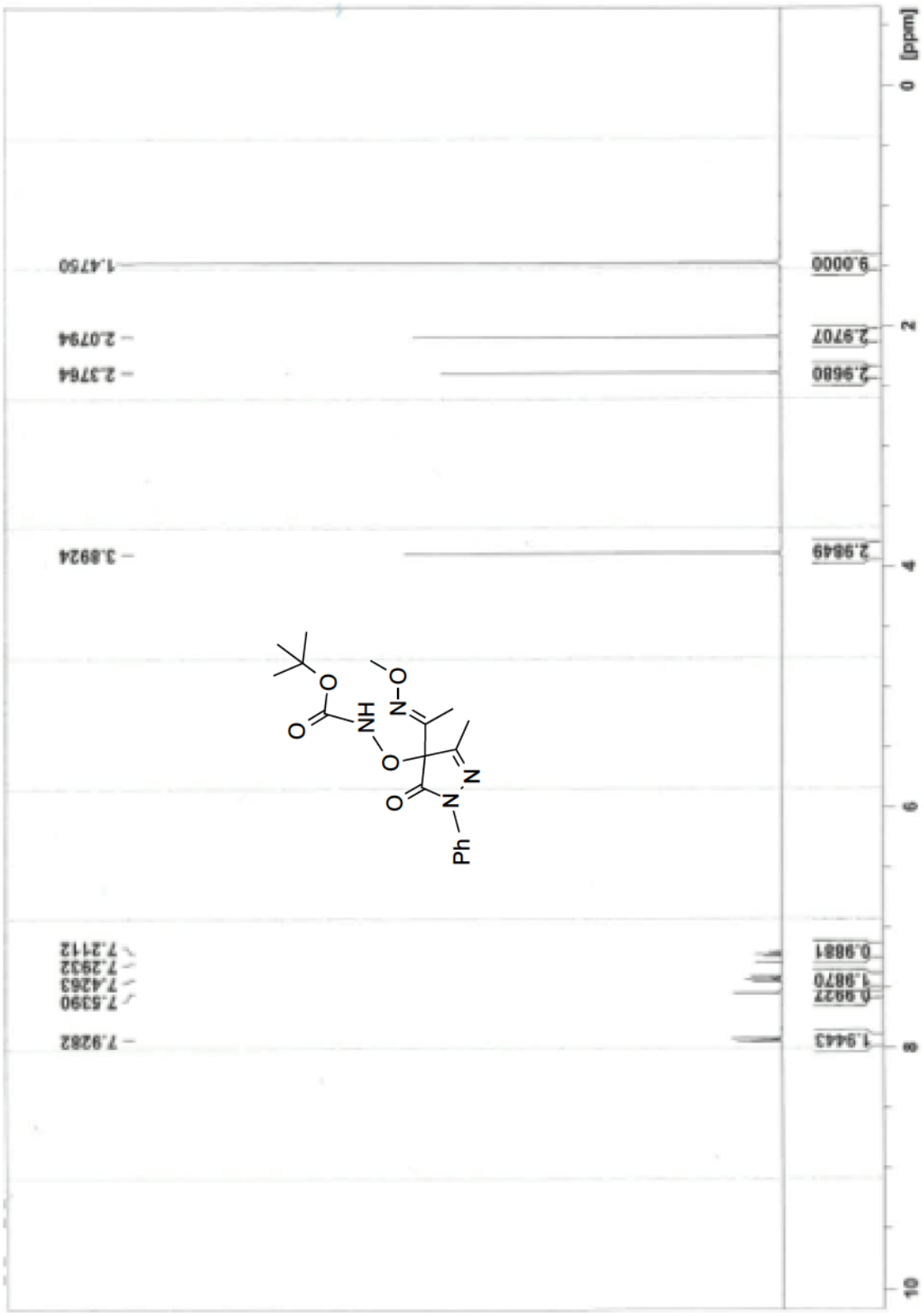
1.4750
2.0794
2.3764
3.8924
7.2112
7.2932
7.4263
7.5390
7.9282
9.0000
2.9707
2.9680
2.9849
0.9881
1.9870
0.9927
1.9443
[ppm]
0
2
4
6
8
10
O
O
NH
O
N
O
N
N
Ph
O

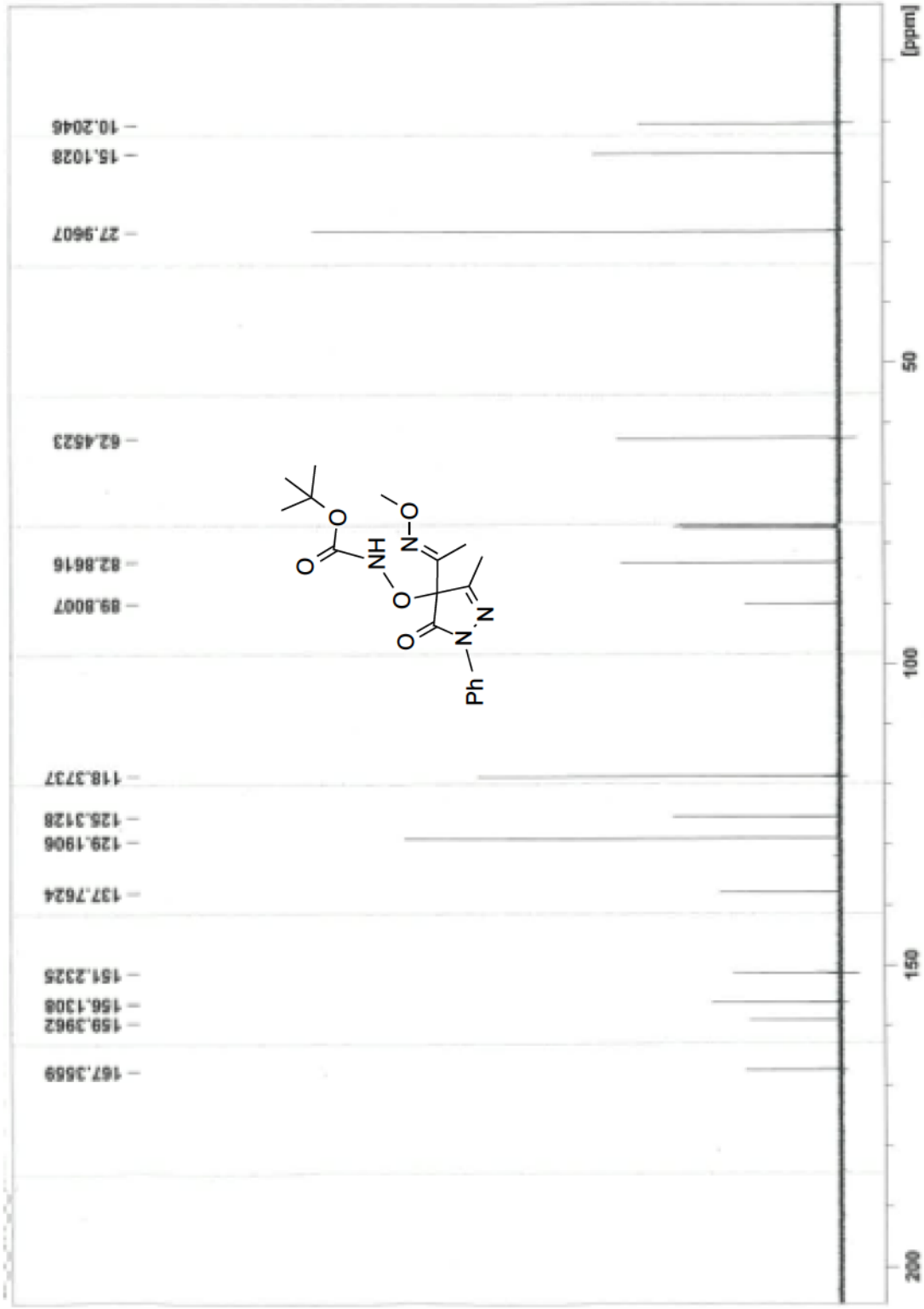
[ppm]
200
150
100
50
167.3559
159.3962
156.1308
151.2325
137.7624
129.1906
125.3128
118.3737
89.8007
82.8616
62.4523
27.9607
15.1028
10.2046
O
O
NH
O
N
O
N
N
Ph

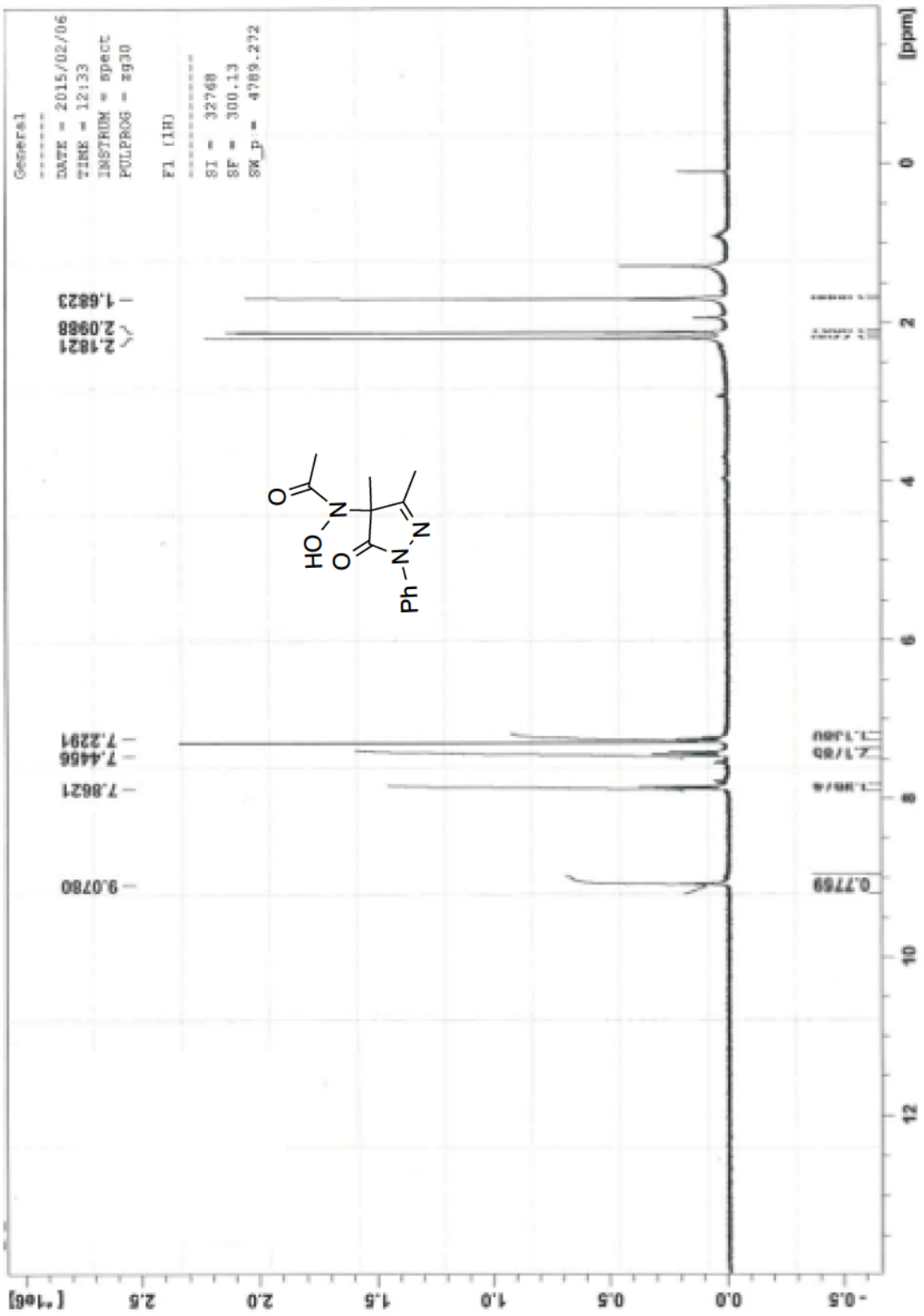
General
DATE = 2015/02/06
TIME = 12:33
INSTRUM = spect
PULPROG = zg30
F1 (1H)
SI = 32768
SF = 300.13
SW_p = 4789.272
1.6823
2.0988
2.1821
7.2291
7.4456
7.8621
9.0780
0.7769
[ppm]
[*10e6]

[ppm]
0
5
10
15
20
M 8.9651
M 7.8517
M 7.3967
M 7.2127
M 3.8629
M 2.3429
M 2.0622
M 1.9169
0.8672
1.9965
2.1643
1.1120
3.0000
2.7658
3.1274
3.3357
O
HN
O
N
O
N
O
N
Ph

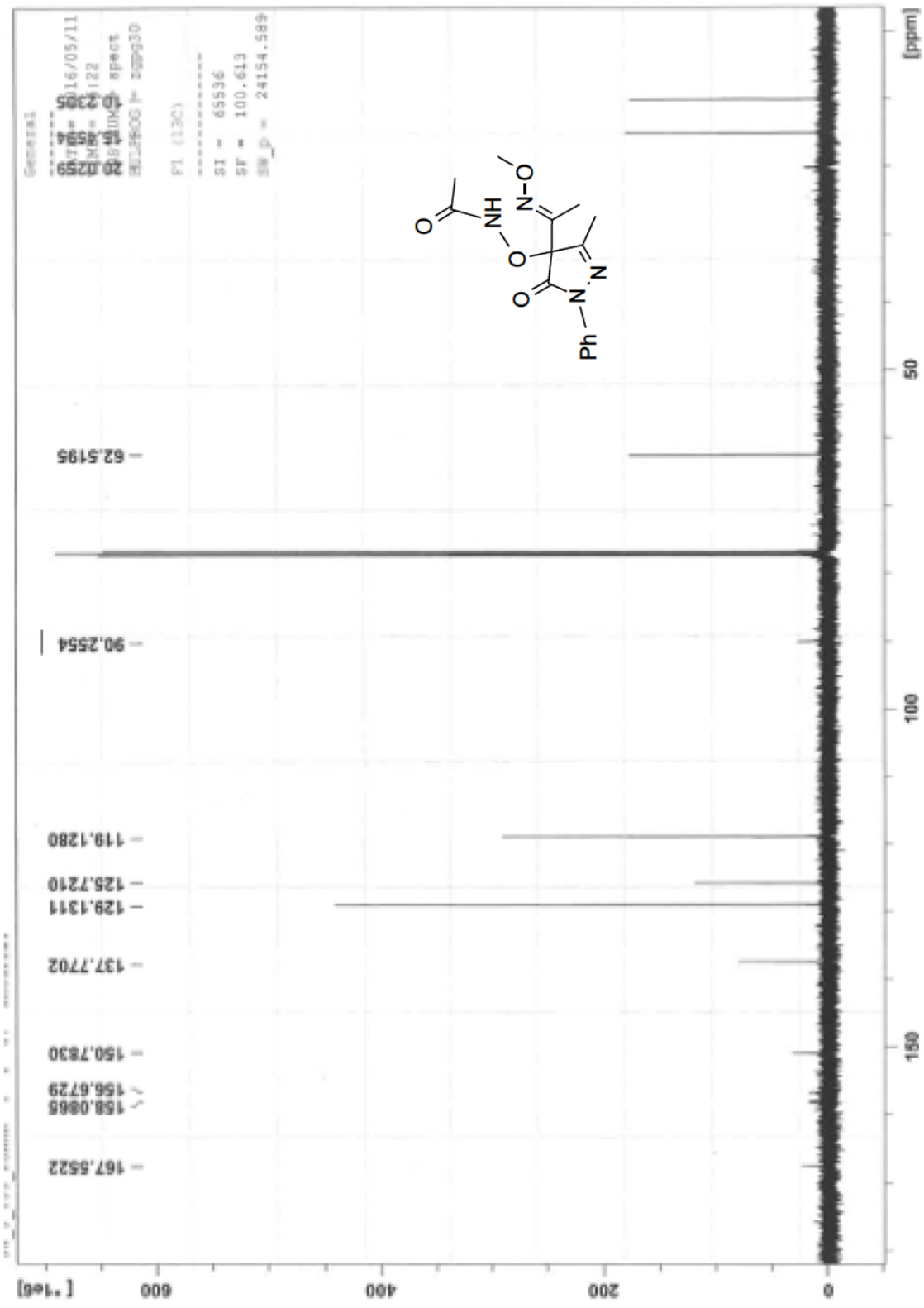
[ppm]
0
50
100
150
200
400
600
[ppm]
167.5522
158.0865
156.6729
150.7830
137.7702
129.1311
125.7210
119.1280
90.2554
62.5195
Ph

Chapter 4.

Reaction of Nitrosocarbonyl Compounds with Pyrazolones as Studied by TRIR Spectroscopy

4.1. Introduction

4.1.1. Nitrosocarbonyl Compounds

Nitrosocarbonyls are transient electrophiles that can react with nucleophiles to generate HNO. The formation of these reactive intermediates was first proposed by pyrolysis of nitrite with aldehydes,[1] and through oxidation of hydroxamic acid derivatives.[2] Originally, because direct detection of nitrosocarbonyls was difficult, isolation of the end products was used as indicators for nitrosocarbonyl release. For example, upon hydrolysis the formation of carboxylic acid and HNO was used to infer the intermediacy of nitrosocarbonyls.

4.1.2. Nitrosocarbonyls Trapping Reactions

As shown in Scheme 4-1, Kirby and co-workers reported the formation of Diels-Alder adducts upon generation of nitrosocarbonyls in presence of different dienes.[3-5] Further studies have suggested that these Diels-Alder adducts are efficient nitrosocarbonyl precursors under elevated temperature.[3].

Scheme 4-1. Thermal Generation and Diels-Alder Trapping of Nitrosocarbonyl Compounds.

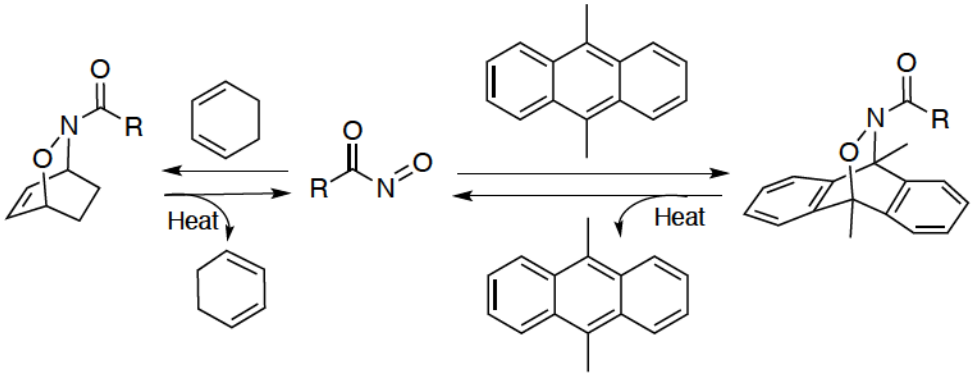

Upon thermal decomposition of Diels-Alder adducts, Kirby and co-workers studied the reactivity of nitrosocarbonyls with triphenyl phosphine.[6] It was proposed that through an oxygen atom transfer, triphenyl phosphine oxide and an isocyanate were formed (Scheme 4-2). The mechanism of the reaction was shown to be more complicated than originally expected, and depending on the nature of the nitrosocarbonyl intermediate, different pathways for product generation is possible.

In presence of olefins, nitrosocarbonyls can undergo an ene reaction to yield *N*-substituted hydroxamic acid derivatives (Scheme 4-2).[7-9] A limitation with developing nitrosocarbonyl ene reactions has been attributed to the strongly

oxidative conditions often required for nitrosocarbonyl generation which can lead to subsequent product decomposition. Keck[10] and Kirby[11] reported a nitrosocarbonyl transfer in the nitrosocarbonyl ene reaction using thermal decomposition of a Diels-Alder adducts, and as the result, the ene adducts were isolated in high yields. Also, Tan and co-workers reported nitrosocarbonyl formation using photoredox catalysis for oxidation of hydroxamic acids.[12] The nitrosocarbonyl ene adducts were isolated in high yields under optimized conditions. Recently, a number of groups have reported mild aerobic conditions for nitrosocarbonyl generation using transition metal catalysis.[13-30] This oxidative protocol is single pot, and can be applied to the ene and Diels-Alder reactions.

Scheme 4-2. Reactivity of Nitrosocarbonyl Compounds

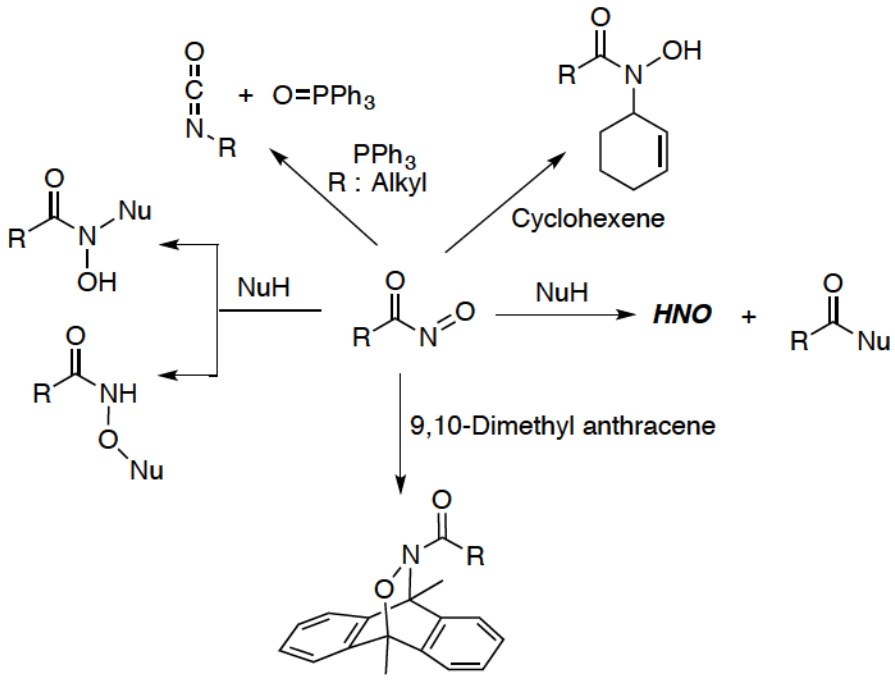

The hydrolysis of nitrosocarbonyls has been used as an efficient pathway for HNO generation. King and co-workers studied the reaction of nitrosocarbonyl compounds with amines resulting in the formation of amides in reasonable yield.[31] Also, detection of N_2O (the product of HNO dimerization) indicated HNO formation. Another recent report studied the reaction of amines with carbamoyl nitroso intermediates (Scheme 4-3).[32] Here, low yields of the expected urea were obtained, and the major product was semicarbazone, which was presumably formed via initial attack at the nitroso nitrogen atom and subsequent dehydration and tautomerization.

Scheme 4-3. Reactivity of Carbamoylnitroso Compounds with Primary Amines

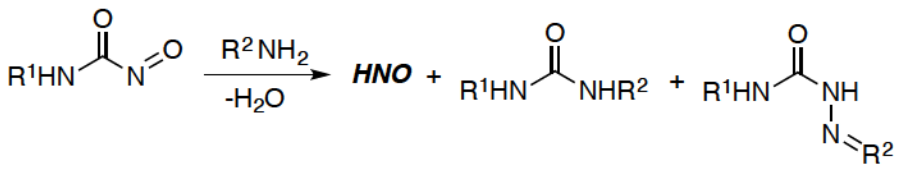

Recently, Read de Alaniz and Yamamoto studied nitrosocarbonyl aldol reaction on the nitrogen and oxygen atoms of nitrosocarbonyls using different carbon based nucleophiles.[17,18] The regioselectivity and enantioselctivity was shown to be controlled through the use of different catalysts. As has been discussed in Chapters 2 and 3, pyrazolones are efficient nitrosocarbonyl traps, undergoing an *N*-selective nitrosocarbonyl aldol reaction to generate *N*-substituted hydroxamic acid derivatives under physiological conditions.[33,34] This reaction can be used to confirm the involvement of nitrosocarbonyl intermediates in different reactions.

In the absence of nucleophiles, nitrosocarbonyls may undergo a dimerization reaction, followed by a series of acyl migrations, to release equimolar amounts of N_2O and anhydride (Scheme 4-4).[35]

Scheme 4-4. Proposed Mechanism for Dimerization of Nitrosocarbonyls in the Absence of Nucleophiles

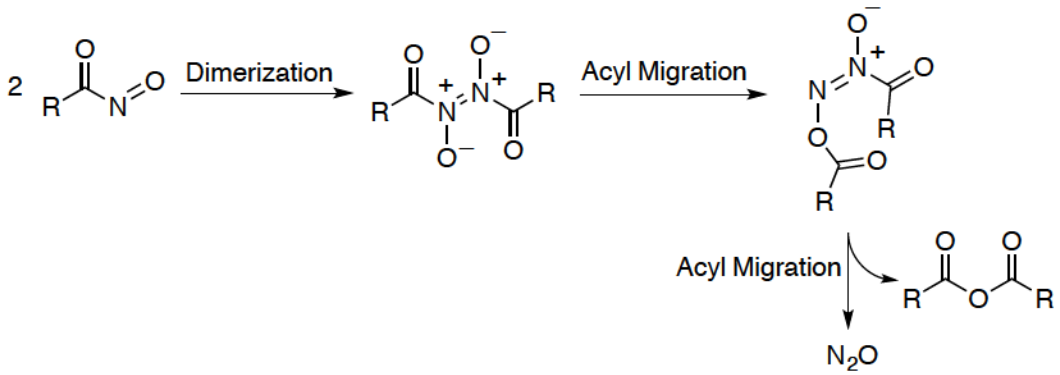

4.1.3. Detection of Nitrosocarbonyl Intermediates

The spectroscopic detection of nitrosocarbonyls in gas phase was first reported by Schwarz and co-workers using charge reversal and neutralization reionization mass spectrometry.[36,37] Recently, Toscano et al. reported the direct detection of nitrosocarbonyls using time-resolved infrared (TRIR) spectroscopy.[38] This technique is very effective for mechanistic photochemical studies, and provides fundamental information about the structure of reactive intermediates.

To study the reactivity of photogenerated nitrosocarbonyl intermediates, a photoprecursor with high quantum yield is desired. For this purpose, 3,5-diphenyl-1,2,4-oxadiazole-4-oxide was used as an efficient nitrosocarbonyl photoprecursor.[39] The reaction of benzonitrile with tertiary amines yields three different products (Scheme 4-5). 3,5-Diphenyl-1,2,4-oxadiazole-4-oxide is one of the products, which

undergoes a photochemical fragmentation in solution to generate equimolar amounts of benzonitrile and nitrosocarbonyl. This nitrosocarbonyl precursor can also undergo thermal cleavage and generate nitrosocarbonyls at elevated temperatures.[40] Different oxadiazole aryl substitutions are reported to release nitrosocarbonyls following the same decomposition mechanism.[39-41]

A practical application of photo generated nitrosocarbonyls has been shown in ene reaction using a variety of alkenes.[39,42] For example, in the synthesis of carbanucleosides, as shown in Scheme 4-6, 3,5-diphenyl-1,2,4-oxadiazole-4-oxide was used as a photo precursor to generate nitrosocarbonyl compounds.[42] In presence of cyclopentenes functionalized with purine heterobases, diastereomeic mixture of ene adducts were isolated.

Scheme 4-5. Synthesis and Photochemical Fragmentation of Oxadiazole

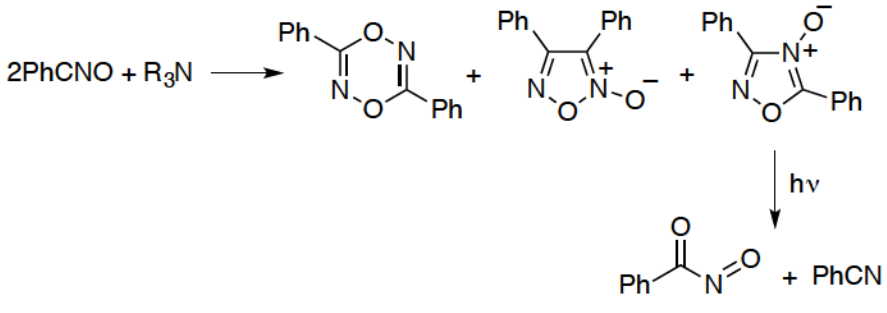

Scheme 4-6. Ene Reaction of Nitrosocarbonyl Compound with Cyclopentene Derivatives.

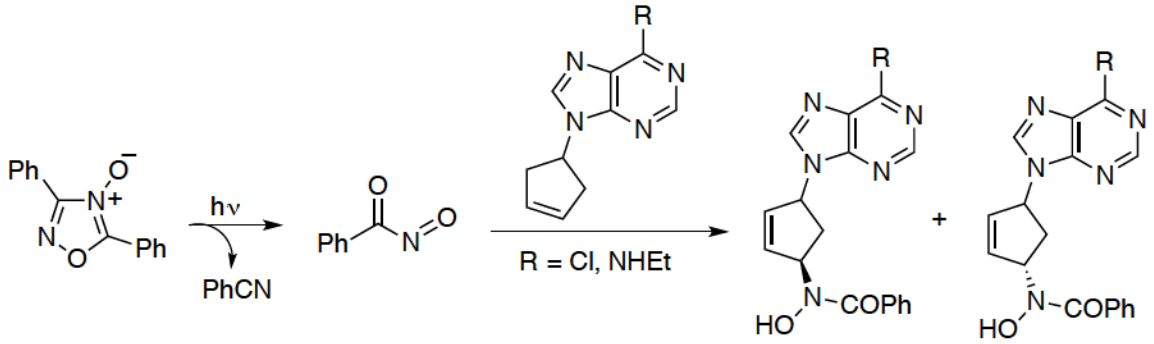

Upon 355 nm laser photolysis of 3,5-diphenyl-1,2,4-oxadiazole-4-oxide in argon-saturated acetonitrile-d_3 or dichloromethane, Toscano and co-workers observed the bleaching of the oxadiazole at 1310 cm^{-1} using TRIR spectroscopy.[38] Also, other bands were observed corresponding to benzonitrile (2265 cm^{-1}) and the nitrosocarbonyl intermediate (1735, 1590, 1560, and 1235 cm^{-1}). In this study, the trapping reaction of the nitrosocarbonyl with diethylamine (DEA) and 1,3-cyclohexadiene (CHD) was monitored to form the corresponding amide and Diels-Alder adduct, respectively, in either acetonitrile-d_3 or dichloromethane.

Scheme 4-7. Reactions of Nitrosocarbonyl Intermediate with Diethylamine and 1,3-Cyclohexadiene

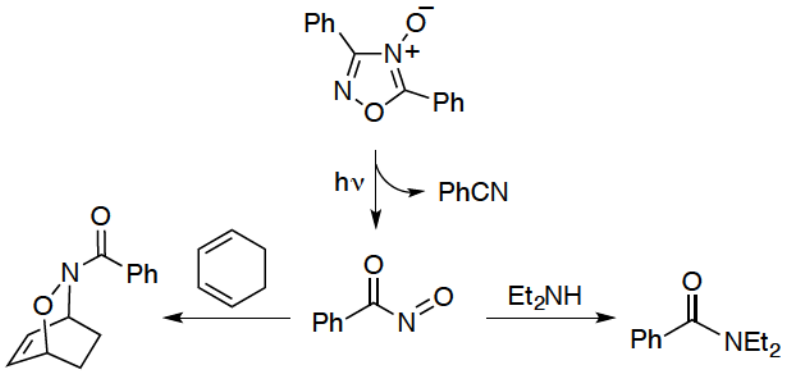

The observed decay rates for the nitrosocarbonyl intermediate in the presence of either DEA or CHD were monitored at 1735 cm^{-1}. Plots of the observed nitrosocarbonyl decay rates versus either concentration of DEA or CHD, which fit well to pseudo-first order rate equations, were used to derive relevant rate constants. Using ($k_{obs} = k_0 + k_{DEA}[DEA]$) and ($k_{obs} = k_0 + k_{CHD}[CHD]$), the second order rate constants $k_{DEA} = (1.3 \pm 0.5) \times 10^5\ M^{-1}\ s^{-1}$ and $k_{CHD} = (6.0 \pm 0.5) \times 10^3\ M^{-1}\ s^{-1}$ were derived.

In another study, upon 266 nm laser photolysis of 9,10-dimethylanthracene adducts **1** and **2** (Scheme 4-8), Toscano and co-workers observed a similar IR band at 1735 cm^{-1}, corresponding to nitrosocarbonyl intermediate formation.[43] In contrast to **2**, laser photolysis of photoprecursor **1** generated an additional IR band at 1820 cm^{-1}, which formed faster than the time resolution of the spectrometer (ca. 50 ns) and decayed with additional increase of the 1735 cm^{-1} nitrosocarbonyl band. This band was assigned to the formation of benzoyl radical, potentially generated through either a secondary photolysis of nitrosocarbonyl compound or Norrish type I cleavage of photo precursor **1** to form benzoyl radical along with an NO/DMA adduct that quickly dissociated to NO and DMA. It was proposed that the excited state of **1** could undergo α-cleavage and cycloreversion, and additional formation of the nitrosocarbonyl intermediate was attributed to the recombination of benzoyl radical with NO, which was released from the aminyl radical intermediate. In contrast, photoprecursor **2** proceeded through cycloreversion to generate nitrosocarbonyl (R = Me) compound with no evidence for the acetyl radical formation. Unlike benzoyl nitroside (R = Ph), acetyl nitroside (Me) was not

expected to have absorbance at 266 nm, and it suggested that upon nitrosocarbonyl (R = Ph) release, secondary photolysis was the pathway that occurred to form benzoyl radical and NO. .

Scheme 4-8. Potential Photochemical Decomposition Pathways for 9,10-Dimethylanthracene Adducts

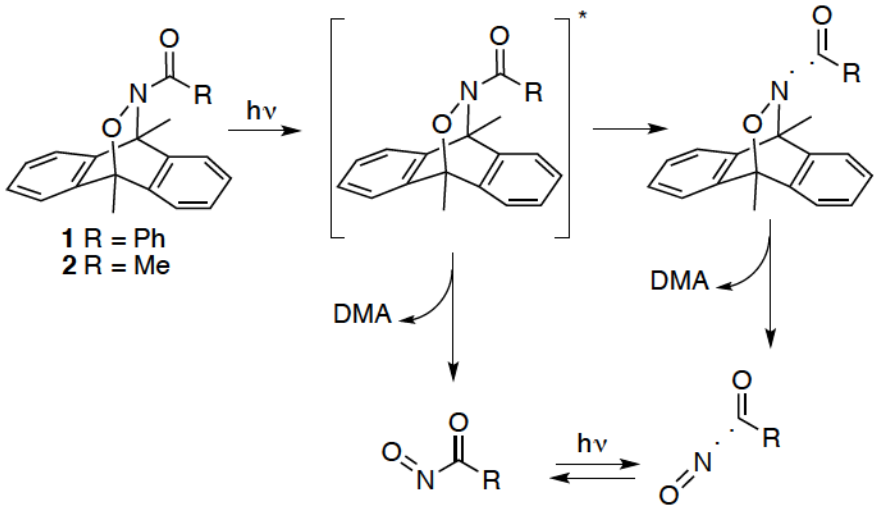

Also, the reactivity of photogenerated nitrosocarbonyl compounds (R = Ph, Me, and 4-Cl-Ph) with different primary and secondary amines was reported using 1,2,4-oxadiazole-4-oxides and 9,10-dimethylanthracene adducts as nitrosocarbonyl precursors. For primary and secondary amines, the observed decay rates were plotted versus amine concentration, and fit well to $k_{obs} = k_0 + k_{amine}[amine]^2$ and $k_{obs} = k_0 + k_{amine}[amine]$, respectively. This indicated that the aminolysis of nitrosocarbonyls is dependent on the amine structure. The mechanism of nitrosocarbonyl aminolysis by secondary amines was proposed to be bimolecular, however, primary amines reacted with nitrosocarbonyls through a general base catalysis mechanism.

Also, the reactivity of photogenerated nitrosocarbonyl intermediates with thiols was studied. No increase in nitrosocarbonyl decay was observed in presence of a thiol (*N*-acetylcysteine methyl ester). However, addition of DEA to the reaction mixture resulted in faster nitrosocarbonyl decay than in the presence of DEA alone. This result suggested that thiols do not react with nitrosocarbonyls on the microsecond timescale, however, thiolates trap nitrosocrabonyls on the microsecond time scale to form thioesters. As shown in Scheme 4-9, the mechanism was proposed to be through formation of a tetrahedral intermediate, which was detected at 1615 cm^{-1} by TRIR spectroscopy.

Scheme 4-9. Proposed Mechanism for the Thiolysis of the Nitrosocarbonyl Compound.

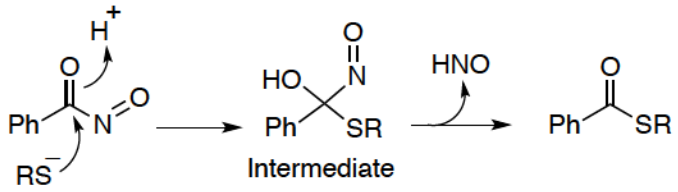

4.2. Results and Discussion

4.2.1. Reaction of a Photogenerated Nitrosocarbonyl Compound with Pyrazolones

As mentioned in Chapters 2 and 3, pyrazolones are efficient nitrosocarbonyl traps in both aqueous and organic solutions. We tried to examine this reaction by TRIR spectroscopy and compare it to the reaction with amines. Previously, **PY-1** was reported to be an efficient trap for HNO to form *N*-substituted hydroxylamine derivatives.[44] Additionally, based on our experiments and consistent with our

expectation, this pyrazolone was shown to be an excellent trap for nitrosocarbonyl intermediates to generate *N*-substituted hydroxamic acid derivatives under physiological conditions.[33] Anionic **PY-1** absorbs light at wavelengths shorter than 300 nm, so it was not possible to use 9,10-dimethylanthracene adducts as the nitrosocarbonyl photoprecursor since 266 nm laser photolysis is necessary in this case. However, 3,5-diaryl-1,2,4-oxadiazole-4-oxide can be photolyzed at 355 nm to generate nitrosocarbonyl intermediates. By conducting this photolysis in presence of **PY-1**, we hoped to study the kinetics of this trapping reaction (Scheme 4-10). Also, we hoped to follow the trapping reactions using **PY-2** and **3**, as well as **PY-1**, in order to compare different pyrazolones trapping rate constants with nitrosocarbonyls. Unlike **PY-1**, high concentrations (80 mM) of anionic **PY-2** and **3** absorb light at wavelengths longer than 300 nm. Therefore, the nitrosocarbonyl trapping reaction was studied with only **PY-1** using TRIR spectroscopy.

Scheme 4-10. Suggested Reaction of Photogenerated Nitrosocarbonyl Intermediate with Pyrazolones.

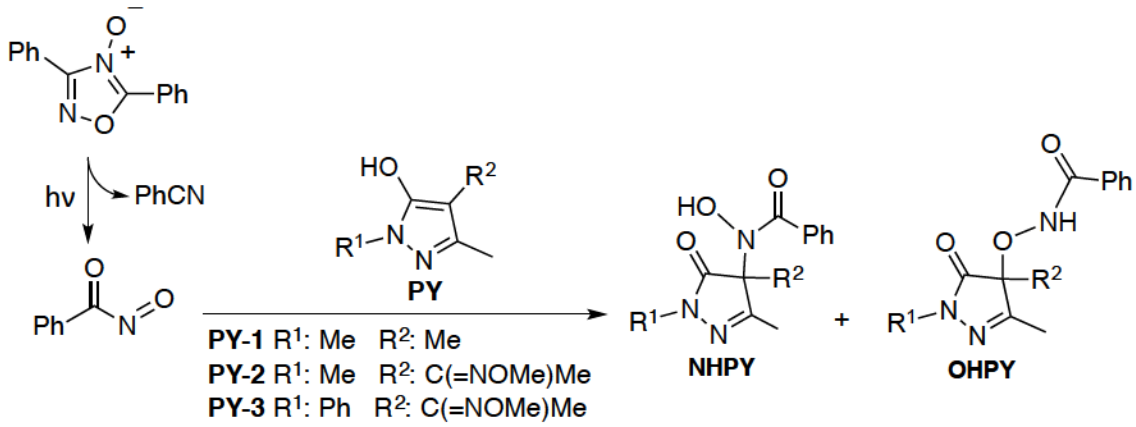

Laser photolysis (355 nm, 5 ns, 2 mJ) of 1 mM 3,5-diphenyl-1,2,4-oxadiazole-4-oxide in acetonitrile produces the TRIR difference spectra shown in Figure 4-1. The observed large positive band at 1738 cm^{-1} corresponds to generation of nitrosocarbonyl (PhC(O)N=O), which is consistent with the previously reported frequency (1735 cm^{-1}) for this intermediate.[38]

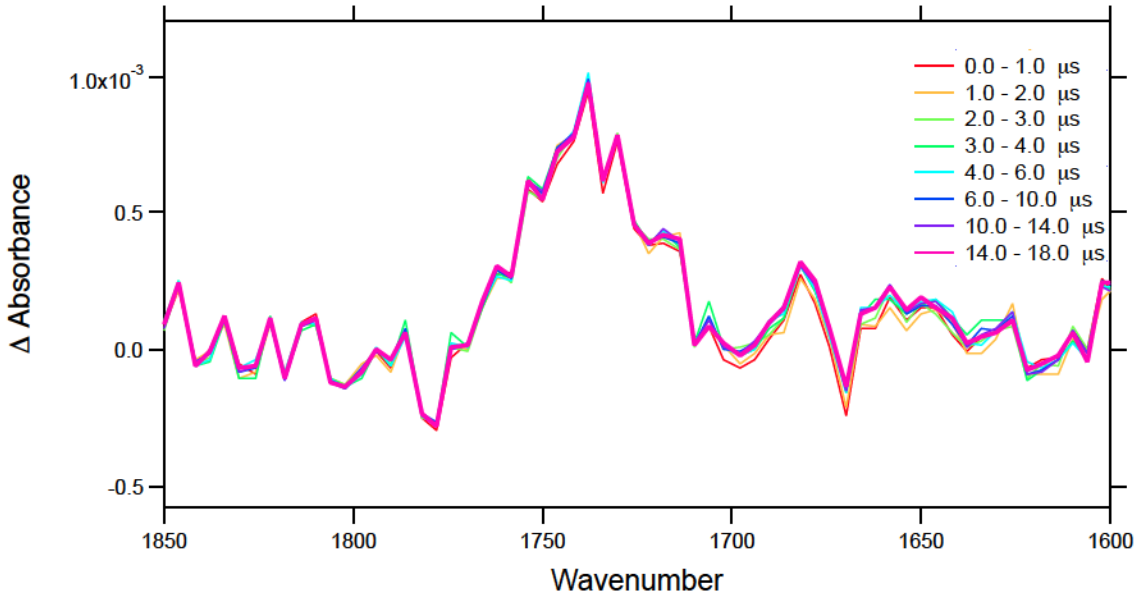

Figure 4-1. TRIR difference spectra averaged over the indicated time frames following laser photolysis (355 nm, 5 ns, 2 mJ) of a solution of 3,5-diphenyl-1,2,4-oxadiazole-4-oxide (1 mM) in argon-saturated acetonitrile.

Based on our previous studies, it was expected that deprotonated pyrazolones should trap nitrosocarbonyls efficiently. To confirm that triethylamine could be used to deprotonate pyrazolones and not interfere with our TRIR experiments, we examined its effect on the rate of nitrosocarbonyl decomposition. Addition of 80 mM triethylamine to a solution of 1 mM 3,5-diphenyl-1,2,4-

oxadiazole-4-oxide in acetonitrile had no effect on kinetic traces observed following 355 nm laser photolysis. This suggests that triethylamine does not react with the nitrosocarbonyl intermediate.

Upon 355 nm laser photolysis of 1 mM 3,5-diphenyl-1,2,4-oxadiazole-4-oxide in presence of 80 mM **PY-1** and 80 mM triethylamine in argon-saturated acetonitrile, the TRIR difference spectra shown in Figure 4-2 were obtained.

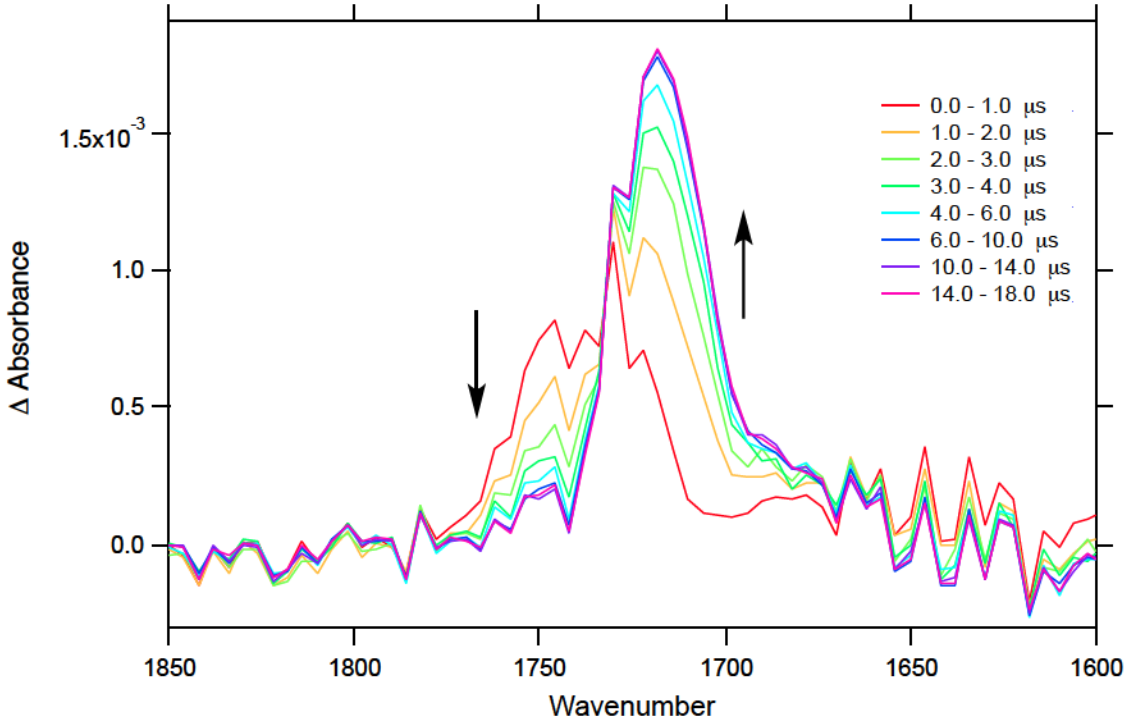

Figure 4-2. TRIR difference spectra averaged over the indicated time scales following laser photolysis (355 nm, 5 ns, 2 mJ) of a solution of 3,5-diphenyl-1,2,4-oxadiazole-4-oxide (1 mM), **PY-1** (80 mM), and triethylamine (80 mM) in argon-saturated acetonitrile.

To gain insight into this reaction, spectra from different experiments were overlaid as indicated in Figure 4-3. Spectra observed over the first 1 μs are similar after laser photolysis of a solution of 1 mM 3,5-diphenyl-1,2,4-oxadiazole-4-oxide with and without added **PY-1**, consistent with the initial formation of a nitrosocarbonyl intermediate. Following nitrosocarbonyl trapping reaction with anionic **PY-1**, it is expected to observe decay of the band at 1738 cm^{-1} band corresponding to a nitrosocarbonyl trapping reaction. Decay of this band, monitored at 1752 cm^{-1}, is observed along with a concomitant growth of the band with the maximum at 1718 cm^{-1}. Comparing the red and green spectra from Figure 4-3 which represent the TRIR difference spectra upon photolysis of 3,5-diphenyl-1,2,4-oxadiazole-4-oxide with and without the presence of anionic **PY-1**, the band monitored at 1752 cm^{-1} is assigned to nitrosocarbonyl intermediate, and its decay is due to nitrosocarbonyl consumption, which is accompanied by concomitant formation of a new product observed with the maximum wavelength at 1718 cm^{-1}. To inhibit the complications due to overlapping spectra of nitrosocarbonyl consumption and product formation at 1718 cm^{-1}, as indicated by red and purple in Figure 4-3, product formation was monitored at 1704 cm^{-1}. Decay of the band due to nitrosocarbonyl consumption was accompanied by the growth of the product at 1704 cm^{-1} with identical kinetics (Figure 4-4).

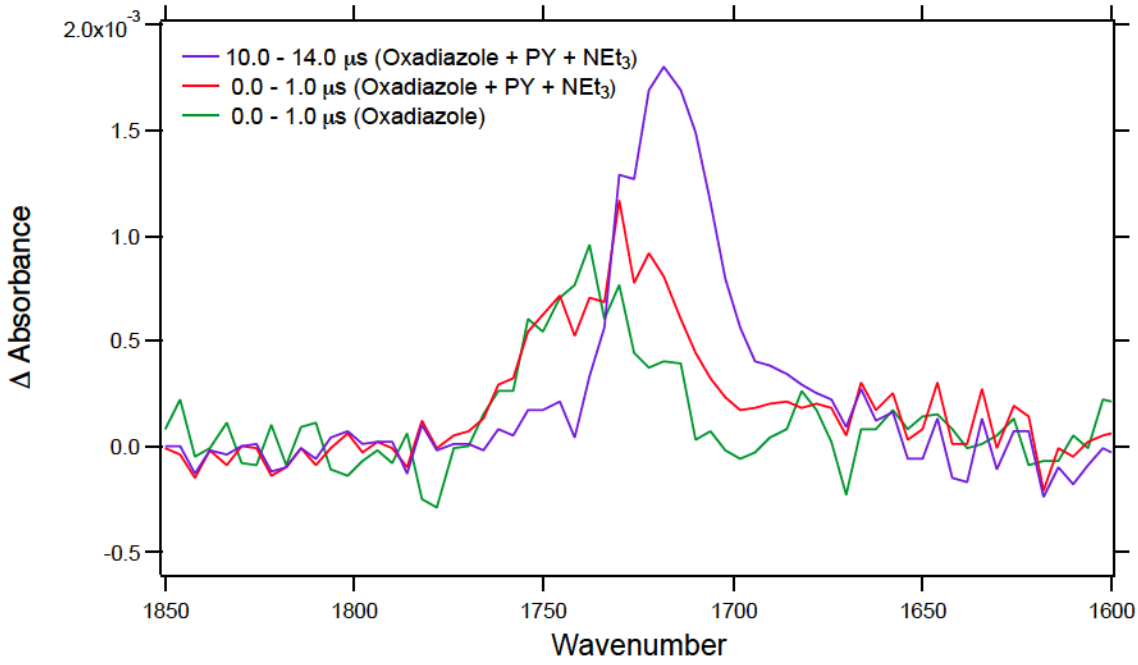

Figure 4-3. Overlaid of TRIR difference spectra for the indicated conditions and time scales following laser photolysis (355 nm, 5 ns, 2 mJ) of 1 mM solution of 3,5-diphenyl-1,2,4-oxadiazole-4-oxide with and without the presence of 80 mM anionic **PY-1**.

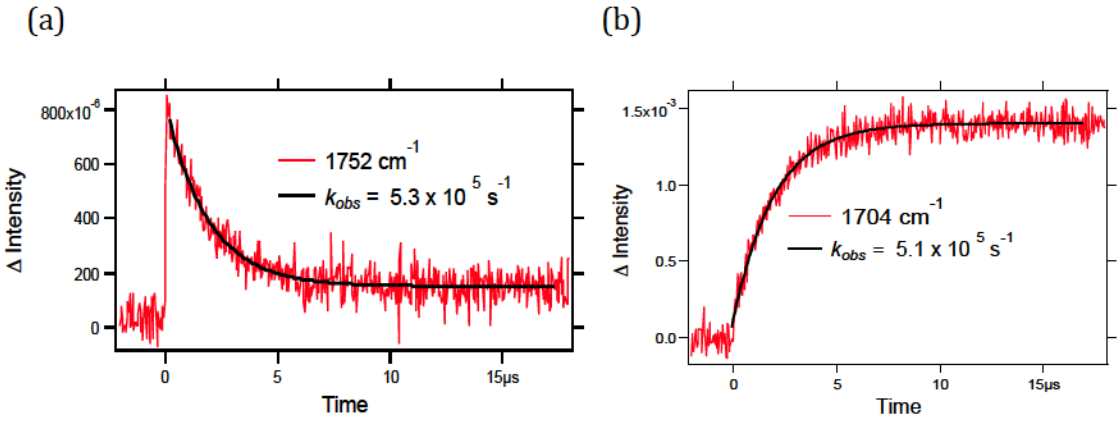

Figure 4-4. Kinetic traces observed following laser photolysis (355 nm, 5 ns, 2 mJ) of 1 mM solution of 3,5-diphenyl-1,2,4-oxadiazole-4-oxide containing 80 mM triethylamine and 80 mM of **PY-1** in argon-saturated acetonitrile at (a)1752 cm^{-1} and (b) 1704 cm^{-1} . Black curves are the calculated best fit to a single-exponential function.

According to Scheme 4-10, it is expected that the reaction of the nitrosocarbonyl intermediate with anionic **PY-1** will generate **NHPY-1** (R^1, R^2 = Me), and under certain conditions, may also yield **OHPY-1** (R^1, R^2 = Me). To assign the observed IR band with the maximum at 1718 cm^{-1} in Figure 4-2, we synthesized **NHPY-1** and **OHPY-1**, and examined their carbonyl IR frequencies in acetonitrile: **NHPY-1** (1718 and 1650 cm^{-1}) and **OHPY-1** (1722 cm^{-1}). It is expected to observe two IR bands corresponding to two carbonyl groups in **NHPY-1** and **OHPY-1** compounds. However, only one IR band was observed corresponding to carbonyl groups in **OHPY-1**. We suggest that two IR bands corresponding to two carbonyl groups are likely overlapping and experimentally, observed as a single band at 1722 cm^{-1} using acetonitrile as the solvent.

The experimental IR frequencies of these authentic samples suggested that the growth of observed IR bands with the maximum at 1718 cm^{-1} in Figure 4-2, is attributed to the formation of **NHPY-1**, and potentially, **OHPY-1**. It is expected that upon formation of **NHPY-1**, the growth of IR band at 1650 cm^{-1} corresponding to the carbonyl of the hydroxamic acid moiety, may be cancel out by the depletion of the corresponding band in **PY-1**. The decay of nitrosocarbonyl and growth of the product fit well to a single exponential as indicated in Figure 4-4, and as shown the kinetic traces in Figure 4-7, the observed rates were dependent on the concentration of added anionic **PY-1**.

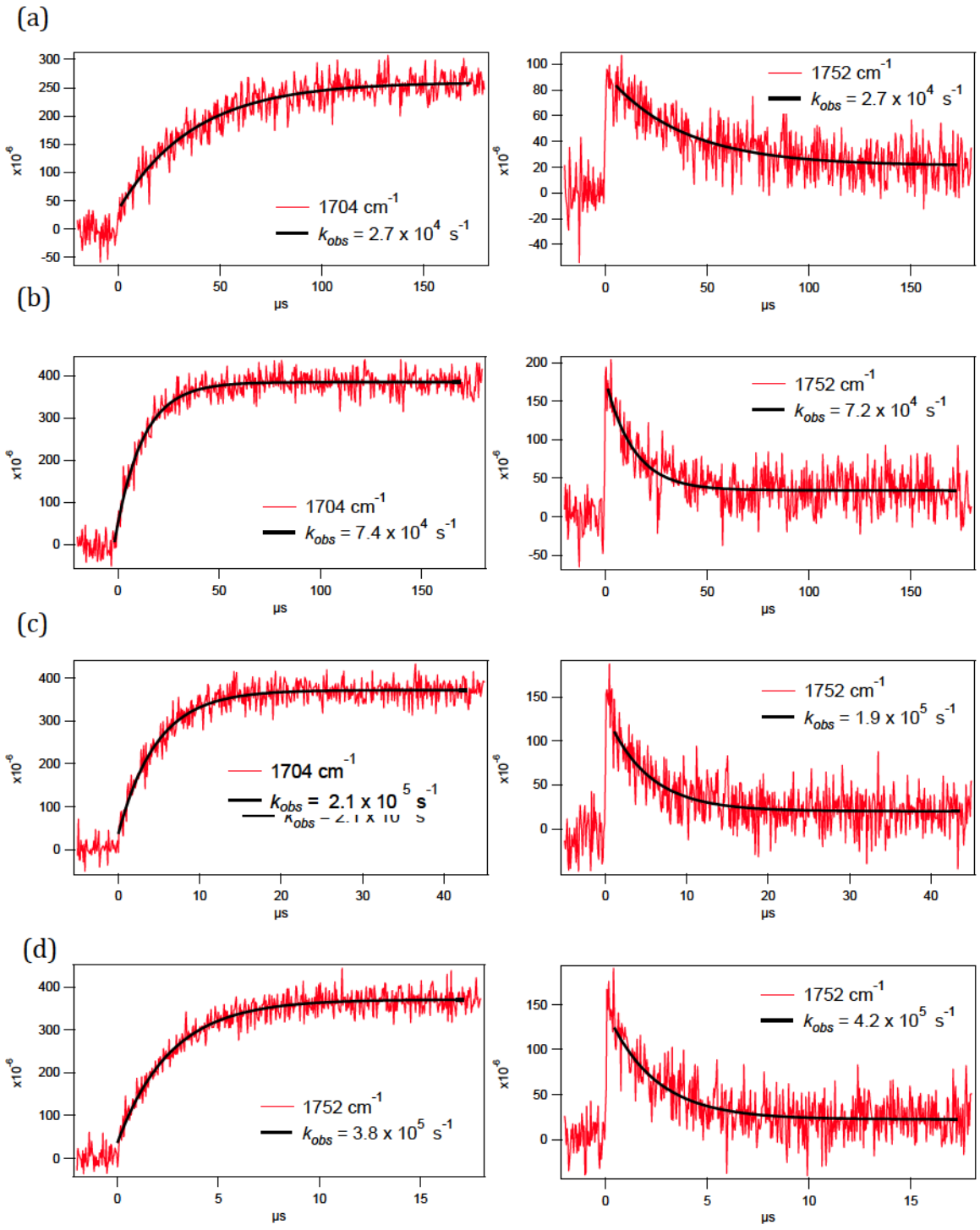

Figure 4-5. Kinetic traces observed following laser photolysis (355 nm, 5 ns, 2 mJ) of 1 mM solution of 3,5-diphenyl-1,2,4-oxadiazole-4-oxide in argon-saturated acetonitrile containing triethylamine and **PY-1** with the at 1752 and 1704 cm^{-1} following concentrations: (a) 10 mM (b) 20 mM (c) 40 mM (d) 60 mM. Black curves are the calculated best fit to a single-exponential function.

The observed rates of nitrosocarbonyl decay and the growth of product in acetonitrile versus the concentration of anionic **PY-1** were plotted and fit well to a pseudo-first-order rate equation (Figure 4-8). Applying $k_{obs} = k_0 + k_{PY}[PY]$, the second-order rate constant for reaction of nitrosocarbonyl with anionic **PY-1** was derived, $k_{NC} = (8.0 \pm 0.5) \times 10^6\ M^{-1}\ s^{-1}$, which is significantly faster than reported rate constant for the reaction of diethylamine with the same nitrosocarbonyl ($k_{DEA} = (1.3 \pm 0.5) \times 10^5\ M^{-1}\ s^{-1}$). [38]

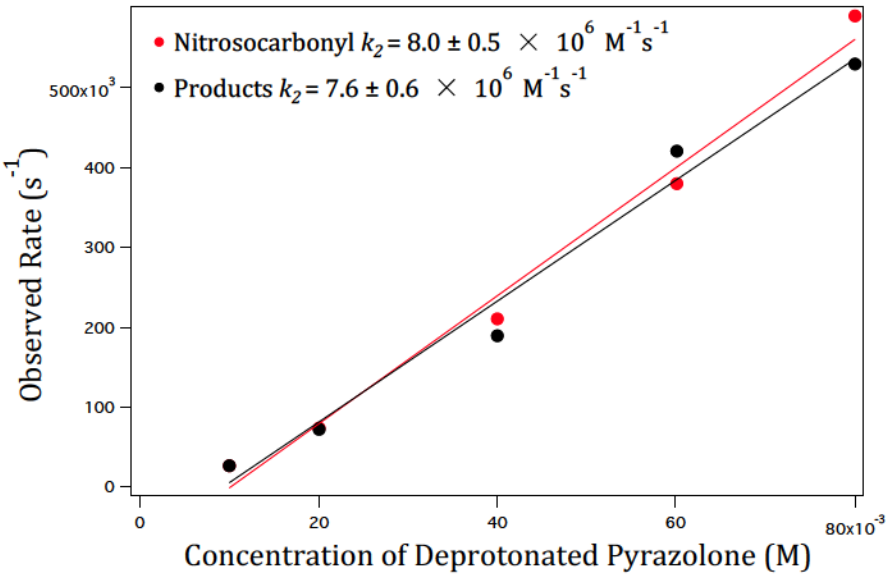

Figure 4-6. Plots of observed rate of decay of nitrosocarbonyl (indicated with red circles and monitored at 1752 cm^{-1}) and growth of the products (indicated with black circles and monitored at 1704 cm^{-1}) as a function of the concentration of deprotonated **PY-1**.

4.2.2. Product Analysis

Beside TRIR spectroscopy experiments that provide information about the involved intermediates, product studies using HPLC at the endpoint of the reaction were used to gain insight into the identity of the final products. Photolysis of 3,5-

diphenyl-1,2,4-oxadiazole-4-oxide was performed in argon-saturated acetonitrile solutions employing 350 nm irradiation with a Rayonet Reactor. The nitrosocarbonyl trapping ability of **PY-1** was studied in presence and absence of equimolar amounts of triethylamine (Figure 4-6). After photolysis, 20 µL of the samples was immediately analyzed by HPLC. In both conditions, we observed the formation of benzonitrile along with mixture of **NHPY-1** and **OHPY-1** (Scheme 4-10). We also observed formation of a product with retention time of 7.01 min; its identification is currently under investigation.

NHPY-1 and **OHPY-1** were synthesized (R^1, R^2 = Me in Scheme 4-7) and used to assign the observed peaks by co-injection. Using these synthesized compounds, the product yields under both conditions were measured and reported in Table 4-1. Results from product analysis of the photolysis of 3,5-diphenyl-1,2,4-oxadiazole-4-oxide (indicated as oxadiazole in Table 4-1 and Figure 4-6) in presence of **PY-1** suggested that both anionic and neutral **PY-1** reacts with nitrogen and oxygen atoms of nitrosocarbonyl intermediate.

Table 4-1. Yield of products following photolysis of 3,5-diphenyl-1,2,4-oxadiazole-4-oxide in presence of deprotonated and neutral PY-1 in acetonitrile.

Compounds	NHPY-1 %	OHPY-1 %	PhCN %
Oxadiazole + PY-1 + NEt_3	47	45	100
Oxadiazole + PY-1	40	53	100

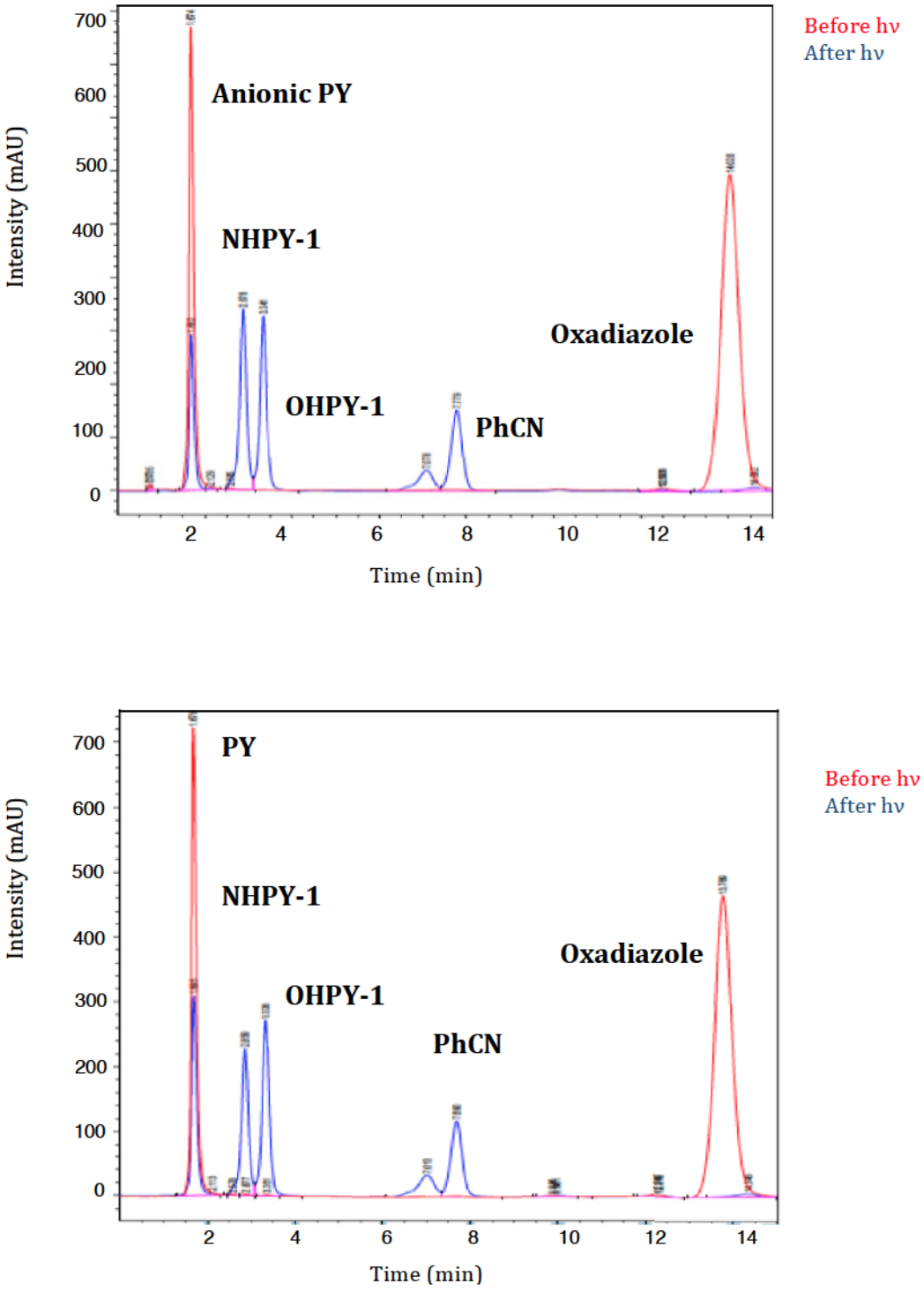

Figure 4-6. HPLC spectra before and after photolysis of 0.4 mM of 3,5-diphenyl-1,2,4-oxadiazole-4-oxide in presence of 0.8 mM **PY-1** with (a) 0.8 mM triethylamine and (b) no triethylamine.

To examine the regioselectivity of the transformation to yield either **NHPY** or **OHPY**, we carried out the photolysis in different solvents (Table 4-2). Samples were analyzed by HPLC after photolysis of 0.4 mM 3,5-diphenyl-1,2,4-oxadiazole-4-oxide in presence of 0.5 mM **PY-1** in aqueous acetonitrile, methanol, and dichloromethane.

The results presented in Table 4-2 suggest that the ability of **PY-1** to trap nitrosocarbonyl intermediate is solvent dependent. For example, pyrazolones are excellent nitrosocarbonyl traps in either methanol or acetonitrile; however, only 24% formation of the trapped product is observed in dichloromethane. Due to the low solubility of 3,5-diphenyl-1,2,4-oxadiazole-4-oxide in water, a 10% v/v aqueous acetonitrile solution was used as the solvent, and as expected, **PY-1** is observed to be an efficient nitrosocarbonyl trap under these conditions. Interestingly, **NHPY-1** is the major product in aqueous acetonitrile, methanol, and dichrolomethane. However, **OHPY-1** is the major product in neat acetonitrile. It seems that the reaction of nitrosocarbonyl compounds with pyrazolones under different solvent conditions is complicated, and more investigations are required to understand and optimize the observed regiochemistry.

Table 4-2. Products Distribution After Photolysis of 3,5-diphenyl-1,2,4-oxadiazole-4-oxide in Presence of PY-1 Using Different Solvents.

Solvent	Trapping	NHPY-1 : OHPY-1
10% Aqueous Acetonitrile	92	85 : 15
Acetonitrile	93	42 : 51
Methanol	100	72 : 28
Dichloromethane	24	100 : 0

4.3. Future Directions

We studied the reactivity of a photogenerated nitrosocarbonyl intermediate with **PY-1** by TRIR spectroscopy, and measured the second-order rate constant for its reaction with the deprotonated **PY-1**, $k_2 = 8 \times 10^6$ M^{-1} s^{-1}. We also characterized the products of this reaction, and interestingly observed formation of both **OHPY-1** and **NHPY-1**, with a product distribution that was dependent on solvent.

Based on discussions in Chapters 2 and 3, the nature of the nitrosocarbonyl intermediate is an important factor that controls its reactivity with pyrazolone nucleophiles. Future TRIR spectroscopy work should involve exploring the photogeneration of different nitrosocarbonyls ($Me_2NC(O)=O$, $MeOC(O)N=O$, and $MeC(O)N=O$), and examining the reaction of these intermediates with a variety of amines. Because 9,10-dimethylanthracene adducts (DMA) are efficient nitrosocarbonyl photoprecursors, we propose to synthesize DMA adducts (R = NMe_2, OMe, and Me) using literature reported procedures.[3,45,46] Photolysis of these DMA adducts in presence of amines should make it possible to study the impact of R group (NMe_2, OMe, and Me) on the reactivity of nitrosocarbonyl intermediates.

4.4. Experimental

4.4.1. Method and Materials

3,5-diaryl-1,2,4-oxadiazole-4-oxide, **NHPY-1**, and **OHPY-1** were synthesized according to previously reported methods.[33,34,41] NMR spectra were obtained on a 400 MHz FT-NMR spectrometer. All chemical shifts are reported in parts per million (ppm) relative to residual $CHCl_3$ (7.26 ppm for ^1H, 77.23 ppm for ^{13}C). Benzonitrile was purchased from Aldrich and used without further purification.

4.4.2. Characterization of NHPY-1 and OHPY-1:

***N*-hydroxy-*N*-(1,3,4-trimethyl-5-oxo-4,5-dihydro-1*H*-pyrazol-4-yl)benzamide (NHPY-1)**: ^1H NMR (400 MHz, $CDCl_3$) δ: 9.33 (s, 1H), 7.76 (m, 2H), 7.44 (m, 1H), 7.35 (m, 2H), 3.33 (s, 3H), 2.03 (s, 3H), 1.61 (s, 3H). ^{13}C NMR (100 MHz, $CDCl_3$) δ: 174.8, 167.0, 160.4, 132.3, 131.8, 129.6, 128.1, 69.3, 31.6, 18.8, 12.5. HR-MS (FAB): found *m/z* = 262.11966 (MH^+); calcd for $C_{13}H_{16}O_3N_3$: 262.11917.

***N*-((1,3,4-trimethyl-5-oxo-4,5-dihydro-1*H*-pyrazol-4-yl)oxy)benzamide (OHPY-1):** ^1H NMR (400 MHz, $CDCl_3$) δ: 7.9 (s, 1H), 7.68 (m, 2H), 7.42 (m, 1H), 7.31 (m, 2H), 3.20 (s, 3H), 2.16 (s, 3H), 1.40 (s, 3H).

4.4.2. Time-Resolved IR Methods

TRIR experiments were performed (with 16 cm^{-1} spectral resolution) following the method of Hamaguchi and co-workers,[47,48] as has been reported previously.[49] The broadband output of a $MoSi_2$ IR source (JASCO) is crossed with excitation pulses from a Continuum Minilite II Nd:YAG laser (355 nm, 5 ns, 2 mJ) operating at 15 Hz. Changes in IR intensity are monitored using an AC-coupled mercury/cadmium/tellurium (MCT) photovoltaic IR detector (Kolmar Technologies, KMPV11-J1/AC), amplified, digitized with a Tektronix TDS520A oscilloscope, and collected for data processing. The experiment is performed in dispersive mode with a JASCO TRIR 1000 spectrometer.

4.5. References

(1) Beckwith, A. L. J.; Evans, G. W. *J. Chem. Soc.* **1962**, 130-137.

(2) Sklarz, B.; Al-Sayyab, A. F. *J. Chem. Soc.* **1964**, 1318-1320.

(3) Kirby, G. W.; Sweeny, J. G. *J. Chem. Soc., Perkin Trans. 1* **1981**, 3250- 3254.

(4) Kirby, G. W. Chem. Soc. Rev. **1977**, *6*, 1-24.

(5) Kirby, G. W.; Sweeny, J. G. *J. Chem. Soc., Chem. Commun.* **1973**, 704- 705.

(6) Corrie, J. E. T.; Kirby, G. W.; Mackinnon, J. W. M. *J. Chem. Soc., Perkin Trans.1* **1985**, 883-886.

(7) Keck, G. E.; Webb, R. R. *J. Am. Chem. Soc.* **1981**, *103*, 3173-3177.

(8) Keck, G. E.; Webb, R. R. *J. Org. Chem.* **1982**, *47*, 1302.1309.

(9) Matsumura, Y.; Aoyagi, S.; Kibayashi, C. *Org. Lett.* **2003**, *5*, 3249-3252.

(10) Keck, G. E.; Webb, R. R.; Yates, J. B. *Tetrahedron* **1981**, *37*, 4007-4016.

(11) Kirby, G. W.; McGuigan, H.; McLean, D. *J. Chem. Soc., Perkin Trans. 1* **1985**, 1961-1966.

(12) Teo, Y. C.; Pan, Y.; Tan, C. H. *ChemCatChem* **2013**, *5*, 235-240.

(13) Frazier, C. P.; Engelking, J. R.; Read de Alaniz, J. *J. Am. Chem. Soc.* **2011**, *133*, 10430–10433.

(14) Fakhruddin, A.; Iwasa, S.; Nishiyama, H.; Tsutsumi, K. *Tetrahedron Lett.* **2004**, *45*, 9323–9326.

(15) Yamamoto, Y.; Yamamoto, H. *Eur. J. Org. Chem.* **2006**, *2006*, 2031–2043.

(16) Chaiyaveij, D.; Cleary, L.; Batsanov, A. S.; Marder, T. B.; Shea, K. J.; Whiting, A. *Org. Lett.* **2011**, *13*, 3442–3445.

(17) Sandoval, D.; Frazier, C. P.; Bugarin, A.; Read de Alaniz, J. *J. Am. Chem. Soc.*

2012, *134*, 18948–18951.

(18) Baidya, M.; Griffin, K. A.; Yamamoto, H. *J. Am. Chem. Soc.* **2012**, *134*, 18566–18569.

(19) Selig, P. *Angew. Chemie Int. Ed.* **2013**, *52*, 7080–7082.

(20) Palmer, L.; Frazier, C. P.; Read de Alaniz, J. *Synthesis.* **2013**, *46*, 269–280.

(21) Baidya, M.; Yamamoto, H. *Synthesis.* **2013**, *45*, 1931–1938.

(22) Frazier, C. P.; Sandoval, D.; Palmer, L. I.; Read de Alaniz, J. *Chem. Sci.* **2013**, *4*, 3857–3862.

(23) Yang, W.; Huang, L.; Yu, Y.; Pflasterer, D.; Rominger, F.; Hashmi, A. S. K. *Chem. Eur. J.* **2014**, *20*, 3927–3931.

(24) Yu, C.; Song, A.; Zhang, F. Wang, W. *ChemCatChem.* **2014**, *6*, 1863–1865.

(25) Sandoval, D.; Samoshin, A. V; Read de Alaniz, J. *Org. Lett.* **2015**, *17*, 4514–4517.

(26) Ramakrishna, I.; Grandhi, G. S.; Sahoo, H.; Baidya, M. *Chem. Commun.* **2015**, *51*, 13976–13979.

(27) Maji, B.; Yamamoto, H. *Angew. Chem.* **2014**, *126*, 14700–14703.

(28) Maji, B.; Yamamoto, H. *Bull. Chem. Soc. Jpn.* **2015**, *88*, 753–762.

(29) Xu, C.; Zhang, L.; Luo, S. *Angew. Chem. Int. Ed.* **2014**, *53*, 4149–4153.

(30) Merino, P.; Tejero, T.; Delso, I.; Matute, R. *Synthesis* **2016**, *48*, 653–676.

(31) Atkinson, R. N.; Storey, B. M.; King, S. B. *Tetrahedron Lett.* **1996**, *37*, 9287–9290.

(32) Paz, J.; Perez-Balado, C.; Iglesias, B.; Munoz, L. *Org, Lett.* **2011**, *13*, 1800–1803.

(33) Nourian, S.; Zilber, Z. A.; Toscano, J. P. *J. Org. Chem.* **2016**, *81*, 9138–9146.

(34) Nourian, S.; Lesko, R. P.; Guthrie, D. A.; Toscano, J. P. *Tetrahedron* **2016**, *72*, 6037–6042.

(35) Cohen, Andrew D. The Time-resolved Infrared Spectroscopic Study of an Iminooxirane, a Nitronic Anhydride, and Acylnitroso Species: The Development of Novel *N*-Hydroxysulfonamides as Physiological Nitroxyl Donors. The Johns Hopkins University, ProQuest Dissertations, Publishing 2007. 3240690.

(36) O'Bannon, P. E.; Suelzle, D.; Schwarz, H. *HelV. Chim. Acta* **1991**, *74*, 2068–2072.

(37) O'Bannon, P. E.; Suelzle, D.; Dailey, W. P.; Schwarz, H. *J. Am. Chem. Soc.* **1992**, *114*, 344–345.

(38) Cohen, A. D.; Zeng, B-B; King, S. B.; Toscano, J. P. *J. Am. Chem. Soc.* **2003**, *125*, 1444–1445.

(39) Quadrelli, P.; Mella, M.; Caramella, P. *Tetrahedron Lett.* **1999**, *40*, 797–800.

(40) Quadrelli, P.; Campari, G.; Mella, M.; Caramella, P. *Tetrahedron Lett.* **2000**, *41*, 2019–2022.

(41) Memeo, M. G.; Quadrelli, P. *Chem. Rev.* **2017**, *117*, 2108–2200.

(42) Scagnelli, L.; Memeo, M. G.; Carosso, S.; Bovio, B.; Quadrelli, P. *Eur. J. Org. Chem.* **2013**, *2013*, 3835–3846.

(43) Evans, A. S.; Cohen, A. D.; Gurard-Levin, Z. A.; Kebede, N.; Celius, T. C.; Miceli, A. P.; Toscano, J. P. *Can. J. Chem.* **2011**, *89*, 130–138.

(44) Guthrie, D. A.; Ho, A.; Takahashi, C. G.; Collins, A.; Morris, M.; Toscano, J. P. *J. Org. Chem.* **2015**, *80*, 1338–1348.

(45) Xu, Y.; Alavanja, M-M; Johnson, V. L.; Yasaki, G.; King, S. B. *Tetrahedron Lett.*

2000, *41*, 4265–4269.

(46) Zeng, B-B, Huang, J.; Wright, M. W.; King, S. B. *Biorg. Med. Chem. Lett.* **2004**, *14*, 5565–5568.

(47) Iwata, K.; Hamaguchi, H.-O. Construction of a Versatile Microsecond Time-Resolved Infrared Spectrometer. *Appl. Spectrosc.* **1990**, *44*, 1431–1437.

(48) Yuzawa, T.; Kato, C.; George, M. W.; Hamaguchi, H. Nanosecond Time-Resolved Infrared Spectroscopy with a Dispersive Scanning Spectrometer. *Appl. Spectrosc.* **1994**, *48*, 684–690.

(49) Wang, Y. H.; Yuzawa, T.; Hamaguchi, H. O.; Toscano, J. P. Time-Resolved IR Studies of 2-Naphthyl(carbomethoxy)carbene: Reactivity and Direct Experimental Estimate of the Singlet/triplet Energy Gap. *J. Am. Chem. Soc.* **1999**, *121*, 2875–2882.

Chapter 5.
Miscellaneous

5.1. Phosphine Reactivity with Nitrosocarbonyl Compounds

5.1.1. Reaction of HNO with Phosphines

HNO represents the smallest nitroso compound. It is a very reactive molecule and dimerizes ($k = 8 \times 10^6$ $M^{-1}s^{-1}$) to hyponitrous acid (HON=NOH), which subsequently dehydrates to produce nitrous oxide (N_2O).[1] Detection of N_2O has been used as a benchmark of HNO formation. HNO reacts with thiols to yield either disulfides or sulfinamides,[2,3] and the biological effects of HNO are mostly attributed to its unique reactivity with protein thiols.[4] Also, metalloproteins redox reactions with HNO is a known trapping pathway, for example, the reaction of HNO with metmyoglobin occurs through reductive nitrosylation reaction to produce NO-myoglobin.[5]

Phosphines, as soft nucleophiles, react with HNO to form chemically distinct products. Preliminary experiments by King and co-workers confirmed formation of triphenylphosphine oxide and aza-ylide after treatment of triphenylphosphine with Angeli's salt in organic/aqueous solutions.[6] The aza-ylide may undergo hydrolysis to yield triphenylphosphine oxide over longer periods of time. (4,6-Dimethyl-3-sulfonatephenyl)phosphine trisodium salt hydrate (TXPTS) is a water soluble phosphine, and was employed to study the HNO reactivity with phophines in aqueous solutions (Scheme 5.1). Applying mass spectrometry and ^{31}P NMR, King and co-workers reported the formation of aza-ylide and phosphine oxide, as the only detectable products. Additionally, the stability of TXPTS-derived aza-ylide was confirmed using ^{31}P NMR. The addition of TXPTS to Angeli's salt was found to quench N_2O formation up to 90%, which also suggested efficient trapping of HNO, andthe potential application of TXPTS as an indicator for HNO detection. To rule out the general TXPTS trapping ability of HNO, different HNO precursors were treated with TXPTS. Upon treatment of ^{15}N labeled para-bromo Piloty's acid, a known HNO precursor, with TXPTS, the formation of aza-ylide was observed by ^{15}N NMR spectroscopy. Also, the formation of aza-ylide was also observed following incubation of horseradish peroxidase (HRP) with hydrogen peroxide in presence of hydroxylamine and addition of TXPTS.[7,8]

Scheme 5-1. Reaction of HNO with TXPTS.

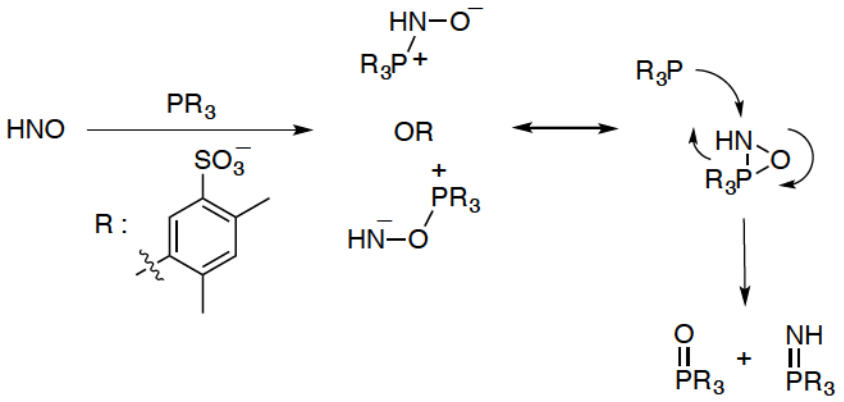

The mechanism for the generation of aza-ylide and phosphine oxide is proposed to occur through formation of a hetero three-membered ring intermediate.[6] Upon reaction of phosphines with either the nitrogen or oxygen atom of HNO, it is expected that zwitterions with structures indicated in Scheme 5-1 are formed. These species are in resonance with a hetero three-membered ring intermediate, which upon addition of a second phosphine, will form equimolar amounts of phosphine oxide and aza-ylide. Based on ^{31}P NMR competition experiments with GSH, King and co-workers reported the reaction of TXPTS with HNO to be a second order reaction with a rate constant of 9×10^5 M^{-1} s^{-1}.[7] Also, Toscano et al. reported an efficient ^{1}H NMR assay to monitor HNO trapping by TXPTS, which was based on distinctive chemical shifts of TXPTS, aza-ylide and phosphine oxide.[9] Thus, formation of aza-ylide can be used as a selective marker for HNO detection in different reactions.

5.1.2. Reaction of *C*-Nitroso Compounds with Phosphines

C-nitroso compounds are known to react with phosphines in organic solvents to release phosphine oxides and different nitrogenous products.[10,11] Cadogen reported formation of azoxybenzene and triphenylphosphine oxide, upon treatment of nitrosobenezene with triphenyl phosphine in benzene.[12] The mechanism was complicated and suggested to involve nitrene intermediates. Kirby and co-workers for the first time studied the reaction of nitrosocarbonyls with phosphines.[13] 9,10-Dimethyl anthracene adducts were used as source of nitrosocarbonyl intermediates, and were treated with triphenyl phosphine in organic solvents at high temperature. After complete decomposition of the nitrosocarbaonyl precursor, 9,10-dimethyl anthracene, triphenyl phosphine oxide, and phenyl isocyanate were observed as the products. The generation of isocyanate was proposed to be through the pathway indicated in Scheme 5-2, and its formation was confirmed by its reaction with aniline. Also, in presence of excess triphenyl phosphine, isolation of $RCON{=}PPh_3$ suggested the intermediacy of nitrenes.

Kirby and co-workers also studied the reaction of nitrosoformates with phosphines,[14] which in contrast to acylnitroso intermediates, do not produce isocyanate. Due to low migratory tendency of alkoxy groups, it was suggested that alkoxycarbonylnitrenes were formed upon deoxygenation of intermediate **2**, as indicated in Scheme 5-2.

Scheme 5-2. Reaction of Nitrosocarbonyl Compounds with Phosphines

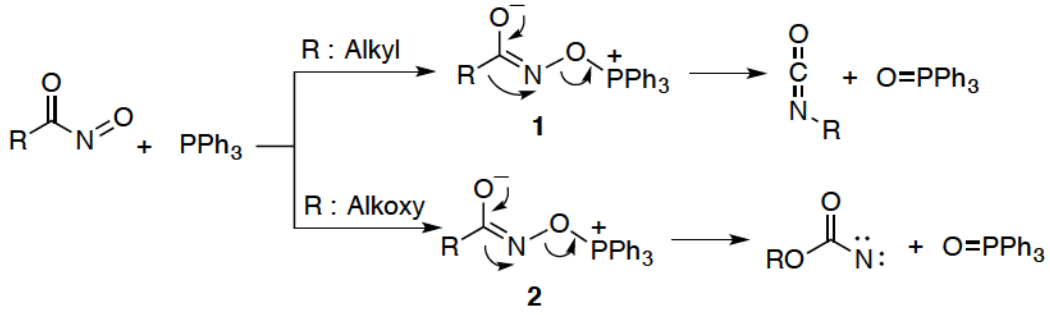

5.1.3. Reaction of Nitrosocarbonyl Compounds with Phosphines under Physiological Conditions

Phosphines are known to be efficient traps for HNO under physiological conditions and have been used as selective tools for HNO detection.[9] As discussed in section 5.1.2, the mechanism of nitrosocarbonyl reaction with phosphines in presence of organic solvents is complicated, and more investigations are required to confirm the formation of nitrenes and other intermediates. By studying the reactivity of nitrosocarbonyls with phosphines under physiologically relevant conditions, we hoped to employ phosphines for nitrosocarbonyl detection. Also, we tried to clarify the reaction mechanism and characterize the products.

As discussed in Chapter 3, **OHPY-1a** is an efficient nitrosocarbonyl precursor under physiological conditions. Upon generation of the nitrosocarbonyl intermediate, there is a competition between hydrolysis (HNO generation) and a nitrosocarbonyl aldol reaction to produce **NHPY-1a** (Scheme 5-3). For example after complete decomposition of 0.5 mM of **OHPY-1a**, the yields of final products are 74% **PY-1**, 26% **NHPY-1a**, and 73% acetate. Based on our discussions in Chapter 3,

higher concentrations of pyrazolone byproducts following decomposition of higher concentrations of **OHPY** donors will favor **NHPY** formation.

Scheme 5-3. Decomposition of OHPY-1a with/without the Presence of TXPTS

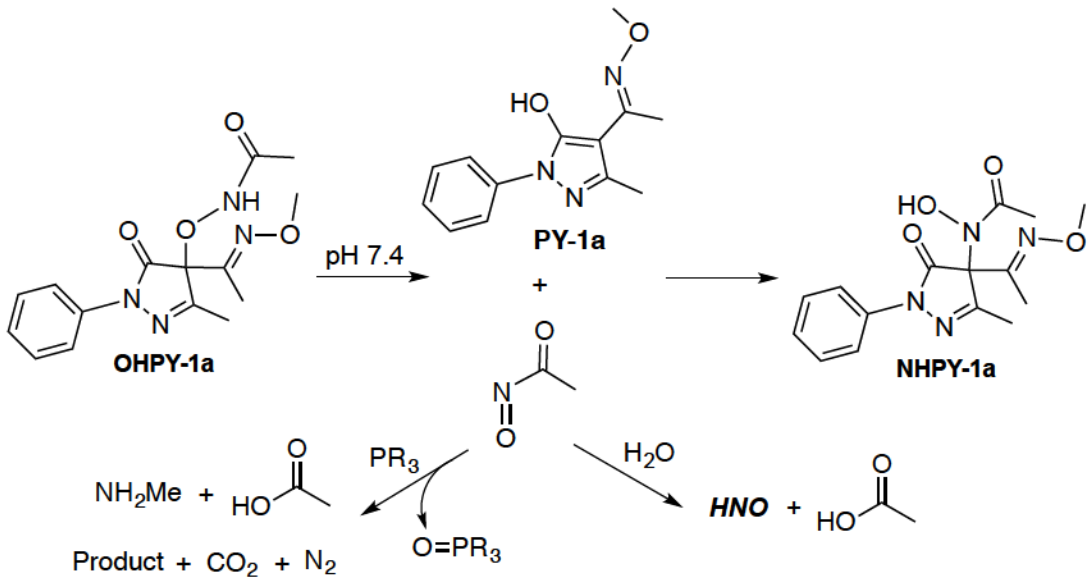

To study the reaction of phosphines with nitrosocarbonyls, we incubated 1 mM **OHPY-1a** with 5 mM TXPTS at pH 7.4 and 37 °C. Upon completion of the reaction, no formation of N_2O was observed by GC headspace analysis. However, TXPTS can react with HNO directly, so from this experiment it was not possible to conclude that the nitrosocarbonyl reacted with TXPTS. Additionally, no formation of **NHPY-1a** was observed by ^{1}H NMR spectroscopy after complete decomposition of the donor, which strongly suggests the trapping of nitrosocarbonyl intermediate by TXPTS (Figure 5-1).

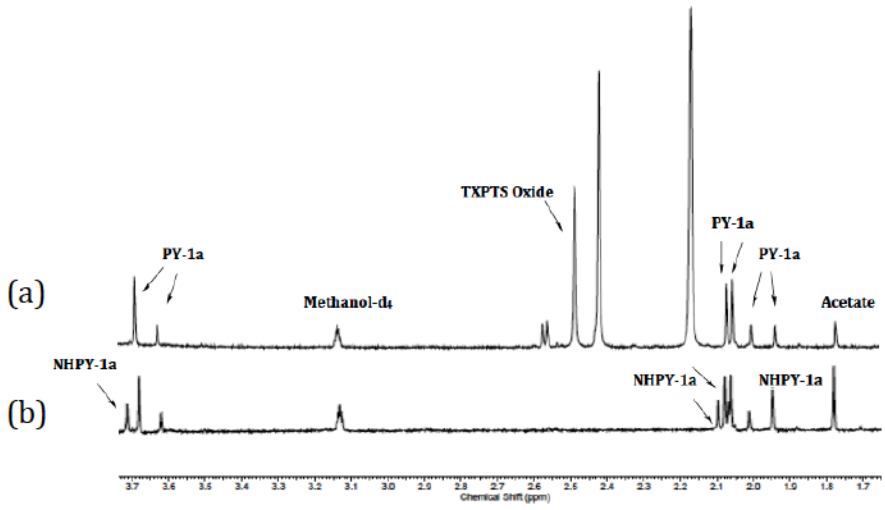

Figure 5-1. Representative ^{1}H NMR spectra after complete decomposition of **OHPY-1a** (a) with (b) without the presence of TXPTS under argon at pH 7.4 and 37 °C.

Based on ^{15}P NMR spectroscopy experiments, TXPTS and TXPTS oxide were found to be the only phosphorous containing compound in the reaction mixture. Formation of equimolar amounts of **PY-1a** and phosphine oxide along with 30% acetate was confirmed after complete decomposition of **OHPY-1a** by ^{1}H NMR spectroscopy (Figure 5-1). The formation of acetate is presumably the result of initial formation of an azoxy compound (as is reported previously in literature for reaction of nitrosobenzene and phosphines), followed by an acyl migration and hydrolysis (Scheme 5-4). Also, growth of two peaks with chemical shifts at 2.58 and 2.57 ppm were observed (Figure 5-1), which corresponds to generation of 30% and 40% of products. We propose that the peak with the chemical shift of 2.57 ppm may correspond to methylamine, which forms through the mechanism indicated in Scheme 5-4. Initial nucleophilic attack of phosphine on oxygen atom of the nitrosocarbonyl is consistent with previously reported nitrosobenzene reactions

with phosphines. Upon methyl migration, the isocyanate formed may undergo hydrolysis to release methylamine and carbon dioxide. The identity of the peak at 2.58 ppm is still under investigation.

Scheme 5-4. Proposed Mechanism for Nitrosocarbonyl Reaction with TXPTS Under Physiological Conditions

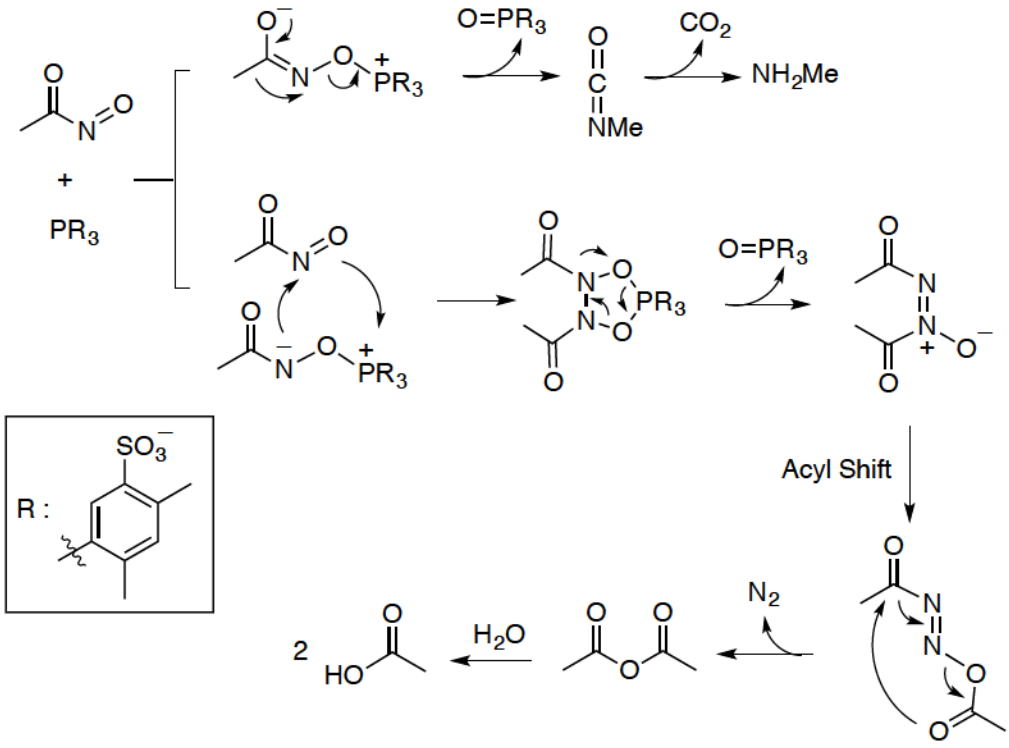

In general, the reaction of phosphines with nitrosocarbonyls is complicated, and this reactivity is expected to be dependent on the structure of nitrosocarbonyl intermediate.

5.2. Synthesis of *N*-Substituted Hydroxamic Acids with Barbituric Acids Leaving Groups.

Recently, Toscano et al. introduced a series of *N*-substituted hydroxylamines with barbituric acid leaving groups (**HABA**) with various half-lives and excellent HNO yields. The synthesis of **HABA** derivatives is based on the HNO aldol reaction using Angeli's salt in presence of barbituric acids. This methodology is very efficient, but requires an HNO precursor to generate HNO, which is further trapped by barbituric acid derivatives to form the final HABA compounds. The product yield is mainly dependent on the structure of barbituric acid byproducts. For example, barbituric acids substituted with bulky groups significantly decrease the product yield. In Chapter 2, the single pot nitrosocarbonyl aldol reaction was introduced for the synthesis of different NHPY compounds. This procedure is straightforward, scalable, and generates products in moderate to high yields (47-75%). This synthetic methodology may also be efficient for the generation of different carbon-based hydroxamic acid derivatives.

We tried to expand nitrosocarbonyl aldol reaction for the synthesis of *N*-substituted hydroxamic acids with barbituric acids leaving groups (**NHBA**). The synthesis was initiated with the oxidation of *t*-butyl-*N*-hydroxycarbamate to generate a nitrosocarbonyl intermediate, which was trapped by barbituric acid derivatives to form NHBA compounds. We could also subsequently generate **HABA** compounds by acid deprotection of the BOC groups.

Scheme 5-5. Nitrosocarbonyl Aldol Reaction of Barbituric Acids

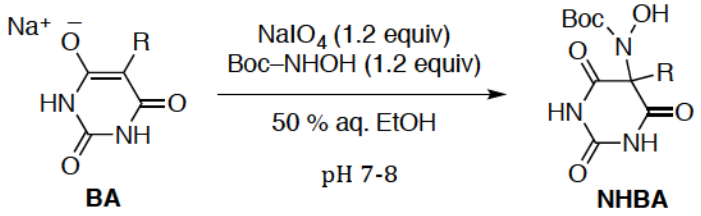

5.3. Experimental

5.3.1. Method and Materials

All starting materials were of reagent grade and used without further purification. Barbituric acid derivatives (BA) were synthesized following previously reported procedures.[15] NMR spectra were obtained on either a 300 or 400 MHz FT-NMR spectrometer. All chemical shifts are reported in parts per million (ppm) relative to residual DMSO (2.5 ppm for ^{1}H, 39.5 for ^{13}C) and methanol (3.31 ppm for ^{1}H).

5.3.2. ^{1}H NMR Procedure of OHPY-1a with TXPTS

The ^{1}H NMR procedure was based on previously reported protocol.[9] To a solution of 0.25 M phosphate buffer solution containing 10% D_2O and 90% H_2O (1 mL) at pH 7.4 under argon with and without the presence of TXPTS (3.3 mg, 5 mM) was added **OHPY-1a** (10 µL of 100 mM in methanol-d_4). The solution was incubated at 37 °C and an ^{1}H NMR spectrum using a 400 MHz FT-NMR spectrometer was collected after complete decomposition of **OHPY-1a**.

5.3.3. Synthesis and Characterization of NHBA and HABA Compounds

Barbituric acid (BA) derivative (0.5 mmol) was added to a solution of *t*-butyl-*N*-hydroxycarbamate (0.6 mmol) in 50% aqueous ethanol (2.5 mL). The pH of the solution was adjusted to 7-8 using 0.2 equiv of potassium carbonate. Sodium periodate (0.6 mmol) was added to the solution and the reaction mixture was sonicated for 10 min and stirred at room temperature for one hour. The reaction mixture was diluted with 25 mL of ethanol and filtered. The filtrate was concentrated *in vacuo*, and redissolved in ethyl acetate (5 mL). The mixture was washed three times with 20 mL of saturated ammonium chloride, water, and brine. The organic solution was collected, dried over magnesium sulfate, and concentrated *in vacuo*. Crystallization from ether and petroleum ether gave the desired NHBA compound as a white solid.

To a solution of **NHBA** (0.25 mmol) in ethanol (10 mL) was added HCl (2 mL) and stirred overnight. The solution was diluted with ethanol (10 mL), and concentrated *in vacuo*. Crystallization from ether and petroleum ether gave the desired **HABA** compound as a white solid.

tert-Butyl-(5-ethyl-2,4,6-trioxohexahydropyrimidin-5-yl)(hydroxy)carbamate (**NHBA-1**): White solid, yield 93 mg (65%) , m.p. 167-169 °C. ^{1}H NMR (300 MHz, DMSO) δ: 11.53 (s, 2H), 9.78 (s, 1H), 2.06 (q, 2H), 1.35 (s, 9H), 0.94 (t, 3H).

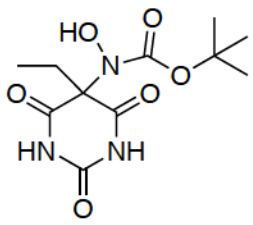

tert-Butyl-hydroxy(5-methyl-2,4,6-trioxohexahydropyrimidin-5-yl)carbamate (**NHBA-2**):): White solid, yield 94 mg (69%), m.p. 187-189 °C. ^{1}H NMR (300 MHz, DMSO) δ: 11.46 (s, 2H), 9.81 (s, 1H), 1.60 (s, 3H), 1.33 (s, 9H). NMR (100 MHz, DMSO-d_6) δ: 171.45, 150.03, 81.82, 66.52, 28.20, 21.89. . HR-MS: found *m/z* = 296.08560 (MNa^+); calc. for $C_{10}H_{15}N_3O_6Na^+$: 296.08531.

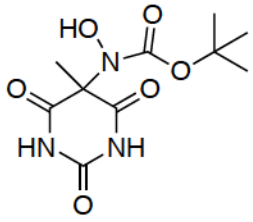

tert-Butyl-hydroxy(5-isopropyl-2,4,6-trioxohexahydropyrimidin-5-yl)carbamate (**NHBA-3**): White solid, yield 96 mg (64%), m.p. 177-180 °C. ^{1}H NMR (300 MHz, DMSO) δ: 11.44 (s, 2H), 9.65 (s, 1H), 2.51 (m, 1H), 1.32 (s, 9H), 0.96 (d, 6H). ^{13}C NMR (100 MHz, DMSO-d_6) δ: 169.85, 150.45, 82.06, 72.88, 33.53, 28.25, 18.28. HR-MS: found *m/z* = 324.116963 (MNa^+); calc. for $C_{12}H_{19}N_3O_6Na^+$: 324.11661.

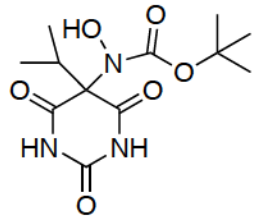

tert-Butyl-hydroxy(2,4,6-trioxo-5-(pentan-2-yl)hexahydropyrimidin-5-yl)carbamate (**NHBA-4**): White solid, yield 118 mg (72%), m.p. 158-161 °C. ^{1}H NMR (300 MHz, DMSO) δ: 11.48 (s, 2H), 9.63 (s, 1H), 2.32 (m, 1H), 1.67 (m, 1H), 1.31 (s, 9H), 1.11 (m, 2H) ,1.07 (m, 1H), 0.94 (d, 3H), 0.83 (t, 3H). ^{13}C NMR (100 MHz, DMSO-d_6) δ: 170.43, 150.81, 82.15, 73.08, 38.26, 33.60, 28.20, 21.09, 14.82, 14.28. HR-MS: found *m/z* = 352.14822 (MNa^+); calc. for $C_{14}H_{23}N_3O_6Na^+$: 352.14791.

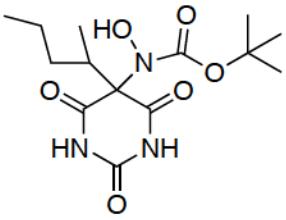

tert-Butyl-hydroxy(5-isobutyl-2,4,6-trioxohexahydropyrimidin-5-yl)carbamate (**NHBA-5**): White solid, yield 118 mg (75%), m.p. 189-192 °C. ^{1}H NMR (300 MHz, DMSO) δ: 11.56 (s, 2H), 9.8 (s, 1H), 1.99 (m, 2H), 1.71 (m, 1H), 1.37 (s, 9H), 0.82 (d, 6H). ^{13}C NMR (100 MHz, DMSO-d_6) δ: 170.93, 150.18, 81.92, 69.16, 44.21, 28.24, 24.34, 23.43. HR-MS: found *m/z* = 338.13232 (MNa^+); calc. for $C_{13}H_{21}N_3O_6Na^+$: 338.13232.

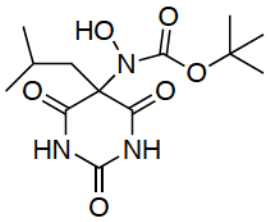

tert-Butyl-(5-(*sec*-butyl)-2,4,6-trioxohexahydropyrimidin-5-yl)(hydroxy)carbamate (**NHBA-6**): White solid, yield 123 mg (78%), m.p. 178-181 °C. ^{1}H NMR (300 MHz, DMSO) δ: 11.51 (s, 2H), 9.67 (s, 1H), 2.26 (m, 1H), 1.77 (m, 1H), 1.33 (s, 9H), 0.96 (d, 3H), 0.85 (d, 3H). ^{13}C NMR (100 MHz, DMSO-d_6) δ: 169.61, 150.42, 82.08, 73.01, 28.21, 27.80, 24.57, 14.27, 12.58. HR-MS: found *m/z* = 338.13255 (MNa^+); calc. for $C_{13}H_{21}N_3O_6Na^+$: 338.13255.

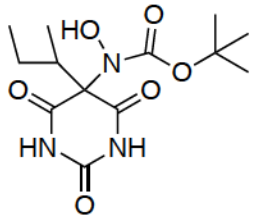

tert-Butyl-(5-allyl-2,4,6-trioxohexahydropyrimidin-5-yl)(hydroxy)carbamate (**NHBA-7**): White solid, yield 108 mg (72%), m.p. 163-165 °C. ^{1}H NMR (300 MHz, DMSO) δ: 11.51 (s, 2H), 9.92 (s, 1H), 5.65 (m, 1H), 5.20 (m, 2H), 2.77 (m, 2H), 1.34 (s, 9H). ^{13}C NMR (100 MHz, DMSO-d_6) δ: 170.07, 150.10, 129.90, 121.79, 82.20, 69.44, 28.58, 28.27. HR-MS: found *m/z* = 322.10085 (MNa^+); calc. for $C_{12}H_{17}N_3O_6Na^+$: 322.10085.

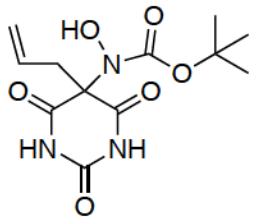

tert-Butyl-hydroxy(2,4,6-trioxo-5-(thiophen-3-ylmethyl) hexahydropyrimidin-5-yl)carbamate (**NHBA-8**): White solid, yield 122 mg (69%), m.p. 175-178 °C. ^{1}H NMR (300 MHz, DMSO) δ: 11.35 (s, 2H), 10.12 (s, 1H), 7.45 (m, 1H), 7.01 (m, 1H), 6.81 (m, 1H), 3.38 (s, 2H), 1.35 (s, 9H). ^{13}C NMR (100 MHz, DMSO-d_6) δ: 170.62, 149.65, 132.97, 129.12, 127.66, 127.13, 82.40, 69.65, 35.93, 28.19. HR-MS: found *m/z* = 378.07320 (MNa^+); calc. for $C_{14}H_{17}N_3O_6SNa^+$: 378.073203.

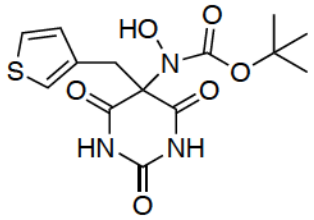

tert-Butyl-hydroxy(2,4,6-trioxo-5-phenylhexahydropyrimidin-5-yl)carbamate (**NHBA-9**): White solid, yield 119 mg (71%), m.p. 180-183 °C. ^{1}H NMR (300 MHz, DMSO) δ: 11.72 (s, 2H), 9.50, 1H), 7.45 (m, 5H), 1.37 (s, 9H). ^{13}C NMR (100 MHz, DMSO-d_6) δ:169.02, 149.84, 131.75, 129.94, 129.10, 128.87, 82.32, 74.68, 28.25. HR-MS: found *m/z* = 358.10136 (MNa^+); calc. for $C_{15}H_{17}N_3O_6Na^+$: 358.10096.

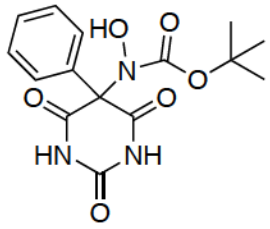

tert-Butyl(5-benzyl-2,4,6-trioxohexahydropyrimidin-5-yl)(hydroxy)carbamate (**NHBA-10**): White solid, yield 140 mg (80%), m.p. 181-183 °C. ^{1}H NMR (300 MHz, DMSO) δ: 11.26 (s, 2H), 10.07 (s, 1H), 7.29 (m, 3H), 7.06 (m, 2H), 3.37(s, 2H), 1.35 (s, 9H). ^{13}C NMR (100 MHz, DMSO-d_6) δ: 170.70, 149.43, 132.17, 130.36, 128.91, 128.36, 82.17, 70.20, 41.89, 28.21. HR-MS: found *m/z* = 372.11694 (MNa^+); calc. for $C_{16}H_{19}N_3O_6Na^+$: 372.11694.

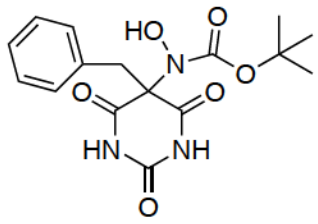

tert-butyl-(5-(2-chlorobenzyl)-2,4,6-trioxohexahydropyrimidin-5-yl)(hydroxy)carbamate (**NHBA-11**): White solid, yield 157 mg (82%), m.p. 190-193 °C. ^{1}H NMR (300 MHz, DMSO) δ: 11.29 (s, 2H), 10.09 (s, 1H), 7.45 (m, 1H), 7.32 (m, 2H), 7.16 (m, 1H), 3.52 (s, 2H), 1.41 (s, 9H). ^{13}C NMR (100 MHz, DMSO-d_6) δ: 170.48, 149.77, 135.01,133.25, 130.39, 120.29, 130.07, 127.75, 82.37, 70.04, 38.10, 28.26. HR-MS: found *m/z* = 406.07763 (MNa^+); calc. for $C_{16}H_{18}N_3O_6ClNa^+$: 406.07763.

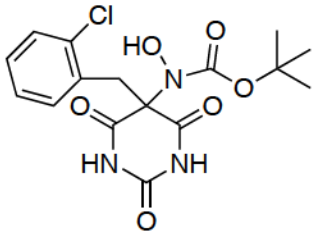

tert-Butyl-(5-(4-chlorobenzyl)-2,4,6-trioxohexahydropyrimidin-5-yl)(hydroxy)carbamate (**NHBA-12**): White solid, yield 134 mg (70%), m.p. °C. ^{1}H NMR (300 MHz, DMSO) δ: 11.3 (s, 2H), 10.08 (s, 1H), 7.37 (m, 2H), 7.03 (m, 2H), 3.28 (s, 2H), 1.34 (s, 9H). ^{13}C NMR (100 MHz, DMSO-d_6) δ: 170.38, 149.55, 133.17, 132.25, 131.34, 128.92, 82.36, 70.04, 41.06, 28.26. HR-MS: found *m/z* = 406.07763 (MNa^+); calc. for $C_{16}H_{18}N_3O_6ClNa^+$: 406.07763.

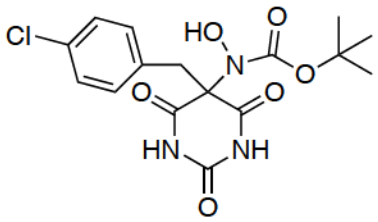

tert-Butyl-hydroxy(5-(4-methoxybenzyl)-2,4,6-trioxohexahydropyrimidin-5-yl)carbamate (**NHBA-13**): White solid, yield 148 mg (78%), m.p. 197-200 °C. ^{1}H NMR (300 MHz, DMSO) δ: 11.24 (s, 2H), 10.03 (s, 1H), 7.01 (m, 2H), 6.90 (m, 2H), 3.24 (s, 2H), 1.32 (s, 9H). ^{13}C NMR (100 MHz, DMSO-d_6) δ: 170.83, 159.27, 149.54, 131.48, 123.77, 114.32, 82.05, 70.18, 55.50, 41.20, 28.23. HR-MS: found *m/z* = 402.12738 (MNa^+); calc. for $C_{17}H_{21}N_3O_7Na^+$: 402.12717.

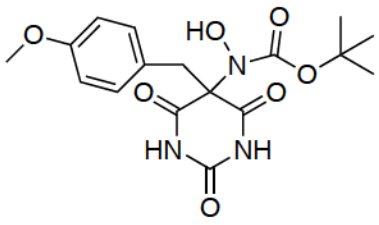

(5-(*N*-hydroxylamino)-5-phenylbarbituricacid (**HABA-1**): White solid, yield 47 mg (69%), m.p. 183-185 °C. ^{1}H NMR (400 MHz, DMSO) δ: 11.76 (s, 2H), 8.60 (br. s, 2H), 7.38 (m, 5H). ^{13}C NMR (100 MHz, DMSO-d_6) δ: 170.17, 149.62, 134.11, 129.34, 128.93, 126.53, 73.14.

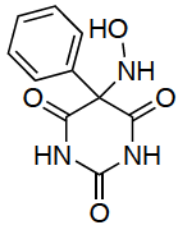

5-(*N*-Hydroxylamino)-5-(4-methoxybenzyl)-barbituric acid (**HABA-2**): White solid, yield 66 mg (95%). ^{1}H NMR (400 MHz, DMSO-d_6) δ: 11.35 (s, 2H), 6.92 (d, 2H), 6.82 (d, 2H), 3.70 (s, 3H), 2.92 (s, 2H). ^{13}C NMR (100 MHz, DMSO-d_6) δ: 171.41, 158.50, 149.36, 130.62, 124.53, 113.90, 71.69, 55.00, 38.45.

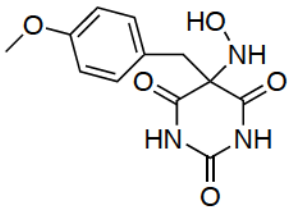

5-(*N*-hydroxylamino)-5-(2-thienylmethyl)-barbituric acid (**HABA-3**): White solid, yield 51 mg (70%), m.p. 175-178 °C. ^{1}H NMR (400 MHz, DMSO-d_6) δ: 11.45 (s, 2H), 8.13 (s, 1H), 7.39 (s, 1H), 6.94 (s, 1H), 6.73 (s, 1H), 6.53 (br. s, 1H), 3.21 (s, 2H). ^{13}C NMR (100 MHz, DMSO-d_6) δ: 171.59, 149.56, 134.24, 127.73, 127.12, 126.02, 71.08, 32.95.

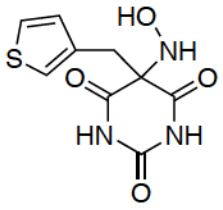

5.4. References

(1) Shafirovich, V.; Lymar, S. V. *Proc. Natl. Acad. Sci. U.S.A.* **2002**, *99*, 7340–7345.

(2) Doyle, M. P.; Mahapatro, S. N.; Broene, R. D.; Guy, J. K. *J. Am. Chem. Soc.* **1988**, *110*, 593–599.

(3) Wong, P. S. Y.; Hyun, J.; Fukuto, J. M.; Shirota, F. N.; DeMaster, E. G.; Shoeman, D. W.; Nagasawa, H. T. *Biochemistry* **1998**, *37*, 5362–5371.

(4) Tocchetti, C. G.; Stanley, B. A.; Murray, C. I.; Sivakumaran, V.; Donzelli, S.; Mancardi, D.; Pagliaro, P.; Gao, W. D.; van Eyk, J.; Kass, D. A.; Wink, D. A.; Paolocci, N. *Antioxid. Redox Sig.* **2011**, *14*, 1687–1698.

(5) Miranda, K. M. *Coord. Chem. Rev.* **2005**, *249*, 433–455.

(6) Reisz, J. A.; Klorig, E. B.; Wright, M. W.; King, S. B. *Org Lett.* **2009**, *11*, 2719–2721.

(7) Reisz, J. A.; Zink, C. N.; King, S. B. *J. Am. Chem. Soc.* **2011**, *133*, 11675–11685.

(8) Donzeli, S.; Espey, M. G.; Flores-Santana, W.; Switzer, C. H.; Yeh, G. C.; Huang, J. Stuehr, D. J., King, S. B.; Miranda, K. M.; Wink, D. A. *Free Rad Biol Med* **2008**, *45*, 578-584.

(9) Guthrie, D. A.; Ho, A.; Takahashi, C. G.; Collins, A.; Morris, M.; Toscano, J. P. *J. Org. Chem.* **2015**, *80*, 1338–1348.

(10) Cadogan, J. I. G. *Quart Rev.* **1968**, *22*, 222–251.

(11) Cadogan, J. I. G.; Mackie, R. K. *Chem. Roc. Rev.* **1974**, *3*, 87–137.

(12) Bunyan, J.; Cadogan, J. I. G. *J. Chem. Soc.* **1963**, 42–49.

(13) Corrie, J. E. T.; Kirby, G. W.; Sharma, R. P. *J. Chem. Soc. Perkin Trans. I.* **1982**, 1571–1574.

(14) Kirby, G. W.; McGuigan, H.; Mackinnon, J. W. M.; McLean, D.; Sharma, R. P. *J. Chem. Soc. Perkin Trans. I.* **1985**, 1437–1442.

(15) Dickey, J. B.; Gray, A. R. *Org. Synth.***1938**, *18*, 8.

5.5. ^{1}H NMR and ^{13}C NMR Spectra

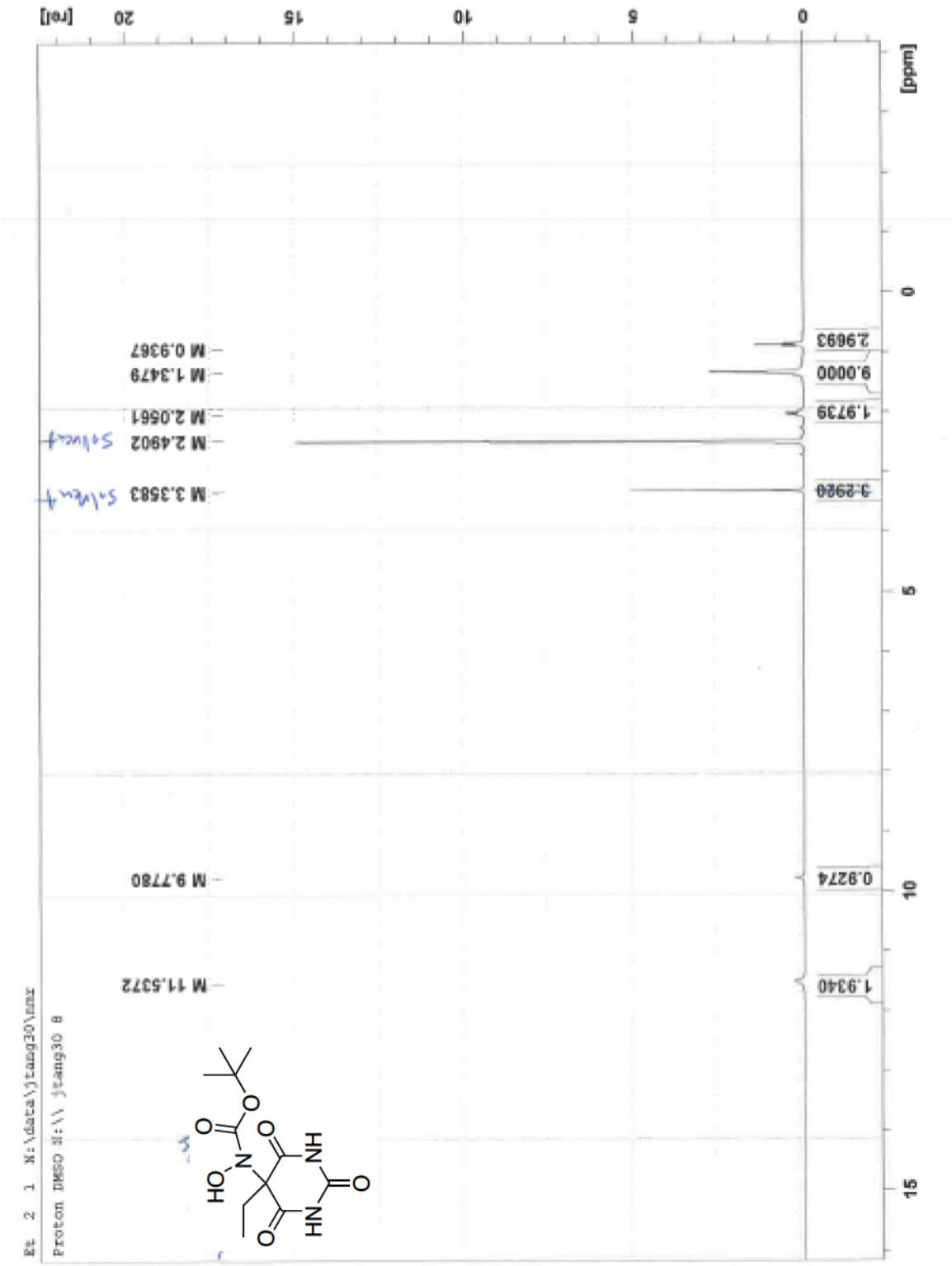

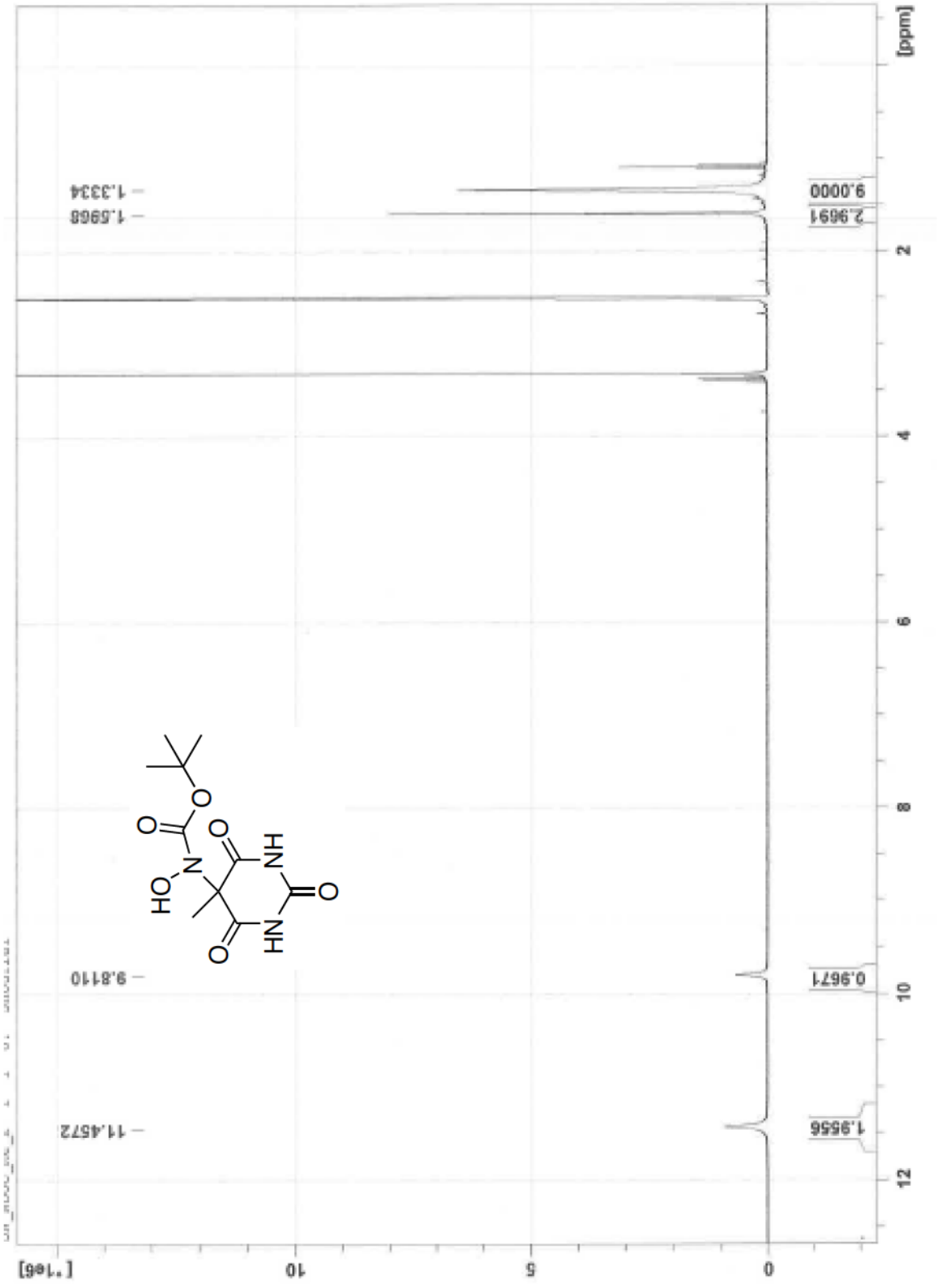
[ppm]
0
2
4
6
8
10
12
1.3334
1.5968
9.8110
11.4572
9.0000
2.9691
0.9671
1.9556
HO
N
O
O
O
NH
NH
O
O

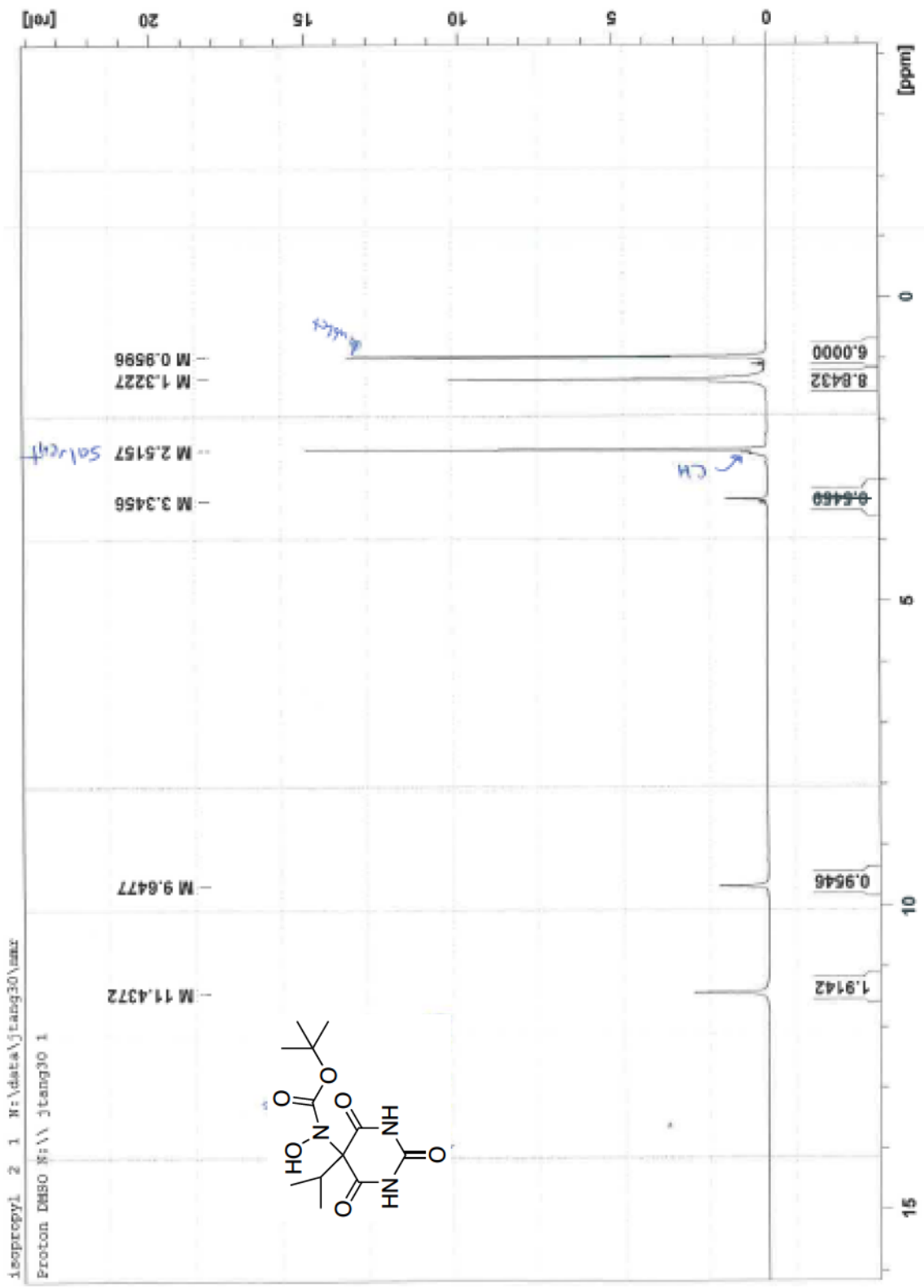
isopropyl 2 1 N:\data\jtang30\sar
Proton DMSO N:\\ jtang30 1
M 11.4372
M 9.6477
M 3.3456
M 2.5157
M 1.3227
M 0.9596
1.9142
0.9546
0.6469
8.8432
6.0000
[ppm]
[rel]
0
5
10
15
20
NH
HN
O
N
OH

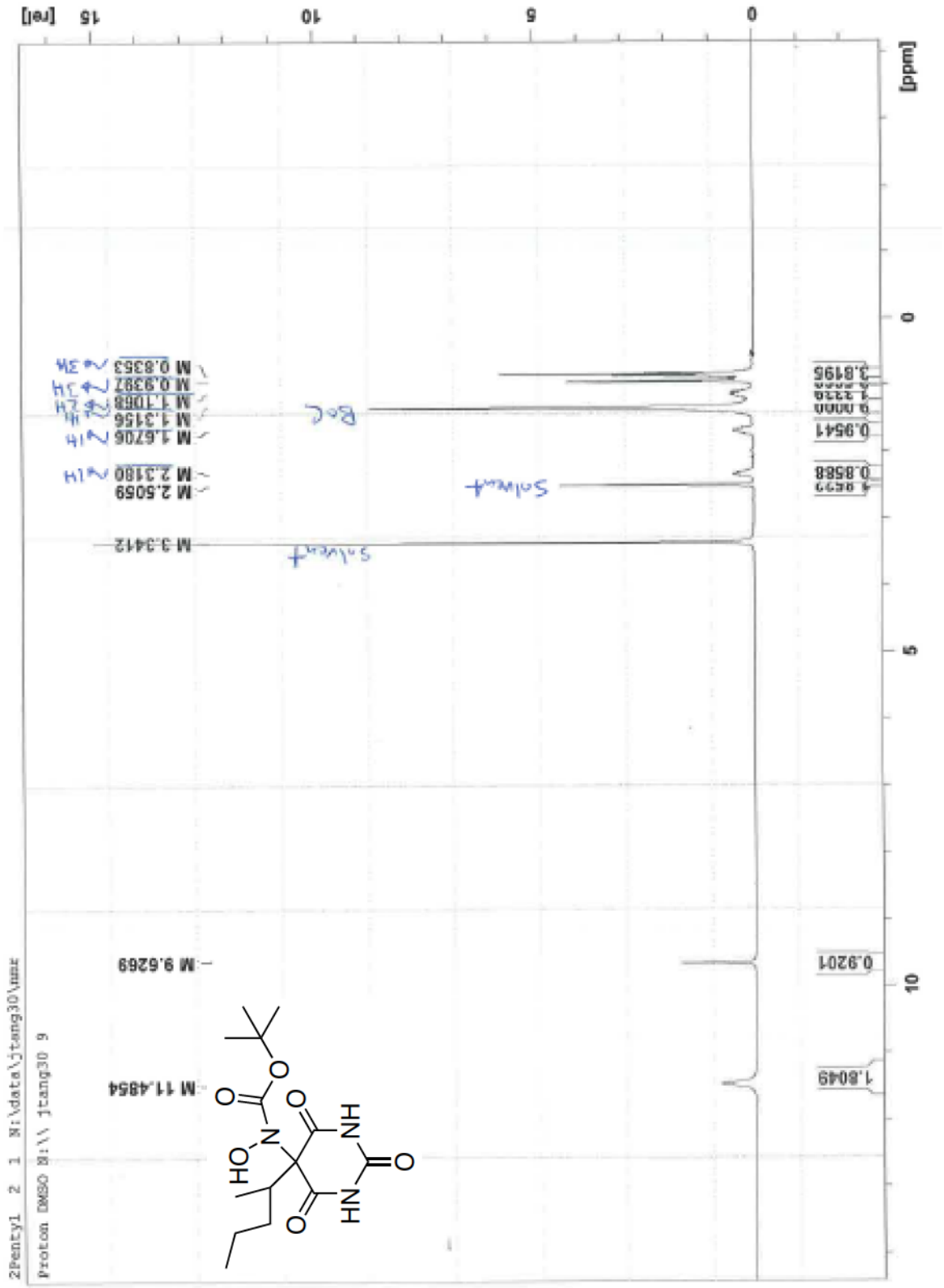
2Pentyl 2 1 N:\data\jtang30\nmr
Proton DMSO N:\\ jtang30 9
M 9.6269
M 11.4854
M 3.3412
M 2.5059
M 2.3180
M 1.6706
M 1.3156
M 1.1088
M 0.9382
M 0.8353
0.9201
1.8049
0.8588
0.9541
3.8195
Boc
Solvent
Solvent
[rel]
15
10
5
0
[ppm]
0
5
10

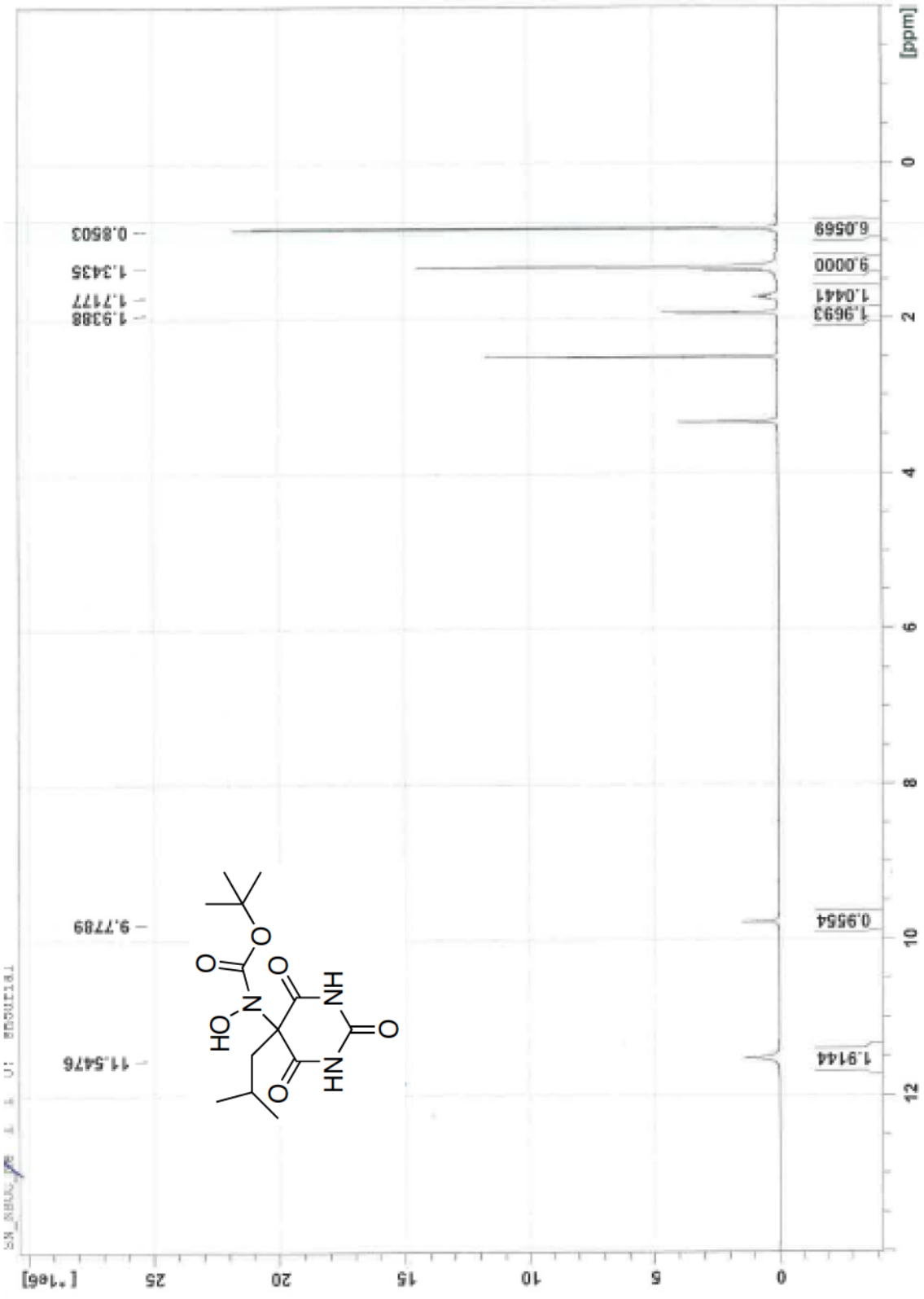
[ppm]
0
2
4
6
8
10
12
6.0569
9.0000
1.0441
1.9693
0.9554
1.9144
0.8503
1.3435
1.7177
1.9388
9.7789
11.5476
NH
NH
O
O
O
O
O
N
OH

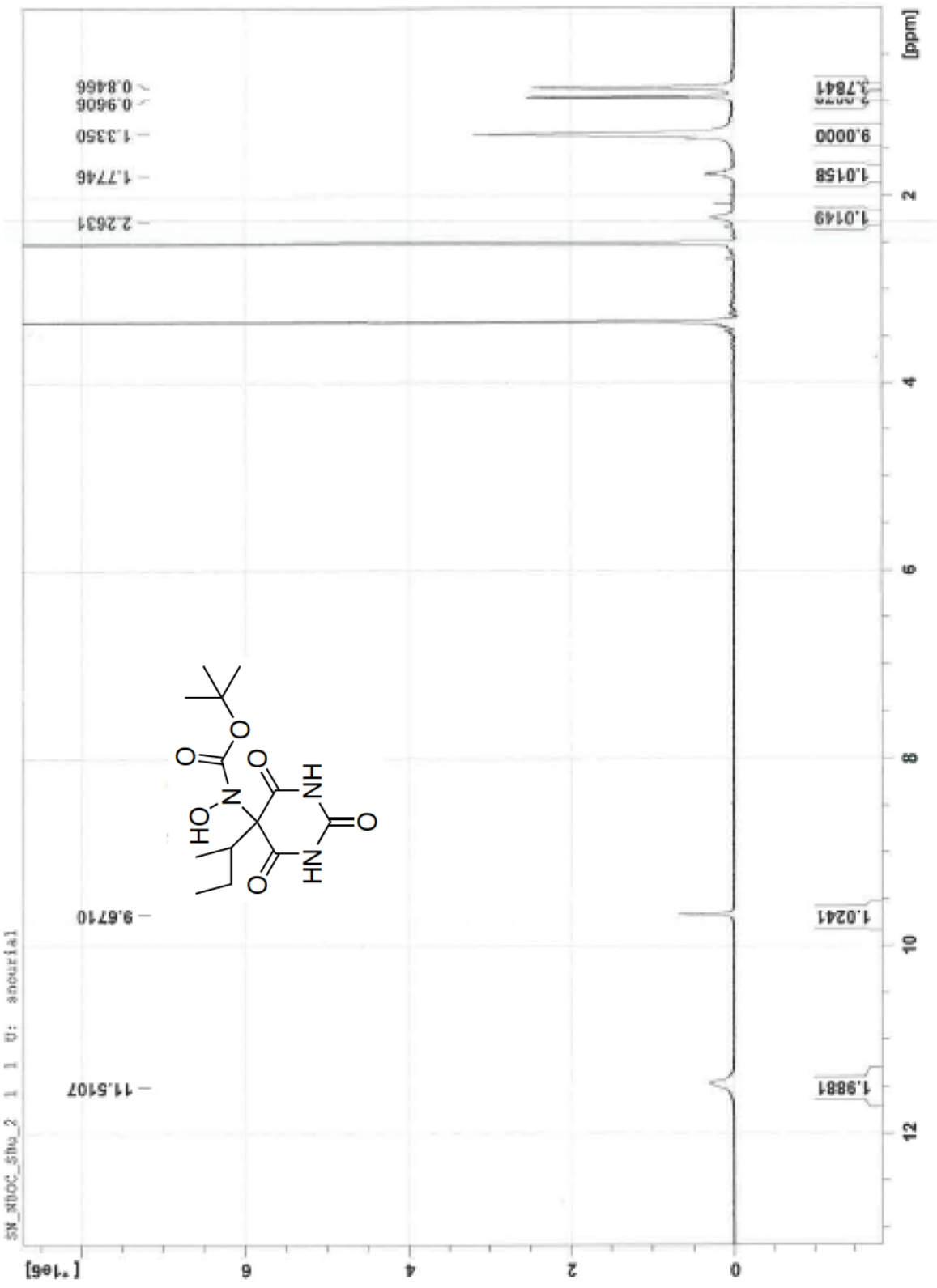
SN_NBOC_5thu_2 1 1 D: anouelal
[ppm]
0.8466
0.9606
1.3350
1.7746
2.2631
9.6710
11.5107
1.7841
9.0000
1.0158
1.0149
1.0241
1.9881
NH
NH
N
O
HO

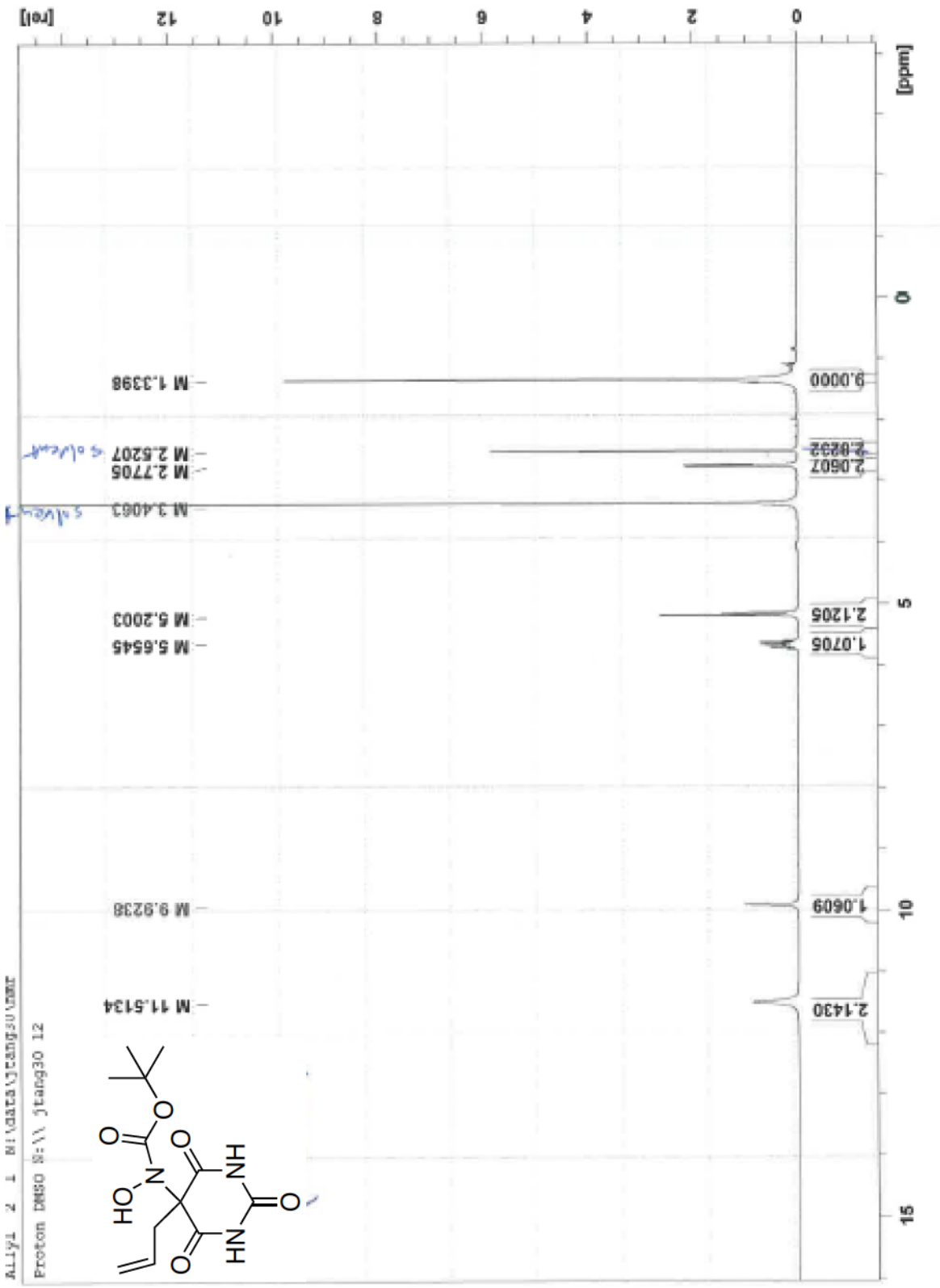
[ppm]
0
5
10
15
9.0000
2.0607
2.0232
2.1205
1.0705
1.0609
2.1430
M 1.3398
M 2.5207
M 2.7705
M 3.4063
M 5.2003
M 5.6545
M 9.9238
M 11.5134
Proton DMSO 8:\\ jtang30 12
ALIYL 2 1 N:\data\jtang30\1

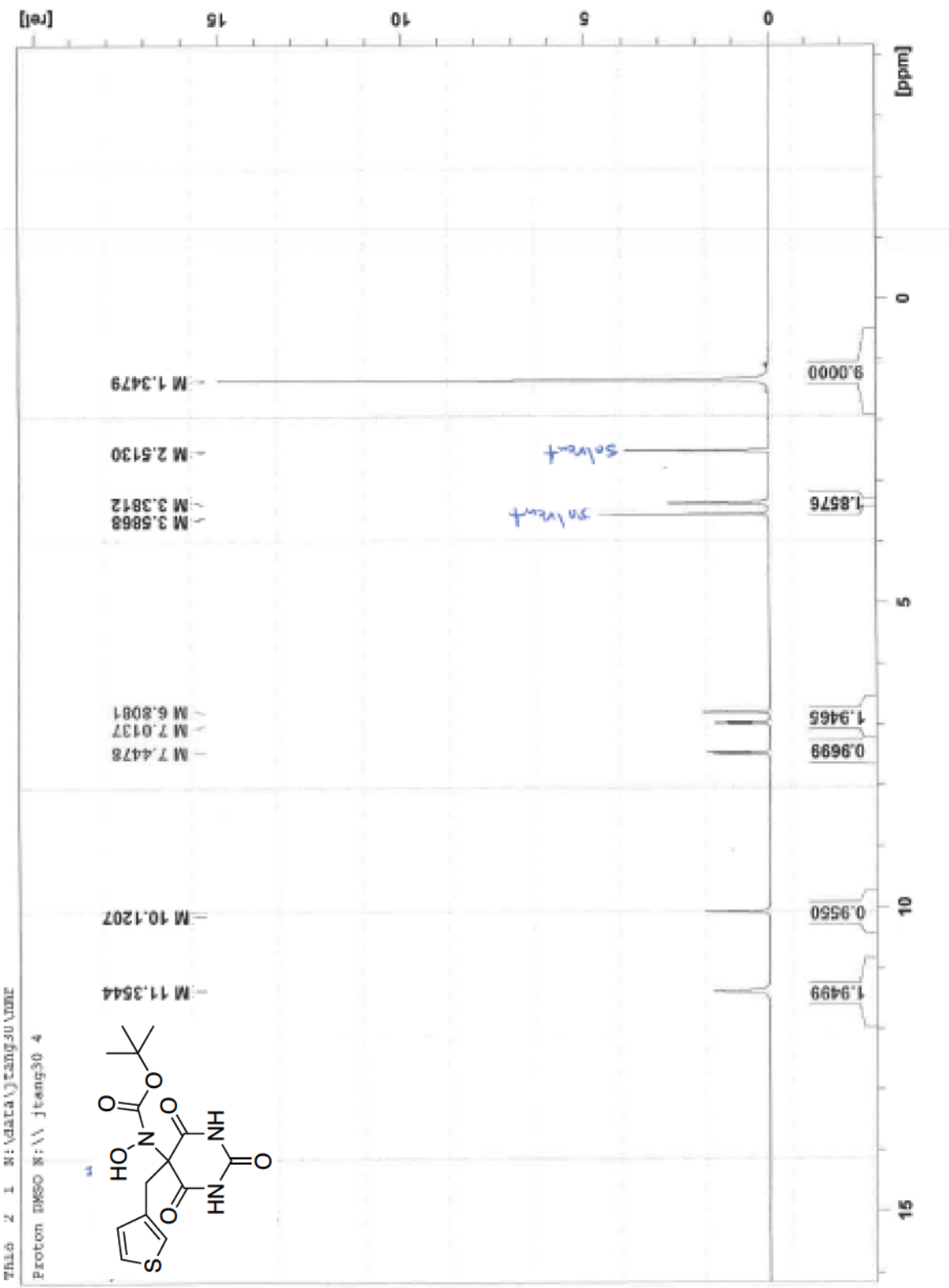
[rel]
15
10
5
0
[ppm]
M 1.3479
M 2.5130
M 3.3812
M 3.5868
M 6.8081
M 7.0137
M 7.4478
M 10.1207
M 11.3544
9.0000
1.8576
1.9465
0.9699
0.9550
1.9499
Proton DMSO N:\\ jtang30 4
THIS 2 1 N:\data\jtang30\1ne
O
O
N
HO
O
NH
HN
O
O
S

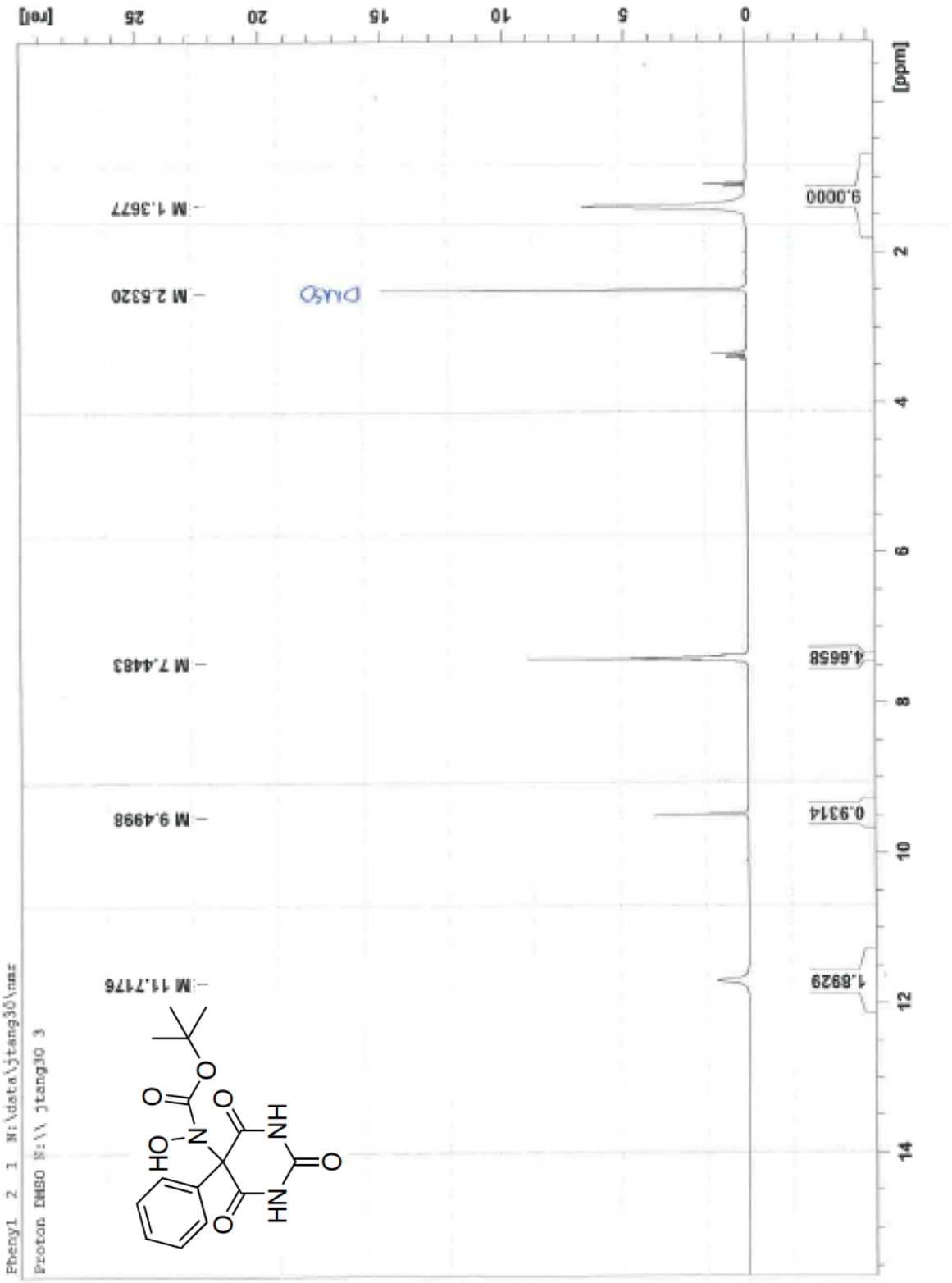
Ebenyl 2 1 N:\data\jtang30\nmr
Proton DMSO N:\\ jtang30 3
M 11.7176
M 9.4998
M 7.4483
M 2.5320
M 1.3677
DMSO
1.8929
0.9314
4.6658
9.0000
[rel]
[ppm]

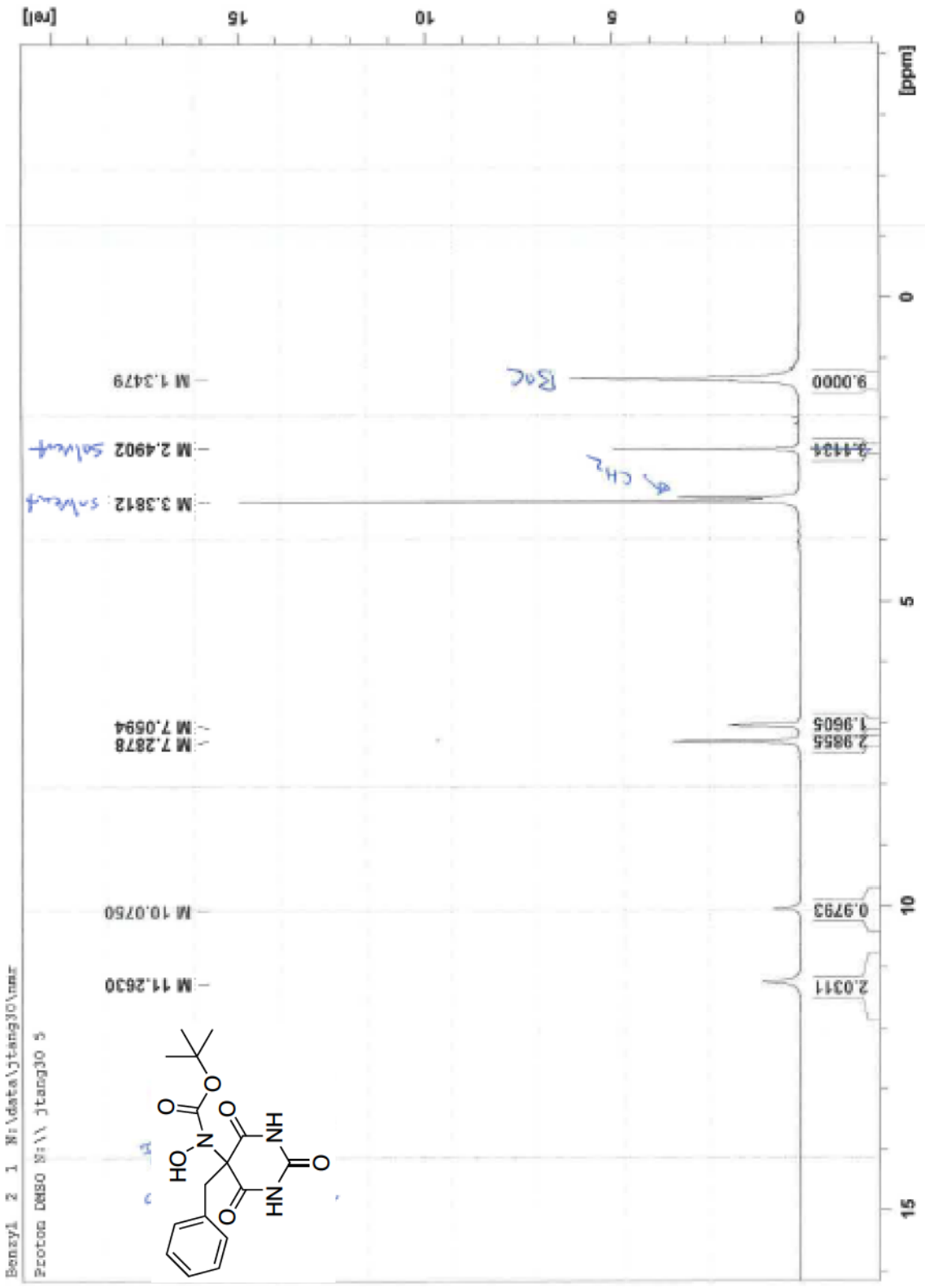
Benzyl 2 1 W:\data\jtang30\nmr
Proton DMSO W:\\ jtang30 5
M 11.2630
M 10.0750
M 7.0594
M 7.2878
M 3.3812
M 2.4902
M 1.3479
2.0311
0.9793
1.9605
2.9855
9.0000
9.1134
[rel]
[ppm]

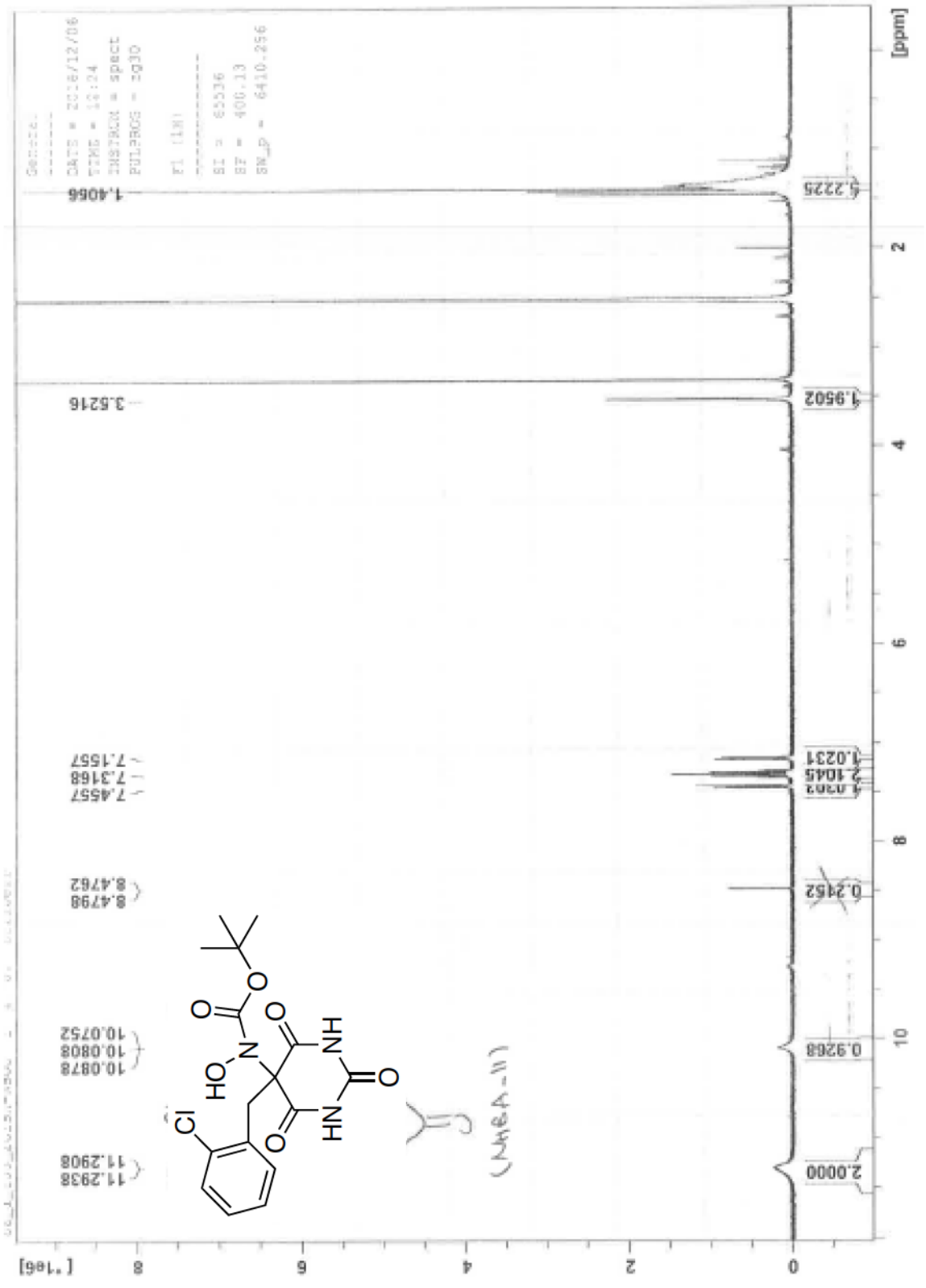
[ppm]
11.2938
11.2908
10.0878
10.0808
10.0752
8.4798
8.4762
7.4557
7.3168
7.1557
3.5216
1.4066
5.2225
1.9502
1.0231
2.1045
0.2152
0.9268
2.0000
(MeA-11)

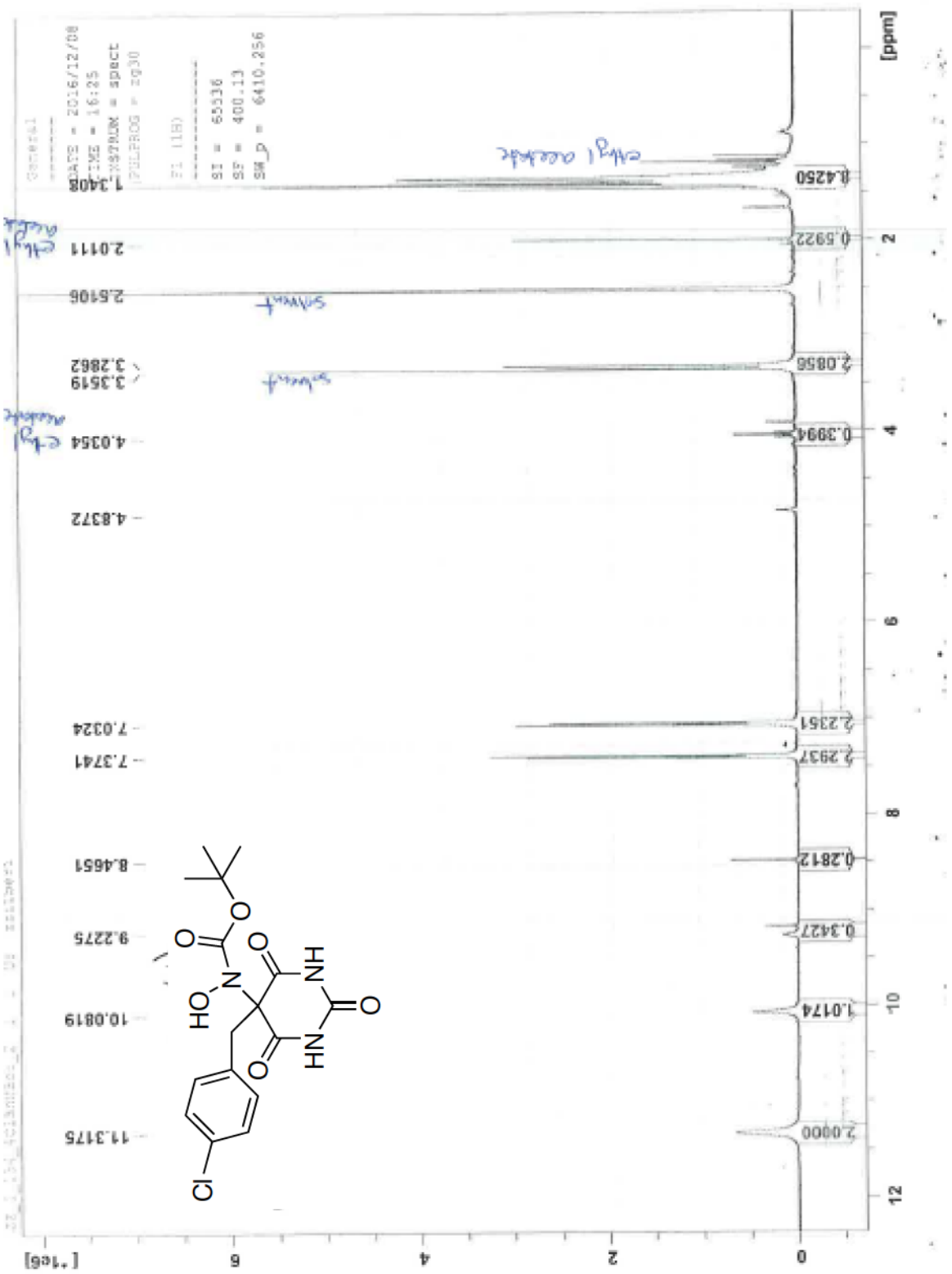
ethyl acetate
ethyl acetate
solvent
solvent
1.3408
2.0111
2.5106
3.2862
3.3519
4.0354
4.8372
7.0324
7.3741
8.4651
9.2275
10.0819
11.3175
0.4250
0.5922
2.0856
0.3994
2.2351
2.2937
0.2812
0.3427
1.0174
2.0000
[ppm]
[*1e6]
0
2
4
6
8
10
12
HO
N
O
O
O
NH
NH
O
O
Cl

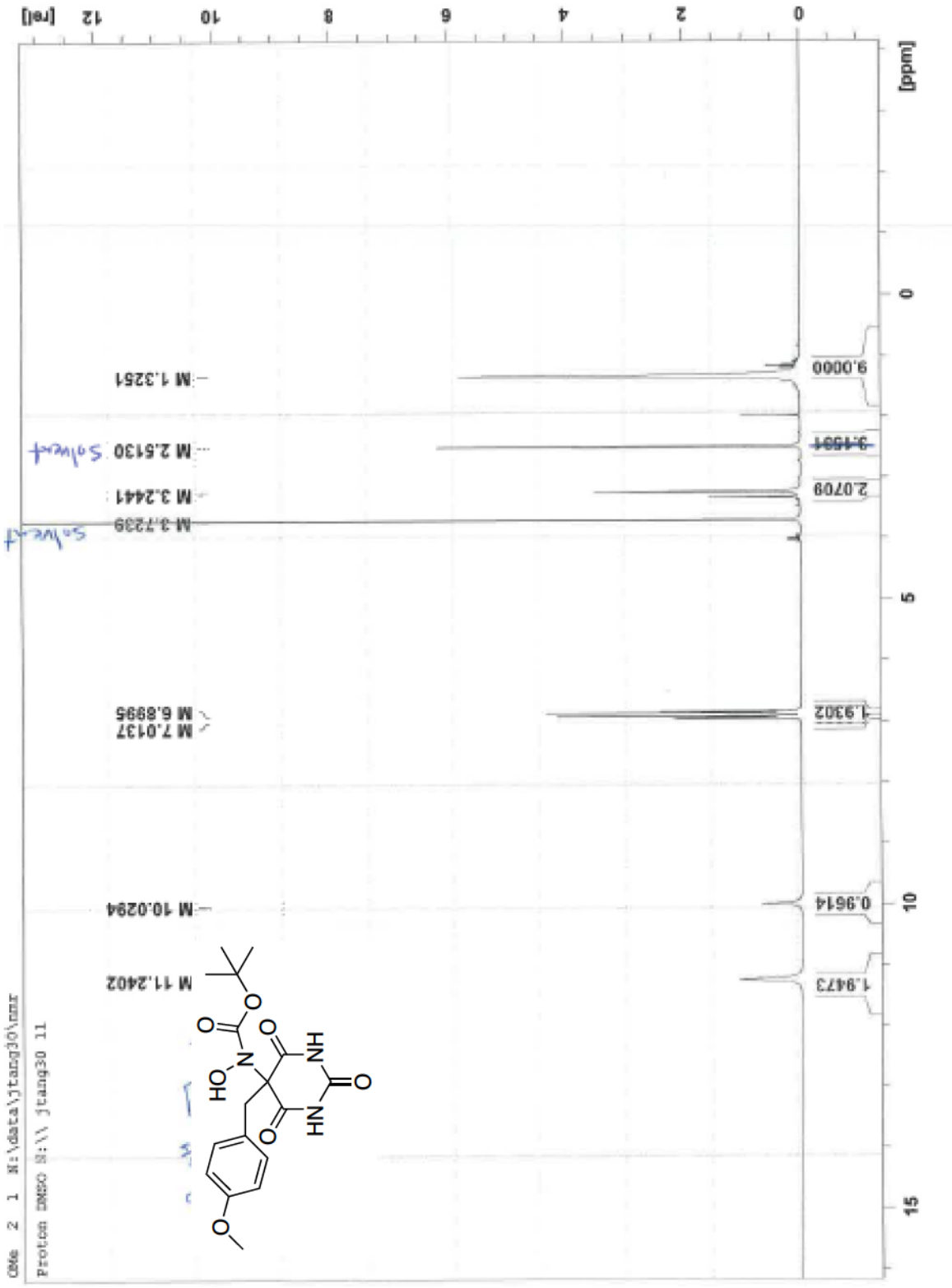
[rel]
12
10
8
6
4
2
0
[ppm]
M 11.2402
M 10.0294
M 7.0137
M 6.8995
M 3.7239
M 3.2441
M 2.5130
M 1.3251
9.0000
3.1581
2.0709
1.9302
0.9614
1.9473
5
10
15
Proton DMSO N:\\ jtang30 11
CMe 2 1 N:\data\jtang30\nmr

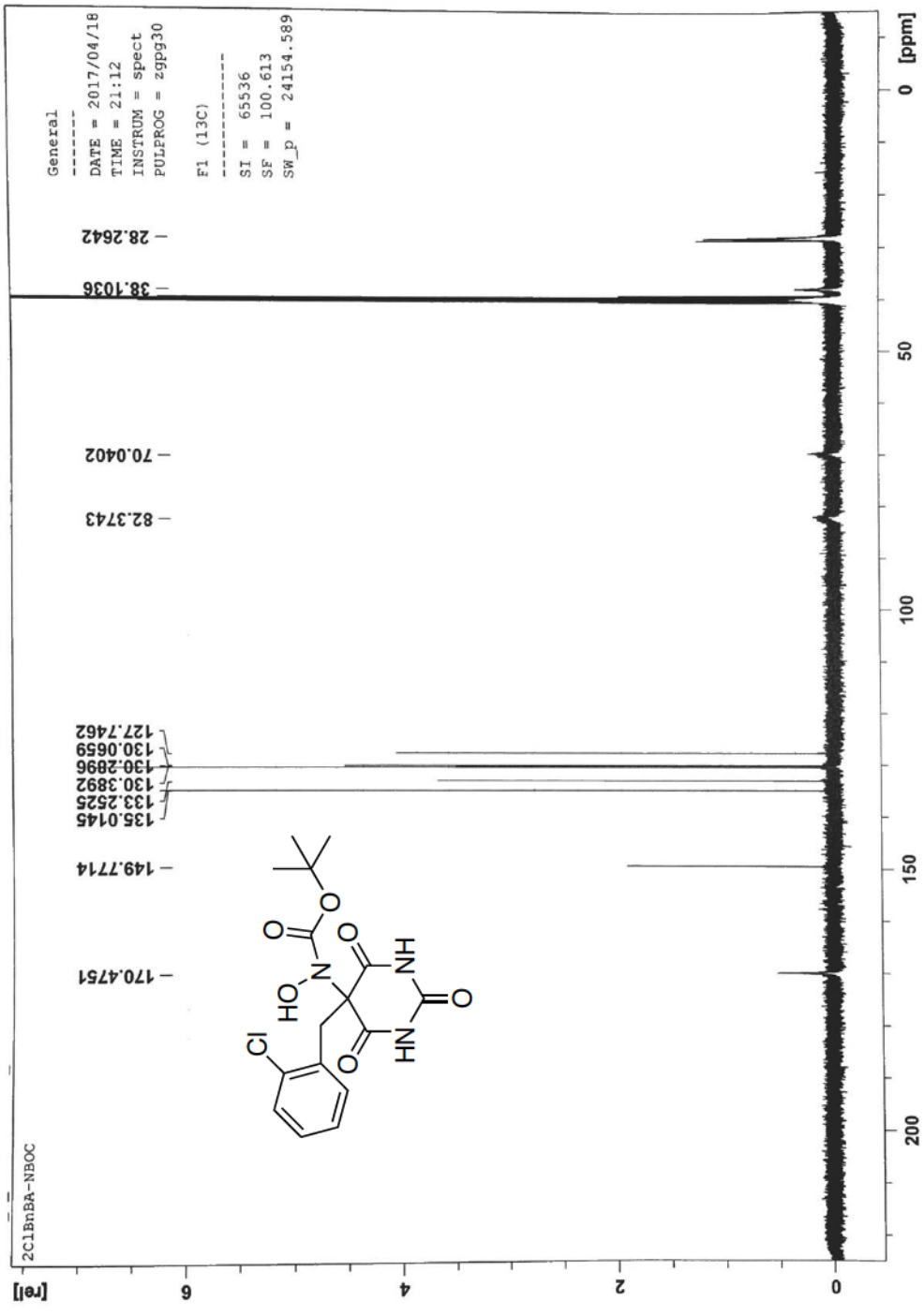
2C1BnBA-NBOC
General
DATE = 2017/04/18
TIME = 21:12
INSTRUM = spect
PULPROG = zgpg30
F1 (13C)
SI = 65536
SF = 100.613
SW_p = 24154.589
28.2642
38.1036
70.0402
82.3743
127.7462
130.0659
130.2896
130.3892
133.2525
135.0145
149.7714
170.4751
[rel]
[ppm]

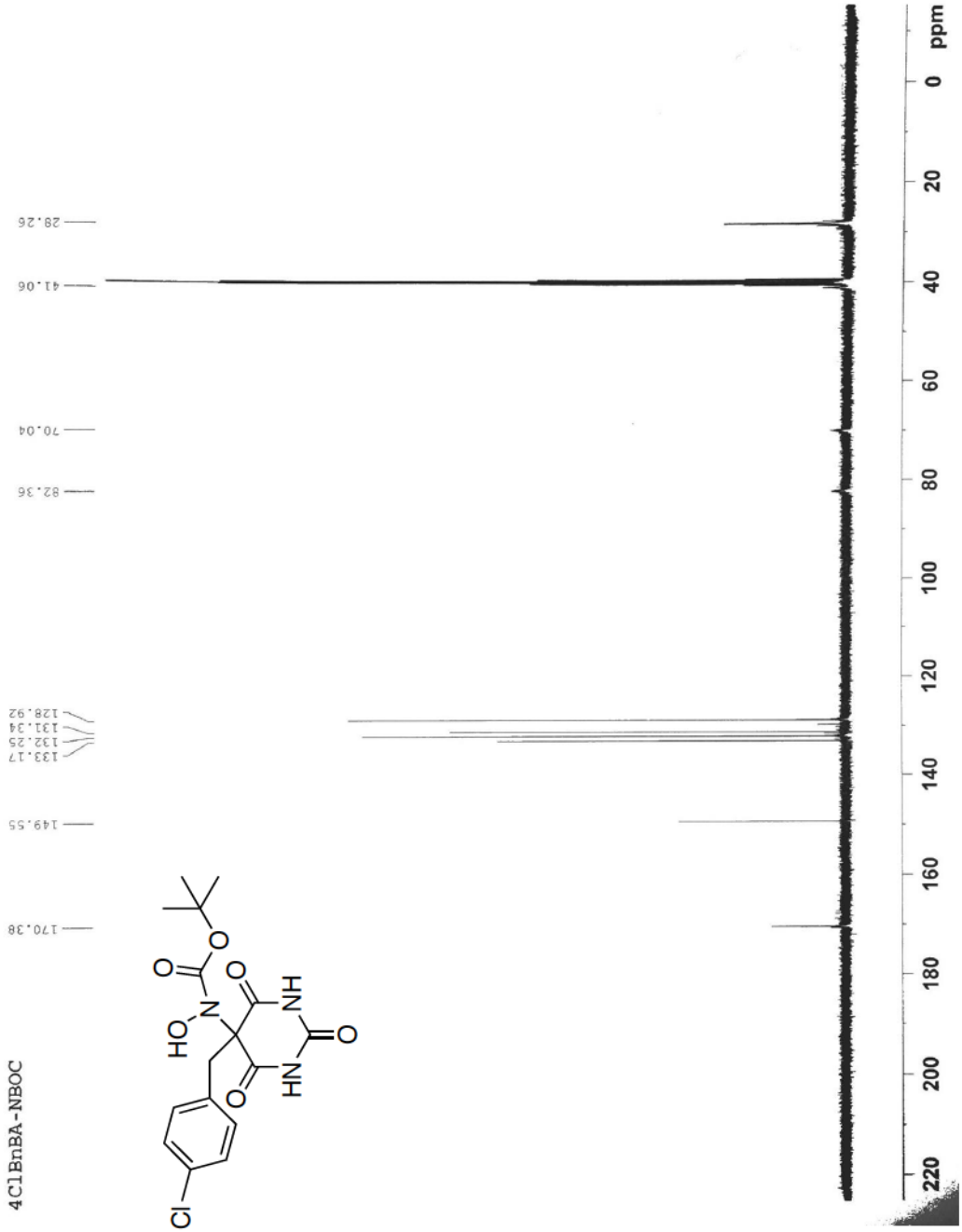
4ClBnBA-NBOC
170.38
149.55
133.17
132.25
131.34
128.92
82.36
70.04
41.06
28.26
ppm
0
20
40
60
80
100
120
140
160
180
200
220
HO
N
O
O
O
NH
HN
O
O
Cl

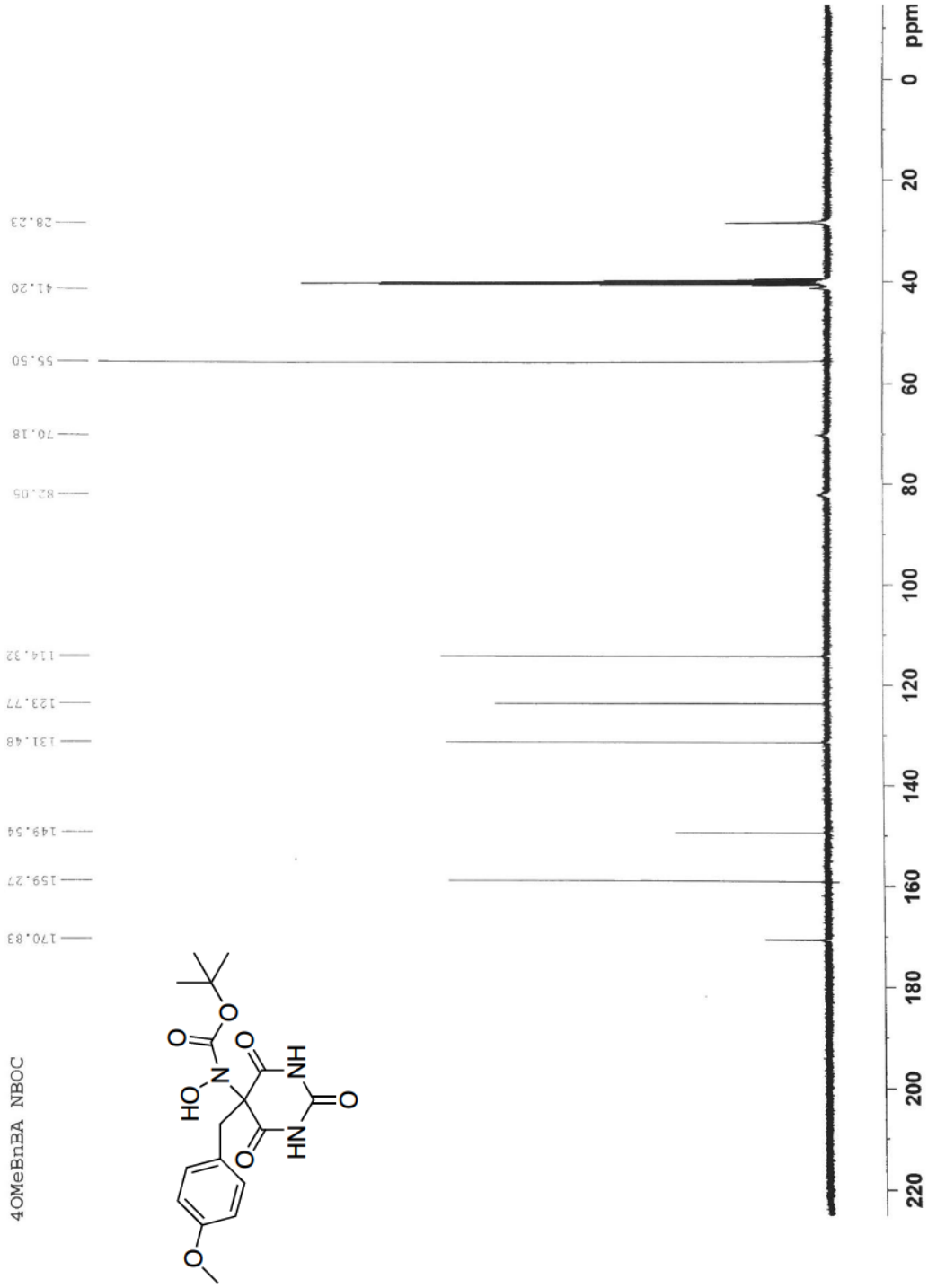
4OMeBnBA NBOC
170.83
159.27
149.54
131.48
123.77
114.32
82.05
70.18
55.50
41.20
28.23
ppm
0
20
40
60
80
100
120
140
160
180
200
220

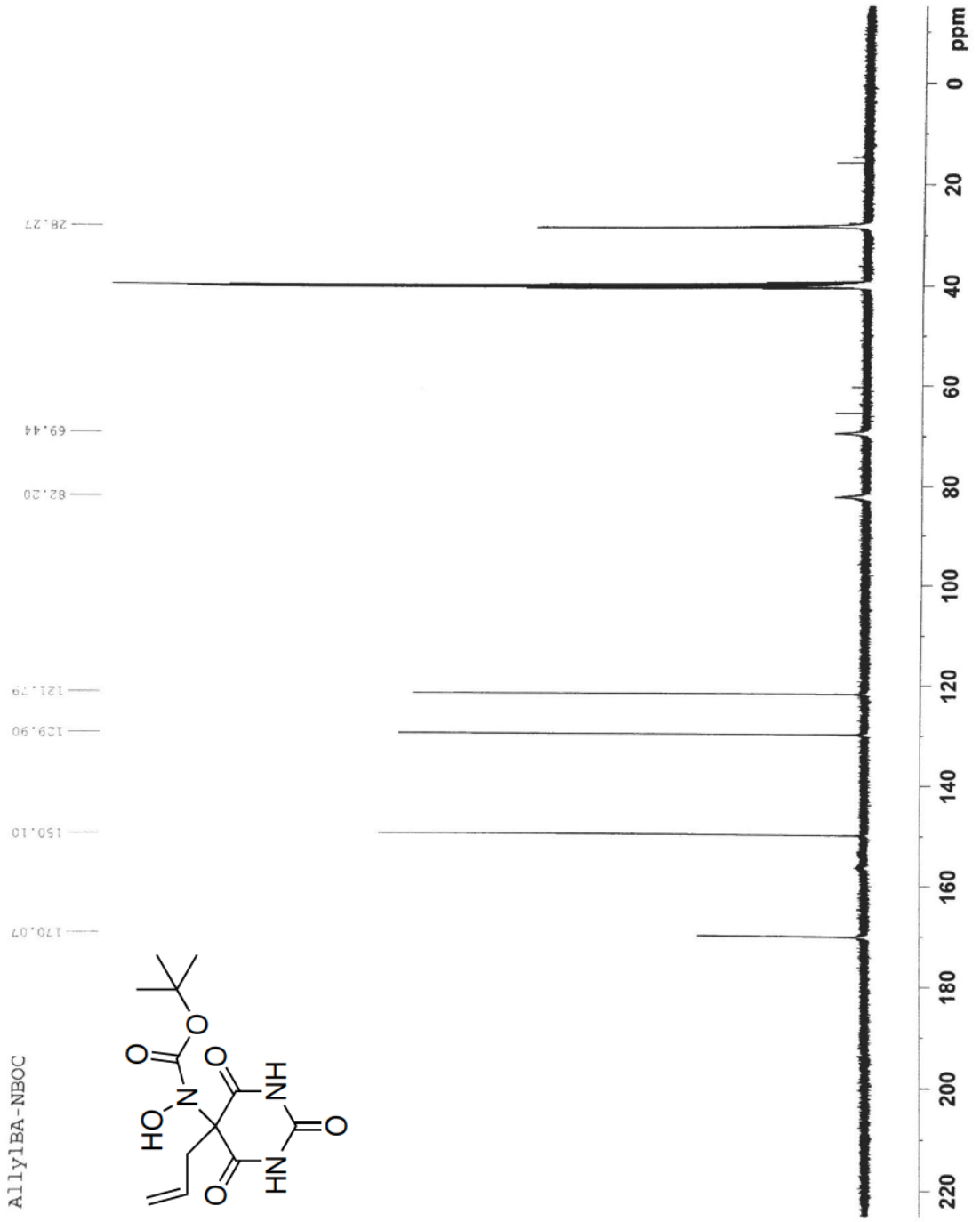
AllylBA-NBOC
170.07
150.10
129.90
121.79
82.20
69.44
28.27
ppm
0
20
40
60
80
100
120
140
160
180
200
220

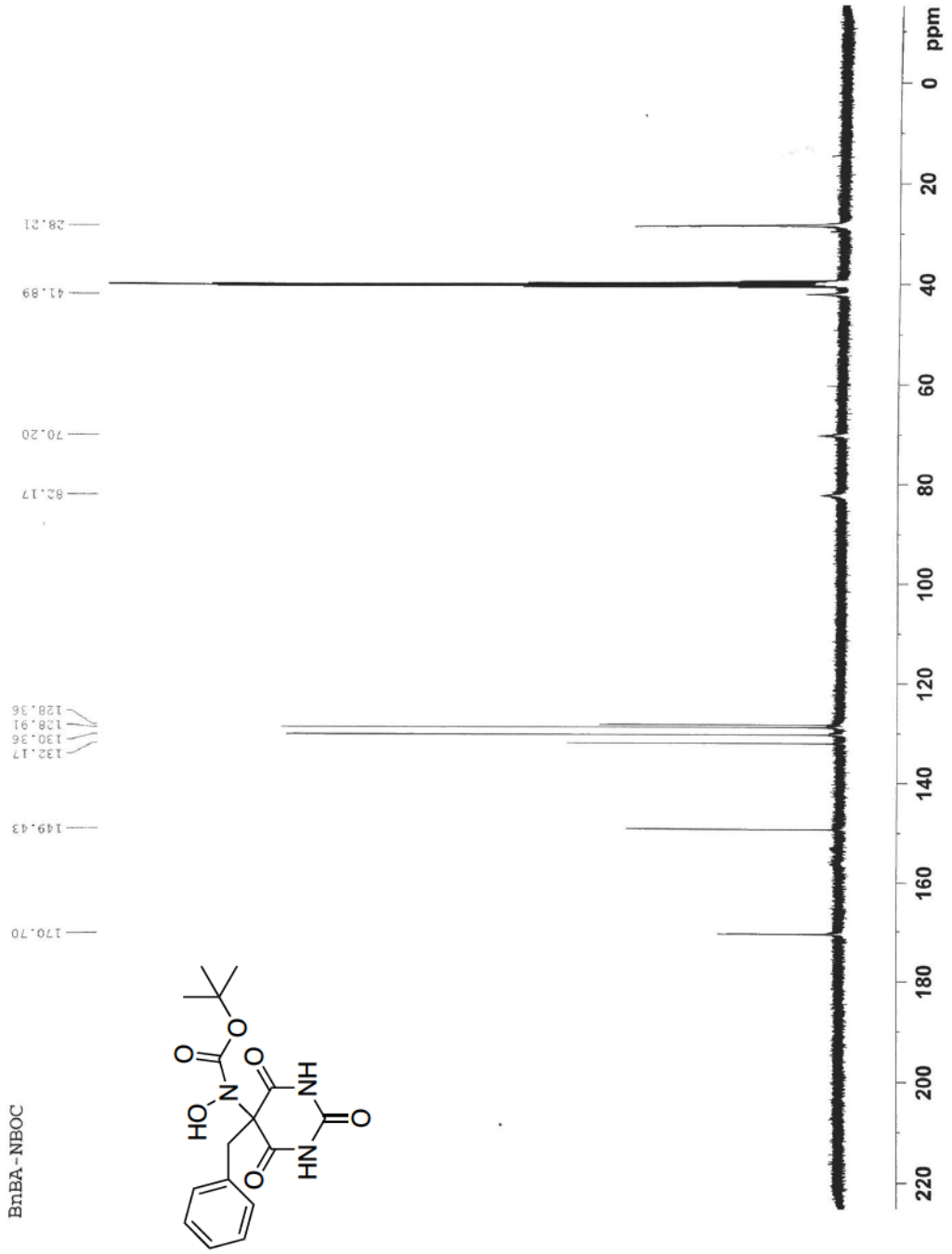
BnBA-NBOC
170.70
149.43
132.17
130.36
128.91
128.36
82.17
70.20
41.89
28.21
ppm
0
20
40
60
80
100
120
140
160
180
200
220

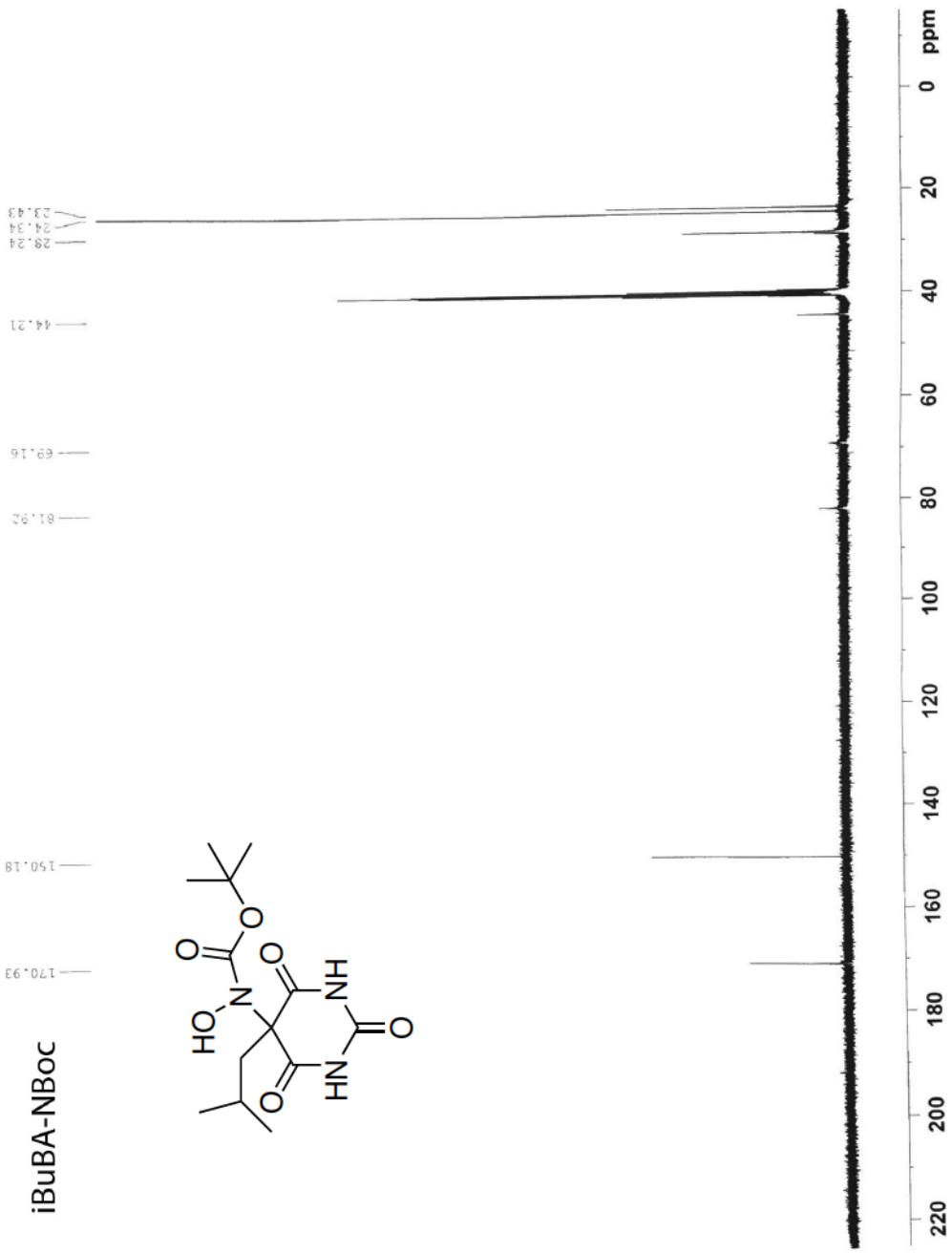
iBuBA-NBoc
170.93
150.18
81.92
69.16
44.21
28.24
24.34
23.43
ppm
0
20
40
60
80
100
120
140
160
180
200
220

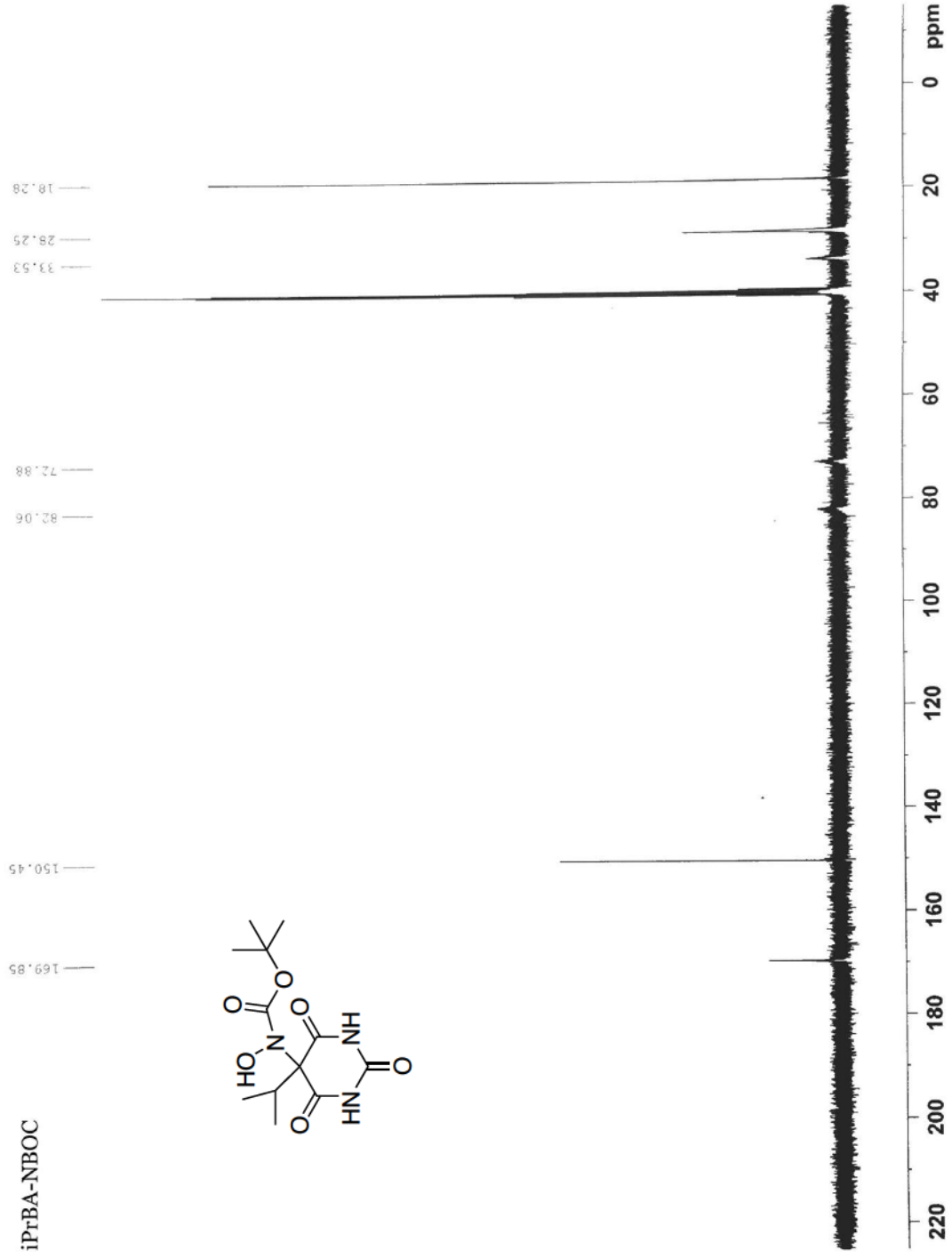
iPrBA-NBOC
169.85
150.45
82.06
72.88
33.53
28.25
18.28
ppm
0
20
40
60
80
100
120
140
160
180
200
220

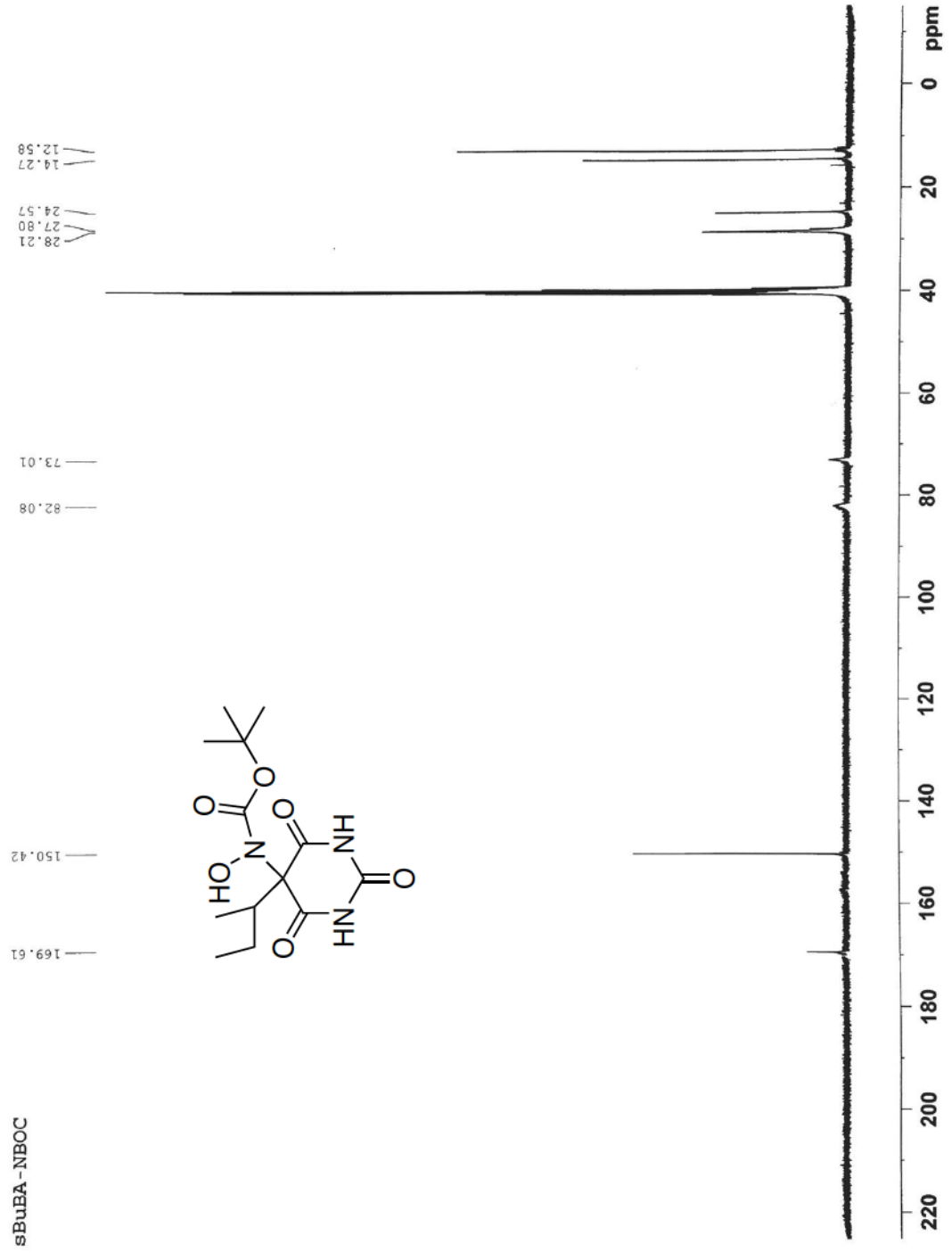
sBuBA-NBOC
169.61
150.42
82.08
73.01
28.21
27.80
24.57
14.27
12.58
ppm
0
20
40
60
80
100
120
140
160
180
200
220

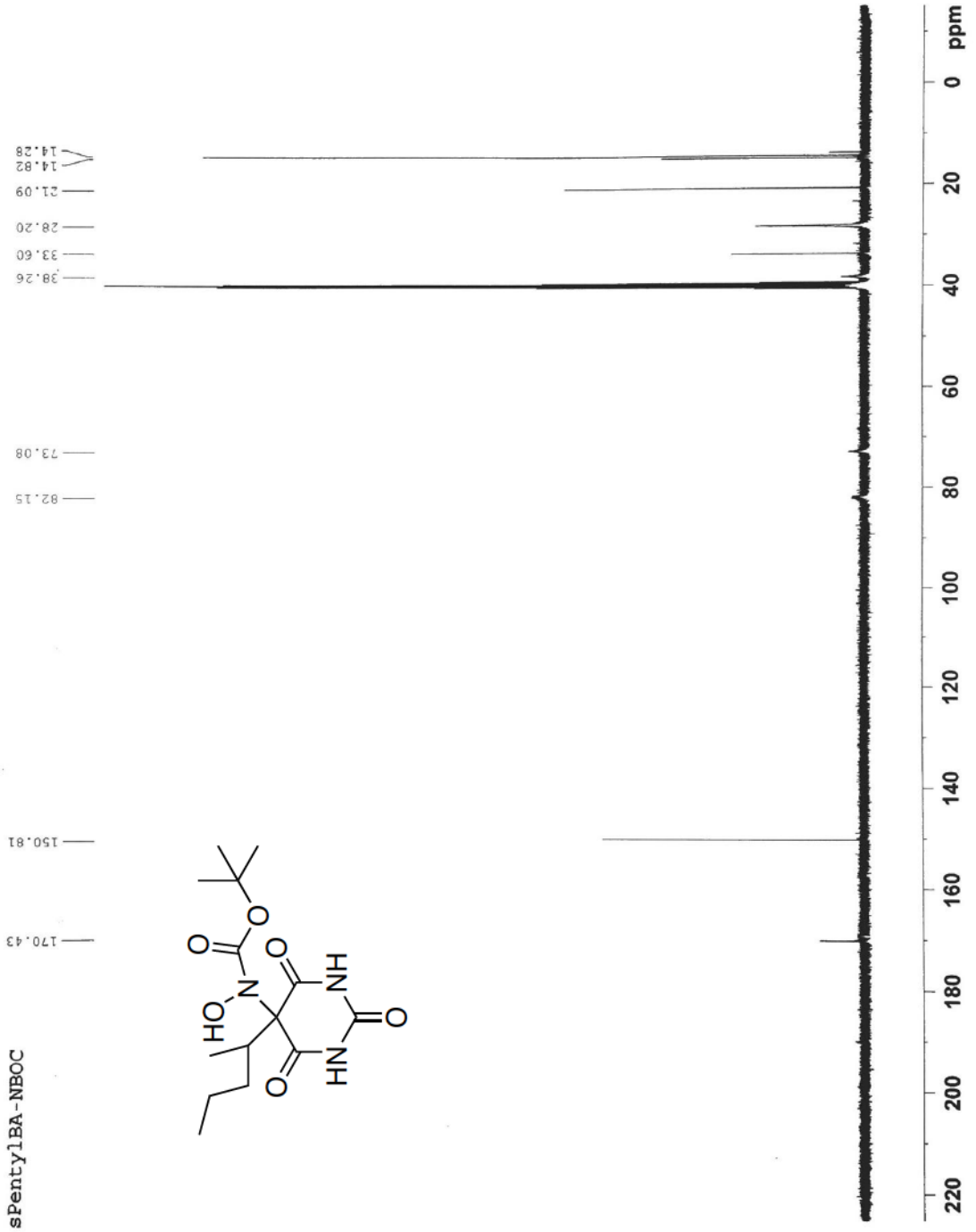
sPentylBA-NBOC
170.43
150.81
82.15
73.08
38.26
33.60
28.20
21.09
14.82
14.28
ppm
0
20
40
60
80
100
120
140
160
180
200
220

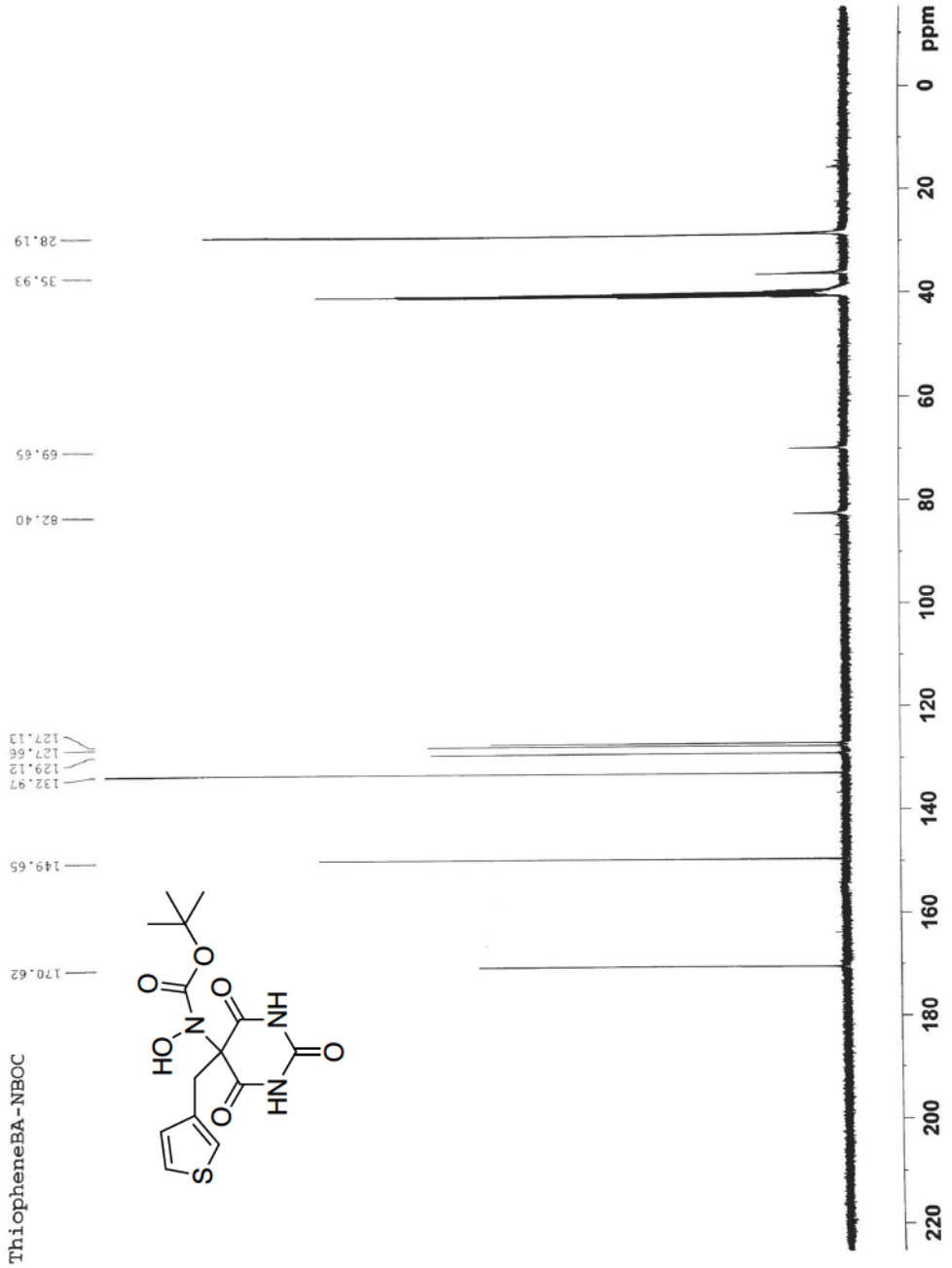
ThiopheneBA-NBOC
170.62
149.65
132.97
129.12
127.66
127.13
82.40
69.65
35.93
28.19
ppm
0
20
40
60
80
100
120
140
160
180
200
220

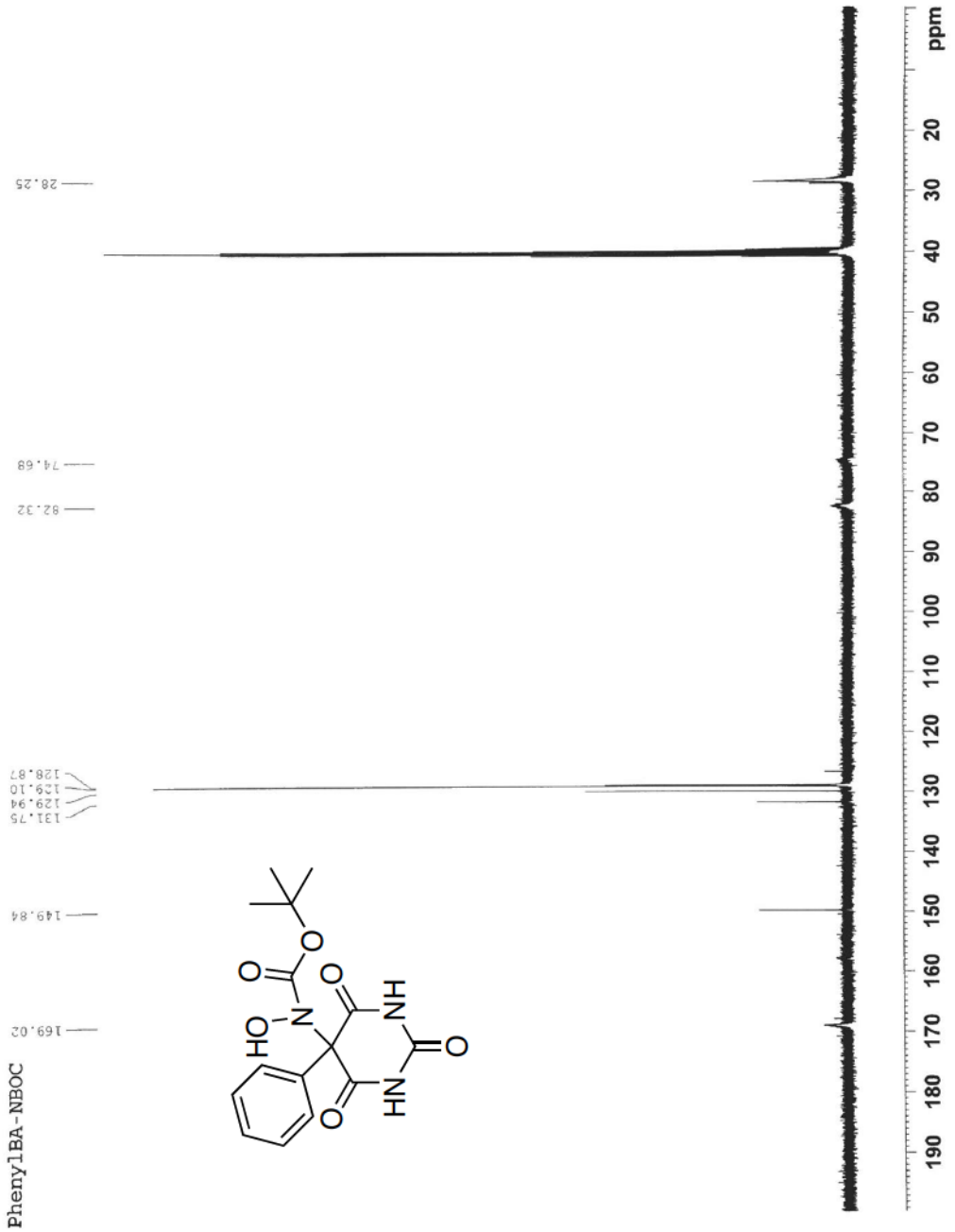
Phenylba-NBOC
169.02
149.84
131.75
129.94
129.10
128.87
82.32
74.68
28.25
ppm
190
180
170
160
150
140
130
120
110
100
90
80
70
60
50
40
30
20
HO
N
O
O
O
O
NH
NH
O

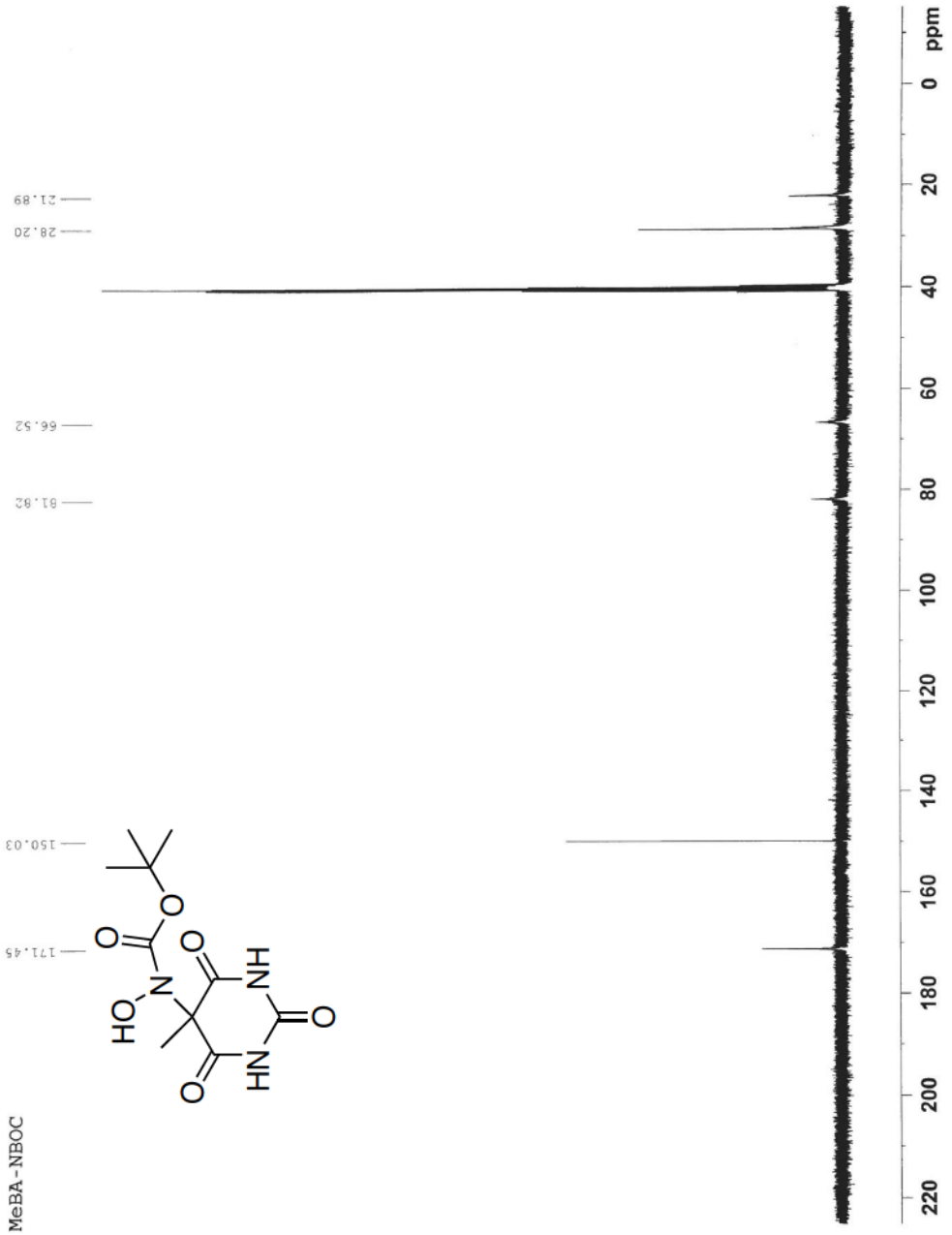
MeBA-NBOC
21.89
28.20
66.52
81.82
150.03
171.45
HO
N
O
O
O
NH
HN
O
ppm
0
20
40
60
80
100
120
140
160
180
200
220

Curriculum Vitae

Saghar Nourian was born in Tehran, Iran on September 16, 1985. Her interest in chemistry started in high school after taking courses in chemistry. In 2003, she enrolled in Sharif University of Technology where she graduated with a B.S. in chemistry. After a brief experience working for a pharmaceutical company, she decided to pursue her education by studying organic chemistry as a Master's student at Sharif University of Technology in 2008. During that time, she performed research under supervision of Professor Firouz Matloubi Moghaddam. She synthesized unique bicyclic systems and α-aminonitrile-type compounds, and it was a beginning for her great interest for science. In 2010, she graduated with her M.S with honor, and decided to follow her education in higher level.

In the fall of 2012, she joined Professor John P. Toscano lab at Johns Hopkins University where her PhD thesis was on the synthesis of precursors and reactivity studies of nitrosocarbonyl intermediates. During her studies as a PhD student, she authored two patent applications and couple of manuscripts. In winter 2017, she was accepted for a three-month internship through Hopkins/MedImmune program, where she worked as a scientist co-op and studied HCPs using different analytical techniques. In July 2017, Saghar received her Doctorate of Philosophy in Chemistry. After receiving her PhD, Saghar will begin a postdoctoral fellowship at NCI/NIH in Fredrick, in the lab of Dr. Martin Schnermann, working on near-IR uncaging chemistry for *in vivo* drug delivery.